Limitations of RNA interference as a potential technique for crop protection against insect pests

CAO, MIN

Limitations of RNA interference as a potential technique for crop protection against insect pests

A thesis submitted by Min CAO in accordance with requirements of Durham University for the degree of Doctor of Philosophy.

School of Biological and Biomedical Sciences
Durham University
March 2016

Abstract

The RNAi response suppresses gene expression at the post-transcriptional level and the potential of this technique to give control of insect pests in crops has been recognised for a decade.

This project focuses on a comparison of RNAi responses in insects of different orders by injecting and feeding dsRNA directed against *thread (APIN)* and *V-Type-ATPase E* homologues in the target species. The results showed systemic RNAi responses, and mortality, occurred in larvae of the *Tribolium castaneum* (*T. castaneum*), Coleopteran, but not a Hemipteran, the *Acyrthosiphon pisum* (*A. pisum*), where comparatively low levels of gene down-regulation were only achieved by injection of dsRNA. DsRNA injection produced both a lethal phenotype and gene down-regulation in larvae of the dipteran species *Musca domestica* (*M. domestica*), and *Delia radicum* (*D. radicum*), although the effects were found to be stage dependent.

Rapid dsRNA degradation in the extracellular environment could lead to a limitation of RNAi reponses. *In vitro* experiments show that dsRNA was degraded rapidly by *A. pisum* haemolymph and gut extracts, and less rapidly by *D. radicum* larval extracts. However, *T. castaneum* larval extracts differ in both the amount and qualitative nature of their RNase activity; dsRNA was degraded at a slow rate, predominantly by exonuclease activity rather than endonuclease activity.

A strategy using recombinant proteins was used to address limitations of RNAi effects after feeding dsRNA in insects. A recombinant protein containing an RNA binding domain (RBD) was selected to conjugate dsRNA forming a protein-RNA complex. The complexed protein enhanced the stability of dsRNA and protected it from degradation from insect extracts. A fusion protein containing snowdrop lectin (GNA) linked to RBD was also developed to produce a "systemic" RNAi effect, by transporting the protein-RNA complex to the insect haemolymph using the lectin as a "carrier".

Table of Contents

Table of Figures

Table of Tables

Declaration and Statement of Copyright

Declaration

No material contained herein has been previously submitted for any other degree. Except where acknowledged, all material is the work of the author

Statement of Copyright

Date: .....

Signed:.....

To my parents, Yuanying Li and Yinglong CAO.

Acknowledgements

I would like to express my sincere gratitude to my supervisor Prof. John A. Gatehouse for the continuous support of my PhD study and research, for his patience, motivation, enthusiasm, and immense knowledge. His guidance and encouragement helped me in research and writing of this thesis. It is a great honour for me to be one of his PhD students. I am also thankful to Prof. Angharad MR. Gatehouse, for her endless support for my experiments.

Many thanks to Dr. Elaine Fithches for help me to design experiments and the suggesions for correcting my thesis. Special thanks go to Dr. Prashant Pyati for his patience, support and advice for my experiments.

I would like to thank Dr. Stepan Fenyk for his help in designing the work of RNA mobility shift assay, and Dr. David R.W. Hodgson for providing me the materials for labelling RNA with FITC. I also thank Dr. Jen Topping for her kind encouragement and advice.

I wish to thank my examiners, Dr. Natalie Ferry and Prof. Marc Knight for their expertise and time spent improving my thesis.

I also acknowledge the other members of lab 1 for their help and advice. Particularly Dr. Dominic Wood and Dr. Sheng Yang.

I am indebted to friends who made my life here in the UK so special, Dr. Beatriz Orosa, Dr. Cunjin Zhang, Dr. Pengwei Wang, Dr. Lisha He and Mr Weiran Shen.

Finally, I would like to thank Bowen Li for the smile, love and company.

Min CAO

Abbreviations

AOX1:	Alcohol oxidase 1
bp:	base pairs
BCA :	Bicinchoninic acid
BSA:	Bovine Serum Albumin
CBB:	Coomassie brilliant blue stain
CDS:	Coding sequences
dNTPs:	deoxyribonucleotide triphosphate
dATP:	deoxyadenosine triphosphate
dCTP:	deoxycytosine triphosphate
dGTP:	deoxyguanine triphosphate
dsRNA:	double stranded RNA
dTTP:	deoxythymine triphosphate
DTT:	Dithiothreitol
ECL:	Enhanced Chemiluminescence
EU:	European Union
FAO:	Food and Agriculture Organization of the United Nations
FITC:	Fluorescein isothiocyanate
FPLC:	Fast Protein Liquid Chromatography
g	gram(s)
GNA	Galanthus nivalis agglutinin or Snowdrop lectin
GSP:	Gene specific primer
HRP:	Horseradish Peroxidase
kD / kDa:	KiloDalton
Kan	kanamycin
L :	litre(s)
L:D:	Light: dark

LD50	Median lethal dose
MWCO:	Molecular weight cut off
OD:	Optical density
ORF:	Open reading frame
PBS:	Phosphate buffered saline
PCR:	Polymerase chain reaction
RT-PCR:	Reverse transcription polymerase chain reaction
RACE:	Rapid Amplification of cDNA ends
RdRP	RNA induced RNA polymerase
RNAi:	RNA interference
RISC :	RNA-induced silencing complex
siRNA	Small interfering RNA
SDS-PAGE:	Sodium dodecyl sulphate polyacrylamide gel electrophoresis
TBE:	Tris Boric EDTA buffer
TEMED:	Tetramethylethylenediamine
TRX:	Thioredoxin
UTR:	Untranslated region
v:	volume
w:	weight
°C :	Degrees Celsius

Chapter 1 Introduction

1.1 Crop protection against insect pests

According to the United Nations (UN), the world population, currently at 7.2 billion, will reach to 9.6 billion people in 2050. Most of the growth of population will take place in developing countries, particularly in Africa. As a consequence, food demand will be increased. The FAO (2009) estimated that overall a 70% increase in agriculture food production will need to be achieved for feeding 9.1 billion people. However, this goal faces many challenges such as soil fertility depletion, arable land limitation, water resources and global warming (FAO, 2011).

As well as limitations to crop production by nutrients, water and other abiotic stresses, crop losses occur due to competition from animal pests, weeds, bacteria and viruses. Insects from orders of Orthoptera, Isoptera, Hemiptera, Thysanoptera, Diptera, Coleoptera, Lepidoptera and Hymenoptera can cause direct damage by eating leaves, buds, fruit and root or feeding on plant juice (Matthews 1999). Insect pests like aphids are also able to cause indirect effects by transmitting bacterial, viral or fungal infections (Kennedy and Collier (2000); Eleftherianos *et al.* (2008)). According to the data investigated by The Global Crop Diversity Trust, approx. 30%-40% of the world's crop yield is lost due to the damage by insect pests and crop diseases (Garthwaite *et al.* 2008).

Pest management through the use of applied insecticides can significantly improve crop production. Although early insecticides exploited naturally occurring compounds, the use of synthetic chemistry to produce more active compounds was a key component in the development of modern intensive agriculture. In 2007, Environmental Protection Agency (EPA) reported that the annual expenditures on insecticides reached $10.25 billion globally, which accounted for 29% of the total crop market value (Grube *et al.* 2011). The commonly used commercial insecticides for controlling insect pests target nervous systems (Casida and Durkin 2013), and include molecular targets such as acetylcholinesterase enzymes (organophosphates and carbamates) (Fukuto 1990); voltage-gated sodium channels (e.g. organochlorides and pyrethroids); and neurotransmitter- gated nicotinic acetylcholine (e.g. neonicotinoids), γ-aminobutyric acid – GABA (e.g. phenylpyrazoles) and L-glutamate (e.g. avermectins) receptors (Raymond-Delpech *et al.* 2005).

The use of such insecticides has largely contributed to increass food production in the past, however, their effects on human health, ecosystems and wildlife populations are poorly understood (Koehler and Triebskorn 2013). In addition, the widespread and

long-time use of chemicals with the same range of molecular targets has resulted in evolution of resistance in insects. Pesticide-resistant insects have been observed in many species which are major crop pests, which can contain mutations on sites of interaction in target proteins, gene duplication/ increased expression of detoxifying enzymes (e.g.,carboxylesterase and P450), or improved systems of excretion of toxic compounds from cells (Heckel (2012); Ffrench-Constant (2013)). Concerns about the environmental effects of synthetic chemical pesticides, and increasing levels of resistance in the target pests, have led to a need for new types of pesticides.

One alternative technology is the development of biological pesticide or biopesticides, which are developed from natural sources including plants, minerals and microorganisms. Spinosad, a mixture containing the secondary metabolites spinosyn A and spinosyn D from the Actinomycete *Saccharopolyspora spinosa*, is the most commonly used biopesticide (Kirst *et al.* 1992). Spinosyn is effective against a broad spectrum of insects (Lepidoptera, Coleopteran, Dipteran and Orthopteran) through contact or ingestion. It is believed to target a subtype of the nicotinic acetycholine receptor (Orr *et al.* 2009). Another widely-used biopesticide is the crystal proteins (Cry) from the entomopathogenic soil bacterium *Bacillus thuringiensis*. These proteins are pore-forming toxins, which interact with receptors in insect and lead to midgut lysis and osmotic shock, result in insect death. These toxins have been widely used as biopesticides for at least 50 years and are particularly effective against Lepidopteran, Coleopteran and Dipteran larvae (Crickmore *et al.* 1998). Since the Bt toxins are proteins, they are good subjects for production via a transgenic organism; genetically engineered crops expressing *Bacillus thuringiensis* (Bt) toxins are widely applied in global agriculture (Toenniessen *et al.* 2003). Bt toxins combine effectiveness against insect pests and safety to non-target organisms, and as a result the area planted with transgenic Bt-expressing crops such as soybean, maize, cotton and canola has been expanded from 1.1 million hectares (ha) in 1996 to 181.6 million ha in 2011 *(*James *et al*., 2015). However, due to the lack of appropriate receptors in the insect to interact with Cry toxin, GM Bt crops cannot be used for controlling hemipteran insect pests such as aphids (Porcar *et al.* 2009). Furthermore, evolving resistance to Bt crops in insects has been reported (Baum *et al.* 2007). Therefore, there is still a requirement for new strategies, which protect crops against insect pests.

1.2 RNA interference

1.2.1 A short history of the discovery of RNAi

The phenomenon of dsRNA-induced gene silencing was first discovered by Napoli et al. in 1990. They overexpressed chalcone synthase in petunias by introducing a construct containing the coding sequence of the gene and a constitutive promoter to identify whether chalcone synthase (CHS) was key enzyme in anthocyanin biosynthesis. The anthocyanin biosynthesis pathway is crucial for the deep violet coloration in petunias. Unexpectedly, the overexpression of CHS by introducing a chimeric CHS gene resulted in white petunia and the level of endogenous CHS was 50-fold lower than in wild-type petunia (Napoli *et al.* 1990). Napoli *et al.* (1990) described this phenomenon as 'co-suppression'. A similar phenomenon in *Neurospora crassa* (an ascomycete fungus) was reported by Romano and Macino. They noticed that introduction of homologous RNA sequences caused 'quelling' of the endogenous gene (Romano and Macino 1992). When they transformed *albino-3* (*al-3*) and *albino-1* (*al-1*) genes in Neurospora, low level of expression of endogenous *al-1* and *al-3* gene were detected. Several years later, mRNA silencing by sense and antisense RNA was found in the animal model, *Caenorhabditis elegans* (Guo and Kemphues 1995). Guo and Kemphues were attempting to knock down *PAR-1* (*partition 1*) gene by introducing antisense (ss)RNA. However, gene silencing was also detected in a control group which was treated with sense RNA.

The mechanism of the gene silencing by both sense and antisense RNA was unknown until 1998 when Andrew Fire and Craig Mello elucidated that it is double-stranded RNA (dsRNA) as the trigger for gene silencing (Fire *et al.* 1998). This also provided the explanation for previous gene silencing observations. Fire et al. suggested that in the case of studies conducted by Guo and Kemphues that effects observed in *C. elegans* following the introduction of ssRNA were actually due to the presence of contaminating dsRNA, produced during the preparation of ssRNA (Fire *et al.* 1998). They purified sense and antisense single-stranded RNA molecules against *C. elegans unc-22* gene product gene resulted in a twitching phenotype in *C. elegans*. Their results showed that ssRNAs were significantly less effective than dsRNA targeting the same mRNA. Moreover, ssRNAs was only effective only when sense strand was injected into worms, followed by the antisense strand RNA (Fire *et al.* 1998) reviewed in Sen and Blau (2006).

1.2.2 Identification of 'dicing' and 'slicing'

The term RNAi is used to describe inhibition of gene expression in a sequence-specific manner by introduction of double-stranded RNAs. It is a conserved mechanism in

many eukaryotes (Geley and Müller 2004). In order to identify the mechanism which dsRNA directs the degradation of endogenous mRNA, Hamilton and Baulcombe (1999) detected antisense RNA with estimated length of 25 nucleotides (nt) in tissue in gene silencing experiment and they suggested that this length was necessary for RNAi specificity. Later, researchers found that 21-23 nt RNA always copurified with RNAi activity by using a *Drosophila melanogaster* cell culture system (Hammond *et al.* 2000) (Zamore and Haley 2005). These findings suggest that dsRNA was converted to short interfering RNAs (siRNAs) before binding to target mRNAs. To confirm that the 21-23nt dsRNA are the effectors for gene silencing, Elbashir *et al.* (2001a) synthesized 21-22nt dsRNAs with sequence identity to part of the firefly luciferase transcript and incubated the dsRNA with Drosophila cell extracts containing firefly luciferase mRNA. They found that these short interfering RNAs, or siRNAs, functioned as guides for cleavage of the mRNA near the centre of the region encompassed by the 21-22nt RNAs, 11 or 12 nt downstream of the first base pair between the siRNA and mRNA. Moreover, siRNAs with 2-3nt overhangs on their 3' ends were proved to be more efficient in silencing mRNA than siRNAs with blunt ends (Elbashir *et al.* 2001b).

Further research characterised the enzymes that were responsible for converting dsRNA into siRNAs ('dicing') and the destruction of complementary mRNAs ('slicing'). Bernstein et al identified two enzymatic activities in Drosophila cell extracts by high-speed centrifugation (Bernstein *et al.* 2001). The activity that degraded the target mRNA, which was referred as RNA-induced silencing complex (RISC), was pelleted by centrifugation whereas the activity that convert dsRNA into siRNA remained in the supernatant (Bernstein *et al.* 2001). They designated these two phases of the RNAi pathway as initiator phase (cleavage of dsRNA into siRNA) and effector phase (RISC-mediated degradation of target mRNA). The activity in the supernatant was caused by a type III RNase III enzyme, named Dicer, which was shown to be able to cleave dsRNA into 21-23nt siRNA. Depletion of Dicer using dsRNAs resulted in loss of dsRNA-induced gene silencing of other genes (Hammond *et al.* 2000). Identification of enzymes that were responsible for RISC-mediated mRNA cleavage resulted in two protein candidates, Argonaute 1 and Argonaute 2, which were found to have the ability of cleaving mRNA by a co-immunoprecipitation study in mammalian cells (Martinez *et al.* 2002). The 'slicer' activity of Argonaute enzymes was not confirmed until Song *et al.* (2004) crystallized an Argonaute protein from the archaebacterium *Pyrococcus furiosus,* and found significant similarity in the Argonaute PIWI (P-element induced wimpy testis) domain to the conserved secondary structure of RNase H enzymes, which hydrolyze the RNA of RNA/DNA hybrids (Cerritelli and Crouch 2009). Moreover, the 'slicer' activity, like RNase H enzyme activity, is dependent on divalent cations and leaves 3'-OH and 5'-phosphate termini (Martinez and Tuschl 2004). Argonaute 2 (Ago2) appears

to be the enzyme with 'slicer' activity present in the active RISC complex; immunoprecipitation of tagged Ago 1, 2, 3 and 4 from human cells showed that all the proteins were able to bind to siRNA, but only Ago2 retained mRNA cleavage activity (Liu *et al.* 2004).

Studies on the assembly of the RISC in *D. melanogaster* have broadened our understanding, and shown that additional proteins are involved in this process. SiRNAs are loaded on to RISC with the aid of RISC-loading complex (RLC) which contains Dicer-2 (Dcr-2) and a partner protein R2D2 (Zamore and Haley 2005). Addition of recombinant Dcr-2 and R2D2 to recombinant Ago2 and duplex siRNA induced RISC activity (Liu *et al.* 2009). Moreover, a RISC enhancer C3PO (component 3 promoter of RISC), which contains translin and TRAX (translin-associated factor-X) was identified as necessary for *in vivo* RNAi in *D. melanogaster*. Liu *et al.* (2009) confirmed the ribonuclease activity of C3PO and proposed that Dcr-2-R2D2 associated with C3PO to form the active RISC complex and remove the passenger strand of siRNA, releasing the guide strand siRNA to Ago2.

1.2.3 Multiple RNAi pathways

In addition to the exogenous (or siRNA-mediated) RNAi pathway observed by Fire et al (1998), further pathways utilising many of the same components have been identified in eukaryotic organisms; these are the endogenous RNAi pathway (mediated by micro RNAs; miRNA), the piRNA (Piwi-interacting short RNA) pathway and RNAi effects mediated by endogenous siRNA (esiRNAs) (Matranga and Zamore 2007). Each pathway has distinct role: the exogenous RNAi response to foreign nucleic acids forms a primary anti-viral defence, while endogenous RNAi acts as one of many controls on endogenous gene expression, and piRNAs protect the genome against transposable elements (Obbard *et al.* 2009).

In the exogenous RNAi pathway, dsRNAs (either experimentally introduced dsRNA or viral RNAs) are cleaved by Dicer dsRNA-specific endonucleases into double stranded fragments 21-23 nucleotides in length which contain a 5' phosphate and 2', 3' hydroxyl termini (named as siRNAs). One strand of the siRNA (guide strand) is loaded into an RNA-induced silencing complex (RISC) with the involvement of an additional argonaute multi-domain protein, which contains an RNaseH-like domain responsible for target mRNA degradation (Filipowicz (2005) and Martinez *et al.* (2002)).The siRNA assembled into a RISC can bind anywhere within the target mRNA sequence provided that there is perfectly matched base pairing. Argonaute protein then cleaves the target mRNA at the position of nt 10 and nt 11 of the siRNA to cause mRNA degradation. The cleaved mRNA is subsequently degraded by cytoplasmic nucleases (Tolia and Joshua-Tor 2007).

Endogenous RNAi functions in the post-transcriptional regulation of eukaryotic gene expression (described in reviews by Du and Zamore (2005); Pillai *et al.* (2007); Matranga and Zamore (2007); Chapman and Carrington (2007)). The endogenous siRNA (esiRNA) pathway has been discovered to function to regulate host gene expression and to control transposable element (TE) levels (Obbard *et al.* 2009). Instead of silencing mRNA, the target for esiRNA is endogenously produced dsRNAs; either TEs, overlapping 3-UTRs from genes on opposite strands or stem-loop structures. RNAi pathway mediated silencing endogenous dsRNA processes in a similar way to the silencing of exogenous dsRNAs in the siRNA pathway. Argonaute-2 and Dicer-2 are involved in the pathway (Chung *et al.* (2008); Czech *et al.* (2008)).

MiRNAs are conserved in both plants and animnals, and are thought to be a vital component of gene regulation (Siomi *et al.* 2011). They are usually produced endogenously by host genomes. They are transcribed by RNA polymerase II into primary miRNAs followed by processing in the nucleus by proteins from Drosha family to form short stem loops, which are termed immature miRNAs. Mature miRNA, containing a 5' phosphate and 3' hydroxyl is processed by another Dicer family protein, Dicer-1, which preferably binds to dsRNAs with imperfectly matching sequences (Lee *et al.* 2004), and a dsRNA-binding domain (dsRBD) protein, Loquacious after the immature RNAs are exported in the cytoplasm. Similar to siRNA, of strand of mature miRNA are loaded into the RNA-induced silencing complex (RISC) and binds to its complementary sequence in endogenous mRNA transcripts, or inhibits translation initiation. The other strand from miRNA duplex is released and degraded. Plants miRNAs are perfectly complementary to the target mRNA they regulate, and result in mRNA cleavage and degradation (Obbard *et al.* 2009) whereas animal miRNAs are less complementary to their target sequence, which results in translation inhibition (Pillai *et al.* 2007).

PIWI-interacting RNAs (piRNAs) are longest small RNAs, and also the largest class in small non-coding RNAs expressed in animal cells (Aravin *et al.* 2007). They are distinct from miRNA in size (24-30 nucleotides in piRNAs), lack of sequence conservation, and increased complexity (Aravin *et al.* (2007); Seto *et al.* (2007). They are produced by a Dicer-independent mechanism; they are found in the germ cells of animals, associated with piwi-class Argonaute proteins, participate in in both epigenetic and post-transcriptional gene silencing (Hartig *et al.* (2007); Aravin *et al.* (2007); Klattenhoff and Theurkauf (2008)). They are thought to be generated from single-stranded precursor RNAs (Matranga and Zamore 2007). PiRNAs contain 5´ monophosphate and 2´-*O*-

methyl, 3´hydroxy termini, are thought to arise from loci rich in transposons and act to silence dispersed copies of the selfish genetic elements present in the original trigger locus (Matranga and Zamore 2007). piRNAs are also implicated to act in silencing transposons during mammalian spermatogenesis (Aravin *et al.* 2007).

1.3 RNAi in insects

1.3.1 Amplification and spreading of silencing

The RNAi-mediated down-regulation of gene expression which has been discovered in plants (Palauqui *et al.* 1997) and nematodes (Fire *et al.* 1998) shows systemic effects, in which gene suppression spreads throughout the organism and persists over different developmental stages. The systemic RNAi effect in *C. elegans* involves multiple steps including export of siRNAs from cells that are exposed to the original RNA signal and a transmission of the effect to other cells. The synthesis of new RNAs (RNA triggers) by an export process enables an amplification of the RNAi effect, which can be persistent with time in the organism, leading to transmission to progeny (Gatehouse and Price 2011). The systemic RNAi effect in *C. elegans* is determined by an RNA-dependent RNA polymerase (RdRP) which can interact with the RISC complex and produce new dsRNA based on partially degraded target template through using the hybridized siRNA strands as primers (Price and Gatehouse 2008). The synthesized dsRNA is then cleaved by Dicer to produce new siRNAs (Secondary siRNAs), thus functioning as an amplification step. A domain, designated PF05183 is characterized as RdRP, and has been found in gene products of many eukaryotic microorganisms, fungi, plants, nematodes, but not in insects. In Drosophila, RNAi-mediated gene knockdown is limited to the location where dsRNA is delivered and systemic long-lasting RNAi effects like *C. elegans* have not been observed (Figure 1-1).

As well as a possible amplification mechanism, the mechanisms of export of RNAs across the cell membrane are not yet fully understood. Currently, three genes, *sid-1,-2* and *-3* are identified as important for RNAs transportation (Winston *et al.* 2002). The product of *sid-1* was characterized as trans-membrane protein in cell plasma membrane. It is predicted that *sid-1* products may function as either a channel for dsRNAs and/or siRNAs or a receptor which is responsible for their endocytosis. SID-2 was identified in intestine, and functions as trans-membrane protein necessary for import of dsRNAs from gut lumen into body cavity in nematode. The function of SID-2 was demonstrated in nematode *Caenorhabditis briggsae*, which is defective in uptake of dsRNA from the gut lumen. A systemic RNAi phenotype was restored after

transformation of *C. elegans* sid-2 into *C. briggsae* (Winston *et al.* 2002). In the model insect *D. melanogaster*, a homologue of *SID-1* is not present, and no systemic RNAi effects are observed. The absence of RdRP in *D. melanogaster* may indicate that systemic RNAi effects from endogenously produced dsRNA will become a limitation for down-regulation of a target gene through a plant host. *Sid-2* homologues have only been identified in nematodes closely related to *C. elegans*. However, and promisingly, homologues of the *C.elegans sid-1* gene have been found in insects like *Tribolium castaneum*, *Bombyx mori* and *Apis mellifera*, and systemic RNAi effects were observed in the *T. castaneum* , *T. castaneum*, which can be transmitted to progeny. Tomoyasu and Denell (2004) injected dsRNA of a homologue of the *Drosophila* sensory bristle-forming gene *Tc-achaete-scute (Tc-ASH)* into larvae, which caused 'loss-of-bristle' phenotype over the whole life of adult insects. Three genes: *Distalless* (leg development gene), *maxillopedia* (homeotic gene) and *proboscipedia* (relevant with labial and maxillary palps formation) were used to construct dsRNA for injection in another study. The phenotype changes caused by the RNAi effect were observed both in injected insects and progeny embryos (Bucher *et al.* 2002). Due to the robust systemic RNAi response and the completion its genome sequence, *T. castaneum* is becoming a model for the study of systemic RNAi in insects. The comparison of genome sequence of *C. elegans* and *T. castaneum* revealed that *T. castaneum* lacks a *C. elegans*-like RdRP which would mediate a systemic RNAi effect (Tomoyasu *et al.* 2008). These results suggest that the RNA amplification in *T. castaneum* is occurring by a mechanism different from that in *C. elegans*, although the mechanism in insects is still unclear.

A possible reason for RNAi systemic effects observed in *T. castaneum* could be the presence of three homologues of *sid-1* gene in the genome, whereas the lack of systemic effects in *Drosophila* might be due to the lack of *sid-1* homologous gene. However, recent studies suggests that in *Drosophila* S2 cells revealed that dsRNA uptake does not involve a sid-1 based pathway but occurs by receptor-mediated endocytosis (Saleh *et al.* 2006). The result shows pharmacological inhibition of endocytosis also inhibited RNAi effects. A similar phenomenon was also observed in *C. elegans*, in that knockdown of components of the endocytotic pathway by RNAi resulted in 'loss-of-RNAi-function' phenotype (Ulvila *et al.* 2006). Moreover, another study in *Locus migratoria* stated that silencing of the *LmSID-1* gene did not influence RNAi effects of other genes through *in vivo* experiments (Luo *et al.* 2012). Further, *in vitro* experiments showed that the *LmSID-1* protein in *Drosophila* S2 cells could not enhance dsRNA uptake, confirming that it is not involved in systemic RNAi effects (Luo *et al.* 2012). The author concluded that the mechanism of insect systemic RNAi is

different from *C. elegans*. Homologues of the *C.elegans SID-1* gene have been identified in aphids (Xu and Han 2008) but the evidence presented above shows that the presence of *SID-1* homologues in insects cannot be the only criteria for robust systemic RNAi effects (Tomoyasu *et al.* 2008).

1.3.2 Insect sensitivity to RNAi

The presence of systemic RNAi effects has been found to vary considerably between insect species, although *C. elegans* exhibited a robust systemic RNAi response. In insects, successful suppression of endogenous gene expression by RNAi has been proposed to depend on intrinsic properties of insects such as species, tissue type and genes (reviewed in Bellés (2010)). As stated, in species such as *T. castaneum*, strong RNAi effects are observed, with the effect even spreading into subsequent generations by germ line transmission (Bucher *et al.* (2002); Liu *et al.* (2004); Lynch and Desplan (2006); Mito *et al.* (2011); Ronco *et al.* (2008)). In contrast, studies using dipteran and lepidopteran species found them to be refractory to systemic RNAi. In some lepidopteran species, even dsRNA delivered by microinjection into insects were not able to provoke RNAi effect (reviewed in Terenius *et al.* (2011)).

Recent studies have focused on the extracellular degradation mechanisms in insects that are able to remove or degrade alien dsRNA before it is able to enter cells. DNA/RNase non-specific activity distinct from that of Dicer has been identified in several lepidopteran species. Arimatsu *et al.* (2007) separated a dsRNase from the digestive juice of the silkworm larvae, *Bombyx mori.* The cDNA they cloned encoded a 51kDa precursor protein containing three domains: a signal peptide, an N-terminal propeptide and a mature Bm-dsRNase which was characterized as a Mg^{2+} dependent alkaline nuclease degrading both DNA and dsRNA, and had conserved catalytic amino acid residues. The identified precursor has an Arg-Ser cleavage site, which generates the 43kDa mature/processed protein by post-translational processing, the mature protein was produced in gut tissue of Day 2 fifth instar larvae, and was coincidently secreted into the gut lumen. Mature proteins were localized in the apical side of midgut cells for extracellular secretion. The identified 43kDa protein is proposed to be responsible for digestion of nucleic acids in the alkaline environment of the midgut of Lepidoptera. Later, Jisheng Liu *et al.* (2012) confirmed that the digestive properties of processed BmdsRNase could interfere with the RNAi response by a reporter assay targeted by transfected homologous dsRNA. Jisheng Liu *et al.* (2012) concluded that BmdsRNase could be involved in the regulation of nucleic acid metabolism in the cytoplasm and the property of degrading dsRNA could be related to an immune response against alien RNA such as RNA viruses. Garbutt *et al.* (2013) demonstrated that the rapid degradation of dsRNA in insect haemolymph could be one of the reasons

for the unsuccessful RNAi. The persistence of dsRNA was compared between tobacco hornworm, *Manduca sexta*, which is an RNAi insensitive insect and German cockroach, *Blattella germanica,* which is known to be highly susceptible to RNAi. They found that the exogenous dsRNA was rapidly degraded in hornworm haemolymph whereas dsRNA persisted much longer in the cockroach haemolymph. Saliva of tarnished plant bug, *Lygus lineolaris,* a Hemipteran species was shown to digest dsRNA by Allen and Walker Iii (2012). The authors proposed that this could be the reason for an inactive RNAi response when dsRNA is delivered by feeding to tarnished plant bug.

The type of insect tissue can be another factor influencing RNAi efficiency. Ciudad *et al.* (2007) observed that the RNAi response was much faster and transient in the fat body than in the ovary of German cockroach. A recent study by Ren *et al.* (2014) investigated the RNAi response in migratory locust, *Locusta migratoria*. The migratory locust is considered to be a susceptible species to RNAi, but its ovary was found to be completely insensitive. They proved that the ovariole sheath was permeable to dsRNA by tracking the labelled dsRNA, but dsRNA was not taken up by follicle cells and oocytes. Salivary glands are generally less sensitive to RNAi than other type of tissues. Boisson *et al.* (2006) demonstrated that the low level expression of *Dicer* and *Argonaute* genes in salivary glands resulted in a high dose of dsRNA being necessary for inducing an RNAi effect in the mosquito *A. gambiae.*

Finally, the type of genes can also affect the RNAi response in insects. Ciudad *et al.* (2007) proposed that genes with efficient feedback mechanisms of regulation might lead to faster rates of transcription of the target mRNA which might counteract the effect of depletion. They observed that lipophorin receptor mRNA levels recovered fast in fat body of German cockroach after RNAi. Moreover, mRNAs with transient expression might make RNAi effects impossible due to a time lag in generating siRNAs. For example, *B. germanica yellow-g* expression gives an acute mRNA peak lasing only a few hours in the ovary, and cannot be knocked down by RNAi procedures, although down-regulation of many other genes in the ovary has been achieved by RNAi (Irles *et al.* 2009).

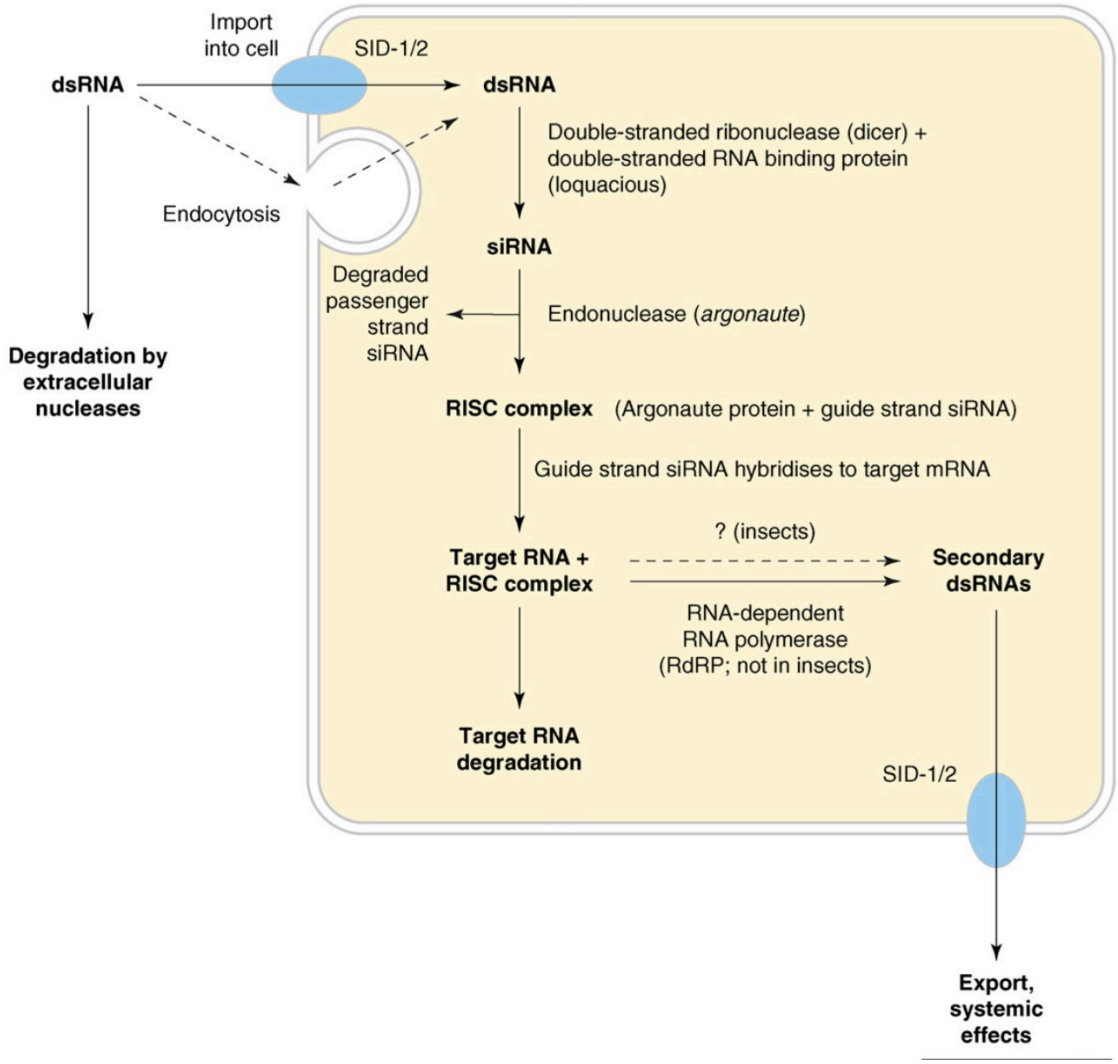

Figure 1-1 **functional stages of RNAi pathway in cells of lower animals.**
Exogenous dsRNA is cleaved by Dicer into small interfering RNA (siRNA) after entering into the cells. SiRNA is then assembled with argonaute protein into RNA-induced silencing complex (RISC). The RISC complex degrades target mRNA based on the guide strand sequence of siRNA. Systemic RNAi are mediated by RNA-dependent RNA polymerase (RdRP) which produce new dsRNAs by useing the target RNA as template primed by siRNA strands. The amplified dsRNA can be exported and spread RNAi effects among cells. SID-1 and SID2 have been identified in *C. elegans* which are responsible for dsRNA transportation, as has the RdRP enzyme. Systemic RNAi effect in insects could be limited by dsRNases in digestive tract and Haemolymph. Source: Gatehouse and Price (2011).

1.3.3 RNAi for insect pest control

In insects, research on RNAi has involved delivery of dsRNAs synthesized *in vitro* into embryos or the haemolymph by microinjection. This method of dsRNA delivery has become a powerful tool for investigating gene function in insect species lacking well-developed genetics. However, in terms of using RNAi-based approaches for crop protection in the field, a robust feeding method in insects that mimics the results obtained in *C. elegans,* where efficient gene suppression and a resulting phenotype can be achieved by orally feeding dsRNA, need to be developed. Two studies published in 2006 performed by Araujo *et al.* (2006) and Turner *et al.* (2006) suggest that RNAi effects can be achieved in insects by oral administration of dsRNA. Araujo *et al.* (2006) produced dsRNA against the gene encoding the anticoagulant heme-binding protein nitrophorin 2 of triatomine bug *Rhodnius prolixus*. The level of anticoagulant activity in salivary glands of nymphs was significantly reduced after feeding dsRNA. Turner *et al.* (2006) demonstrated an RNAi effect after dsRNA feeding in larvae of the light brown apple moth (*Epiphyas postvittana*). Third instar larvae of the light brown apple moth were fed with dsRNA against *carboxyesterases* incorporated into artificial diet. Down-regulation of gene expression was detected as early as two days after feeding, and repression reached a maximum after several days feeding. Gene downregulation was detected not only in the gut, but also in adult antenna after feeding dsRNA to larvae, suggesting that the persistence of the RNAi effect throughout the larval and adult stages, and a systemic transport signal of RNAi from the midgut cells to the eye/antennae disc. These two studies demonstrated that systemic RNAi can be induced by oral administration of dsRNA. Subsequently, RNAi induced in insects by topical application of dsRNA was demonstrated in the mosquito *Aedes aegypti*. Pridgeon *et al.* (2008) demonstrated that expression of *an inhibitor of apoptosis protein 1* gene (AaeIAP1) was significantly reduced and result in mortality by applying dsRNA in diluted acetone to the dorsal thorax of adult females. Another study by Wang *et al.* (2011) investigating RNAi in the Asian corn borer *Ostrinia furnacalis Guenee* demonstrated that RNAi-induced larval development stunting or death was achieved by spraying with an aqueous solution of dsRNA. Evidence showed that eggs soaked in dsRNA solution caused delayed rates of hatching compared to control treatment. Moreover, the fluorescently labelled dsRNA could be found in larval gut, haemocytes and silk fibre after delivery to eggs, indicating that topical application of dsRNA could lead to gene repression in other types of tissue cells via the tracheal system. These observations show a promising future of using RNAi for crop protection, as dsRNA delivery is not limited by oral administration to insect midgut where is not protected by chitin (Gu and Knipple 2013).

In most RNAi studies of insects, dsRNA are produced through *in vitro* transcription synthesis or chemical synthesis. However, this is not practical for field application for pest control due to the high cost. Previous researchers have developed several alternative systems for the production of dsRNA *in vivo* via vector constructs harbouring segments of target gene sequence. These systems involve using bacteria, host plants and host plant viruses to produce dsRNA, and have made significant progress toward using RNAi as tool for crop protection against insect pests.

In the bacterial expression system, dsRNAs against insect genes are prepared by *in vivo* transcription using a plasmid with T7 promoters in inverted orientation flanking the inserted cDNA sequence targetting an insect gene in an engineered *E.coli* strain containing a chromosomal gene encoding T7 polymerase. DsRNA is produced in the induced bacterial cells and both strands of dsRNA are annealed at the same time. The ingestion of bacteria cells expressing dsRNA has been shown to induce gene repression as well as a phenotype in *Spodoptera frugiperda* (Tian *et al.* 2009), *Bactrocera dorsalis Hendel* (Li *et al.* 2011) and *Leptinotarsa decemlineata* (Zhu *et al.* 2011). Although the gene silencing effects in all three studies were caused by feeding, the silenced signals were observed beyond the gut which indicate a systemic spread RNAi effect.

Alternatively, transgenic plants capable of inducing RNAi in insect pests have been produced. The host plants are transformed via *Agrobacterium tumefaciens* with vectors containing inverted repeats of target insect gene sequences. The genes are transcribed to form hairpin RNAs (hpRNAs) in transgenic plants that are functionally equivalent to linear dsRNAs, followed by cleavage of hpRNAs into siRNA by endogenous plant Dicer enzymes. These plants expressing hpRNA deliver sufficient amounts of intact dsRNA for oral uptake by insect pests to show enhanced resistance, and protection against several economically important agricultural pests from different insect orders has been claimed. This approach has been used to cause mortality in the western corn rootworm (WCR) *Diabrotic virgifera* by expressing dsRNA against *V-type ATPase A* gene (Baum *et al.* 2007). The rapid downregulation of endogenous mRNA can be detected as early as 24h after ingestion of dsRNA at low concentration. A systemic silencing of genes was triggered by orally delivered dsRNA. Knockdown of *V-type ATPase A* results in disruption of electrochemical gradients across the insect gut epithelia, affecting the insect's ability to transport nutrients out of the gut, which leads to high mortality as a consequence. To investigate the specificity of RNAi-mediated insecticidal effects, dsRNA directed against *b-tubulin, V-ATPase A and V-ATPase E* of WCR were delivered to other coleopteran pests: Southern corn rootworm (SCR) *Diabrotica undecimpunctata*, Colorado potato beetle (CPB) *Leptinotarsa decemlineata*,

and cotton boll weevil *Anthonomus grandis*. Significant larval mortality in SCR and CPB were achieved with higher concentration of dsRNA than those used in WCR but cotton boll weevil was completely insensitive, emphasizing the species-specificity of RNAi effects, which require a high level of sequence identity between the dsRNA and the target gene. Mao *et al.* (2007) engineered Tobacco and *Arabidopsis* plants to express dsRNA against a *cytochrome P450* gene, *CYP6AE14*, which is highly expressed in the insect midgut. The expression of *CYP6AE14* is related to tolerance to gossypol, a cotton secondary metabolite, via detoxification of this compound. Knockdown of *CYP6AE14* could increase the sensitivity of the insect larvae to gossypol. In larvae feeding on plants expressing the *CYP6AE14 dsRNA*, effective gene silencing of endogenous *CYP6AE14* gene was found, and the insects showed enhanced sensitivity to gossypol. Interestingly, knocking out the Arabidopsis dicer genes *DCL2*, *DCL3* and *DCL4* in transgenic plants producing dsRNA resulted in substantially higher levels of long dsRNA and resulted in more effective repression of the *CYP6AE14* gene, indicating that longer dsRNA shows more efficient RNAi in the insect than siRNA already cleaved and processed by the host plant (Mao *et al.* 2007). Subsequently, several studies using transgenic plants expressing dsRNA were published, using tobacco hornworm *Manduca Sexta (Kumar et al. 2012)* and two phloem sap feeders, the brown plant hopper *Nilaparvata lugens* (Zha *et al.* 2011) and the green peach aphid *Myzus persicae* (Pitino *et al.* 2011). Instead of focusing on silencing gut specific genes, a gene to produce dsRNA directed against aphid salivary gland genes was constructed and expressed in transgenic plants. This also achieved effective gene suppression, suggesting systemic RNAi in aphid (Pitino *et al.* (2011); Kumar *et al.* (2012)).

Finally, in plants, virus-induced gene silencing (VIGS) provides a more simple and efficient alternative to knockdown of endogenous gene expression (Gu and Knipple 2013). Infection of host plants by recombinant viruses containing target sequences triggers the antiviral RNA-silencing pathway with slight viral disease symptoms in the host plants (Bachan and Dinesh-Kumar 2012). Kumar *et al.* (2012) demonstrated a rapid and robust RNAi effect was achieved against an herbivore *Manduca sexta* by this VIGS system. The author Agro-infiltrated *Nicotiana attenuate* with tobacco rattle virus (TRV), a bipartite positive-sense RNA virus, as the silencing vector to target three *cytochrome P450* (*CYP*) genes expressed in insect mid-gut. Transgenic plant mediated RNAi was also developed for comparison. Both stable and transient expression of *CYP* dsRNA resulted in specific and robust RNAi in *M. sexta* larvae. But, the advantage of VIGS system is the speed of this technique taking only 4-5 weeks to complete, whereas transgenic lines are much time-consuming. Therefore, this system is more suitable for high throughput screening of potential targets in insect pests (Bachan and Dinesh-Kumar 2012).

1.4 Targets in Insects for RNAi

1.4.1 Inhibitor of apoptosis

Apoptosis is an evolutionarily conserved pathway of programmed cell suicide triggered by a large number of extracellular and intracellular stimuli including developmental signals, environmental and intracellular stress (Reviewed by Berthelet and Dubrez (2013). Apoptosis is a genetically controlled process, which is significant for normal development and tissue homeostasis (Vaux *et al.* 1994). It is recognized as an important mechanism for removal of supernumerary, undesirable or damaged cells. It also involved in immune responses and antivirus defence (Clarke and Clem 2003). In order to overcome the protection mechanism, viruses have developed strategies to allow replication and spreading. Inhibitor of Apoptosis (IAP) has been identified as a potent inhibitor of apoptosis in insect cells (Crook *et al.* 1993). IAP was originally discovered in insect baculoviruses (*Cydia pomonella granulosis* virus and *Orgyia pseudotsugata* nuclear polyhedrosis virus) (Crook *et al.* 1993), (Birnbaum *et al.* 1994). Subsequent studies revealed that IAPs also existed as endogenous genes in insects (Wang *et al.* 1999), yeast (Walter *et al.* 2006), and human (Ambrosini *et al.* 1997), (Vitte-Mony *et al.* 1997). However, only a subset of IAPs are functionally involved in apoptosis regulation, with many genes encoding proteins with similar sequences having non-apoptosis functions (Marivin *et al.* 2012); (Beug *et al.* 2012). For example, Drosophila IAP2 (DIAP2) has been shown to be involved in Tumour Necrosis Factor (TNF) Receptor (TNFR) superfamily and Nuclear Factor-kappaB (NF-kB) activating signalling pathways (Gyrd-Hansen and Meier 2010); (Wertz and Dixit 2010); (Silke and Brink 2010), regulating cell differentiation (Dupoux *et al.* 2009) cell motility (Dogan *et al.* 2008), and pro-inflammatory and immune responses (Beug *et al.* 2012).

1.4.1.1 Structure of IAPs

The *Drosophila melanogaster* (Dipteran) gene thread (*th*) encodes a protein referred to as DIAP1 (Drosophila Inhibitor of Apoptosis Protein 1) (Figure 1-2). The IAP family is identified by the presence of 1-3 Baculovirus Iap Repeat (BIR) domains at the N-terminal, each of which contains about 70 residues with a consensus Cys/His motif coordinating a single zinc ion ((Birnbaum *et al.* 1994); (Hinds *et al.* 1999). BIRs function as protein interacting modules with specific binding properties (Eckelman *et al.* 2008). The BIR hydrophobic groove can only bind processed, activated caspases. Type II BIRs are functionally involved in anti-apoptotic properties of IAPs whereas Type I BIRs are found to be essential for cell signalling pathways (Lu *et al.* 2007). Another conserved motif present in IAPs is the C-terminal RING zinc-finger that exhibits an E3-

ubiquitin ligase activity. This motif enables IAPs to catalyse the covalent conjugation of ubiquitin to a lysine of target partner proteins, such as NEDD8 (neural precursor cell expressed developmentally downregulated protein 8) (Broemer *et al.* 2010);(Zhuang *et al.* 2013); the conjugation can result in addition of a single ubiquitin molecule (monoubiquination) or polyubiquitin chains. Furthermore, IAPs can mediate their own ubiquitination as well (Silke *et al.* 2005).

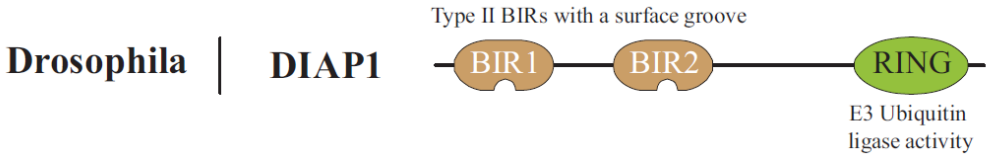

Figure 1-2 **Drosophila IAP1 involved in the regulation of apoptosis.** Type II BIRs highlighted in brown contain a surface hydrophobic groove that binds a tetrapeptide motif called IAP Binding Motifs (IBM) observed in caspase sub-units and IAP antagonists. The RING domain offers IAP with an E3-ubiquitin ligase activity. Source: Berthelet and Dubrez (2013).

1.4.1.2 *Drosophila* IAPs as Caspase Inhibitors

In Drosophila, the apoptotic initiator caspase DRONC (DROsophila Nedde-2-like Caspase) takes part in all forms of apoptosis (Meier *et al.* 2000). It is activated by the Apaf-1 (Apoptotic protease activating factor 1) orthologue DARK (Drosophila Apaf-1 related killer) at the caspase-activating platform apoptosome (Yuan *et al.* 2011). Following a death signal, signalling caspases is activated by proteolytic processing, then these signal caspases proteolytially activate effector caspases which will cleave and degrade targets such as lamins, kinases, DNA repair enzymes and proteins involved in mRNA splicing and DNA replication, and this is presumed to trigger many of the morphological processes of cell death defined as apoptosis (Thornberry and Lazebnik 1998). When the apoptotic signal is absent, the cell death machinery is frozen by several regulatory mechanisms which involve the inhibition of assembly of apoptosome and caspase cascade activation by IAPs (Orme and Meier 2009).

Therefore, inhibition of caspase activity inhibits apoptosis. In *D. melanogaster*, DIAP1, referred as a 'gatekeeper of death' (Orme and Meier 2009), interacts with the caspase DRONC (*Drosophila* Nedd-2-like caspase) through BIR2 and prevents activation of protease either by binding to the pro-region of the protease or blocking the active site of the enzyme. DRONC is capable of self-activation through an oligomerising factor DARK. During apoptosis, DIAP activity is inhibited by the protein products of *reaper*, *hid* and *grim* genes, which induce DIAP ubiquitinylation and subsequent degradation, thus releasing DRONC, leading to apoptosis activation. Loss-of-function mutations in *thread* (gene encoding DIAP1) result in early embryonic death with a caspase-dependent apoptosis (Wang *et al.* 1999); (Lisi *et al.* 2000) and (Chandraratna *et al.* 2007).

There have been several studies on the effectiveness of *inhibitor of apoptosis* genes as a target for RNAi, in dipteran (*Drosophila*, *Aedes aegypti*), and Heteropteran (*Lygus lineolaris*) species. Igaki *et al.* (2002) reported that cell death in *Drosophila* S2 cells was achieved through downregulation of *DIAP1* by introduction of dsRNA. And *DIAP1* downregulation induced cell death was proved to be depended on the loss of DRONC and Dark function. Another study on *Aedes aegypti* showed that topically applied *AaeIAP1* double-stranded RNA products were able to kill female adults. Three different *IAP1* isoforms (*IAP1-B, IAP1-C*, *IAP1-D*) were targetted, and dsRNA was delivered using two carriers, acetone and transIT-siQUEST transfection reagent (Mirus Bio Corporation, Madison, WI), which is proprietary cationic polymer/lipid formulation supplied in ethanol. TransIT-siQUEST has been successfully applied in transfection of cell culture with siRNA (Pridgeon *et al.* 2008). The result showed that IAP1-D dsRNA with siQUEST caused the highest level of *AaeIAP1* mRNA suppression. DNA fragmentation assays were applied for the confirmation of specific RNAi effects. They

also concluded that a specific formulation could be developed as an efficient carrier for introducing dsRNA into insects, allowing dsRNA to be sprayed as a pesticide.

1.4.2 V- type ATPase

The eukaryotic vacuolar-type adenosine triphosphatase (V-ATPase) is a multi-subunit membrane protein complex that functions as a rotary proton-pumping nano-motor by transforming the energy of ATP hydrolysis to electrochemical potential differences of protons across various biological membranes. V-type ATPases and F-ATPases are evolutionary related with similar structural and functional characters (Nishi and Forgac 2002). F-ATPases produce ATP and V-ATPases consume ATP. When the ionic electrochemical potential is greater than the free energy of ATP hydrolysis, ATP is synthesized. In contrast, ATP is hydrolysed to drive the uphill transport of ions when free energy of ATP hydrolysis is greater than the ionic electrochemical potential (Beyenbach and Wieczorek 2006).

1.4.2.1 Structure and mechanism of V-type ATPase

Eukaryotic V-type ATPases are multi-subunit proteins that consist up to 14 different polypeptides have a bipartite structure which assemble as two major ring structures: a soluble cytoplasmic V_1 sector ($A_3B_3CDEFG_2H_{1-2}$,400-600 kDa) that interacts with ATP, ADP and inorganic phosphate and a membrane-integrated V_0 sector ($ac_4c'c''de$, 150-350kDa) that mediates the transport of H^+. V_1 and V_0 are connected to assemble V_1V_0 holocomplex. As shown in Figure 1-3 A, the subunits of V_1 and V_0 are distinguished by large and small letters. The V_1 complex consists of: (1) a globular structure contains three alternating copies of A and B subunits to form a ring. Subunit A and B mediate the hydrolysis of ATP at three reaction sties. (2) a central stalk contain single copies of subunit D and F and (3) a peripheral stalk composed of subunit C, E, G and H. Both the central rational stalk and peripheral stalk connected V_1 complex with central hydrophobic c ring structure (c,c',c'') consist of six or more c subunits of proton transporting V_0 complex. V_1 complex is hold in place by fixed peripheral stalk and subunits B and C which are capable of binding to actin to stabilize the structure (Vitavska *et al.* 2005). It is recognized that V-type ATPase contains a stationary and a mobile parts, named as stator and rotor (Figure 1-3 B). Subunits D, F and c-ring belong to rotor and rest of subunits are considered as stator. Reviewed by Beyenbach and Wieczorek (2006).

During the process of ATP-driven proton pumping, conformational changes of subunits A and B of V_1 are caused by ATP hydrolysis that drives the rotation of c-ring. There is a H^+ binding site on each c subunit of the c-ring and inner half channel of subunit and the middle of the lipid bilayer enable cytoplasmic H^+ to bind to glutamate residues on the c-

ring. After 360° clockwise rotation of the c-ring when viewed from the cytoplasm (Meier *et al.* 2005), H^+ is released and exited the membrane though middle of the lipid bilayer and other side of the membrane (Junge *et al.* (1997); Junge and Nelson (2005)). As a consequence, an electrochemical proton gradient of proton motive force (*pmf*) is generated across the membrane, which will lead to acidification of intracellular compartments (Marshansky *et al.* 2014). V-ATPase dependent acidic luminal pH is necessary for all intracellular compartments of eukaryotic cells (Marshansky and Futai 2008). Moreover, V-ATPase is essential for vesicular trafficking along both the exocytotic and endocytotic pathways of eukaryotic cells (Marshansky and Futai 2008).

1.4.2.2 Regulation of the V-type ATPase

A unique fundamental character of V-type ATPase is the reversible assembly/ disassembly of the V_1 and V_0 complexes. It was first identified during the process of molting of *M.sexta*, revealing the relationship of transepithelial transport of V-type ATPase and insect growth (Sumner *et al.* (1995); Beyenbach and Wieczorek (2006)). In *M. sexta*, secreting K^+ into the lumen of the midgut drives growth through inducing feeding activity. High activity of V-ATPase at the apical membrane proved by large transepithelial, lumen-positive voltages across the midgut, offers the electrical force for K^+ secretion through $2H^+/k^+$ antiport, In response to ceased feeding or starvation in *M.sexta*, transepithelial voltage drops to zero, and the hydrolysis of V-type ATPase as well as ATP-dependent proton transport decreased to less than 15%, suggesting the inactivation of the V-type ATPase (Beyenbach and Wieczorek 2006). Later, separation of V_1 and V_0 complexes was observed by gel electrophoresis and immunoblot (Sumner *et al.* 1995).The dissociation of holoenzyme was identified in yeast *Saccharomyces cerevisiae* (*S. cerevisiae*) as well (Kane (1995); Kane (2000); Kane (2012)). 70% dissociation of holoenzyme is observed after glucose deprivation for as short as 5 min, and reassembly of V_1 and V_0 complexes is recovered after addition of glucose. Interestingly, new protein synthesis is not required for dissociation or reassociation of holoenzyme of V-type ATPase. And V-type ATPase V_1 and V_0 complexes association/dissociation is now considered as a universal regulatory mechanism of V-type ATPases.

1.4.2.3 V-type ATPase knockouts

Due to the function involvement in fundamental cellular mechanism, intact v-type ATPase are required for the normal function of the Golgi complex, endoplasmic reticulum, vacuoles and endocytotic and exocytotic vesicles in almost every eukaryotic cell (Beyenbach and Wieczorek 2006). Disruption of genes encoding the V_1 subunit B or the V_0 subunit c in yeast lead to failure to survive at physiological pH (Nelson and

Nelson 1990). Subsequently, inactivation of subunit B in *Drosophila* and subunit c in mice were proved to cause lethal phenotypes (Davies *et al.* (1996); Inoue *et al.* (1999)). Different subunit isoforms are normally observed at different locations, when a V-type ATPase subunit is encoded by more than one gene (Beyenbach and Wieczorek 2006). In multicellular higher eukaryotes, several subunit isoforms were found to be expressed in various cell types and located in specific tissues. For example, several subunit isoforms in mammals have been identified in the kidney (Chung *et al.* 2008), inner ear (Dou *et al.* 2003) and brain (Murata *et al.* 2002). Disruption of tissue-specific isoforms may not lead to lethal phenotype, but could cause inherited disorders. As mentioned above, ingestion of dsRNA against V-type ATPase A subunit lead to mortality in western corn rootworm, which suggest that knockdown of midgut V-type ATPase A subunit affects the electrochemical gradient across the gut epithelia and results in the subsequent lethal phenotype (Baum *et al.* 2007). A similar effect was also observed in *Leptinotarsa decemlineata*. *V-type ATPase E subunit* mRNA was expressed consistently at high level in ileum and rectum, moderately in Malpighian tubules, midgut and foregut, and less expressed in fat body, ventral ganglion, epidermis and haemolymph of fourth instar larvae (Fu *et al.* 2014). Larval growth and survival were significantly affected after continuously ingested dsRNA against *V-type ATPase E subunit* (Fu *et al.* 2014).

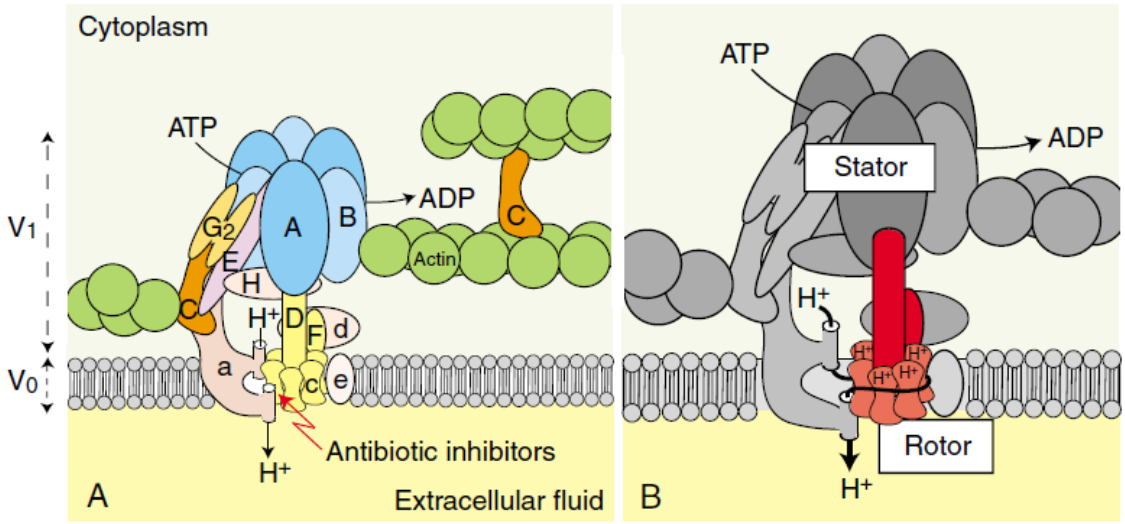

Figure 1-3 **V-type ATPase in eukaryotic cell membrane.**

(A) Molecular model. Eight different subunits labelled with capital letters A-H are identified in V1 complex. Subunit G presents as the dimer G2. Four different subunits shown as small letters (a,c,d,e) are found in integral membrane V0 complex. H+-binding rotor ring (c-ring) composed of c subunit and its isoforms c' and c''. Subunit B and C has acting binding site.

(B) Mechanistic model. V1 and V0 complexes are connected by central stalk (subunit D, F) and a peripheral stationary stalk (subunit C,E,G,H,a). Rotor sector consists of central stalk of V1 complex and c-ring of V0 complex (highlighted in red), and rest of the subunits are considered as stator (highlighted in grey). Hydrolysis of ATP releases energy and drive the rotation of central stalk and c-ring. H+ is transported from the inner half channel to the outer half channel with the aid of H+ binding step to on c subunit. Inhibitors of V-type ATPase like pleomacrolides bafilomycin, concanomycin, and macrolactone archazolid bind to the c subunit in V0 complex (Beyenbach and Wieczorek 2006).

1.5 Using GNA as a molecular carrier

Lectins are sugar-binding proteins, which comprise a group of proteins that are found in all plants, and many other organisms, including bacteria. In plants, they are considered as nitrogen-storage proteins and involved in plant defence against biotic stresses. They also present deleterious effects against several invertebrates (Peumans and Van Damme 1995). The mannose-specific lectin from snowdrop (*Galanthus nivalis* agglutinin: GNA) (Figure 1-4) is a 50kDa tetrameric protein composed of 12.5kDa subunits, which agglutinates rabbit erythrocytes (Van Damme *et al.* 1987). The gene and mRNA code for a 157 amino acid polypeptide, with 23 residues forming an N-terminal signal sequence and 29 residues composing C-terminal extension. Mature GNA is formed when C-terminal peptide is cleaved during post-translational processing. Mature GNA is highly resistant to proteolytic activity in the insect gut and binds specifically to terminal mannose residue of insect gut epithelial glycoproteins. Binding to the gut surface results in effective transport by endocytosis, which allows the protein to cross the midgut epithelium of insects. After feeding, the transported GNA was observed in haemolymph, fat bodies and ovarioles in brown plant hopper *Nilaparvata lugens* (Hemipteran) (Powell *et al.* 1998). The ability of GNA transport to the haemolymph after oral administration to insects has also demonstrated in other orders such as Coleopteran, Neuropteran and Lepidoptera (Hogervorst *et al.* 2006); (Fitches *et al.* 2001). However, the mechanism behind this phenomenon is still not fully characterised.

The ability of GNA to transport across insect midgut barrier after orally ingestion by insects opened the potential possibility of delivering toxic molecules to the effective site in insect by fusing them to GNA. Fitches *et al.* (2004) developed a fusion protein which contained SFI1, a spider toxin from *Segestria florentina* to GNA. Injection of SFI1 into *Heliothis virescens* (Lepidoptera) induces paralysis (Lipkin *et al.* 2002) whereas orally feeding to larvae failed to induce toxic activity. 100% mortality was observed in *Nilaparvata lugens* after feeding artificial diet containing the fusion protein SFI1/GNA after 7 days and 49% survival was recored in *Myzus persicae* after 14 days (Down *et al.* 2006). Other insecticidal peptides were also fused with GNA and tested against several insect species; the fusion proteins showed effective toxicity in rice brown planthopper *Nilaparvata lugens* (Trung *et al.* 2006), *T. castaneum* (Fitches *et al.* 2010). More recently, insect calcium channel blocker ω-ACTX-Hv1a was selected to fuse with GNA. Fitches *et al.* (2012) demonstrated that GNA was delivering ω-ACTX-Hv1a to its target sites in the central nervous systems (CNS) of *M.sexta*.

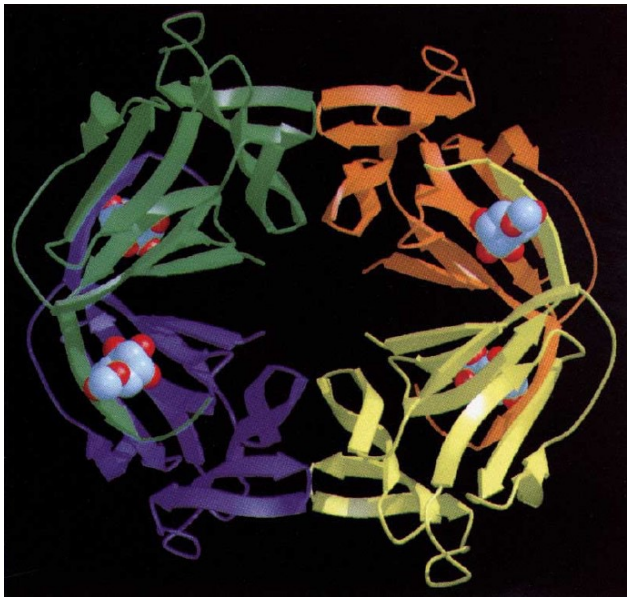

Figure 1-4 **GNA tetramer Structure**. Each subunit is distinguished in colour (green, orange, yellow and purple). High affinity carbohydrate binding sites in each subunit contains a bound sugar molecule. Source: Hester *et al.* (1995)

1.6 Aims and objectives

The present project explores the RNAi responses in insects of three orders, including *T. castaneum* (Coleopteran), *M. domestica and D. radicum* (Dipteran) and *A. pisum* (Hemipteran). Potential effectors for various RNAi responses in insects were investigated. In order to apply RNAi as a potential method for crop protection, recombinant proteins containing a dsRNA binding domain, RBD3, derived from the *Drosophila* staufen protein were produced and evaluated for their ability to protect dsRNA against degradation. A fusion protein containing RBD3 and *Galanthus nivalis* agglutinin was designed to both protect dsRNA and transport it across the insect gut after feeding. This fusion protein was produced and evaluated for controlling insect pests.

The objectives are:

1. To produce dsRNAs against *V-type ATPase E subunit* and *APIN* gene of 3 insects species for the evaluation of RNAi responses by injection and feeding (Results are shown in chapter 3).

2. To investigate the stability and persistence of introduced dsRNAs affecting RNAi responses in insect haemolymph and gut tissues (Results are shown in chapter 5).

3. To express Trx/RBD and Trx/RBD/GNA proteins in *E. coli* and *P. pastoris* system for testing dsRNA binding abilities (Results are shown in chapter 4).

4. To improve the dsRNA stability in insects tissues by conjugation with Trx/RBD Trx/RBD/GNA and RBD and RBD/GNA proteins (Results are shown in chapter 5).

5. To evaluate the RNAi reponse of dsRNA-Trx/RBD conjugates in insects (Results are shown in chapter 5).

Chapter 2 Methods and materials

2.1 Insects cultures

Acyrthosiphon pisum (*A. pisum*) were maintained on broad bean plants (*Vicia faba*) at 25°C, under a lighting regime of 16h: 8h (L: D). Before the bioassays, adults were collected and transferred from plants to chambers containing artificial diet described by (Febvay *et al.* 1988). The liquid diets (50μl) was sealed between two layers of parafilm in a feeding chamber described by (Down *et al.* 1996). Neonate nymphs were collected with paint brush after 24 hours for feeding assays, and 5 days old aphids were used for injection assays with dsRNA.

Tribolium castaneum (*T. castaneum*) larvae and adults were reared continuously in whole flour containing 5% brewer's yeast at 25°C, under a lighting regime of 16h:8h (L:D) with 75% relative humidity. For the feeding assays, flour was passed through a sieve with aperture size 300μm (Glenammer Engineering) in order to separate the larvae and eggs. Newly hatched larvae less than 1 week old were used for feeding assay whereas pre-pupa stage larvae were used for injection assays.

Musca domestica (*M. domestica*) eggs were kindly supplied from FERA and larvae were fed on an organic bran based diet (0.2g/g bran; 0.1g/g grassmeal w/w; 0.05g/g dried brewers yeast; 0.015g/g malt extract [Stortex 70D] and 0.015g/g skimmed dried milk powder; 0.62ml/g water). *Delia radicum* (*D. radicum*) cultures were kept according to (Finch and Coaker 1969). The larvae were fed on organic swede covered by sand, whereas adults were maintained in a bug dorm (Megaview Science Education Services Co., Ltd) supplied with cotton wool swabs soaked with solutions of sugar (10% [w/v]), yeast extract (1.25% [w/v]) and dried milk powder. Both *M. domestica* and *D. radicum* were kept in same environment as *T. castaneum*.

2.2 RNA extraction and complementary DNA (cDNA) synthesis

Total RNA was purified from whole insect bodies at different stages by using Quick-RNA™ Miniprep from ZYMO Research according to the manufacturer's protocol. Insects were placed in 1.5ml microcentrifuge tubes and submerged in liquid nitrogen to 'snap freeze' the samples. Insect tissue homogenisation was performed by grinding the tissue by using RNase-free pellet pestle (Anachem) in lysis buffer provided by kit. DNA contamination was removed by using on column digestion provided by RNA extraction kit. RNA was quantified by using Nano-drop spectrophotometer (Model ND-1000, Thermo Scientific). cDNA synthesis was performed from 1μg total RNA by using a mixture of oligo-d(T) and random hexamer primers from SensiFAST™, and the components of a cDNA synthesis kit (Bioline) as described in the protocol supplied.

2.3 Isolation of target gene sequence from *M. domestica* and *D. radicum*

For isolating the *APIN* gene in *M. domestica* and *D. radicum*, degenerate primers (Table 2) were designed based on the conserved amino acid sequence alignment among several dipteran species, including *Drosophila melanogaster*, *Anopheles gambiae*, *Aedes aegyptica* and *Culex pipiens*. The same primer pair was used for both *M. domestica* and *D. radicum*. PCR conditions were: 94 °C for 5 minutes (1 cycle), 94 °C for 30 seconds, 58 °C for 30 seconds, 72 °C for 30 seconds (30 cycles) and 72 °C for 7 minutes (1 cycle). The primer pair gives a predicted PCR product of 470bp followed by extraction (QIAquick Gel Extraction kit, QIAGEN) from agarose gel and cloned into pJET1.2 (CloneJET PCR Cloning kit, Thermo Scientific Life Science Research) as described in the manufacturer's protocol. The identity of the resulting DNA fragments was confirmed by DNA sequencing based on Sanger sequencing method. Based on the partial coding sequences obtained, the following gene specific primers used for amplification of RNAi region were designed (错误! 未找到引用源。).

2.4 RACE for obtaining full-length genes from *M. domestica* and *D. radicum*

For obtain the full-length *APIN* gene from *M. domestica* and *D. radicum*. 3' and 5' primer RACE of *M. domestica* and *D. radicum APIN* gene was prepared and sequenced. First-strand cDNA synthesis was prepared from incubating 1μg total RNA with 1μl 12μM 3-CDS primer A (Listed in Table 1) at 70°C for 2 minutes, the volume was adjusted to 5μl with PCR-grade water. The reaction was then transferred to ice for 2 minutes. 10μl reaction was carried out according to the manufacturer's protocol from TAKARA Primer Script. RACE PCR reaction was prepared according to Advantage 2 polymerase Mix from Clontech. RACE cDNA was amplified by 10X Universal Primer Mix and gene-specific primer listed in Table 1. The conditions are: 94 °C 30 seconds repeated 5 cycles; 94 °C 30 seconds, 70 °C 30 seconds, 72 °C 3 minutes, repeated 5 cycles followed by 94 °C 30 seconds, 68 °C 30 seconds 72 °C 3 minutes repeated 30 cycles. PCR product was eluted from agarose gel by using QIAquick gel extraction kit metioned above and ligated with pJET1.2 vector for sequencing. Sequences are assembled by Sequencher 5.0.

2.5 Cloning of gene templates for Double-stranded RNA (dsRNA)

V-type ATPase E subunit and *thread* transcripts from insects were amplified from 200ng cDNA template using synthetic oligonucleotides from IDT (Integrated DNA Technologies http://www.idtdna.com/CodonOpt). All the primers for cloning including

restriction enzyme sites (*XhoI* and *XbaI*) (Fermentas) are listed in Table 2. A sequence from a kanamycin-resistance gene (*nptII*) from the plasmid PSC-A-amp/Kan vector (Ahgilent Technologies) was amplified as a negative control. PCR amplification was performed by using Phusion High-Fidelity DNA polymerase (Thermo Scientific) with conditions as follows: 98 °C for 30s, followed by 15 cycles of 10s 98°C, 30s at 58°C and 30s at 72°C, final extension step was 72°C for 10min. The amplified PCR product of 277bp or 254bp were separated by 1% DNA agarose gel and eluted from gel by using QIAquick column (Qiagen). Eluted PCR products were ligated with pJET1.2 vector (CloneJET PCR cloning kit, Thermo Scientific Life Science Research) following the manufacturer's protocol. The ligation was then transformed into one shot *E. coli* TOP10 competent cells (Invitrogen) and plated on selective Carbenicillin (50µg/ml) LB media. Colonies were screened by colony PCR with standard Taq polymerase using pJET1.2 forward and reverse sequencing primers provided by the kit. The conditions were 94°C For 10 mins, followed by 25 cycles of denaturation at 94°C for 30s, annealing at 60°C for 30s, and extension at 70°C for 1 min, with a final extension at 72°C for 7 mins. Selected colonies giving a PCR product of the predicted size (400 bp) were picked off. Recombinant plasmids containing confirmed DNA sequences were minipreped by using Wizard plus SV Minipreps (Promega) followed by double digestion with *Xho I* and *Xba I* restriction enzymes. The digested products were ligated to RNAi vector L4440 that had been digested with same two enzymes. The ligation mixture was then transformed into *E. coli* TOP10 and HT115 (DE3) competent cells. Positive colonies were screened by colony PCR described above using T7 promoter and terminator primers. The selective recombinant clone was verified by DNA sequencing again.

2.6 *In vitro* transcription

Recombinant plasmids containing confirmed DNA sequence were extracted from cells and linearized with either *XhoI* or *XbaI* restriction enzymes for production of sense and antisense strands of the dsRNA. Both digestion reactions were performed in 1X tango buffer overnight at 37°C. Linear plasmids were precipitated with 3M NaOAc (Sodium acetate, 1/10 reaction volume) and three volumes of absolute ethanol in -20°C overnight. The pellets were then collected by centrifuge and resuspended in nucleases free water. Sense and antisense RNA were prepared by *in vitro* T7 RNA polymerase transcription separately (Megascript T7 transcription kit, Ambion). 1µg linearised DNA templated were used for sense and antisense reactions in a total volume of 20µl, following the manufacturer's protocol. The reactions were incubated at 37 °C for 6 hours. Remaining DNA templates in the reactions were removed by DNase digestion (Enzyme provided by transcription kit). Single-strand RNAs produced were then

purified by phenol chloroform extraction and precipitated with 3M NaOAc described above. The pellets were collected by centrifuge and then washed with 70% ethanol. Finally, the pellets were air-dried and resuspended in nuclease free water.

Single stranded RNAs were quantified by using Nano-drop spectrophotometer (Model ND-1000, Thermo Scientific) and equal amount of sense and antisense RNAs were mixed together. The mixture was then annealed by heating at 85°C for 5 mins and then slowly cooled down to room temperature. Resulting dsRNAs was analysed by agarose gel electrophoresis to confirm the size and quality. The yield of ssRNA from 1µg of DNA template was routinely around 100µg.

2.7 Quantitative real-time PCR (qRT-PCR)

Total RNA was isolated from 3-5 individual insects after injection or feeding using Quick-RNA^{TM} Miniprep from (ZYMO Research). DNA contamination was digested with DNase provided by the kit. The quality of isolated RNA was validated by Nano-drop. cDNA synthesis was performed from 1µg total RNA by using a mixture of poly-T oligo d(T) and random hexamer primers from SensiFAST^{TM} cDNA synthesis kit (Bioline) described in the protocol supplied. Quantitative real-time PCR was performed on 96 wells ABI Step one Plus real-time PCR instrument by using GoTaq® qPCR Master Mix (Promega). CXR was used as reference dye in each reaction. GAPDH was used as the endogenous control for normalisation of target gene expression and triplicates were performed for each sample. qPCR primers listed in

were designed using ABI primer express software for real-time PCR.

2.8 Biotin-labelled RNA

RNA biotinylation was performed by using PierceTM RNA 3' End Biotinylation kit from Thermo scientific. ssRNAs generated from *in vitro* transcription were first heated at 85°C for 5 minutes and placed on ice immediately. 10pmol ssRNAs was used in 30µl biotin ligation reaction prepared according to the manufacturer's protocol. The reactions were incubated at 16°C for 2 hours followed by adding 70µl of nuclease-free water. Same volume of chloroform: isomyl alcohol was mixed to extract the RNA ligase by centrifuge 3 minutes at 12,000xg in a microcentrifuge to separate the phases. Top the aqueous phase was collected and concentrated by ethanol precipitation. The biotin-ssRNAs were finally stored in 20µl nuclease-free water. Biotin-dsRNAs were prepared by heating a mixture of biotin-sense and biotin-antisense RNA at 85°C and cool down to room temperature slowly. 50pmol dsRNA which prepared from *in vivo* transcription also used to perform labelling reaction.

Labelling efficiency was determined by dot blotting using Thermo Scientific Chemiluminescent Nucleic Acid Detection Module. Briefly, 2500-fold diluted biotin-

ssRNAs, biotin-dsRNAs as well as control biotinylated IRE RNAs were dotted on positively charged nylon membrane which was equilibrated with TE buffer. Excess buffer was absorbed by dry paper towel followed by crosslinking the membrane for 60 seconds at 120mJ/cm^2 by UV-light crosslinking instrument. The immobilized nucleic acids were first blocked on positively charged nylon membrane by incubated with blocking buffer provided by detection kit. Then the biotinylated RNAs were conjugated with stabilized streptavidin-horseradish peroxidase. The membrane was incubated in a mixture of luminol enhancer solution and stable peroxide solution for 5 minutes after washing. Membrane was then placed in a film cassette and exposed to X-ray film for 2-5 minutes to obtain the desired signal.

Biotinylated dsRNA was also checked on 6% polyacrylamide gel in 0.5XTBE (45mM Tris, 45mM boric acid, 1mM EDTA, pH8.3) under 100V for 8X8X0.1cm gel for 4hours at 4°C. After electrophoresis completed, gel and nylon membrane were sandwiched in a clean electrophoretic transfer unit. Transfer was performed at 400mM (35V) for 30 minutes at 4 °C. The membrane was crosslinked and detected according to the method mentioned above.

2.9 RNA Electrophoretic Mobility Shift Assays (RMSA) to detect protein-RNA interactions

RNA mobility shift assays were applied using LightShift Chemiluminescent RNA EMSA kit from Thermo scientific. The binding reactions which contain binding buffer (10mM HEPES, pH 7.3, 10mM KCL, 1mM $MgCl_2$ and 1mMDTT), glycerol and tRNA were performed using same amount of biotinylated dsRNA (10ng) with different protein samples or various amounts (ng-µg) of a particular protein sample. Control binding reactions which used control biotinylated IRE-RNA (28bp) and liver extract provided by the kit was performed as a positive control. The binding reactions were incubated at room temperature for 30 minutes and mixed with 5Xlodaing buffer provided by the kit. The reactions were electrophoresed, transferred and detected according to the steps described before.

2.10 FITC labelled dsRNA

Instead of using linearized DNA template, purified PCR products containing T7 promoter sequences on each strand was used as template for *in vitro* transcription. Primers used for PCR amplification are shown in Table 2. PCR products amplified using gene specific sequences with T7 promoter sequences on both strands was checked and extracted from agarose gel followed by ethanol precipitation. *In vitro* transcription reaction was performed on a 20µl scale with 1µg purified PCR template

according to the manufacturers' protocol; 0.08mM 5'-deoxy-5'-hydrazinylguanosine initiator 1 (from a 50 mM stock in 50 mM NaOH) was added in the reaction. The reagents were mixed and collected in the bottom of the tube by brief centrifugation. The reaction was incubated at 37°C for 4 hours followed by DNase treatment. To remove any precipitated inorganic pyrophosphate, the mixture was centrifuged at 1500g for 30 seconds. The reaction was then precipitated by adding 30μl 7.5M lithium chloride and 30μl water and kept at -20°C overnight. After centrifugation, the pellet was washed with 75% ethanol and dissolved in 20μl nuclease-free water. The quality of dsRNA was checked on agarose gel and the concentration value was measured by nanodrop before continuing to the next step.

The pH of the dsRNA solution was increased by adding 3.75μl 1M sodium carbonate (pH 10.7). Ninety-seven nanogram fluorescein isothiocyanate (FITC, isomer I, Sigma) was weighed and resuspended in 25μl DMF to make 0.1M stock solution. The dsRNA extract was mixed with 1μl prepared FITC and covered by foil. The reaction was allowed to proceed overnight at 4°C on end over end rotator. The reaction was quenched by addition of 7.5μl 1M sodium acetate and then precipitated with 5μl 7.5M lithium chloride and 90μl 100% ethanol in -20°C overnight. The mixture was then centrifuged into pellet, followed by washing with 75% ethanol. The FITC-dsRNA pellet was resuspended in water and purified by Zeba^{TM} spin desalting column, 7K MWCO (Thermo scientific) according to the manufacturer's protocol. Finally, the FITC-dsRNA was stored in 70μl nuclease-free water and kept in dark at -20 °C. FITC-dsRNA was checked on 6% TBE polyacrylamide gel and visualized on Typhoon phosphorimager. Once the electrophoresis was completed, the polyacrylamide gel was fixed in 10% methanol and 7% acetic acid for 15 minutes. The signal was detected at wavelength 520nm laser with cy2 blue module.

2.11 FITC-dsRNA Electrophoresis Mobility shift assays

The binding reactions were prepared in 20μl reaction which contains 1Xbinding buffer (50mM Tris-HCL (pH 8), 5mM EDTA, 1mM DTT, 100ug/ml BSA and 5% glycerol). For visualizing FITC-dsRNA mobility shift based on the signal of FITC dye, 5ng FITC-dsRNA was incubated with much excess of Trx/RBD3 protein extract (1-8μg in 1XPBS), and allowed to react for 30 minutes at room temperature before loaded onto 6%TBE polyacrylamide gel. Binding reactions containing 100ng FITC-dsRNA and Trx/RBD3 protein extract (1-8μg in 1XPBS) loaded on 6% polyacrylamide gel was also stained with ethidium bromide at final concentration of 0.5mg/ml in 200ml 0.5XTBE buffer for visualization.

2.12 RNAi experiment with *T. castaneum*

2.12.1 Injection of dsRNA into *T. castaneum* larvae

Larvae were gassed with CO_2 for at least 1min and were then aligned on a sticky tape. In terms of the injection bioassays, glass capillaries (3.5'' Drummond # 3-000-203-G/X) were prepared with a needle puller (PC-10 puller, Narishige Group), programmed as: weight heavy 100g, temperature 58°C. Tips of the needles were broken off with a forceps to create a sharp end. The needles were filled with mineral oil without any bubbles and assembled into a Nanoject II™ injector (Drummond Scientific Company). dsRNAs were loaded onto the needles through the end and injected as summarised in Table 2. dsRNA was injected into dorsal side of the segment of each larva. After injection, larvae were carefully removed from the tape by using forceps and raised in whole wheat flour (with 5% yeast) at the condition described above. For analysing *TcVTE* and *TcAPIN* gene expression pattern in developmental stages, larvae were collected every 5 days started from 5 days old larvae to adults. 50ng *TcAPIN* dsRNA and *TcVTE* dsRNA were injected into pre-pupa stage larvae. Injected larvae were collected at 48h and 10days post injection for investigating the duration of RNAi effect. Mortality data of dsRNA injected larvae was also performed, 100ng *TcAPIN* dsRNA and *TcVTE* dsRNA were injected. The survival data was recorded for 13 days. Less dose 10ng *TcAPIN* dsRNA were also injected and larvae were collected after 24h and 48h. The amount of 150ng and 300ng dsRNA against *V-type ATPase E* subunit from beetle *T. confusum* were also injected into *T. castaneum* pre-pupa stage larvae to validate the cross species RNAi effect. Samples were collected at 48h and 10days post injection followed by q-PCR analysis. To investigate the efficiency of RNAi response in *T. castaneum,* 10ng *TcAPIN* dsRNA was injected into pre-pupa stage larvae and injected samples were collected at 2h, 5h, 48h and 10 days post injection, followed by q-PCR. Insect injection bioassays are summarised in Table 4.

2.12.2 Feeding dsRNA to *T.castaneum* larvae

For *T. castaneum* feeding assays, *TcAPIN* dsRNA and *TcVTE* dsRNA were delivered by flour discs prepared as described by Xie *et al.* (1996). 12.5μg and 25μg dsRNAs (*Kan, TcAPIN* and *TcVTE*) in 200μl volume of nuclease-free water were mixed to 50mg of sieved whole wheat flour (with 5% yeast). Ten microlitre of the mixture was added to each well of 96-well microtiter plate with a flat bottom. The mixture was then allowed to dry in a Laminar flow hood for 8h. The final concentration of dsRNAs were 250ng/mg and 500ng/mg. Less than 1 week old *T. castaneum* larva was added to each well. The feeding assay was carried out for 30 days. Fed larvae were collected for qPCR analysis after 5 days post feeding. Insect feeding bioassays are summarised in Table 5.

2.12.3 Stability of dsRNA in *T. castaneum* diet

Stability of dsRNA in *T. castaneum* diet was evaluated with the presence of larvae. The flour disc was prepared as described above with the *TcAPIN* dsRNA concentration of 250ng/mg. Five 1week old larvae were added to each wells. Larvae were removed after different time points (1h, 3h, 20h, 48h, 72h and 120h) from each wells post feeding. The flour diet were then resuspend in 10μl Nucleases-free water followed by vortex briefly and centrifuge for 10min at room temperature. 2μl of clear supernatant were loaded from 6 samples on 1% agarose gel.

2.13 RNAi experiments with *M. domestica* and *D. radicum*

2.13.1 Injection of *MdAPIN* and *DrAPIN* dsRNA into *M. domestica* and *D. radicum* larvae and *M. domestica* adult.

For injecting *M. domestica* and *D. radicum* larvae, pre-pupa stage larvae were gassed with CO_2 for 20s prior to injection. Larvae surface were dried on tissue and then placed on sticky tape adhered to the back of pertri dish. The larvae were positioned ventral side down and were injected on their dorsal side using a glass needle and a Drummond injector. Initial assays were based on observations of subsequent mortality of insects, over a period up to 7 days, comparing insects injected with *APIN* dsRNA with insects injected with *Kan*dsRNA. Subsequent assays investigated a range of RNAi-induced effects, depending on the developmental stage of the insects assayed. *APIN* gene downregulation in *M. domestica* and *D. radicum were* subsequently investigated by qPCR. Doses at 150ng and 500ng APIN dsRNA were injected to pre-pupa stage (3rd instar) larvae. Injected larvae were frozen at 24h and 48h post injection.

For investigating whether the RNAi effect could be effective on closely related Dipteran species, 150ng and 500ng *DrAPIN* dsRNA were cross-injected into 3rd *M. domestica* larvae. Initial injection bioassays were recorded for 5 days period for phenotype observation. Subsequent experiment of injected larvae with same doses were collected after 48h and 72h post injection. Collected samples were used for investigating changes of APIN mRNA by quantitative Real time-PCR (qRT-PCR) described above.

The RNAi experiment was also investigated in *M. domestica* adult. Newly emerged *M. domestica* adults were gassed with CO_2 for 1min prior to injection. 150ng and 500ng *MdAPIN* dsRNA were injected into fly haemolymph through thorax using a 10μl syringe (Hamilton, 701N). After injection, flies were supplied with 20% sucrose solution. Injected samples were collected at 48h and 72h for detecting RNAi induced effect in gene expression by qPCR.

2.13.2 Feeding dsRNA to *M. domestica* larvae

Two different feeding methods were developed for administering dsRNA to *M. domestica* larvae through feeding. Three days old *M. domestica* larvae were used for feeding assays. Initially, *MdAPIN* dsRNA were simply mixed with bran based diet at final concentration of 100ng/mg (dry weight). This was based on the does necessary to show RNAi response by injection. Briefly, this was done by adding 100μg dsRNA in a volume of 5ml nuclease-free water to 1,000mg dry diet. Ten larvae were placed in each pot and 20 larvae in total were assayed for each treatment. The survival data was recorded for 7 days after oral feeding dsRNA mixed in artificial diet.

A subsequent feeding experiment was performed by adding induced bacteria that expressing dsRNA in diet. The yield of 50ml induced HT115 *E. coli* cells is approx.100μg. After collecting induced cell pellet by centrifugation. Pellet was washed twice with 1XPBS. Pellet from 100ml cell culture was resuspended in 5ml volume of nucleases-free water and mixed with 1,000mg diet. The final concentration was 200ng/mg. Ten larvae were placed in each pot and 20 larvae in total were assayed for each treatment. The survival data was recorded for 7 days after oral feeding dsRNA mixed in artificial diet.

2.14 RNAi experiments with *A. pisum*

2.14.1 Injection of dsRNA into *A. pisum*

For the RNAi experiments in *A. pisum*, both microinjection as well as feeding were used to administer the dsRNA to aphids of different stages. 5 days old aphids were prepared by rearing aphid's mothers on artificial diet (Based on the protocol described by Douglas and Prosser (1992) for 24h, neonates were removed next day and fed on artificial diet.

ApVTE dsRNA, *ApAPIN* dsRNA and control *Kan* dsRNA were delivered to five days old aphid nymphs through microinjection under the dissecting microscope (SX-45, Vision). Aphids were first chilled on ice for 15 minutes prior to injection. 30ng, 15ng and 7.5ng dsRNA were injected into abdomen on the ventral side of each aphid and then aphids were supplied with artificial diet in the close chamber. Aphid samples were collected at 24h, 48h and 72h post injection for detecting the target gene expression change.

2.14.2 Feeding dsRNA in *A. pisum*

ApVTE dsRNA and *Kan* dsRNA were administered to neonate aphid nymphs through feeding assay. dsRNAs were mixed to aphid artificial diet at a final concentration of 7.5ng/μl and 100ng/μl between two layers of Parafilm sachet, nymphal survival and

development were followed. After initial feeding for 2 days, diet without dsRNA was replaced in order to avoid contamination. The size of fed aphids were recorded after 7 days. Details are described in Table 5.

2.14.3 The stability of dsRNA in *A. pisum* liquid diet

For investigating the stability of dsRNA in aphid diet, 2μg FITC-labelled *ApVTE* dsRNA was mixed in 50μl artificial diet. 10 newly born nymphs were placed in dsRNA treatments and control treatments were prepared without aphids. Diet was collected after 5h and 72h followed by phenol chloroform isoamyl alcohol extraction. The extracts were then electrophoresis on 6% TBE polyacrylamide gel. Labelled dsRNA were visualised by Typhoon phosphorimager described before.

2.14.4 The stability of dsRNA in *A. pisum* honeydew *in vitro*

Honeydew was prepared by collecting 20 late stage *A. pisum* in 1.5ml centrifuge tube. Aphids were removed from the tube after 2 hours until enough honeydew was collected. 1XPBS was used for diluting honeydew followed by vortex and centrifugation. Total protein was estimated with BCA assay described above. The concentration of total protein in honeydew was 10μg/μl in 30μl volume. For testing the persistence of dsRNA in *A. pisum* honeydew, 200ng dsRNA were incubated with 20μg, 50μg and 100μg total protein from honeydew in 20μl reaction at 25°C for 30min. dsRNA in 1XPBS was used as positive control and honeydew containing 100μg total protein was treated as negative control.

2.15 The stability of dsRNA against insect tissues

2.15.1 Insect haemolymph and gut extract preparation

Insect haemolymph samples were collected in ice cold 1XPBS in 1.5ml Eppendorf tubes containing 1 mg phenylthiourea (PTU) to inactivate polyphenol oxidase and prevent the haemolymph sample from melanisation (Arakawa,1995). To collect haemolymph for *A. pisum*, legs of aphid are all removed and the body was squeezed gently by forceps to collect the clear liquid exuded. For flour beetle larvae and *D. radicum* larvae, a fine steel needle was used to stab a small hole on their skin, and exuded haemolymph was collected. Haemocytes were removed from all haemolymph samples by centrifugation at 17500g for 20 minutes at 4°C.

Insect gut extracts (including contents) were prepared by extraction in 1xPBS. For aphids and flour beetle larvae, when heads are removed from their body with forceps, the gut remains attached to insect head and will be pulled out with the head. In

D. radicum larvae, the skin of the larvae was gently torn apart by forceps, and the hook-shaped mouthparts were pulled out with the guts. Gut samples were then homogenized by grinding in a clean micro-pestle, followed by centrifugation as described above, discarding the pellet.

The concentrations of total protein in haemolymph samples and gut extracts were estimated by BCA assay using BSA as a standard.

For investigating the persistence of dsRNA in different insect gut extracts, dsRNA were firstly incubated with different amount of protein from different insect species. For *A. pisum* gut extract, 200ng dsRNA were incubated with total protein from 1μg, 2μg, 4μg, 8μg and 10μg in 20μl reaction and incubated for 30min at 25°C. *D. radicum* and *T. castaneum* larval gut extracts containing total protein 3μg, 7μg, 14μg, 21μg and 28μg were used for incubation with dsRNA. 200ng dsRNA incubated in 1XPBS was used as positive control whereas gut samples alone ran on the gel were used as negative control. After incubation, the integrity of the dsRNA subsequently analysed on 2% agarose gel.

2.15.2 Comparison of the rate of persistence of dsRNA against insect haemolymph and gut extracts

For comparing the ability of dsRNA degradation of RNases presented in different insect species. Total proteins from 3 insect gut extracts were normalised to same amount (3μg). 200ng dsRNA were used for incubating with gut extracts for various time: 1min, 5min, 15min and 30min at 25°C. Another assay regarding insect gut extracts were performed by using 200ng dsRNA incubated with total protein from insects equal to single insect gut to three insects. The incubation were performed for 1min, 15min and 30min at 25°C. 200ng dsRNA incubated in 1XPBS was used as positive control whereas gut samples alone ran on the gel were used as negative control.

Similar assay was carried out with insect haemolymph samples. For comparing the dsRNA degradation ability of RNases presented in haemolymph from insects, 200ng dsRNA was mixed with haemolymph samples contain 25μg protein from three different insects in 20μl reaction and incubated at 25°C for 1min, 5min, 15min and 30min. dsRNA incubated with 1XPBS containing PTU was used as positive control and haemolymph samples only were used as negative control. After incubation, the reactions were mixed with DNA loading dye and run on a 2% agarose EtBr gel. Visualization of dsRNA using a UV transilluminator.

2.16 Recombinant Proteins preparation in *E. coli*

2.16.1 Preparation of constructs encoding Trx/RBD1 and Trx/RBD3 fusion proteins for expression in *E. coli*

Coding sequences for the RNA-binding domains RBD1 and RBD3 from the *D. melanogaster* staufen gene (NP_476751.1) (Figure 4-1) were codon-optimised for expression in yeast by using an online website tool from Integrated DNA Technologies (http://www.idtdna.com/CodonOpt). The resulting sequences were synthesised directly by Shinegene (Figure 4-2). The sequences were supplied as inserts in pUC57 plasmid cloning vector. The coding sequences were extracted from the plasmid supplied by PCR, using RBD1/3 forward and reverse primers containing BamH1 and HindIII restriction enzymes (Table 2). PCR products were amplified by Phusion DNA polymerase. PCR conditions were: pre-treatment at 98°C for 30s, followed by 30 cycles of denaturation at 98°C for 30s, annealing at 58°C for 30s, and extension at 72°C for 30s, with a final incubation at 72°C for 10 mins. The PCR product was separated by 1% agarose gel electrophoresis, giving a band at 219 bp as predicted, which was excised. DNA was eluted from the gel by using QIAquick column (QIAGEN) according to the manufacturers' instructions and ligated with pET 32α vector which was restricted with BamH1 and HindIII resctriction enzymes. Samples from the ligation mixture were transformed into one shot *E. coli* TOPO10 competent cells (Invitrogen) and plated on selective Carbenicillin LB media. Colonies were screened by colony PCR using T7 promoter and terminator primers. The conditions were 94°C For 10 mins, followed by 25 cycles of denaturation at 94°C for 30s, annealing at 60°C for 30s, and extension at 70°C for 1 min, with a final extension at 72°C for 7 mins. Selected colonies giving a PCR product of the predicted size (1200 bp) were picked off. Plasmid DNA was prepared from the selected clones by using Wizard plus SV Minipreps (Promega) and was analysed by DNA sequencing. Confirmed RBD1- and RBD3-containing plasmids were then transformed into the expression host, *E. coli* BL21(DE3) by chemical transformation using commercial competent cells (Invitrogen), according to the manufacturer's protocol.

2.16.2 Preparation of constructs encoding Trx/RBD1/GNA and Trx/RBD3/GNA fusion proteins for expression in *E. coli*

The GNA coding sequence, amino acids 1-105 of the mature GNA polypeptide (as described in Fitches *et al.* (2004) was prepared by PCR amplification from a plasmid containing a NotI restriction site which was kindly provided by Dr Prashant Pyati. The template was amplified by using pGAP forward primers and specific reverse primer

XhoI (3' end) restriction sites. Phusion DNA polymerase was used to minimise PCR errors. PCR conditions were as follows: 25 cycles of denaturation at 98°C for 30s, annealing at 58°C for 20s, extension at 72°C for 1min, followed by a final incubation at 72°C for 7 min. The PCR product was separated by agarose gel electrophoresis, giving a band at 1000bp as predicted, which was excised. DNA was extracted using QIAquick column (QIAGEN). The PCR product, and DNA from the recombinant Trx/RBD1 pET32 plasmid, were digested separately with the restriction enzymes NotI and XhoI at 37°C for 2h. The digested products were combined and ligated using T4 DNA ligase overnight at 4°C. Samples from the ligation reaction were then transformed into competent cells of *E. coli* strain TOPO10 (Invitrogen) by electroporation accoding to the manufacturers' protocol, and plated on carbenicilin LB media. Colonies were screened by PCR using T7 promoter and terminator sequence primers and selected colonies giving a PCR product of the predicted size 1200bp were picked off. Plasmid DNA was prepared from the selected clones by the standard miniprep protocol, and was analysed by DNA sequencing. DNA from a plasmid which gave the correct RBD1-GNA coding sequence (Figure 4-5) was then transformed into *E. coli* expression strain BL21(DE3) by standard chemical transformation. Clones containing the expression construct were obtained by plating on selective carbenicillin media, and screened by colony PCR using T7 promoter and terminator primers. Clones giving a product of the predicted size (1200 bp) for the Trx/RBD1/GNA fusion protein coding sequence were selected.

The expression construct encoding Trx/RBD3/GNA in pET32 was prepared in a similar manner, ligating the GNA coding sequence as described above into the Trx/RBD3 pET32 plasmid, and similarly verified by DNA sequencing prior to transformation into the expression host.

2.16.3 Expression of Trx/RBD1,Trx/RBD3, Trx/RBD1/GNA and Trx/RBD3/GNA fusion proteins in *E. coli*

Two mililitre of an overnight cell culture of a verified expression construct clone were added into 100ml LB medium with carbenicilin at final concentration 50μg/ml. The cultures were incubated at 37°C with shaking at 225rpm until the OD at 600nm reached 0.6. The culture were induced by adding IPTG to a final concentration of 0.5mM, 1mM, 2mM and 2.5mM and incubated at varying temperatures (15°C - 30°C) to allow recombinant protein expression. The induced empty pET32 vector was used as a negtive control. After induction, cultures were centrifuged at 4°C 4000g for 10 minutes. The cell pellets were collected and resuspended in 2.5ml 1X "Bugbuster" reagent (Novagen) to release proteins from the cell. The reactions were incubated with gentle shaking for 20 minutes at room temperature, followed by centrifugation to separate

soluble and insoluble material at 4°C, 22,000g for 15 minutes. The supernatant after this centrifugation was taken as the soluble protein fraction. The pellet formed the insoluble protein fraction, which was solubilised by adding 2.5 ml 6M urea and mixing using a vortex mixer. The mixture was then centrifuged again as same conditon, and the supernatant was collected. Protein fractions were analysed by SDS-polyacrylamide gel electrophoresis (Laemmli 1970), followed by staining with Coomassie blue.

2.16.4 Purification of Trx/RBD1, Trx/RBD3, Trx/RBD1/GNA and Trx/RBD3/GNA recombinant proteins in *E.coli* by *Ni-NTA* affinity chromatography

Culture supernatant containing soluble recombinant proteins were subsequently diluted with 4Xbinding buffer (BB) which contained 0.02M sodium phosphate buffer, 0.4M sodium chloride, pH7.4 to 1XBB. The culture supernatant was loaded onto 5ml HisTrap crude nickel columns (GE healthcare) with a flow rate of 5ml/min for 2-3 hours after clarifying by filtration through 0.7µM glass fibre filters (GFF Whatman). The columns containing Trx/RBD1 and Trx/RBD/GNA fusion proteins were first washed with 1XBB until the OD came to a baseline on FPLC recorder and then washed with 1XBB containing 0.01M imidazole. Recombinant proteins were eluted with 1XBB with 0.4M imidazole. Eluted proteins as well as washed fractions were analysed by SDS-PAGE gel electrophoresis stained by Coomassie Blue. In terms of Trx/RBD3, column containing fusion protein was washed with 1XBB containing 0.025M and 0.2M imidazole. Trx/RBD3 fusion protein was eluted with 1XBB containing 0.4M imidazole. Induced Thioredoxin cell supernatant used as negtive control was first washed with 1XBB containing 0.025M imidazole and eluted with 1XBB containing 0.2M imidazole.

2.16.5 Protein desalting by dialysis and PD-10 column

Purified Trx/RBD3/GNA fractions were then pooled and dialysed against a 5 times dilution of sodium chloride, sodium phosphate and 10% glycerol after identification on SDS-PAGE. The starting concentration of sodium chloride and sodium phosphate were 0.4M and 0.02M (pH: 7.4) and protein sample was stored at 0.05M sodium chloride and 10% glycerol. All the procedures were carried out at 4°C. Protein samples were then centrifuged at 20.000g for 1min at 4°C and pellets were resuspended in 6M urea. Both dialysed supernatant and pellet were checked on SDS-PAGE.

Eluted Thioredoxin, Trx/RBD3 and Trx/RBD3/GNA were desalted using a PD-10 column (GE Healthcare) according to the manufacturer's protocol. The column was first equilibrated with deionised water and then 2.5ml of purified fusion proteins in 1XBB containing 0.2M/0.4M imidazole were loaded onto the columns. Proteins were eluted with 3.5ml deionised water in 6X1.5ml eppendorf tubes (around 600µl each). Each fraction was checked on SDS-PAGE. Eluted Thioredoxin and Trx/RBD3 fractions in

1XBB containing 0.2M imidazole were also dialysed against deionised water at 4°C and freeze dried as powder.

2.16.6 Refolding of induced insoluble Trx/RBD1 and Trx/RBD/GNA fusion protein by dialysis

The insoluble Trx/RBD1 and Trx/RBD/GNA fusion proteins in 6M urea were first renatured by dialysis against 20mM sodium phosphate buffer (pH 7.4) containing decreasing concentrations of DDT at each change, from 1mM, 0.5mM to 0.1mM. Each dialysis step was carried out at 4°C for a hour. Finally protein samples were stored in 20mM sodium phosphate buffer (pH7.4). The dialysed Trx/RBD1 and Trx/RBD/GNA protein samples were then centrifuged at 20,000g for 1min. Clear supernatants of renatured dialysed fusion proteins were analyzed on SDS-PAGE with known amounts of GNA as standards. Alternatively, insoluble Trx/RBD1 and Trx/RBD/GNA dissolved in 6M urea were dialysed against a series dilution of urea containing 1mM DTT. The urea concentraion was reduced from 6M to 0.5M over 6 dialysis changes. DTT concentration was reduced to 0.5mM at the last diaysis step. Protein samples were stored in 0.5M urea and 0.5mM DTT. Insoluble Trx/RBD1 was also diluted 10 times and dialysed against deionized water overnight, followed by lyophilisation.

2.16.7 Preparation of constructs encoding pelB/RBD3/GNA fusion proteins for expression in PET22b+ in *E. coli*

The RBD3/GNA coding sequence was assembled into the vector PET22b+ which contains the *pelB* signal sequence, directing secretion of the recombinant protein into the periplasm. To assemble the plasmid, the RBD3/GNA sequence was amplified with primers shown in table 2; the forward primer contains BamHI restriction enzyme sequence with an extra C added into the sequence to correct the reading frame, whereas the reverse primer contains XhoI sequence (Table 1). The PCR product was amplified by Phusion DNA polymerase with annealing at 60 °C for 30s. The PCR product was then separated by 1% agarose gel electrophoresis, giving a band around 220bp, followed by gel extraction. The extracted PCR product was then ligated with pet22b+ vector which had been double digested with BamHI and XhoI. The ligation mixture was then transformed into *E. coli* BL21(DE3) expression host by chemical transformation. The sequence was confirmed by DNA sequencing (Figure 4-19).

2.16.8 Expression of pelB/RBD3/GNA fusion protein in PET22b+ in *E. coli*

Two mililitre of *E. coli* overnight cell culture harbouring construct RBD3/GNA in PET22b+ was inoculated into 100ml LB medium with carbenicilin at final concentration 50μg/ml and incubated at 37°C overnight with shaking at 225rpm until the absorbance

at OD600 reached 0.6. IPTG was added to a final concentration of 1mM and culture was induced for 4 hours with constant shaking at 225rpm. The culture was then cooled prior to centrifugation at 8,000g for 10 minutes to collect the supernatant and cells. The cell pellet was used for extraction of periplasmic proteins.

The osmotic shock method was performed for the extraction of periplasmic protein (Nossal and Heppel 1966). The cell pellet was re-suspended in hypertonic buffer which contains 20% sucrose, Tris/HCL (pH 8.0) and Na_2EDTA. After incubation with gentle shaking at 4°C for 30 minutes, cells were harvested by centrifugation for 10 min at 17,000Xg at 4°C. The supernatant was saved and checked on SDS-PAGE as periplasmic fraction. Cell pellet was then re-suspended in hypotonic solution which contain 5mM $MgSO_4$ and was incubated with vigorous shaking at 4°C for 30 min. Cell pellet and the supernatant were separated by centrifugation for 10 min at 17,000xg at 4°C. The supernatant was treated as cytoplasmic fraction. The insoluble pellet was saved and re-suspended in same volume of 6M urea and was treated as insoluble fraction.

2.17 Recombinant Proteins preparation in *P. pastoris*

2.17.1 Preparation of constructs encoding RBD3/GNA fusion proteins for expression in *P. pastoris*

RBD3 coding sequence was amplified by primers containing restriction enzymes (see 错误！未找到引用源。) to introduce PstI and NotI restriction sites on each side, followed by extraction from agarose gel. The extracted PCR product was double digested with PstI and NotI. Expression vector pGAPZαB containing a GNA coding sequence (described in Yang *et al.* (2014)) was digested with same restriction enzymes. Ligation of insert and vector using T4 DNA ligase followed standard procedures. The expression cassette was transformed into TOP10 *E. coli* cells followed by plasmid extraction and sequencing.

Plasmid DNA was prepared from confirmed RBD3/GNA clones by mini-prep. Isolated plasmid DNAs from 5X10ml LB were pooled and linearized with BlnI restriction enzyme, following standard restriction protocol. The plasmid was checked on agarose gel for confirmation of linearization. Linearized plasmid DNA was ethanol precipitated overnight. The pellet was collected by centrifugation at 12,000xg for 15 minutes at 4°C, and then washed with 70% ethanol. Finally, pellet was re-suspended in nuclease free water. More than 3μg linearized plasmid in 10μl was transformed into 50μl competent cells of protease deficient *P. pastoris* (SMD1168 Invitrogen) according to the manufacturer's protocol. One mililitre solution II was added into the mixture and incubated at 30°C for 1 hour with intermittent mixing-vortexing after every 15 minutes.

The cells were then heat shocked in water bath at 42°C for 10 minutes. The plasmid/ cell mixture was transferred into 15ml falcon tube containing 2ml YPG culture. The cells were incubated at 30°C for 2 hours to allow expression of Zeocin resistance. Cells were then centrifuged at 3000g for 5 minutes at room temperature and pellet was washed with 1ml solution III gently. The cells were centrifuged again as above and pellet was re-suspended in 100-150μl solution III. The transformed cells were then plated on 25μg/ml Zeocin YPG-agar plate and incubated at 30 °C for 2-4 days.

Selected transformant clones were streaked out and grown in 10ml liquid YPG with Zeocin at final concentration 25μg/ml for 2-3 days at 30°C with shaking. Cultures were centrifuged at 4,000xg for 15 minutes at room temperature. Thirty microlitre supernatant was then separated by SDS-PAGE followed by western blotting. Supernatant from plasmid pGAPαB without insert was included during screening as an expression background control. The best-expressing clone was selected for large-scale fermentation.

2.17.2 Large-scale expression (Fermentation) of recombinant proteins in *P. pastoris.*

Three replicates of 100ml liquid YPG media containing the selected clones for expression of RBD3 or RBD3/GNA were inoculated in 250ml baffled flasks at 30 °C for 2-3 days with shaking. These cultures were then added into 2.5L of sterile minimal media (Higgins and Cregg 1998) supplemented with PTM1 salts (Cino 1999) growing in a 5L Bio-Control ADI1010 bench-top fermenter (APPLIKON BIOTECHNOLOGY, Holland). The method was modified from Fitches *et al.* (2004). The fermentation was cultured at 30 °C with continuous agitation. The dissolved oxygen level was maintained at 30% at pH 4-5. Fifty percent glycerol (v/v with distilled water) feed (5-10ml/h) was initiated when 30% dissolved oxygen could not be preserved. After 3-4 days, when the dissolved oxygen level began to rise indicating yeast growth had stopped, the fermentation run was terminated. Culture supernatant from fermentor was collected after centrifugation at 8,000rpm for 30 minutes at 4 °C. The supernatant was then filtered through 2.7μM, and 0.7μM glass microfiber filters (Whatman, UK) using a vacuum manifold.

2.17.3 Purification of recombinant protein RBD3 from *P. pastoris* culture supernatant by Ni-NTA column chromatography.

RBD3 fermented supernatant was adjusted to 0.02M sodium phosphate buffer, 0.4M sodium chloride, pH7.4 by adding 4Xbuffer stock. RBD3 recombinant protein was purified by metal affinity chromatography. Culture supernatant was loaded onto a 5ml Ni-NTA column for 3 hours and washed with 10-fold column volume of 1XBB followed

by washing with 1XBB containing 0.01M imidazole. RBD3 was eluted by 1XBB containing 0.4M imidazole. A second purification was performed by washing the column with 1XBB containing 0.025M imidazole followed by elution with 0.4M imidazole. Wash and eluted fractions from both purification experiments were checked by SDS-PAGE followed by CBB stain as described earlier. Protein fractions containing RBD3 were pooled, diluted twice and dialysed against water overnight (9 changes). Dialysed RBD3 was concentrated using a centrifugal concentrator (5,000 MWCO; Vivascience). Concentrated RBD3 was diluted in 1XREMSA buffer and centrifuged at bench speed for 2 minutes at room temperature. Supernatant and pellet were re-suspended in 1XREMSA buffer. All protein fractions were checked by SDS-PAGE.

2.17.4 Purification of recombinant protein RBD3/GNA *P. pastoris* culture supernatant by Ni-NTA column chromatography.

A. Purification of RBD3/GNA under native condition at different pH

Purification of RBD3/GNA from *P. pastoris* culture supernatant was performed by using Ni-NTA column, as described for RBD3. Culture supernatant was diluted to 0.02M sodium phosphate buffer, 0.4M sodium chloride, pH7.4 by adding 4XBB. RBD3/GNA culture supernatant was normally loaded for 3 hours followed by washing with 1XBB, 0.01M imidazole and eluted with 0.2M imidazole. 0.4M imidazole was used for eluting any tightly bound protein. The purified fractions were pooled and separated into 2 samples. One sample was dialysed against distilled water. Another sample was dialysed against 0.02M sodium phosphate buffer overnight at 4°C.

To improve RBD3/GNA fusion protein purification efficiency, modified methods were applied. First, the pH of culture supernatant was adjusted by adding 4XBB to pH 9. The final pH of adjusted culture supernatant before loading onto nickel column was 5.5. Loaded RBD3/GNA was purified by washing with 0.01M imidazole and eluted with 0.2M imidazole as above. Fractions containing RBD3/GNA were pooled and dialysed against 0.02M sodium phosphate buffer. In a second experiment, culture supernatant containing RBD3/GNA was dialysed against water overnight with 5-6 changes at 4 °C followed by freeze drying. The freeze dried supernatant powder was then re-suspended in 1XBB, pH 7.4. Purification was performed as described above. Fractions containing RBD3/GNA were pooled and dialysed against distilled water or 0.02M sodium phosphate buffer. All purifications were performed from 300ml culture supernatant, and elution was normally repeated twice until most of RBD3/GNA was eluted. All fractions were checked on SDS-PAGE and RBD3/GNA identity was confirmed by western blotting.

B. Purification of RBD3/GNA by gel filtration chromatography.

Three grams freeze-dried culture supernatant powder (see above) containing approx. 6mg RBD3/GNA recombinant protein was re-suspended in 7ml 20mM sodium phosphate buffer. The sample was then centrifuged at 12,000xg for 2 minutes at room temperature to remove any insoluble material. RBD3/GNA solution was loaded onto a Sephacryl S-200 (Amersham) column which was equilibrated with 20mM sodium phosphate buffer to separate the RBD3/GNA from yeast background proteins. RBD3/GNA was eluted in 20mM sodium phosphate buffer at a flow rate of 0.4ml/min, monitoring absorbance at 280nm in the eluate. Fourty-six separated fractions were collected in total and 12 fractions from 21-44 (a green colour indicative of the presence of yeast pigment was observed in fractions) were checked on SDS-PAGE.

C. Purification of RBD3/GNA under denaturing condition

RBD3/GNA culture supernatant was adjusted to pH 6, 6M urea by adding 4XBB pH 9 and solid urea. The solution was loaded onto a nickel-NTA column as described above, and the column was washed with 1XBB containing 6M urea and 0.01M imidazole containing 6M urea. RBD3/GNA was finally eluted in 0.2M imidazole containing 6M urea. Fractions containing RBD3/GNA were pooled and dialysed against a gradient dilution of urea in 0.02M sodium phosphate buffer overnight at 4°C. The dialysed RBD3/GNA solution was finally stored in 0.02M sodium phosphate buffer and the presence of recombinant protein in soluble and insoluble fractions was analysed by SDS-PAGE and western blotting.

2.18 Confirmation of Protein activity by Agglutination

Five mililitre of Alsever's solution containing 1/30 volume anticoagulant was added to equal volume of venous whole rabbit blood in a 10ml heparinized tube which already contains 5ml of Alsever's-anticoagulant. 40μl of the mixture was re-suspended in 1ml 1XPBS followed by quick spin (12,000Xg, 30 sec). The supernatant was discarded and pellet was re-suspended in 1ml 1XPBS to make 2% erythrocyte suspension.

50μl 1XPBS was added to each well in round (U) bottom microtitre plate. 50ul of tested protein with known concentration was added in first well in each row followed serially diluted in preceding wells. Finally, fifty microlitre 2% erythrocyte suspension was added to each well and gently mixed with pipette. The reaction was incubated at room temperature and agglutination was visualized after 2 hours.

2.19 Stability of dsRNA conjugated with Trx/RBD3, Trx/RBD3/GNA and RBD3/GNA against degradation by insect haemolymph and gut extract.

Two hundards nanograms dsRNA was first mixed with 1XPBS or 10μg Trx/RBD3 in 20μl reaction and incubated on ice for binding reaction for 15 minutes. After the incubation, *A. pisum* gut sample containing 2μg protein, *T. castaneum* larvae gut sample containing 25μg protein and *D. radicum* larvae gut sample containing 15μg protein were mixed in binding reaction for 1min, 15min, and 30min separately. In terms of the insect haemolymph samples, *A. pisum* haemolymph sample containing 5μg protein, *T. castaneum* larvae haemolymph sample containing 25μg protein and *D. radicum* larvae haemolymph sample containing 25μg protein were added in binding reactions and incubated for different time periods. DsRNA incubated with 10μg thioredoxin or GNA was used as a negative control and dsRNA in 1XPBS containing PTU was treated as positive control. The amount of protein from insect extracts used for stability assays were determined by results from previous assays. The amounts of protein from insects that completely degrade 200ng dsRNA were applied. The reactions were then extracted with phenol / chloroform/ isoamyl alcohol (25:24:1) to recover the residual dsRNA. The extract was then mixed with DNA loading dye and run on 2% agarose gel stained with EtBr for visualization.

2.20 Detection of Trx/RBD3 and RBD3/GNA in insect tissue by western blotting.

To investigate potential transportation of Trx/RBD3 (*E. coli*) and RBD3/GNA (*P. pastoris*) in *A. pisum*, tissues were dissected and collected from *A. pisum* fed on artificial liquid diet containing either Trx/RBD3 or RBD3/GNA. GNA was included as a positive control. 20μg GNA, Trx/RBD3 and RBD3/GNA were mixed in 40μl diet to make a final concentration of 250ng/μl. Fifteen aphids were picked for each treatment and feeding for 48h followed by dissection in 1XPBS. The dissection procedure was described above. Protein samples collected from different tissues were macerated in 5X sample buffer and boiled at 100 °C for 10 minutes followed by separating on 17.5% SDS-PAGE. After electrophoresis, protein on SDS-PAGE was transferred to nitrocellulose membranes and screened for the presence of GNA, Trx/RBD3 and RBD3/GNA by western blotting. The detection of Trx/RBD3 was performed by using anti-His antibody whereas anti-GNA antibody for detecting GNA and RBD3/GNA.

2.21 Comparison of gene downregulation by injection of dsRNA against insect specific genes and dsRNA-Trx/RBD3 conjugates.

Samples containing 1μg dsRNA (*ApVTE*, *TcAPIN* or *DrAPIN*) were prepared in 0.5μl volumes of nuclease-free water. Trx/RBD3 was prepared as a 3mg/ml solution in 20mM sodium phosphate buffer. For injecting the conjugates into the insects, 5μg dsRNAs (*ApVTE*, *TcAPIN* or *DrAPIN*) was mixed with 35μg Trx/RBD3 in a volume of 17.5μl in total. The binding reactions were performed as described above. The final concentration of dsRNA was 333ng/μl. 35μg Trx/RBD3 mixed with 2.5μl nuclease-free water was used as an additional control.

In experiments using aphids, 15nl of the *ApVTE* dsRNA-Trx/RBD3 conjugates, or Trx/RBD3, or 5ng dsRNA, was injected into 5 days old aphid nymphs. The injected aphids were collected at 48h and 72h post injection. For microinjection of *T. castaneum*, 30nl of *TcAPIN* dsRNA-Trx/RBD3 conjugates was injected in pre-pupal stage larvae. Each larvae received a dose of 10ng *TcAPIN* dsRNA. Injected larvae were collected at 2h, 5h, 24h and 10days post injection. For *D. radicum*, 300nl of *DrAPIN* dsRNA-Trx/RBD3 conjugates was injected into 3rd instar larvae. Each larva received a dose of 100ng *DrAPIN* dsRNA. Injected *D. radicum* larvae were collected at 48h and 72h after injection. The injection bioassays are summarised in Table 6. In all experiments, insects injected with 20mM sodium phosphate buffer and Trx/RBD3 were used as controls.

5 insects from different treatments were collected and subjected to RNA extraction followed by qRT-PCR as previously described.

2.2.2 Statistical analysis

All data were analysed using Prism (v. 5) software. Survival data were analysed using survival curve Log-rank (Mentel-Cox) test. Significant differences were compared to each treatment. Analysis of gene down-regulation was conducted using two-way ANOVA to determine significant differences between treatments.

Primer Name	Primer Sequence
12μM 3-CDS primer	5'AAGCAGTGGTATCAACGCAGAGTAC$(T)_{30}$N-3' (N=A,C,G, or T; V=A, G or C)
10X Universal Primer Mix	Long-UPM (0.4μM): 5'CTAATACGACTCACTATAGGGCAAGCAGTGGTATCAACGCAGAGT-3'
	Short-UPM (2μM):5'-CTAATACGACTCACTATAGGGC-3'
M. domestica	5'GCTGCGGGGGTGGTCTTAAGGACTGGGACG-3'
***M. domestica* 5' RACE**	5' CGGACGAGGCGCATTTGGCACAGGCCAC-3'
***D. radicum* 3' RACE**	5'ACAGTATCGGAACAGGCTTCTCGCATACACC-3'
***D. radicum* 5' RACE**	5' ACCTACAGCTTGTGCTTGTTGCAACTCCCCCTC-3'
Degenerate primers	Fwd: 5' GYTTCAGYTGYGGBGGWGGBY-3' Rev: 5' BACVGANGADGCGCAYTTGGC-3'

Table 1 Degenerate primers used for isolating *APIN* gene and RACE primers for full-length gene sequence of *M. domesitca* and *D. radicum APIN*.

Gene	Access code	Template	Primer sequence	Size
V-type ATPase E subunit	XM_965528	*T. castaneum* cDNA	Fwd: 5'-TATCTCGAGACCAGGCGAGATATTCACAGC-3' Rev: 5'-TATCTCGAGACCAGGCGAGATATTCACAGC-3'	277bp
V-type ATPase E subunit	None	*T. confusum* cDNA	Fwd: 5'-TATCTCGAGTGGTGAGAGTCAGGCAACAG-3' Rev: 5'-ATATCTAGACCAAACAAGGCCGTACGAATTTC-3'	253bp
Thread (APIN: Inhibitor of Apoptosis)	XM_969968.2	*T. castaneum* cDNA	Fwd: 5'-ATATCTAGACATCCGGAACGTCTCACTCT-3' Rev: 5'-ATACTAGACATCCGGAACGTCTCACTCT-3'	277bp
V-type ATPase E subunit	XM_001946489	*A. pisum* cDNA	Fwd: 5'-TAT CTCGAG GGCCGCCTGGTC-3' Rev: 5'-TAT CTCGAG GGCCGCCTGGTC-3'	277bp
Thread (APIN: Inhibitor of Apoptosis)	XM_001944122.3	*A. pisum* cDNA	Fwd: 5'-TATCTCGAGGGTCTGAAGGACTGGGAAGAA-3' Rev: 5'-TATCTCGAGGGTCTGAAGGACTGGGAAGAA-3'	277bp
Thread (APIN: Inhibitor of Apoptosis)	XM_011292268.1	*M. domestica* cDNA	Fwd: 5'-ATAGAATTCGCGGGGGTGGTCTTAAGG-3' Rev: 5'- TATAAGCTTGCGACTGCAACCGTTGTATG-3'	277bp
Thread (APIN: Inhibitor of Apoptosis)	None	*D. radicum* cDNA	Fwd: 5'-ATAGAATTCCAGCTGTGGTGGTGGTC-3' Rev: 5'-TATAAGCTTGCGAGAAGCCTGTTCCG-3'	277bp
Kanamycin resistance (nptII)	JN638547 (synthetic construct)	pSC-A-amp/kan	Fwd: 5'-AGGCTATTCGGCTATGAC-3' Rev: 5'-CGATAGAAGGCGATGCG-3'	600bp
Tread (APIN: Inhibitor of Apoptosis)	XM_969968.2	*T. castaneum* cDNA (with T7 promoter sequences)	Fwd: 5'-TAATACGACTCACTATAGGG ACAAGAAGGCGCGGTTAGAG-3' Rev: 5'-TAATACGACTCACTATAGGG ACATTACTCGCCGACACACC-3'	277bp
To clone *Staufen RBD1* in pET32 vector	NP_476751.1	Synthesed gene in pUC50 vector	Fwd: 5'-ATAGGATCCAAGGCAAGACCCCA-3' Rev: 5'-CGTAAGCTTATGCTTGTACATGGTTTC-3'	219bp
To clone *Staufen RBD3 in pET32 vector*	NP_476751.1	Synthesed gene in pUC50 vector	Fwd: 5'-ATAGGATCCGACAAGAAGTCGCCC-3' Rev: 5'-CGTAAGCTTCGGCAGCTTTTGCAA-3'	219bp
To clone *Staufen RBD3* cloned in pelB vector containing GNA	NP_476751.1	Synthesed gene in pUC50 vector	Fwd: 5'-TGCTCGAGTCCAGTGGCCCAA-3' Rev: 5'-TCGGATCCCGATAAGAAGTCTCC-3'	219bp
To clone *Staufen RBD3* cloned in pGAPαB	NP_476751.1	Synthesed gene in pUC50 vector	Fwd: 5'-TGAAGCTGCAGCAGATAAGAAGTCTCCA-3' Rev: 5' ATCGGCGGCCGCTGGCAACTTTTG-3'	219bp

Table 2 Primer pairs used for cloning RNAi region prior to dsRNA production, primers used for cloning RBD1 and RBD3 into *E. coli* and *P. pastoris.*

Gene	Access code	Insect	Primer sequence
V-type ATPase E subunit	XM_969968.2	*T. castaneum*	Fwd: 5'-CCAAGCATTTTTAATGCA CCAC-3' Rev: 5'-5-CCAAGCATTTTTAATGCA CCAC-3'
Thread (APIN: Inhibitor of Apoptosis)	XM_969968.2	*T. castaneum*	Fwd: 5- AAGCGAAAAGTTGAGGCAAGC-3' Rev: 5- AACCATTGCTTTCTTACTCGAAGG-3'
GAPDH	XP_974181.1	*T. castaneum*	Fwd: 5'-CCGGGATGGCGTTCAG-3' Rev: 5'-CCAAACGCACCGTCAAATC-3'
V-type ATPase E subunit	XM_001946489	*A. pisum*	Fwd: 5'-CCGAGTATAAGGCAGCATCCA-3' Rev: 5'-CTTATGTGCCAACAACTCAATACCA-3'
Thread (APIN: Inhibitor of Apoptosis)	XM_001944122.3	*A. pisum*	Fwd: 5'-GATTATTGGCAACAAGGTGATGATC-3' Rev: 5'-AACCAGCAGAAGAATCGTTAAAAAA-3'
GAPDH	NM_001293474.1	*A. pisum*	Fwd: 5'-CAATGGAAACAAGATCAAGGTGTT-3' Rev: 5'-ACCAGCAGATCCCCATTGG-3'
Thread (APIN: Inhibitor of Apoptosis)	XM_011292268.1	*M. domestica*	Fwd: 5'-GGTTCCGCTGCAACAAAAGT-3' Rev: 5'-GGGTGCCTGTTCGTTGGA-3'
GAPDH	XP_001364734.2	*M. domestica*	Fwd: 5'-AGGCCATCACCGTTTTCAGT-3' Rev: 5'-GCGCTGGCCCAGTTGA-3'
Thread (APIN: Inhibitor of Apoptosis)	In this work	*D. radicum*	Fwd: 5'- GCCACGCAACAAGAAATAACAC Rev: 5'- GCCACGCAACAAGAAATAACAC-3'-3'
GAPDH	In this work	*D. radicum*	Fwd: 5'- CCATGTTTGTGTGCGGTGTT-3' Rev: 5'-TGCAGGAAGCATTGGAGACTAC-3'

Table 3 Primer pairs used for qPCR analysis in *A. pisum*, *M. domestica*, *D. radicum* and *T. castaneum*.

Insect	dsRNA	Insect age	Insect weight	dsRNA (ng)/insect
A. pisum	*Kan*	5 days	0.7mg	7.5, 15 and 30ng
	ApVTE dsRNA	5 days		7.5, 15 and 30ng
	ApAPIN dsRNA	5 days		7.5, 15 and 30ng
M. domestica	*Kan*	Pre-pupa	18mg	150, 250 and 500ng
	DrAPIN dsRNA	Pre-pupa		150, 250 and 500ng
	Kan	1 day fly adult		150 and 500ng
	MdAPIN dsRNA	1 day fly adult		150 and 500ng
D. radicum	*Kan*	Pre-pupa	16.7mg	100ng
	DrAPIN dsRNA	Pre-pupa		100ng
T. castaneum	*Kan*	Pre-pupa	3.1mg	10,50 and 100ng
	TcAPIN dsRNA	Pre-pupa		10,50 and 100ng
	TcVTE dsRNA	Pre-pupa		50 and 100ng
	T.cfmVTE dsRNA	Pre-pupa		150 and 300ng

Table 4 Injection bioassays with *A. pisum, M. domestica* and *T. castaneum*.

Insect	Treatment	Insect stage	dsRNA concentration
A. pisum	*Kan*	neonate	7.5ng/μl, 100ng/μl
	ApVTE dsRNA	neonate	7.5ng/μl, 100ng/μl
M. domestica	*Kan*	3 days old larvae	100ng/mg, 200ng/mg
	MdAPIN dsRNA	3 days old larvae	100ng/mg, 200ng/mg
M. domestica	*Kan* (Bacteria)	3 days old larvae	200ng/mg
	MdAPIN dsRNA (Bacteria)	3 days old larvae	200ng/mg
T. castaneum	*Kan*	<one week old	250ng/mg, 500ng/mg
	TcAPIN dsRNA	<one week old	250ng/mg, 500ng/mg
	TcVTE dsRNA	<one week old	250ng/mg, 500ng/mg

Table 5 Oral delivery of dsRNA to *A. pisum, M. domestica* and *T. castaneum*

Insect	Stage	DsRNA-Trx/RBD3	Volume	dsRNA/ insect
A. pisum	5 days old	*ApVTE* dsRNA	13.8nl	5ng
T. castaneum	Pre-pupa stage	*TcAPIN* dsRNA	30nl	10ng
D. radicum	3rd instar	*DrAPIN* dsRNA	300nl	100ng

Table 6 dsRNA-Trx/RBD3 conjugate injection bioassay against different insect orders

Chapter 3 RNAi responses in insects of different orders

3.1 Introduction

The possibility of exploiting the high level of specificity of RNAi, based on transcript sequences, to give insecticidal effects specific to target insect pests has led to much research being directed towards using an RNAi approach in crop protection. However, two technical problems have limited the application of this strategy in the field.

First, delivery of dsRNA to the insect is a significant problem; although successful gene knockdowns have been achieved in many cases via microinjection into insect haemolymph this method is not possible for practical application of insecticide. More effective delivery methods have been focused on topical or oral administration. Although oral delivery of dsRNA to produce RNAi effects is feasible in some insects, continuous feeding is often needed if this is to result in mortality. In this respect, delivering dsRNA via production in transgenic plants offers significant advantages. Baum *et al.* (2007) constructed a transgenic corn plants to express dsRNAs against specific target genes in Western corn rootworm (WCR), which resulted in significantly reduced WCR feeding damage. Similarly, Mao *et al.* (2007) generated transgenic *Arabidopsis thaliana* and *Nicotiana tabacum* engineered to express dsRNA specific to an insect cytochrome P450, resulting in disruption of insect's ability to detoxify gossypol.

A second problem in applying RNAi to crop protection is variable responses in target pests. Recent studies which have focused on differences in the RNAi efficiency between insect species have found that not all insect species are equally susceptible to the RNAi effect, and some insect species even appear to be completely insensitive (Terenius *et al.* (2011); Bellés (2010)). In this chapter, RNAi effects are compared between insect species of three different orders: *Tribolium castaneum* (*T. castaneum*), red flour beetle from Coleopteran, *Musca domestica* (*M. domestica),* housefly and *Delia radicum* (*D. radicum*), cabbage root fly from Dipteran, and *Acyrthosiphon pisum* (*A. pisum*), pea aphid from Hemiptera. RNAi was directed against two target genes, the *thread* gene which encodes Inhibitor of Apoptosis (APIN) protein, and *V-type ATPase E subunit* gene and dsRNA was delivered both by microinjection and feeding.

3.2 Results

3.2.1 RNAi in *T. castaneum*

3.2.1.1 *TcAPIN* and *TcVTE* gene expression pattern analysed by real time qPCR

In order to determine appropriate developmental stages at which dsRNA administration could be used to show RNAi effects, the expression of the target genes was assessed in *T. castaneum* at different life stages, from early larva to adult. Total RNA was extracted from insects, and used to prepare cDNA. Expression of the target genes was estimated relative to an endogenous control, the *GAPDH* gene, by quantitative PCR (qPCR). These experiments demonstrated that *V-type ATPase E subunit* (*VTE*) gene was ubiquitously expressed in different life stages of *T. castaneum* (Figure 3-1). Although *TcVTE* transcripts were more abundant relative to *GADPH* in pupal stage, the change in ratio was less than 2-fold compare to the pre-pupa larval stage, and within experimental error for technical replicates. In contrast, the *APIN* gene (*TcAPIN*) was expressed in a much more development-specific manner, with the highest level at egg and pre-pupa and pupa stage and relatively low levels in other stages (Figure 3-2).

3.2.1.2 Injection of dsRNA results in significant gene down regulation in *T. castaneum* larvae

Injection of dsRNA in *T. castaneum* larvae at the pre-pupal stage induced robust target gene down-regulation. Representative results are shown in Figure 3-3 and Figure 3-4, and demonstrate that 50ng *TcVTE* dsRNA and *TcAPIN* dsRNA were able to reduce the relative levels of *VTE* and *APIN* gene transcripts by >85%. The down regulation effect persisted for at least 10 days post injection (latest time point assayed). Both genes showed significant difference in gene downregulation compared to control treatment in all tested time points (ANOVA with $P<0.0001$). The assays showed that the *TcVTE* dsRNA was approx. 2x as effective in down regulation as *TcAPIN* dsRNA when the same amount was injected (approx. 16-fold downregulation by *TcVTE* dsRNA, 8-fold by *TcAPIN* dsRNA); the dsRNAs were designed to be of the same length, so the *TcVTE* dsRNA was also more effective on a molar basis (i.e. effect per molecule of dsRNA). Based on the qPCR result, *TcVTE* expression gives Ct value at 21 when normalised to endogenous control GAPDH (21) whereas *TcAPIN* expression is 26. This observation agreed well with the expression levels of *DmVTE* (CG1088) and *DmAPIN* (CG12284) in Drosophila data from Flybase (http://flyatlas.org/atlas.cgi). In larval tissues, *DmVTE* transcripts are 2-4 fold higher than *DmAPIN* transcripts, and both genes express at high level in midgut, hindgut, Malpighian tubules, salivary gland

and fat body. *TcVTE* dsRNA could be targeting *VTE* transcript more easily than *APIN* transcript due to the greater abundancy.

As well as down-regulation of gene expression, a phenotype was observed in larvae injected with both both *TcVTE* and *TcAPIN* dsRNA. Mortality was observed in treated larvae from 3 days post injection and continued throughout the assay. Larvae injected with *TcAPIN* dsRNA exhibit blackened symptom over whole body (Figure 3-51C and 2). Survived larvae failed to complete pupation, showing pupal-like phenotype, but with larvae form (Figure 3-51D). Control larvae were able to go through to the pupal stage with only low levels of mortality. A further assay was performed in order to record survival for larvae after injection (Figure 3-6). Twenty larvae each at the pre-pupal stage were injected with 100ng *TcAPIN* dsRNA or *TcVTE* dsRNA for each treatment. A control treatment was made by injecting 100ng *Kan* dsRNA. A steady decline in survival from 2 days after injection was observed in treated larvae, resulting in 100% larval mortality by day 11 for larvae injected with *TcVTE* dsRNA and by day 12 for larvae injected with *TcAPIN* dsRNA. Survival curves for the treated larvae were significantly different (Mentel-Cox test with $P<0.0001$) from controls, where the control treatment (injected with *Kan* dsRNA) showed approx. 90% survival at 13 days post injection when the assay finished. The two survival curves for injection of *TcVTE* dsRNA or *TcAPIN* dsRNA were not significantly different according to Mentel-Cox test.

3.2.1.3 Species-specificity of RNAi effects in *Tribolium* spp.

The species-specificity of gene down-regulation caused by *VTE* dsRNA was assessed by injecting sequences specific for *VTE* from *T. confusum* (confused flour beetle), a closely-related *Tribolium* species, into *T. castaneum*, and assaying transcript levels in the injected insects by qPCR. One hundard and fifty and 300ng *T. confusum VTE (TcfVTE)* dsRNA with 253bp length were injected into *T. castaneum* pre-pupal stage larvae, and injected larvae were collected after 48h for RNA extraction. The subsequent qPCR results (Figure 3-7) showed effective down-regulation, with transcripts down-regulated by approx. 10-fold in both treatments compared to the control (injected with *Kan* dsRNA), differences are significant between control and *TcfVTE* dsRNA treatments for both doeses (ANOVA, $P<0.0001$). These results are comparable to injection of 50 ng of *T. castaneum VTE* dsRNA (Figure 3-4). The sequence used to prepare the *T. confusum* dsRNA (253bp) is aligned with the *T. castaneum* target in Figure 3-8; although there are sequence differences between the species, several stretches of ≥20 bases with sequence identity are present. The result suggests that cross-protection against related species by RNAi is possible, providing that suitable dsRNA regions are selected.

3.2.1.4 Time course for gene down-regulation in *T. castaneum* larvae.

To determine whether dsRNA injection into *T. castaneum* larvae can induce an RNAi effect in the short term, experiments were carried out in which 10ng *TcAPIN* dsRNA was injected into pre-pupa stage larvae, followed by harvesting insects after 24h and 48h for estimation of transcript levels by qPCR. Results are shown in Figure 3-9A (ANOVA, $P<0.0001$). RNAi effect, nearly 2-fold reduction in transcript level, was observed after 24h compare to control treatment; the effect only increased slightly after 48h. Comparison to the previous assay, in which 50ng of *TcAPIN* dsRNA was injected, shows dose-dependency of the RNAi effect, in that gene down-regulation is approx. 8-fold after 48h at the higher dose.

The time-course of the RNAi response was clarified in a further experiment in which 10ng *TcAPIN* dsRNA was injected into pre-pupal stage larvae, and insects were collected at 2h, 5h, 24h and 10 days after injection, for analysis of *APIN* gene expression by qPCR. Results are shown in Figure 3-10. These data demonstrate that no RNAi effect is detectable at 2h after injection, but is observed at 5h (approx. 2-fold) showing that the interval required observing the effect is <5h. A significant difference was compared between treatment of injection of *TcAPIN* dsRNA at 2h time point and 5h time point (ANOVA, $P<0.0001$). Gene down-regulation by injected dsRNA increases slightly over the interval 5h to 24h (and, from the previous experiment, to 48h), but increases significantly (ANOVA, $P<0.0001$). to approx. 5-fold, after 10 days. Injection of control *Kan* dsRNA has no significant effect on expression of the target gene over the time points tested. These results suggest that the RNAi effect in *Tribolium* involves longer-term RNAi amplification when low doses of dsRNA are used, since levels of gene down-regulation are greater at 10 days (ANOVA, $P<0.0001$) after injection than in the short term.

3.2.1.5 Oral feeding of dsRNA to *T. castaneum* larvae induces target gene down-regulation

Although injection of dsRNA in *T. castaneum* larvae gives reliable gene down-regulation, use as a pesticide in crop protection would require a different method of delivery; oral delivery would be most convenient. Experiments were therefore carried out to evaluate this method of delivery, mixing the dsRNA into the wheat flour diet used for this insect. DsRNA against *TcVTE* and *TcAPIN* gene was incorporated into wheat flour diet at 250 ng/mg (250 ppm) and 500 ng/mg (500 ppm), with 500ng/mg *Kan* dsRNA as a control. *T. castaneum* larvae at ≤7 days after emergence were exposed to the diets for 30 days, after which period control larvae had started to pupate. Survival of controls fed *Kan* dsRNA over the complete assay period was 90%. Both dsRNA treatments, at both levels of incorporation, caused significant mortality (Mentel-Cox test,

p<0.002) when compared to control (result shown in Figure 3-11). Larvae fed with *TcVTE* dsRNA at 500 ng/mg showed a steady decline in survival over the assay, resulting in 100% mortality after 25 days. Larvae fed with the lower dose (250 ng/mg) *TcVTE* dsRNA also declined in survival up to 20 days feeding, with no further mortality over the remaining 10 days, resulting in 55% mortality at the end of the assay. Larvae fed with *TcAPIN* dsRNA at 500 ng/mg and 250 ng/mg also showed declines in survival which reduced at the later stages of the assay, resulting in approx. 70% and 40% mortality over the assay period, respectively. Both dsRNAs showed dose-dependent effects on survival of the *T. castaneum* larvae when fed, demonstrating their activities as biopesticides.

To show that oral administration of dsRNA caused down-regulation of gene expression, *T. castaneum* larvae were fed on wheat flour containing 500 ng/mg *TcVTE* dsRNA for 10 days, then collected and pooled for RNA extraction, followed by qPCR. Results are shown in Figure 3-12 (ANOVA, p<0.0001). Same experiment was performed to show *APIN* gene downregulation after feeding *TcAPIN* dsRNA (Figure 3-13, ANOVA, p<0.0001). *VTE* and APIN gene transcripts were reduced by approx. 2-fold compared to control (*Kan* dsRNA) treatment. This relatively low level of gene down-regulation compared to injection of *TcVTE* dsRNA (Figure 3-3) and *TcAPIN* dsRNA (Figure 3-4) may explain the more gradual decline in survival in the feeding assay (shown by comparing Figure 3-6 and Figure 3-11), and suggests that delivery of dsRNA in the field may limit insecticidal activity and thus use as a biopesticide.

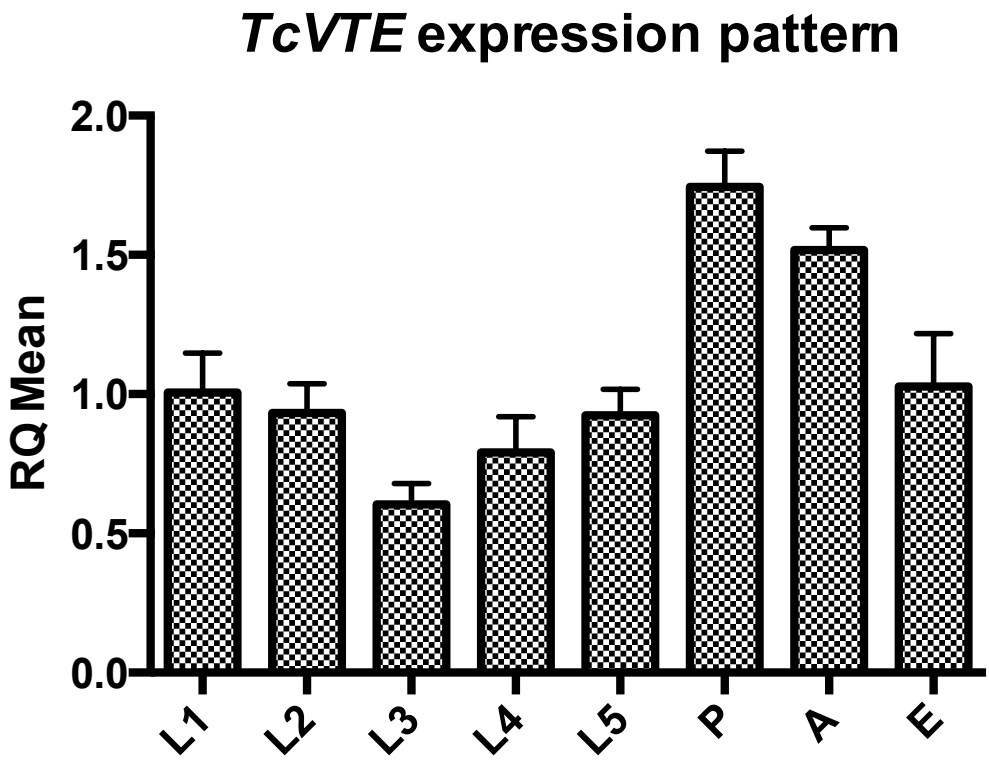

Figure 3-1 ***TcVTE* expression profiles in different life stages of *T. castaneum.*** Columns show the levels of transcript relative to *GADPH* transcript (internal standard) as estimated by qPCR, normalised to *TcVTE* level in adult = 1.0. Error bars indicate standard errors of the mean for 3 technical replicates. L1= 1^{st}-2^{nd} instar, L2= 2^{nd}-3^{rd} instar, L3= 3^{rd}-4^{th} instar, L4= 4^{th}-5^{th} instar, L5= 5^{th}-6^{th} instar (pre-pupa stage), P=pupa, A=adult, E=egg. Number of insects used for each stages n=5.

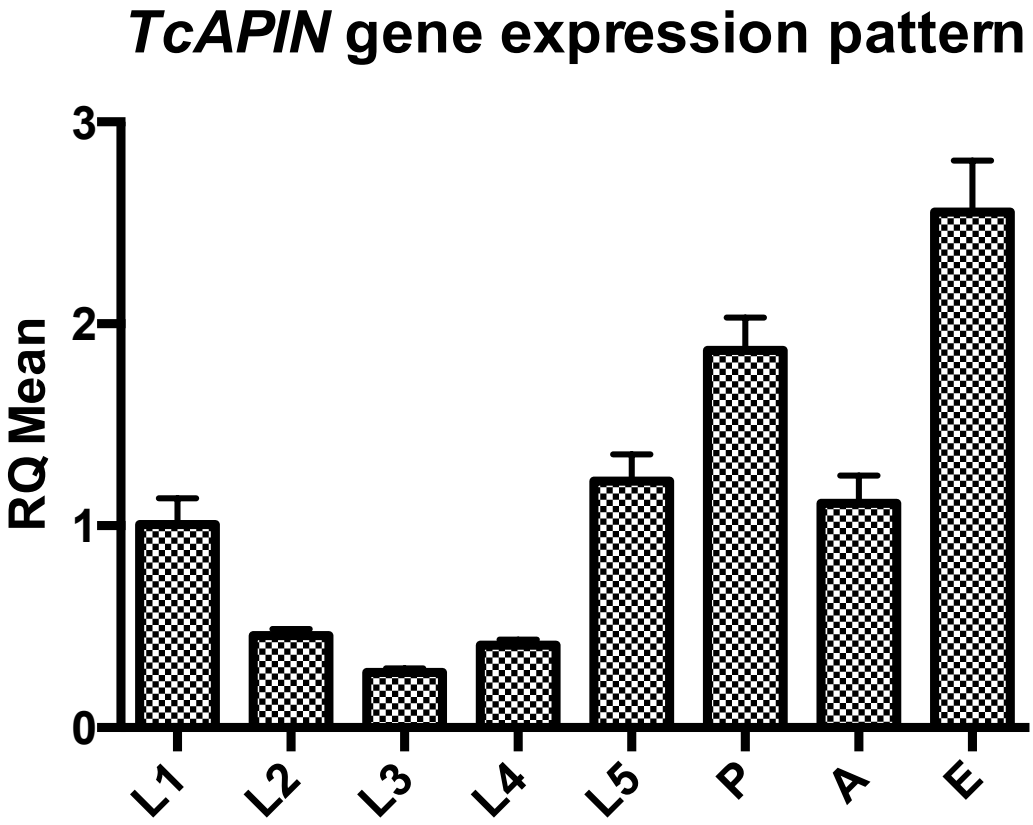

Figure 3-2 ***TcAPIN* expression profiles in different life stages of *T. castaneum.*** Columns show the levels of transcript relative to *GADPH* transcript (internal standard) as estimated by qPCR, normalised to *TcAPIN* level in adult = 1.0. Error bars indicate standard errors of the mean for 3 technical replicates. L1= 1^{st}-2^{nd} instar, L2= 2^{nd}-3^{rd} instar, L3= 3^{rd}-4^{th} instar, L4= 4^{th}-5^{th} instar, L5= 5^{th}-6^{th} instar (pre-pupa stage), P=pupa, A=adult, E=egg. Number of insects used for each stages n=5.

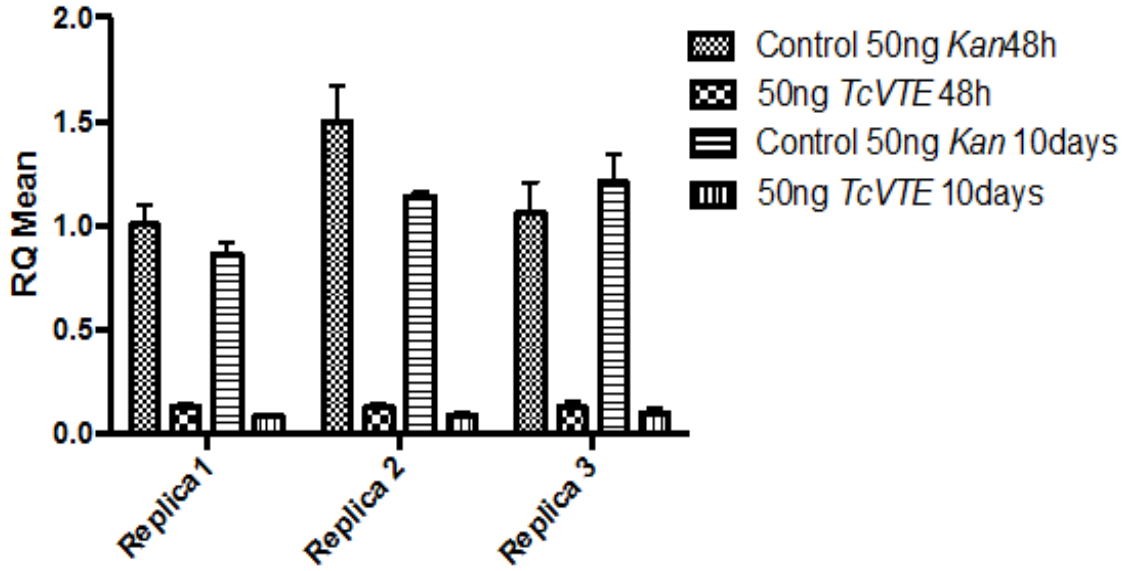

Figure 3-3 **Down-regulation of *TcVTE* gene in pre-pupal *T. castaneum* larvae**. Larvae were injected with 50ng *TcVTE* dsRNA or *Kan* dsRNA as indicated; transcript levels were estimated by qPCR at different times after injection as shown. Columns show the levels of transcript relative to *GADPH* transcript (internal standard), normalised to *Kan* level in replica 1 control 48h = 1.0. Error bars indicate standard errors of the mean for 3 technical replicates; replicas are independent 3 biological replicates. Number of insects for each treatment n=5. Differences are significant between control and *TcVTE* treatment at both time points tested by ANOVA with $p<0.0001$, ****.

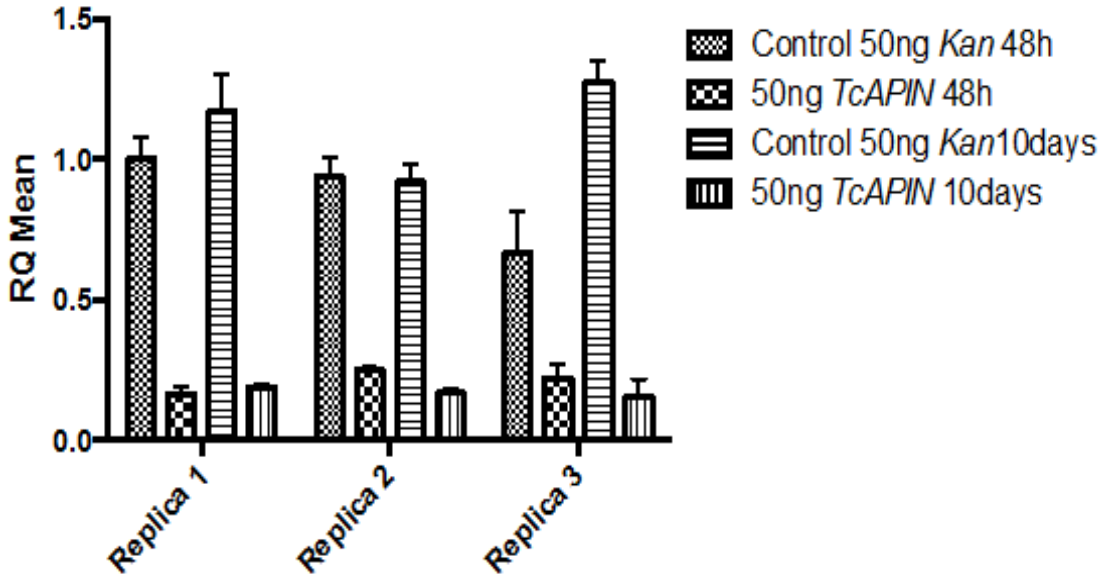

Figure 3-4 **Down-regulation of *TcAPIN* gene in pre-pupal *T. castaneum* larvae.** Larvae were injected with 50ng *TcAPIN* dsRNA or *Kan* dsRNA as indicated; transcript levels were estimated by qPCR at different times after injection as shown. Columns show the levels of transcript relative to *GADPH* transcript (internal standard), normalised to *Kan* level in replica 1 control 48h = 1.0. Error bars indicate standard errors of the mean for 3 technical replicates; replicas are 3 independent biological replicates. Number of insects for each treatment n=5. Differences are significant between control and *TcAPIN* treatment at both time points tested by using ANOVA with $p<0.0001$, ****.

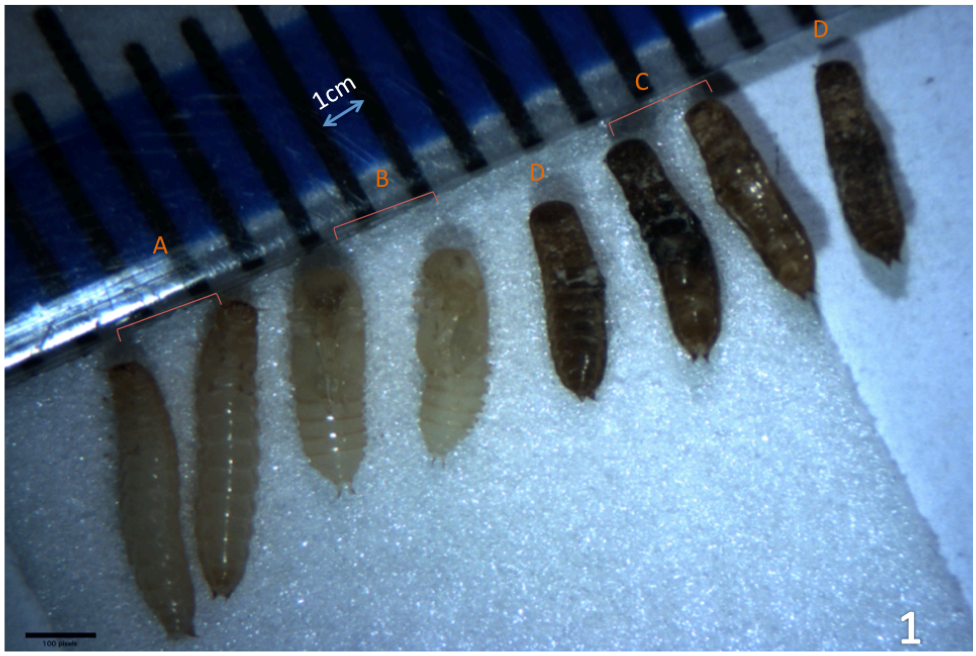

Figure 3-5 **Phenotypes observed after injection of *TcAPIN* and *TcVTE* dsRNA into pre-pupal stage larvae**.

1: Group A and B: *T.castaneum* larvae and pupae injected with *Kan* dsRNA.

Group C and D: *T.castaneum* larvae and pupae injected with *TcAPIN* dsRNA.

2: Control treatment: larva injected with *Kan* dsRNA

Blackened larvae were observed in treatment of injection of *TcAPIN* dsRNA

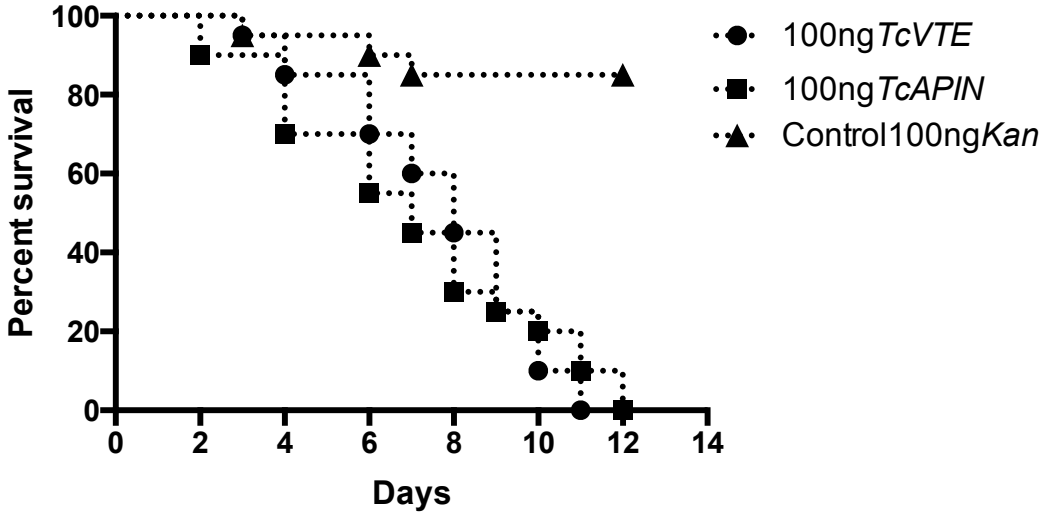

Figure 3-6 **Survival of *T. castaneum* larvae after injection with dsRNAs.** Prepupal larvae were injected with dsRNAs as indicated, and survival was monitored daily. Number of insects for each treatment n=20. Mentel-Cox test with $p<0.0001$, ****.

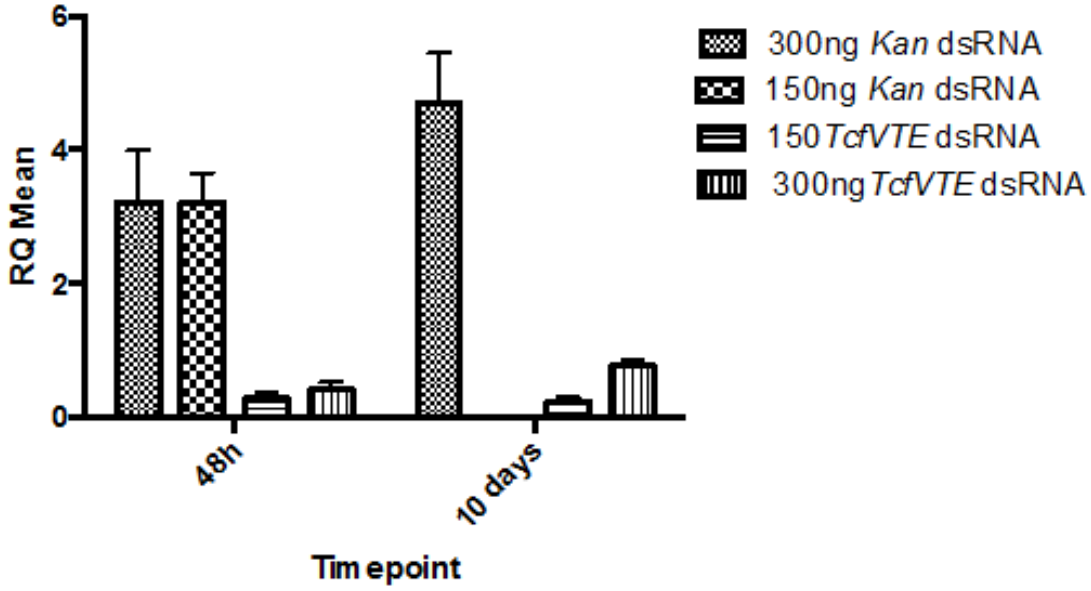

Figure 3-7 **Down-regulation of *TcVTE* gene in pre-pupal *T. castaneum* larvae injected with dsRNA directed against confused flour beetle *VTE* gene.** Five larvae were injected with *TcfVTE* dsRNA or *Kan* dsRNA as indicated; transcript levels were estimated by qPCR at different times after injection as shown. Columns show the levels of transcript relative to *GADPH* transcript (internal standard), normalised to level in 300ng *Kan* level control 48h = 1.0. Error bars indicate standard errors of the mean for 3 technical replicates. Control treatment 150ng Kan dsRNA at 10 days time point was contaminated; therefore it is removed from figure. ANOVA with $p<0.0001$, ****.

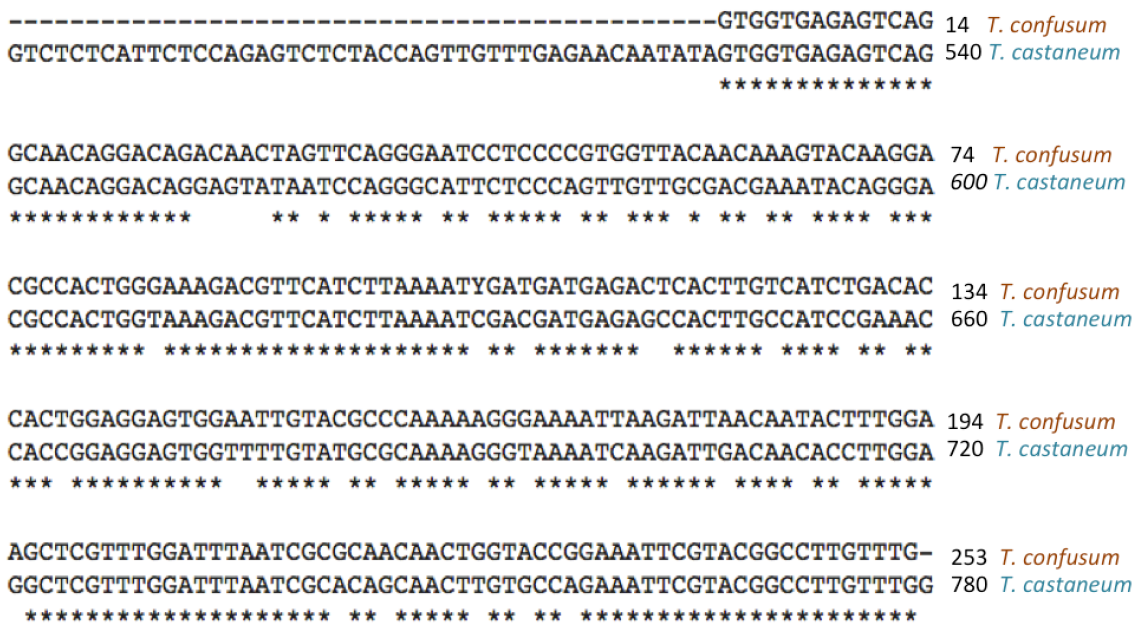

Figure 3-8 **Sequence alignment of *T. castaneum* and *T. confusum VTE* gene fragments used for producing dsRNA**. Asterisks indicate sequence identity. *VTE* dsRNA prepared from *T. confusum* is 253bp whereas 277bp in *T. castaneum.*

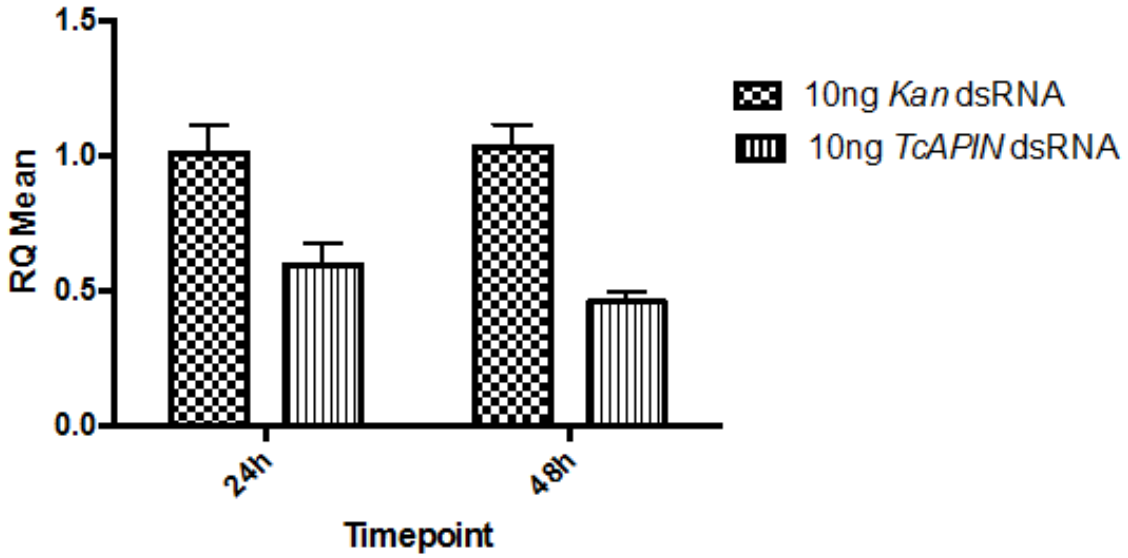

Figure 3-9 **Down-regulation of *TcAPIN* gene in pre-pupal *T. castaneum* larvae.** Larvae were injected with 10ng *TcAPIN* dsRNA or *Kan* dsRNA as indicated; transcript levels were estimated by qPCR at different times after injection as shown. Columns show the levels of transcript relative to *GADPH* transcript (internal standard), normalised to *Kan* level in control 24h = 1.0. Error bars indicate standard errors of the mean for 3 technical replicates**.** Number of insects for each treatment n=5. ANOVA with $p<0.0001$, ****.

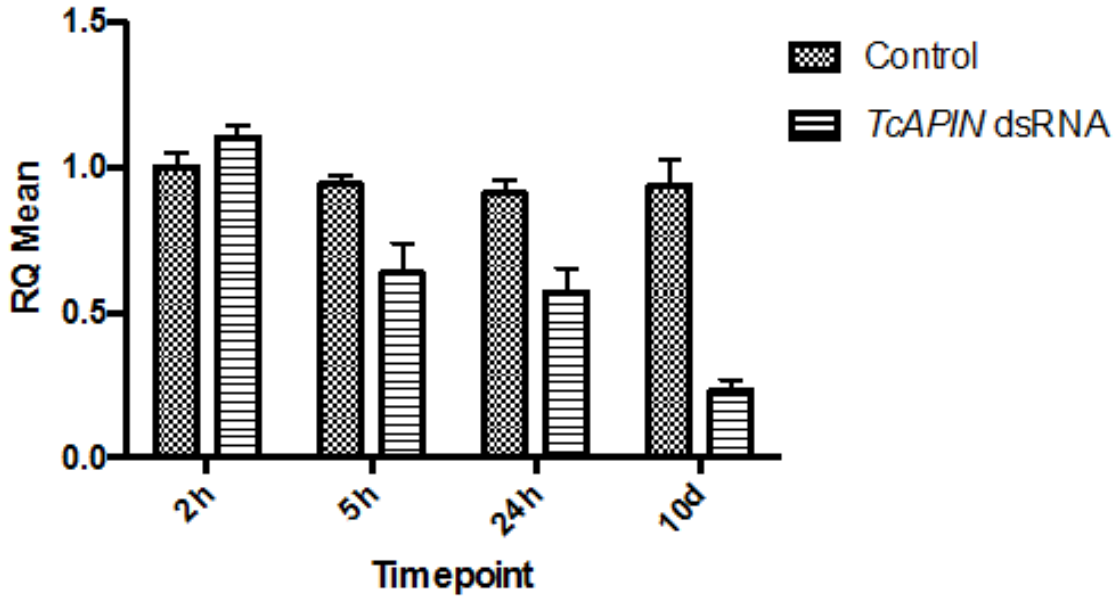

Figure 3-10 **Down-regulation of *TcAPIN* gene in pre-pupal *T. castaneum* larvae.** Larvae were injected with 10ng *TcAPIN* dsRNA or *Kan* dsRNA (control); transcript levels were estimated by qPCR at different times after injection as shown. Columns show the levels of transcript relative to *GADPH* transcript (internal standard), normalised to *Kan* level in 2h control = 1.0. Error bars indicate standard errors of the mean for 3 technical replicates. Number of insects for each treatment n=5. ANOVA with $p<0.0001$, ****.

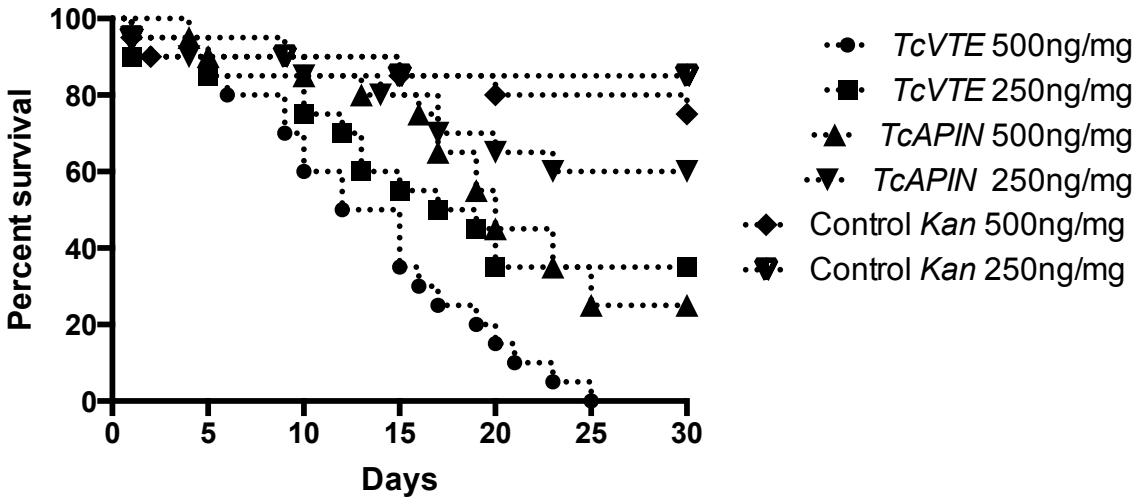

Figure 3-11 **Survival of *T. castaneum* larvae fed on flour disks containing *TcVTE* dsRNA and *TcAPIN* dsRNA.** Less than one week old larvae were fed on disks containing dsRNAs as indicated; survival was monitored daily. Number of insects for each treatment n=20. According to Mentel-Cox test, treatments between control *Kan* 250ng/mg is significant different from *TcVTE* 250ng/mg with P<0.02, **. Significant difference in treatment between Control *Kan* 500ng/mg and *TcVTE* 500ng/mg with P<0.0001, ****. No significant difference between Control *Kan* 250ng/mg and *TcAPIN* 250ng/mg. Significant diffrerent with P<0.0027,** between Control *Kan* 500ng/mg and *TcAPIN* 500ng/mg.

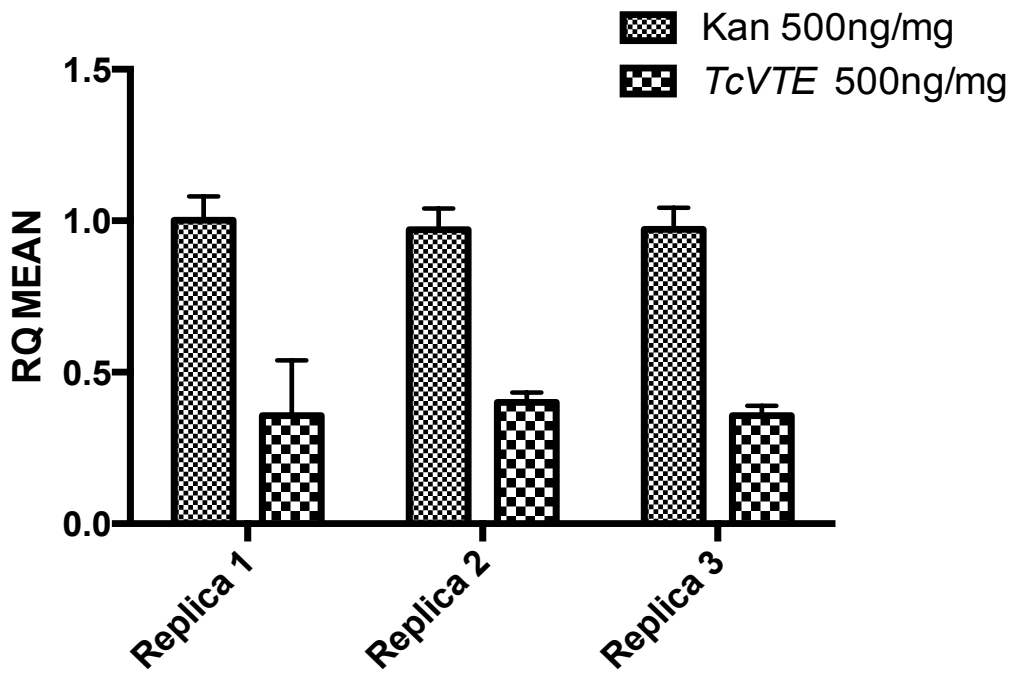

Figure 3-12 **Down-regulation of *TcVTE* gene in *T. castaneum* larvae fed on diets containing dsRNAs.** Larvae were fed on diet containing 500 ng/mg *TcVTE* dsRNA or *Kan* dsRNA (control) for 10 days; transcript levels were estimated by qPCR. Columns show the levels of transcript relative to *GADPH* transcript (internal standard), normalised to *Kan* control = 1.0. Error bars indicate standard errors of the mean for 3 technical replicates. Number of insects for each treatment n=5. Differences are significant between control *Kan* fed and *TcVTE* fed in 3 different biological replicas (Two-way ANOVA with $p<0.0001$, ****).

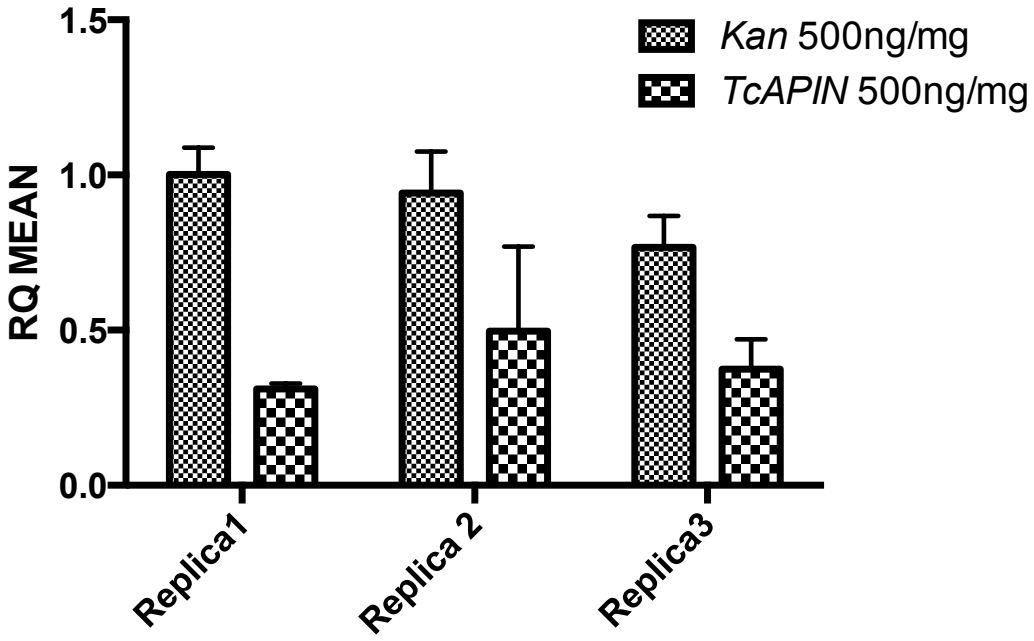

Figure 3-13 **Down-regulation of *TcAPIN* gene in *T. castaneum* larvae fed on diets containing dsRNAs.** Larvae were fed on diet containing 500 ng/mg *TcAPIN* dsRNA or *Kan* dsRNA (control) for 10 days; transcript levels were estimated by qPCR. Columns show the levels of transcript relative to *GADPH* transcript (internal standard), normalised to *Kan* control = 1.0. Error bars indicate standard errors of the mean for 3 technical replicates. Number of insects for each treatment n=5. Differences are significant between control *Kan* fed and *TcVTE* fed in 3 different biological replicas (ANOVA with $p<0.0001$, ****).

3.2.2 RNAi in *M. domestica* and *D. radicum*

3.2.2.1 Isolation of coding sequence and completion of *APIN* transcripts of *M. domestica* and *D. radicum*.

For isolating orthologues of the selected *Drosophila* gene targets were present in *M. domestica* and *D. radicum*, degenerate primers which could potentially be functional in a range of dipteran species were firstly designed based on the conserved amino acid sequence among model dipteran *D. melanogaster*, and other well-characterised dipteran spices including *Anopheles gambiae*, *Aedes aegyptica* and *Culex pipiens*. PCR products amplified from cDNA preparations were isolated and cloned, followed by sequencing. Gene specific primers for dsRNA region were then designed based on the sequence analysis. Sequences were extended to give complete coding sequences for the IAP proteins of *M. domestica* and *D. radicum* by 3' and 5' RACE (Rapid Amplification of cDNA Ends). The assembled *APIN* gene sequences of *M. domestica* and *D. radicum* are shown in Figure 3-14 and Figure 3-15 and predicted amino acid sequences are shown in Figure 3-16.

3.2.2.2 *APIN* gene expression pattern in *M. domestica* and *D. radicum*.

To identify suitable developmental stages to evaluate RNAi effects, the expression of the *APIN* gene was evaluated by qPCR. Under the growth conditions used (25°C) the *M. domestica* larval stage lasts for approx. 10 days, whereas for *D. radicum*, the larval stage lasts for approx. 3 weeks. *M. domestica* and *D. radicum* larvae were collected at time intervals after egg hatch corresponding to the developmental stages 1st-2nd instar, 2nd instar, 2nd-3rd instar and 3rd instar prepupal, followed by pupae and adult. Five insects per developmental stage were pooled and snap frozen in liquid nitrogen for RNA extraction. cDNA prepared from RNA was used as a template for evaluation of endogenous *APIN* expression by real-time quantitative PCR. The results shown in Figure 3-17 and Figure 3-18 demonstrate that in both species *APIN* gene expression can be detected throughout the whole life cycle, with a peak of expression at the pupal stage when tissue remodeling is taking place. Administering dsRNA to the pupal stage would be difficult as the injection process itself often causes mortality, and thus the 3rd instar pre-pupal stage was selected as the best developmental stage to observe RNAi responses.

3.2.2.3 Injection of *APIN*dsRNAs induced *APIN* gene downregulation and mortality in *M. domestica* and *D. radicum* larvae

Injection of *MdAPIN* dsRNA into third instar *M. domestica* larvae induced a significant APIN gene downregulation (Figure 3-19). The level of the *APIN* transcript was not affected 2h post injection, but *APIN* gene down-regulation, by approx. 3-fold, was observed after 24h compared to control treatment (ANOVA with $p<0.0001$). After 48h post injection, a slightly increased level of gene down-regulation was shown. Similar results were observed when *DrAPIN* dsRNA was injected into third instar *D. radicum* larvae. Significant (ANOVA with $p<0.0001$) *APIN* gene downregulation (approx. 3-fold) was detected both 24h and 48h after injection (Figure 3-20). These data show that dsRNA targeting *APIN* gene gives an efficient RNAi response in *M. domestica* and *D. radicum* larvae.

Injection of *APIN* dsRNAs into *M. domestica* and *D. radicum* larvae caused significant mortality (Mentel-Cox test with $p<0.0001$), which was dose dependent when injections were performed with different doses of *APIN* dsRNAs. Results for *M. domestica* are shown in Figure 3-21(2). Surviving in control treatment (injected with Kan dsRNA) was 90% over 6 days, similar to insects injected with water only. In contrast, 100% mortality was found after 3 days in insects injected with 500ng *MdAPIN*, and after 5 days in insects injected with 250ng *MdAPIN* dsRNA. Injection of 125ng *MdAPIN* dsRNA resulted in 60% mortality after 6 days. A similar result was recorded in early third instar *D. radicum* larvae treated with injection of *DrAPIN* dsRNA in Figure 3-22 (2), Mentel-Cox test with $p<0.0001$). Less than 10% mortality was found in control treatment and a dose-dependent effect in *DrAPIN* dsRNA treatment was detected. 100% mortality was found in 3 days after injection of 500ng *DrAPIN* dsRNA, whereas 85% and 75% mortality were recorded in treatment with 250ng and 150ng *DrAPIN* dsRNA treatment respectively after 7 days. The results suggest that *APIN* gene is a good gene candidate for using RNAi to control dipteran species.

M. domestica larvae injected with *MdAPIN* dsRNA exhibited blackened symptoms, which indicate excess apoptosis is occurring leading to necrosis (shown in Figure 3-21 (1)). *D. radicum* larvae injected with *DrAPIN* dsRNA resulted in similar phenotype (Figure 3-22 (1)). Survived larvae failed to reach full pupation stage, even though darkening of the cuticle took place, the insects remain in larviform (phenotype of injected *M. domestica* larvae are shown in Figure 3-21 (1) C-F and *D. radicum* are shown in Figure 3-22 (1) D). Injection of *MdAPIN* dsRNA in *M. domestica* pupae also leads to serious developmental abnormalities, with extensive melanisation of tissues taking place, suggesting uncontrolled apoptosis (Figure 3-21 (1) G-H). Adult *M.*

domestica emerged from *MdAPIN* injected pre-pupa stage larvae, show severe malformation of the abdominal regions (Figure 3-21 (1) J-K).

3.2.2.4 Species-specificity of RNAi effects in *Dipteran* spp.

To investigate whether RNAi effects induced by injection of dsRNA can affect closely related Dipteran species, like the pattern observed previously in Coleopteran species, three different doses (150ng, 250ng and 500ng) of dsRNA against the *D. radicum DrAPIN* gene were injected into 3rd instar *M. domestica* larvae. Alignment of sequences from *M. domestica* and *D. radicum APIN* genes used in templates for dsRNA preparation are shown in Figure 3-23. Results are shown in Figure 3-24. Control survival of larvae injected with water or *Kan* dsRNA were >85%. The larvae injected with *DrAPIN* dsRNA showed a dose-dependent effect on larval mortality. Approx. 50% mortality *M. domestica* larvae injected with 500ng *DrAPIN* dsRNA was observed after 5 days compare to Kan 500ng dsRNA (Mentel-Cox test with P=0.0478), whereas mortality from 150ng and 250ng doses was approx. 30% and 40% after 5 days.

Down-regulation of *MdAPIN* gene expression by injected *DrAPIN* dsRNA was confirmed. One hundard and fifty nanograms and 500ng *DrAPIN* dsRNA were injected into 3rd instar *M. domestica* larvae. The insect samples were collected at 48h and 72h post injection. qPCR results for *APIN* transcript levels are shown in Figure 3-25. House fly larvae injected with 150ng *DrAPIN* dsRNA showed 60% *APIN* gene down-regulation compared to control treatments after 48 (ANOVA test with P=0.040). Significant *APIN* gene down-regulation was also observed in insects injected with 500ng dsRNA (ANOVA test with P=0.024), although there was no dose-dependency in the degree of down-regulation observed. Levels of *APIN* gene transcripts did not decrease further after 72 h compared to 48h post injection.

3.2.2.5 RNAi effects in *M. domestica* adults

The specificity of RNAi effects to specific developmental stages in *M. domestica* was investigated by injecting newly emerged *M. domestica* adults with dsRNA. Flies injected with 150ng and 500ng *MdAPIN* dsRNA were firstly monitored for 6 days to record survival data. The results shown in Figure 3-26 give no indication of any mortality resulting from injection with *APIN* dsRNA. However, this could be due to a phenotype not being observed as gene expression is not essential at this developmental stage.

To show whether injection of dsRNA caused down-regulation of gene expression in adult flies, injected flies were also collected after 48h and 72h, and used to prepare cDNA for analysis of *APIN* transcript levels by qPCR. Results are shown in Figure 3-27. In agreement with survival data, the *APIN* transcript was not down

regulated by injected *APIN* dsRNA in fly adult. Flies injected with 150ng dsRNA shows similar *APIN* transcript level compared to control treatment. Unexpectedly, flies injected with 500ng *MdAPIN* dsRNA show increased (approx. 2-fold) *APIN* gene expression compared to the control treatment after 48h. These results indicate that the RNAi effect induced by dsRNA injection is dependent on developmental stage in *M. domestica*, with larvae showing a robust effect, which is absent in adults.

3.2.2.6 Oral feeding bioassays targeting *APIN* gene in *M. domestica* larvae

A concentration of 100ng *MdAPIN* dsRNA/mg diet was used in a feeding bioassay to determine whether RNAi effects could be produced in *M. domestica* larvae. The survival data was recorded over 7 days continuous oral feeding of dsRNA mixed in artificial diet. No significant mortality due to the MdAPIN dsRNA was observed compared to control treatment，as shown in Figure 3-28; both treatment and control gave approx. 10% mortality.

In a second feeding bioassay, bacteria expressing MdAPIN dsRNA were mixed in diet at final concentration 200ng/mg and fed directly to *M. domestica* larvae. Survival data was recorded for 6 days. No significant differences on larval survival were found between treatments (Figure 3-29).

Insects fed on diets containing *MdAPIN* dsRNA were also analysed by qPCR after varying times of exposure. Results are shown in Figure 3-30, and confirm that the *APIN* gene was not down-regulated by this treatment; although marginal effects on transcript levels are observed, differences between treatment and control are not significant (ANOVA test) over 96 hours feeding.

```
   1  AAGCAGTGGT ATCAACGCAG AGTACGCGGG GAGTCTTCAA TTTTCTACTC
  51  AACAAAAGAA AGAAACAAAC TTAAAACAAA AAAACTGTTA AAAATGTAAA
 101  TGAAAAAATC AATATATTTT TTTTTATCAT GGCTGTTGTG AACAACAATC
 151  TACAAAATAC AGCCGCAGCA ACATTTGAAT TCCTTGTAAG AAAAAACGCA
 201  ACAACAACAC CAACAACAAC GTCATATTTT GAAAATAAAC AAGATAACAT
 251  CAACAATTAT GAAAATGTCT GGAAATGTAG CAACCGAAAT ATGGGCCTCA
 301  CAGCCACAGC TATGGTTGGT ACCATTCCCA AGTAATTTAT TGAAACATAT
 351  ACCATCCAAT CCGACACCAG CAGCATTAGC AAGTGTCCCA AATCAGGACG
 401  AAACGGATAA TAATACACAT AACGAGTTTC TACAAATTGG CCAATTAAAG
 451  CCACGTTATG CCATGGACGA TAGATTCCAT CGTGAAGATG AACGCCTCAA
 501  GACGTACGAA AATTGGCCAT TGAATTTCTT GGATCCCAAC GAATTGGCTC
 551  GTTCGGGCAT GTTCTATATG GGCGAATCGG ATAAAACCAA ATGCTATTTC
 601  TGTGAGGTGG AAATTGGCCG GTGGGAACGT GAAGATCAAC CTGTACCTGA
 651  ACATCTGCGC TGGTCGCCCA ATTGCCCCTT GCTGAGGAGG CGCACTACCA
 701  ACAATGTGCC CATCAATGCT GAACTCTTAG AGCGTACCTT ACCCGCCCCC
 751  AGTTATGATA TTTGCGGAGC GAATGACATT GAAATCAGAC GAAATGCATT
 801  TGCTGAAGGC ACCATCCCAG CACCACTAAT GTCCGATGTA CCACCTGGCT
 851  CACCAATGGT TATGGCGGCC GGCAGCAGTA GCGCTGGTGG TGGCAGTGCA
 901  ATGACAACTG GAGGCACATT TTTCCCCGAG GTGCCCGAAT ATGCCATCGA
 951  AACAGCCCGT ATACGATCCT TTGCCGAATG GCCACGAAAC ATGAAACAAA
1001  AACCTGAACA GTTGGCCGAG GCCGGTTTCT TCTATACTGG TGTGGGCGAT
1051  CGTGTCAAGT GCTTCAGTTG TGGCGGTGGT CTTAAGGACT GGGACGATGA
1101  TGATGAACCC TGGGAACAGC ATGCCTTGTG GATGAATAAA TGTCGTTTTG
1151  TAAAATTGAT GAAAGGCGAT GCATTCATTG AAGCTGTGGC AAATAAATTC
1201  ATGAAAAATA AACCAGCTGC AAGCAACAAC AGAACTCCTA CACCAACGTC
1251  GGAATCGCCT CTCTCCTCGT CGGAAGAAGA GGGGGAGCCT GCAGTGCATT
1301  TGGCGGAGGG AAATCAAGAA ACAACACATA CAACGGTTGC AGTCGCCGGT
1351  TCCGCTGCAA CAAAAGTATC ATCCGCTTCA ATTCCCAAGC CTTGTTCCAA
1401  CGAACAGGCA CCCTCCACAA CTGCTGTCGC CGGTGTCAAT GCCTTGGAAC
1451  AGAAAAGGTC GAGCTCCACA ATACCCGAGG AGAAATTGTG CAAAATCTGC
1501  TATGCCAACG AATACAATAC AGCGTTTTTA CCCTGTGGCC ACGTTGTGGC
1551  CTGTGCCAAG TGCGCCTCGT CTGTTACAAA ATGTCCAATG TGTCGGAAAC
1601  CTTTTGCCGA TGTTATGAGG GTTTATTTCT CTTAAATTCG GAACAACAGC
1651  CACAACCGAG AATAATAACA GATAGCTGTA AAAAACTAAG AAAGCGTTTC
1701  CTCCTGATAT ACGTCGATGA TGTACATACT AATTTTATAA TACCCCGCCT
1751  TTGTAATACA TTTCTTCTAA TCAAACGAGT TTAACGGCCA GTTGAGATTT
1801  GTGCGAAACA TGCTAACGAG CTGAATGATG GGTATAAGTC TTAACTGGCC
1851  GTTAAATTTG CAAACAAACC AACCAACAAA GGAAGAAGAA TGAGAAGAAA
1901  ATAAGTTTAT TATTCCCATA AGAACTTATA ATTACATTAG GATAAAGATA
1951  AATCCATAAT TTATGTATAA AACCATAGAG GAAATAAATC CTTTGTAAAT
2001  AAAAGCATCA TTTGCAATTA CTTTAAAATA CAATTAAAAT TAATGCCCAA
2051  CATATTTATA TTTTCACCAA CCATTGTAAT AG(A)n
```

Figure 3-14 **Assembled sequence of housfly *APIN* transcript.**

This sequence is 98% identical to GenBank entry XM_011292268.1 *Musca domestica* apoptosis 1 inhibitor (LOC101889679), transcript variant X3, mRNA. Differences are as follows:

Extra bases at 5' end (1-39) highlighted in blue

Extra bases at 3' end (1663-2082) highlighted in green

Two base insertion bases 76-77

12 base deletion between bases 198-199

Extra bases at 1336-1341

Single base changes at bases 549, 856, 915, 927, 951, 1029, 1258.

Coding sequence = bases 259 – 1632, highlighted in bold.

```
   1  TAGCAGATCT AATACGACTC ACTATAGGGC AAGCAGTGGT ATCAACGCAG
  51  AGTACGCGGG GATTCGTAAA ACTGAATCTC TAATAACAAG TCATAAAAAT
 101  ATATTTTCAA CTTACAAGTC TTAATTTTTT TTAATTTTAA ATTAAAAAGA
 151  AAAGTAAAAA ATATGAAAGA TATATAAAAA AATATTTATC GCACTATCTG
 201  TTTAAAACAA TTGTTAACTG TTTATCACTG TTGTAATATC GTTTCTTGAA
 251  AACAATAGTA AAACGTATCT CAAACAAAAT GCCTGGAGAT TTATTAACGG
 301  AAAGACCGCC GCTGTCTAAT GGCCAGGTAT TTCCAACTAA CCTATTCTAT
 351  TCGTCCTCAA CGGGTCGTTT CAACAATCCA TTGAGTTTTA TACGAAAGTT
 401  CTCGACTCAA GCGTTATCAC ACGGCCGGGA CGAAATTGAT AATAATACGC
 451  ATAGTGATTT TTTGCAAACT GGCATATTTA AACCACGCTA TGAAATGAAT
 501  GATATATTCC ATAGAGAAGA TGAACGCTTA AAAACATTTG AAAGTTGGCC
 551  GTTGGAATGG TTGGATAAGA AACAATTGGC CATGTCGGGA ATGTTTTATA
 601  TGGGTGATGG TGATAAGACA AAGTGTTATT TTTGTGAAGT CGAAATTGGT
 651  CGTTGGGAAA GAGAGGATCA ACCTGTACCT GAACATCTGC GCTGGTCGCC
 701  AAATTGTCCT CTTCTCAGAA GACGTACTAC CAACAATGTA CCCATTAATT
 751  GTGAGGCTTT AGAGCGATTA CTACCGCCAC CCAGCTATGA CATCTGTGGT
 801  CTCAATGAAC CCATAGAAAT ACGTCGTAAT GCTTTTGCCG AGGGCACTAT
 851  ACCAGCTGTT AACTTTTCCG CTATGGATGT ACCACCGGGA TCACCAGCCA
 901  ACGTTAGCTC AAGTAGTAAT AGTAGTACAG GGACATTTTA TCCCGAATTT
 951  CCCGAATATG CTATAGAAAC TGCACGTTTA AGATCATTTG CGGAATGGCC
1001  GCGACATATG AAACAAAAAC CACCACAATT GGCCGAGGCT GGTTTCTTTT
1051  ATACCGGTGT AGGTGATCGT GTTAAATGTT TCAGTTGTGG TGGTGGTCTT
1101  AAGGATTGGG ATGAAGATGA CGAACCCTGG GAACAACATG CATTGTGGAT
1151  GGGTAAATGT CGTTTTTTGA AACTAATGAA AGGAGAAAAT TATATAGAAG
1201  CTGTTGTAAA TAAATTTAAA AAACCAGACG CTTCAACATC ATCCTCTACA
1251  TCATCACCTT CTCCTACCAA CTCCTCTACT GAAGAAGAGG GGGAGTTGCA
1301  ACAAGCACAA GCTGTAGGTG TAACTACTCA ACAAGTTTTA GCACAGAAAT
1351  CAGCAGCTAC TATCAATCTT CCAAAAGAGG AAGAGATTTT AACAGTATCG
1401  GAACAGGCTT CTCGCATACA CCATATGGCC ACGCAACAAG AAATAACACC
1451  ATCATCACAT CAAGCAGCCT CCATTACAAA TTGCTGCAAT ATAGAACAGA
1501  ACAAACCATC ATCATCATCG TTCTCTTCAG TCATACCCGA AGAGAAATTA
1551  TGCAAAATTT GTTATGCCAA CGAATACAAT ACAGCGTTTT TACCCTGCGG
1601  TCATGTAGTG GCTTGTGCCA AATGTGCATC GTCCGTTACA AAGTGTCCCC
1651  TGTGTCGAAA ACCTTTTGCC GATGTTATGC GTGTATATTT CTCTTAAGAT
1701  CTAACCTCAA TTATTACTAC ATATATAATC ATAGTGATTT CTATTGCAAA
1751  CAATTAAAAA CTGTTTTTCT ACTCTCTCTG TTTCTTTATC AACTTTCCCC
1801  AAATAGTTTT AGAAATGTAT ATAATTTTGT ATTAACAACC TGCCTTGAAA
1851  TATATTTAAA TCTAGAAAAA AGTCTTTAAC GGCCAGTTAG GATTTGTTTC
1901  AACATCATTC TACGATGTGA GTCTTAACTG GCCGTTAAAT TTTCTACATT
1951  ATATTGGCAA ACATATTGAA AGAAAATCCC AAAAACTTAC ACTATATCCA
2001  AACAAATTTA ATTTATAAAA AAAAAAGTAA ATCAT(A)n
```

Figure 3-15 **Assembled sequence of *D. radicum APIN* mRNA.**

Coding sequence = bases 279 – 1694, highlighted in bold.

Extra bases at 5' end (1-271) highlighted in blue

Extra bases at 3' end (1697-2001) highlighted in green

M. domesctia APIN predicted polypeptide：

```
  1 MKMSGNVATE IWASQPQLWL VPFPSNLLKH IPSNPTPAAL ASVPNQDETD
 51 NNTHNEFLQI GQLKPRYAMD DRFHREDERL KTYENWPLNF LDPNELARSG
101 MFYMGESDKT KCYFCEVEIG RWEREDQPVP EHLRWSPNCP LLRRRTTNNV
151 PINAELLERT LPAPSYDICG ANDIEIRRNA FAEGTIPAPL MSDVPPGSPM
201 VMAAGSSSAG GGSAMTTGGT FFPEVPEYAI ETARIRSFAE WPRNMKQKPE
251 QLAEAGFFYT GVGDRVKCFS CGGGLKDWDD DDEPWEQHAL WMNKCRFVKL
301 MKGDAFIEAV ANKFMKNKPA ASNNRTPTPT SESPLSSSEE EGEPAVHLAE
351 GNQETTHTTV AVAGSAATKV SSASIPKPCS NEQAPSTTAV AGVNALEQKR
401 SSSTIPEEKL CKICYANEYN TAFLPCGHVV ACAKCASSVT KCPMCRKPFA
451 DVMRVYFS
```

D. radicum APIN predicted polypeptide:

```
  1 MPGDLLTERP PLSNGQVFPT NLFYSSSTGR FNNPLSFIRK FSTQALSHGR
 51 DEIDNNTHSD FLQTGIFKPR YEMNDIFHRE DERLKTFESW PLEWLDKKQL
101 AMSGMFYMGD GDKTKCYFCE VEIGRWERED QPVPEHLRWS PNCPLLRRRT
151 TNNVPINCEA LERLLPPPSY DICGLNEPIE IRRNAFAEGT IPAVNFSAMD
201 VPPGSPANVS SSSNSSTGTF YPEFPEYAIE TARLRSFAEW PRHMKQKPPQ
251 LAEAGFFYTG VGDRVKCFSC GGGLKDWDED DEPWEQHALW MGKCRFLKLM
301 KGENYIEAVV NKFKKPDAST SSSTSSPSPT NSSTEEEGEL QQAQAVGVTT
351 QQVLAQKSAA TINLPKEEEI LTVSEQASRI HHMATQQEIT PSSHQAASIT
411 NCCNIEQNKP SSSSFSSVIP EEKLCKICYA NEYNTAFLPC GHVVACAKCA
451 SSVTKCPLCR KPFADVMRVY FS
```

Figure 3-16 **Predicted *APIN* gene products in *M. domestica* and *D. radicum*.**
BIR repeat domain, IPR001370 is highlighted in red and Zinc finger domain, RING/FYVE/PHD-type (IPR013083) is highlighted in blue.

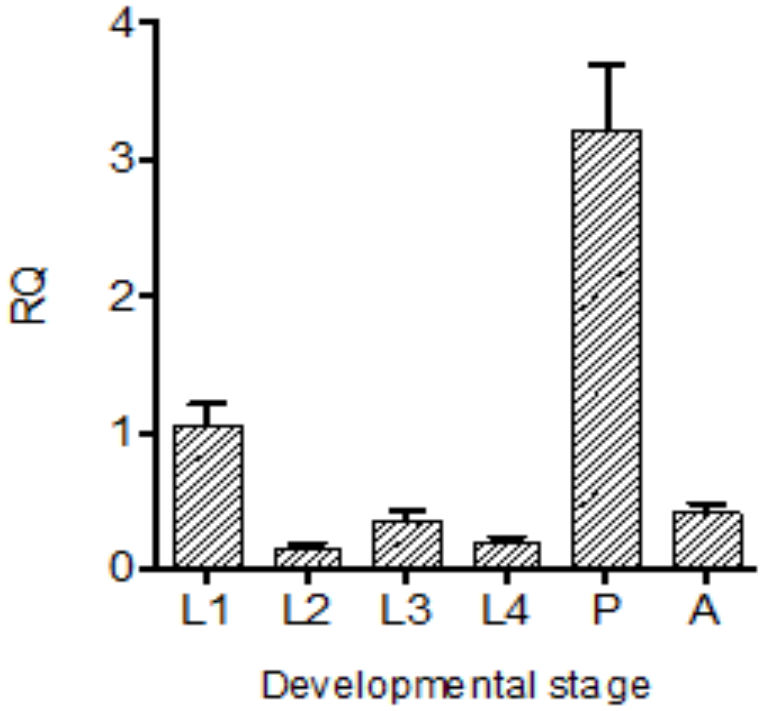

Figure 3-17 ***MdAPIN* expression profiles in different life stages of *M. domestica.*** Columns show the levels of transcript relative to *GADPH* transcript (internal standard) as estimated by qPCR, normalised to *MdAPIN* level in at stage L1 = 1.0. Error bars indicate standard errors of the mean for 3 technical replicates. L1 = stage 1, 1st-2nd larval instar; L2 = stage 2, 2nd larval instar, L3 = stage 3, 2nd-3rd larval instar, L4 = stage 4, 3rd larval instar prepupal, P = pupae, A = adult. Number of insects for each treatment n=5.

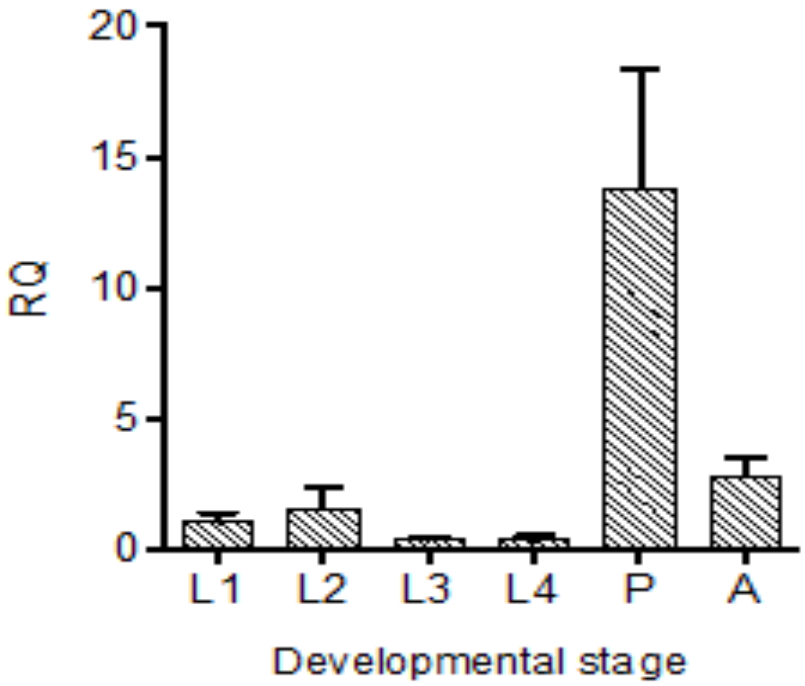

Figure 3-18 ***DrAPIN* expression profiles in different life stages of *D. radicum*.** Columns show the levels of transcript relative to *GADPH* transcript (internal standard) as estimated by qPCR, normalised to *DrAPIN* level in at stage L1 = 1.0. Error bars indicate standard errors of the mean for 3 technical replicates. L1 = stage 1, 1st-2nd larval instar; L2 = stage 2, 2nd larval instar, L3 = stage 3, 2nd-3rd larval instar, L4 = stage 4, 3rd larval instar prepupal, P = pupae, A = adult. Number of insects for each treatment n=5.

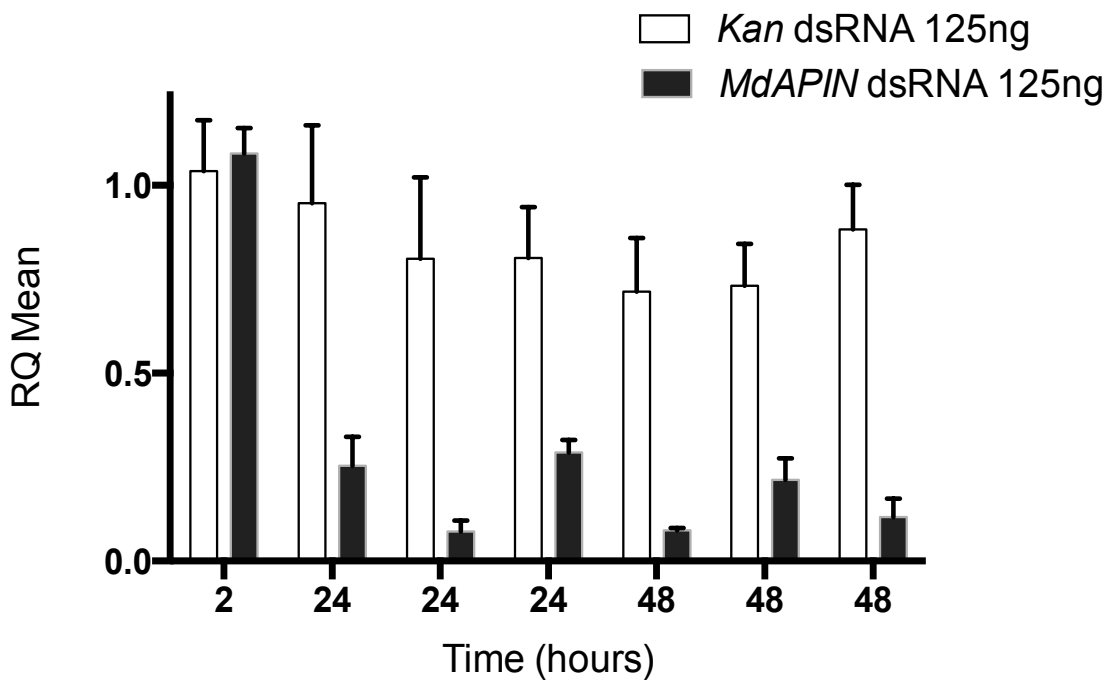

Figure 3-19 **Down-regulation of *MdAPIN* gene by injection of *MdAPIN* dsRNA.** 3rd instar *M. domestica* larvae were injected with 125ng dsRNA, and collected at times as shown after injection for estimation of transcript levels by qPCR. Error bars indicate standard errors of the mean for 3 technical replicates; 24 and 48h timepoints .are shown as 3 separate biological replicates. Number of insects for each treatment n=5. Significant difference was analysed by two-way ANOVA with $p<0.0001$, ****.

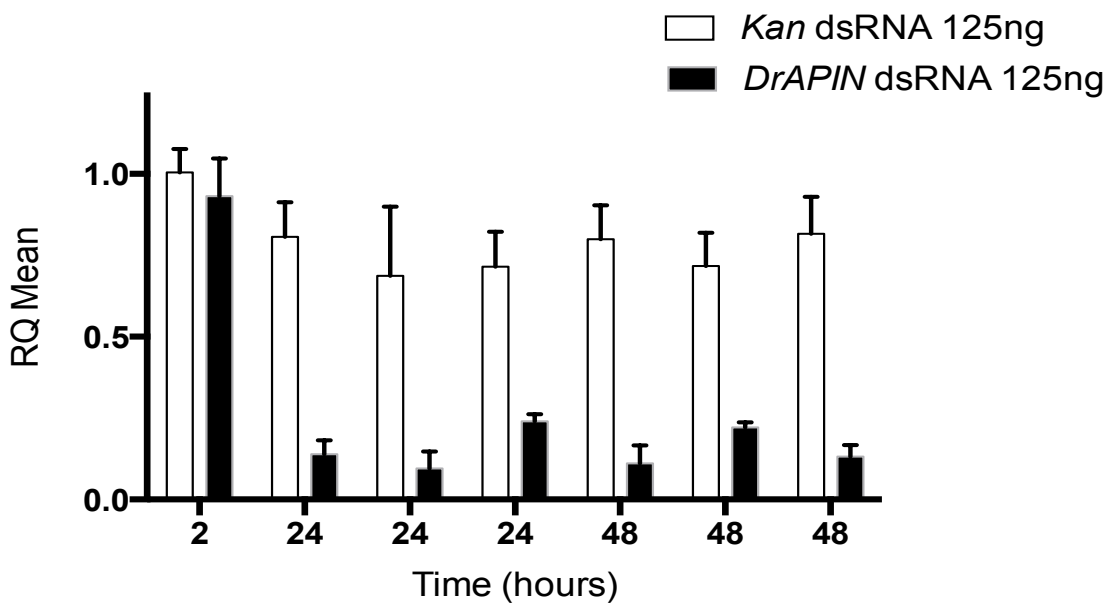

Figure 3-20 **Down-regulation of *DrAPIN* gene by injection of *DrAPIN* dsRNA.** 3rd instar *D. radicum* larvae were injected with 125ng dsRNA, and collected at times as shown after injection for estimation of transcript levels by qPCR. Error bars indicate standard errors of the mean for technical replicates; 24 and 48h timepoints .are shown as 3 separate biological replicates. Number of insects for each treatment n=5. Significant difference was analysed by ANOVA with $p<0.0001$, ****.

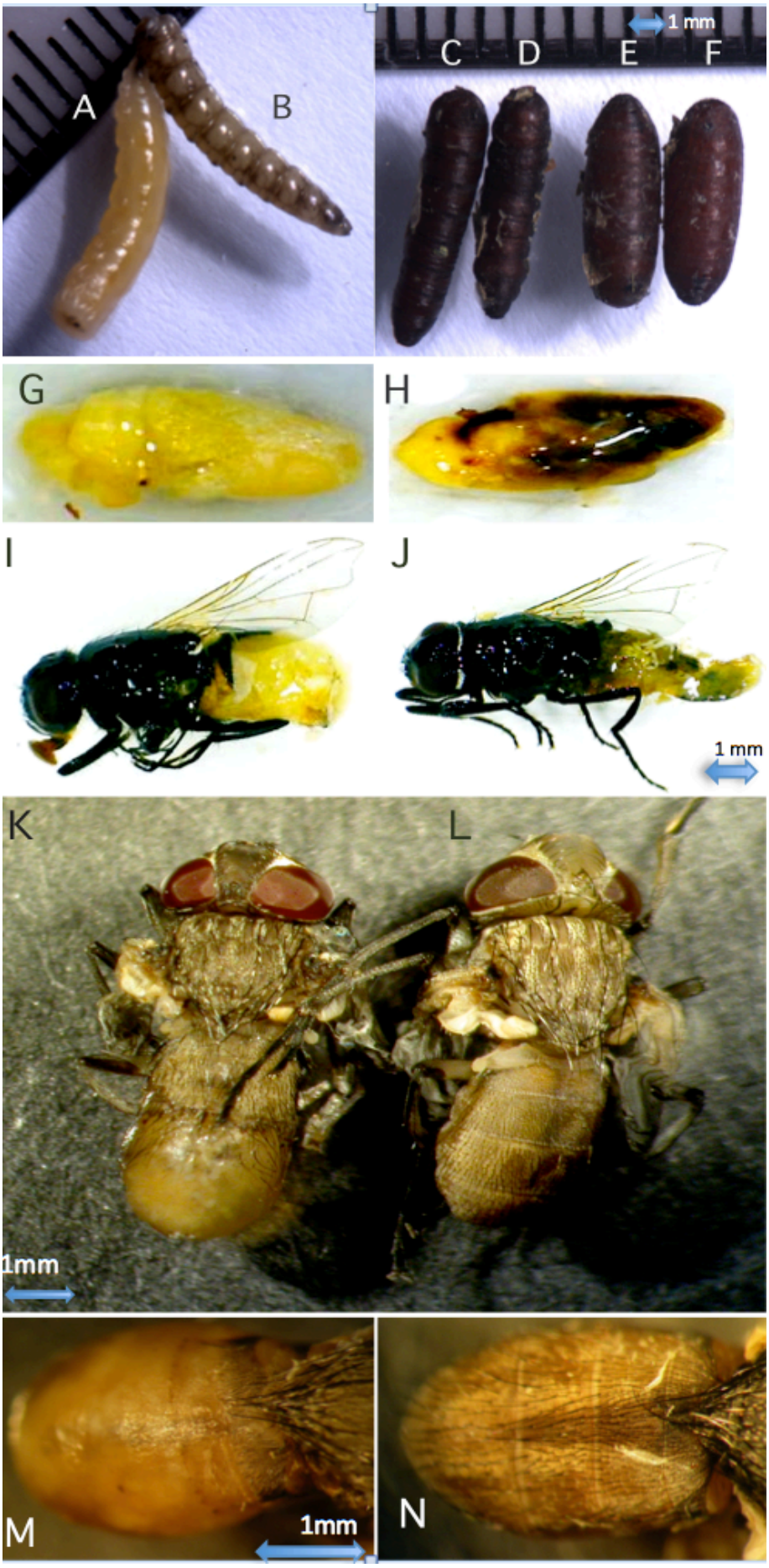

(1)

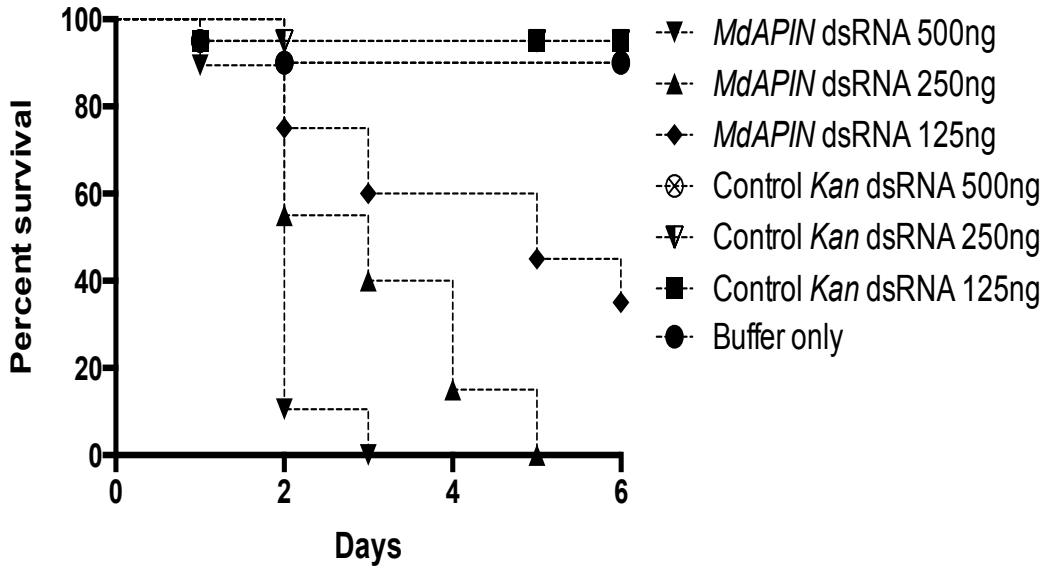

(2)

Figure 3-21 **Mortality of *M. domestica* larvae after injection of *MdAPIN* dsRNA. N=20**

Larvae were injected with varying doses of MdAPIN dsRNA as indicated (2);

Phenotypes observed in this experiment are shown below (1):

A and B: Control and *APIN* dsRNA (respectively) injected 3rd instar larvae (300ng/larva) 48 hours post injection.

C & D and E & F: *MdAPIN* dsRNA and control (respectively) injected pupae (300ng/larva). G and H: Dissected pupae injected with 500ng control and *MdAPIN* dsRNA, respectively. I and J: Emerged adults injected (as pre-pupal larva) with 500ng control and *M dAPIN* dsRNA, respectively.

K and L: Pulled-out adult injected (as pre-pupal larva) with 500ng control and *MdAPIN* dsRNA (resp.) M and N close-up pictures of K and L.

Significant difference was analysed between control and tested treatment with same dsRNA dose by Mentel-Cox test with $p<0.0001$, ****.

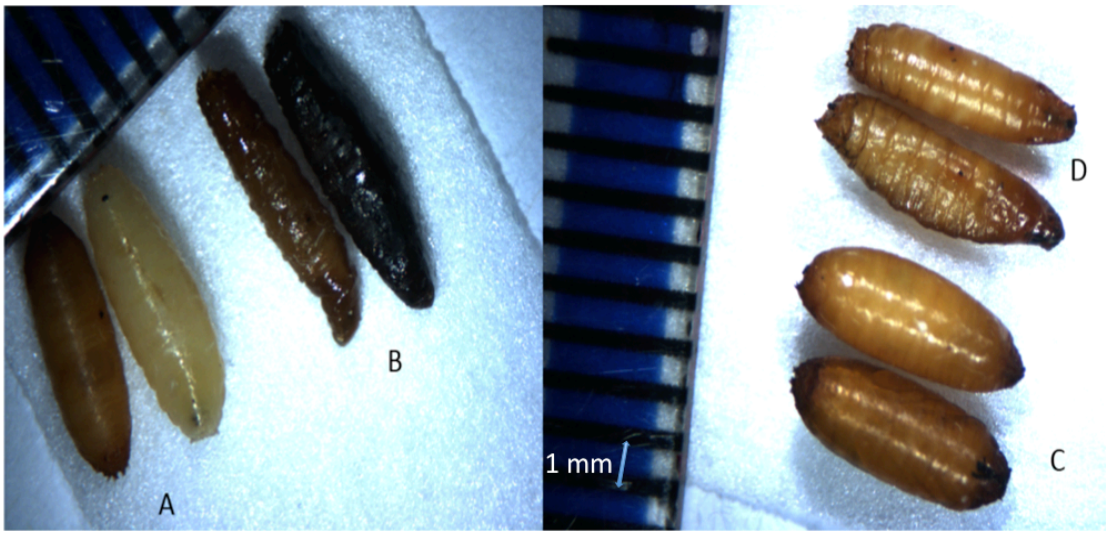

(1)

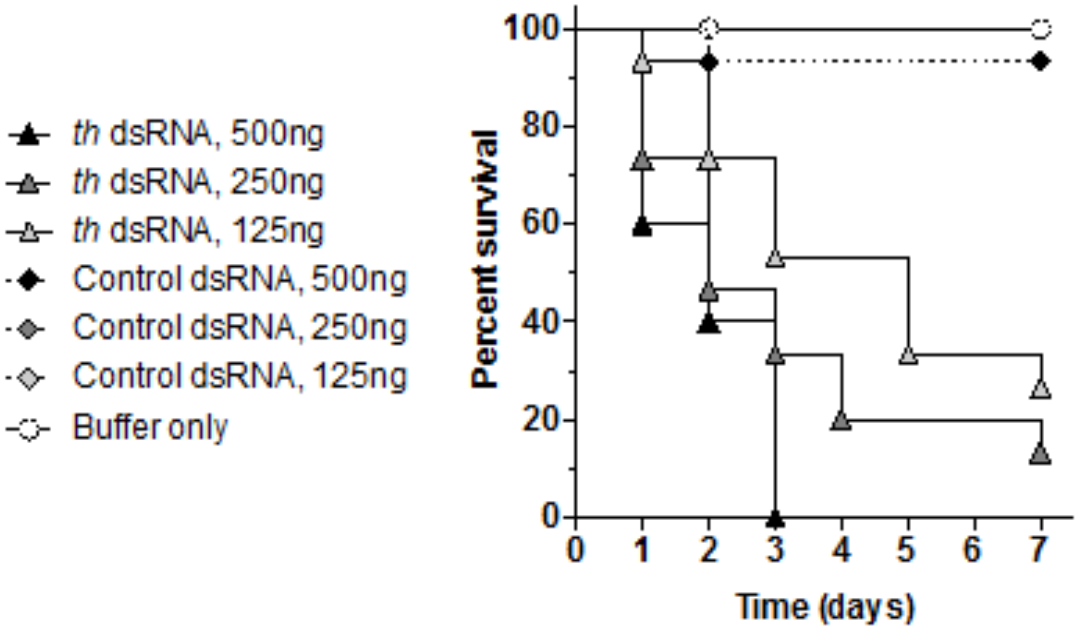

(2)

Figure 3-22 **Mortality of *D. radicum* larvae after injection of *DrAPIN* dsRNA. N=20**
Larvae were injected with varying doses of *DrAPIN* dsRNA as indicated (2);
Phenotypes observed in this experiment are shown below (1):
150ng Kan dsRNA (A) and *DrAPIN* dsRNA (B) injected into pre-pupal stage larvae. Misformed pupae were observed in *DrAPIN* dsRNA injected treatment (D) whereas healthy pupae injected with Kan dsRNA is shown in (C). Significant difference was analysed between control and tested treatment with same dsRNA dose by Mentel-Cox test with $p<0.0001$, ****.

```
Md         TGGCGGTGGTCTTAAGGACTGGGACGATGATGATGAACCCTGGGAACAGCATG
Dr TCAGTTGTGGTGGTGGTCTTAAGGATTGGGATGAAGATGACGAACCCTGGGAACAACATG
          *** ************** ***** ** ***** ************** ****

Md CCTTGTGGATGAATAAATGTCGTTTTGTAAAATTGATGAAAGGCGATGCATTCATTGAAG
Dr CATTGTGGATGGGTAAATGTCGTTTTTTGAAACTAATGAAAGGAGAAAATTATATAGAAG
   * *********  ************* * *** * ******** **    *  ** ****

Md CTGTGGCAAATAAATTCATGAAAAATAAACCAGCTGCAAGCAACAACAGAACTCCTACAC
Dr CTGTTGTAAATAAATTTAAAAAA------CCAGACGCTT-CAACATCA----TCCT----
   **** * ********* *  ***      ****  **   ***** **    ****


Md ------CAACGTCGGAATCGCCTCTCTCCTCGTCGGAAGAAGAGGGGGAGCCTGCAGTGC
Dr CTACATCATCACCTTCTCCTACCAACTCCTCTACTGAAGAAGAGGGGGAG-TTGCAACAA
          ** *  *     *  *   ******  * ***************  ****


Md ATTTGGCGGAGGGAAATCAAGAAACAACACATACAACGGTTGCAGT
Dr GCACAAGCTGTAGGTGTAACTACTCAACAAGTTTTAGCACAGAAATCAGCAGCTACTATCA
                      *    *****      *       * *


Md ATCTTCCAAAAGAGGAAGAGATTTTAACAGTATCGGAACAGGCTTCTCG
```

Figure 3-23 **Alignment of sequences from *M. domestica* and *D. radicum APIN* genes used in templates for dsRNA preparation.**

The sequences correspond to bases 1071 - 1343 of the sequences of *MdAPIN* mRNA, and bases 1081 - 1414 of the *DrAPIN* mRNA, given above.

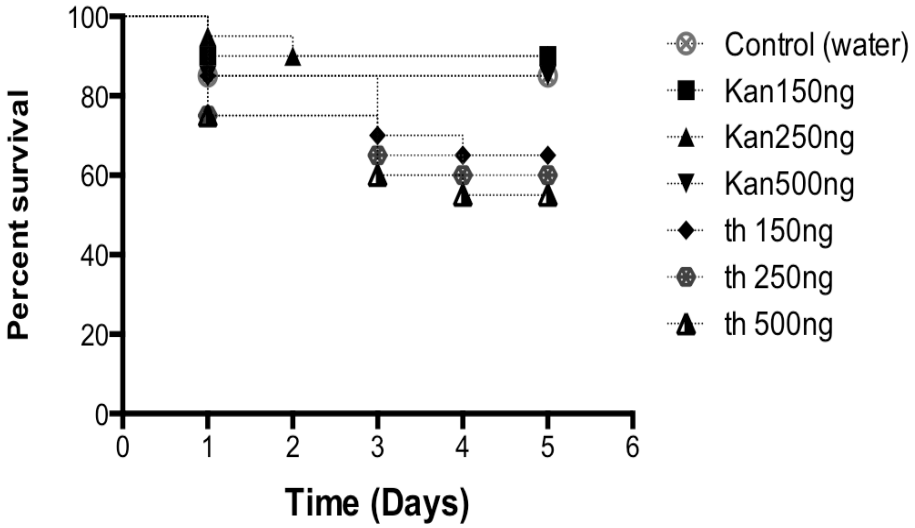

Figure 3-24 **Mortality of *M. domestica* larvae after injection of *DrAPIN* dsRNA.** Larvae were injected with varying doses of *MdAPIN* dsRNA as indicated. Number of insects for each treatment n=20. Significant different was analysis by Mentel-Cox test between Kan 500ng and *DrAPIN* 500ng with P=0.0478, *

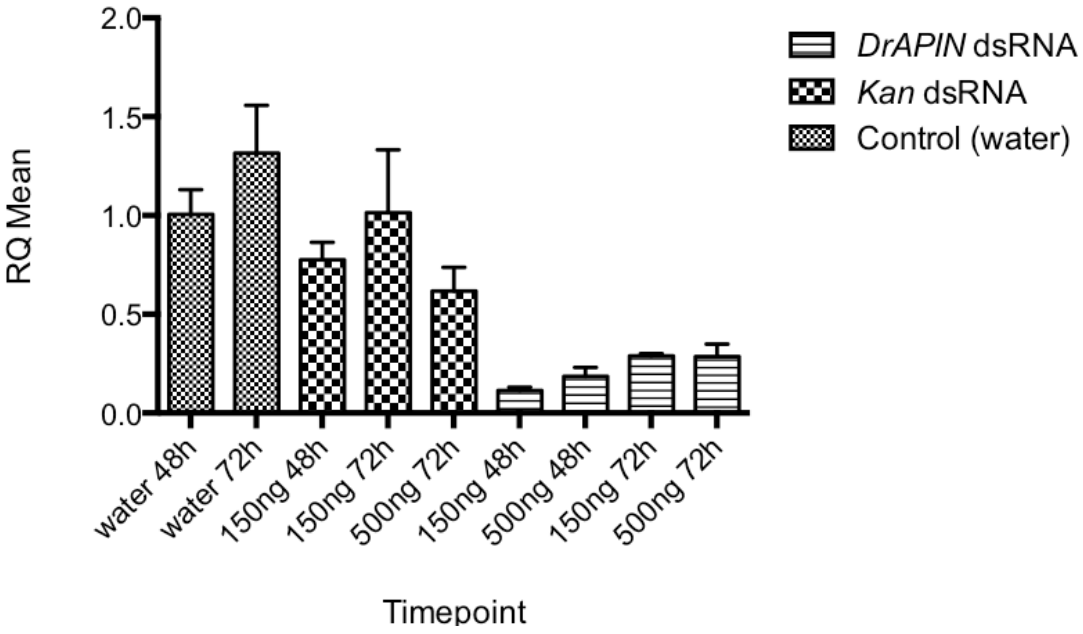

Figure 3-25 **Down-regulation of *MdAPIN* gene in *M. domestica* larvae injected with *DrAPIN* dsRNA.** 3rd instar *M. domestica* larvae were injected with dsRNA as shown, and collected at times as shown after injection for estimation of transcript levels by qPCR. Error bars indicate standard errors of the mean for 3 technical replicates. Number of insects for each treatment n=5. Differences are significant in *Kan*150ng and *DrAPIN*150ng dsRNA treatment according to ANOVA with P=0.0040, **. P=0.0024, ** in treatment between *Kan*500ng and *DrAPIN*500ng.

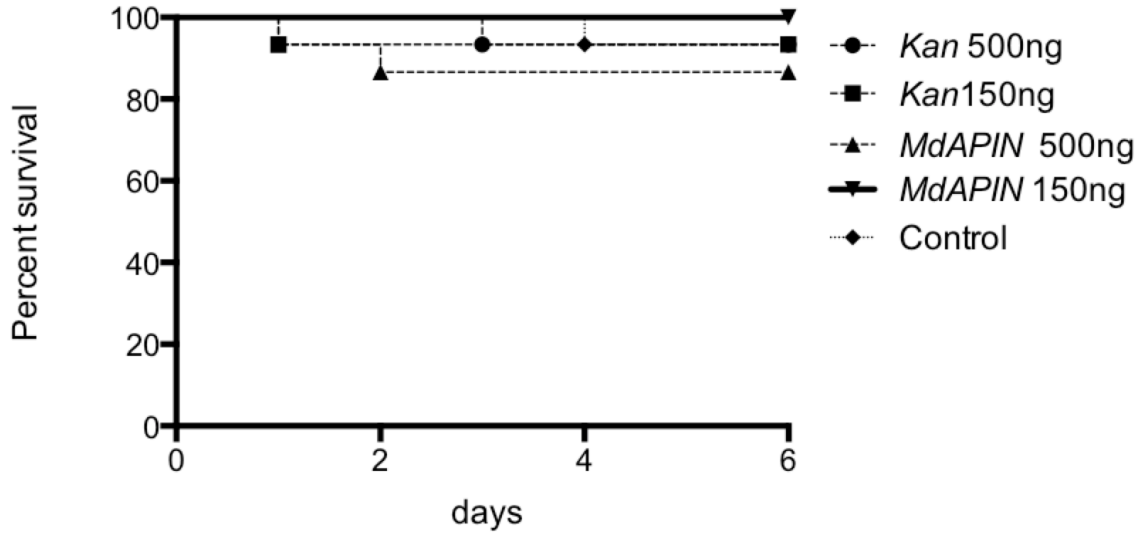

Figure 3-26 **Mortality in *M. domestica* adults after injection of *MdAPIN* dsRNA.** dsRNA was injected at two doses, as indicated. Number of insects for each treatment n= 20. No significant difference between treatemts (Mentel-Cox) test.

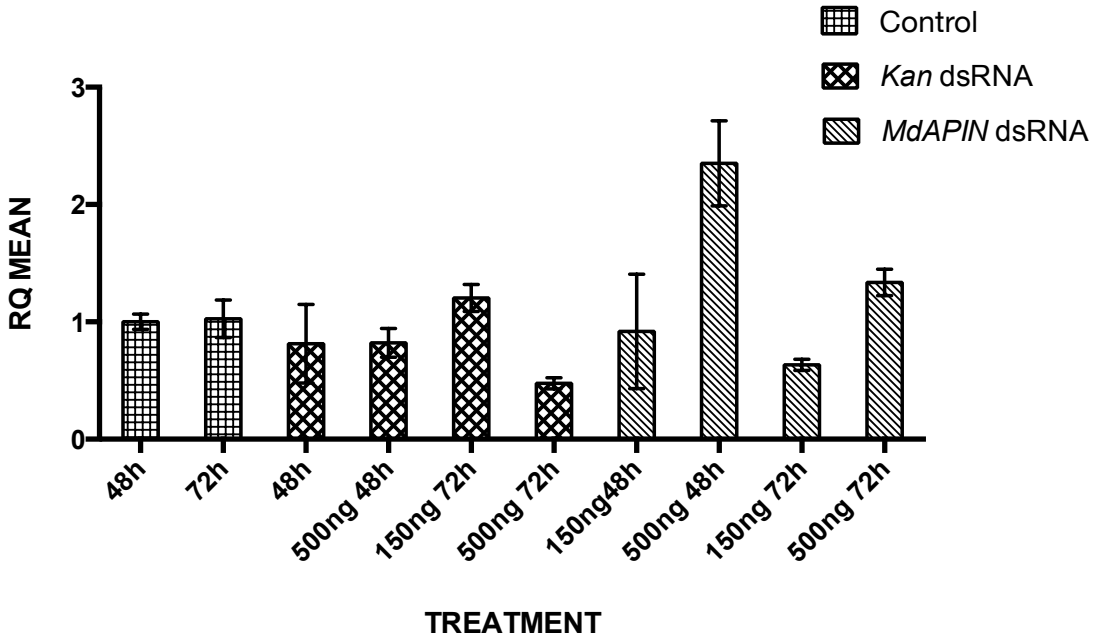

Figure 3-27 **Assay of *APIN* mRNA transcripts in *M. domestica* adults after injection of *MdAPIN* dsRNA.** *M. domestica* adults were injected with dsRNA as shown, and collected at times as shown after injection for estimation of transcript levels by qPCR. Error bars indicate standard errors of the mean for 3 technical replicates. Number of insects for each treatment n=5. Difference is not significant analysed by ANOVA.

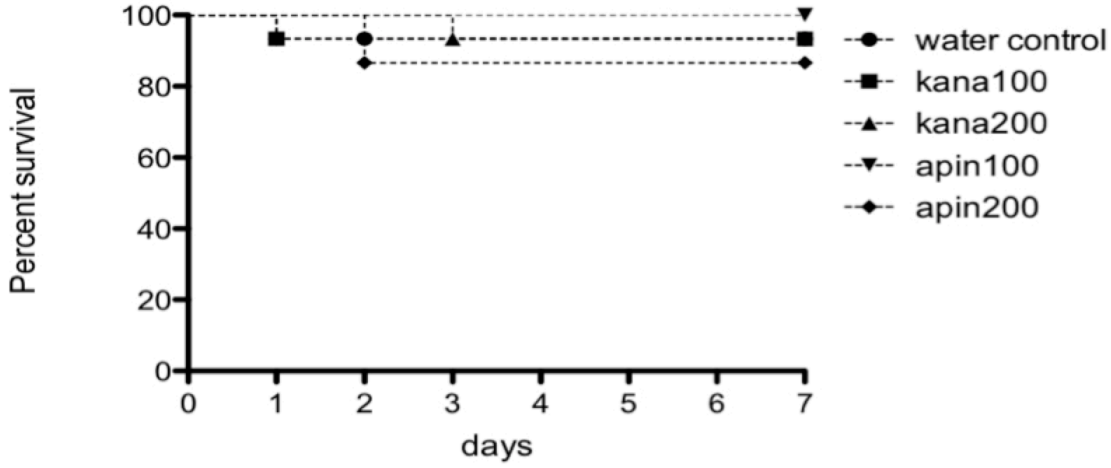

Figure 3-28 **Survival of *M. domestica* larvae after feeding diet containing *MdAPIN* dsRNA.** Number of insects for each treatment n=20. Difference is not significant analysed by ANOVA.

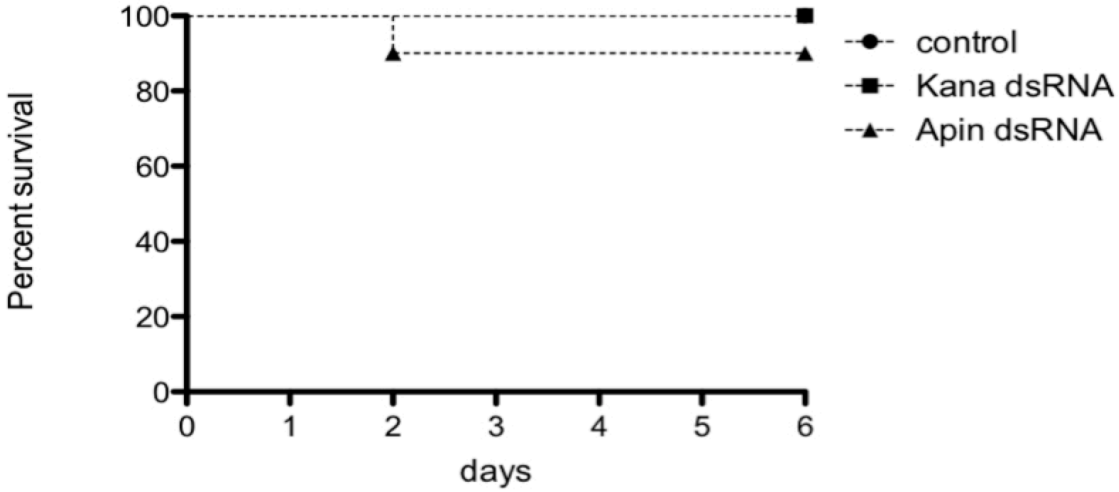

Figure 3-29 **Survival of *M. domestica* larvae after feeding diet containing bacteria expressing *MdAPIN* dsRNA.** Number of insects for each treatment n=20. Difference is not significant analysed by ANOVA.

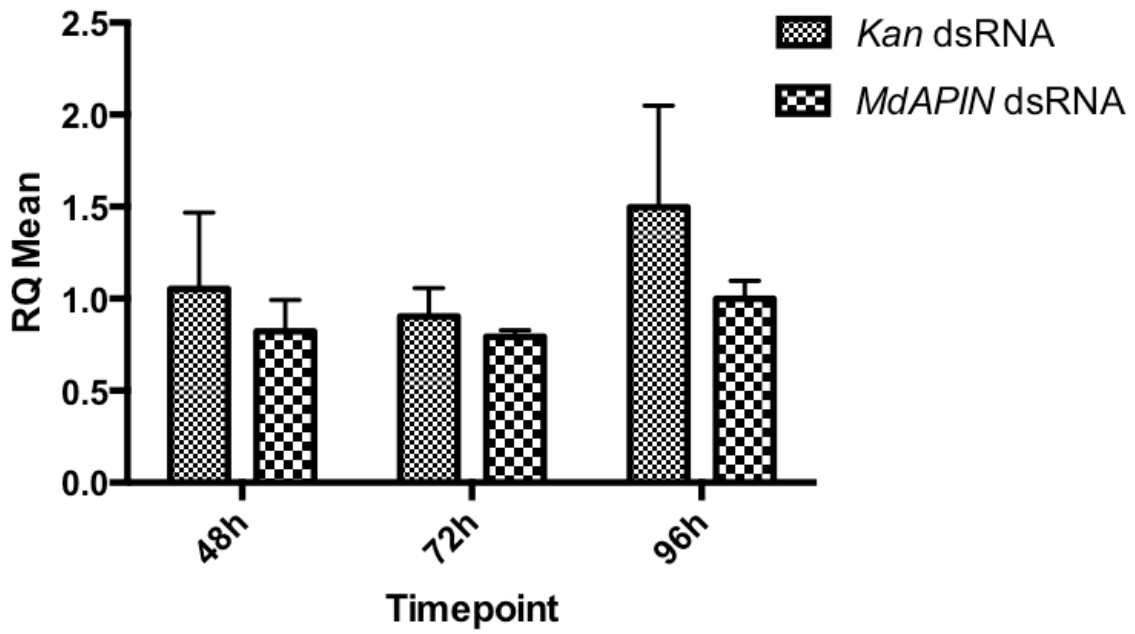

Figure 3-30 **Assay of *APIN* mRNA transcripts in *M. domestica* larvae after feeding on diet containing *MdAPIN* dsRNA.** *M. domestica* larvae were fed on diet containing dsRNA as shown, and collected at times as shown after transfer to diet for estimation of transcript levels by qPCR. Error bars indicate standard errors of the mean for 3 technical replicates. Number of insects for each treatment n=5. No significant difference between treatemts (ANOVA test).

3.2.3 RNAi in *A. pisum*

3.2.3.1 *ApAPIN* and *ApVTE* gene expression profile

Expression profiles for the *A. pisum* target genes for RNAi, *ApAPIN* and *ApVTE* were analyzed over developmental stages by qPCR. Under insectary conditions, the life cycle of *A. pisum*, from neonate to maturity (onset of nymph production) took 10-11 days. Newly born aphid nymphs were transferred to and reared on broad bean plants, collecting samples for qPCR at day 1, day 3, day 5, day 7 and day 9, for investigating gene expression profiles at different stages. The *ApVTE* gene was expressed throughout the whole life cycle (Figure 3-31), varying by about 2-fold relative to internal standard; expression was relatively low when aphids were about 7 and 9 days old. The *ApAPIN* gene (shown in Figure 3-32), was also expressed throughout the life cycle, and varied only about 2-fold relative to the internal standard; in this case expression was highest at day 7.

3.2.3.2 Injection of dsRNA in *A. pisum*

Injections of dsRNAs were carried out on 5 days old *A. pisum*, the earliest stage at which injection was feasible with the equipment available. Three different doses (7.5ng, 15ng and 30ng) of *ApVTE* and *ApAPIN* dsRNA were tested. Aphids injected with 30ng *Kan* dsRNA was used as control treatment, and samples were collected at 24h, 48h and 72h after injection.

Results for *ApVTE* injection are shown in Figure 3-33. Although dsRNA injection consistently resulted in reduced levels of the target transcript after 24h and 48h, the level of down-regulation was <2-fold relative to the *Kan* dsRNA injected control, and did not show a clear dose dependency on the amount of dsRNA injected. Injection of 30ng *ApVTE* dsRNA showed the most effective gene down-regulation against *ApVTE* gene at 24h post injection (Two-way ANOVA with $p<0.0001$), but not at 48h post-injection. Results for samples collected 72h post-injection showed that the levels of *ApVTE* transcripts were not significantly different to the control treatment (ANOVA) The results show that RNAi effect induced by injection of *ApVTE* dsRNA is weak and transient in *A. pisum*.

Results for injection of *ApAPIN* dsRNA in *A. pisum* did not show any significant *ApAPIN* gene downregulation in any *ApAPIN* dsRNA treatment compared to control treatment (Figure 3-34). The results demonstrate that RNAi effect in *A. pisum* can be affected by the sequence of dsRNA. *ApAPIN* dsRNA failed to induce any measurable RNAi effect in *A. pisum* by injection whereas *ApVTE* dsRNA did cause *VTE* gene downregulation, although only by less than 2-fold.

Although injection of *ApVTE* dsRNA had only a transient effect on gene expression, a phenotype was observed in treated aphids. Thirty nanograms *ApVTE* dsRNA was injected into 5 days old *A. pisum*, and survival was recorded for 7 days. Control aphids injected with water or *Kan* dsRNA showed a small decrease in survival (≤20%) over the first three days of the assay, However, aphids injected with 30ng *ApVTE* dsRNA showed 60% mortality over the first three days (Figure 3-35A). No further mortality was observed in either treatment or control after day 3. Differece is significant between control and 30ng *ApVTE* dsRNA treatment (Log-rank (Mantel-Cox) test with P=0.0299). By the end of the assay (corresponding to day 12 of the life cycle) 3-5 nymphs per adult were produced from control treatments, whereas no nymphs were produced by surviving aphids from the *ApVTE* dsRNA injection treatment (Figure 3-35 B).

3.2.3.3 Oral feeding bioassays targeting *ApVTE* gene in *A. pisum*

The artificial diet for aphids is a liquid containing sucrose, amino acids and vitamins, and is particularly well suited for feeding dsRNA. On the basis of injection assays, the *ApVTE* gene was selected as the target for a bioassay using orally delivered dsRNA. Neonate aphids were fed with artificial diet containing 7.5ng/µl and 100ng/µl *ApVTE* dsRNA for 48h, after which they were transferred to fresh diet containing no dsRNA to avoid any contamination. The bioassay was monitored for 12 days until nymphs were observed. No mortality was found in any treatment (data not shown), suggesting that aphid survival was unaffected. After feeding aphids for 10 days, the sizes of the aphids fed on *ApVTE* dsRNA and controls were measured to investigate whether growth was affected by the treatment. Aphid length and width were recorded and results are shown in Figure 3-36. The data show that aphids treated with *ApVTE* dsRNA at 100ng/µl (Figure 3-36A) showed significant reductions in both length (ANOVA, $P<0.001$) and width (approx. 20%, ANOVA, $P<0.01$) compared to controls of aphids fed *Kan* dsRNA. Compared to controls fed no dsRNA, the *Kan* dsRNA had only a marginal effect on size. The effect of dsRNA feeding on growth is shown in retardation of growth. The effect of the *ApVTE* dsRNA was dose-dependent; at 7.5 ng/µl, no significant effect on size compared to Kan dsRNA was observed, although both dsRNA treatments decreased size compared to a no dsRNA control (Figure 3-36 B). Growth has been significantly depressed by feeding 100ng/µl dsRNA. To show *ApVTE* gene down-regulation by feeding *ApVTE* dsRNA, aphids were collected 24h and 48h after feeding on dsRNA-containing diets, and transcript levels were assessed by qPCR. Unexpectedly, *ApVTE* gene transcripts were not reduced significantly in aphids fed on *ApVTE* dsRNA (Figure 3-37).

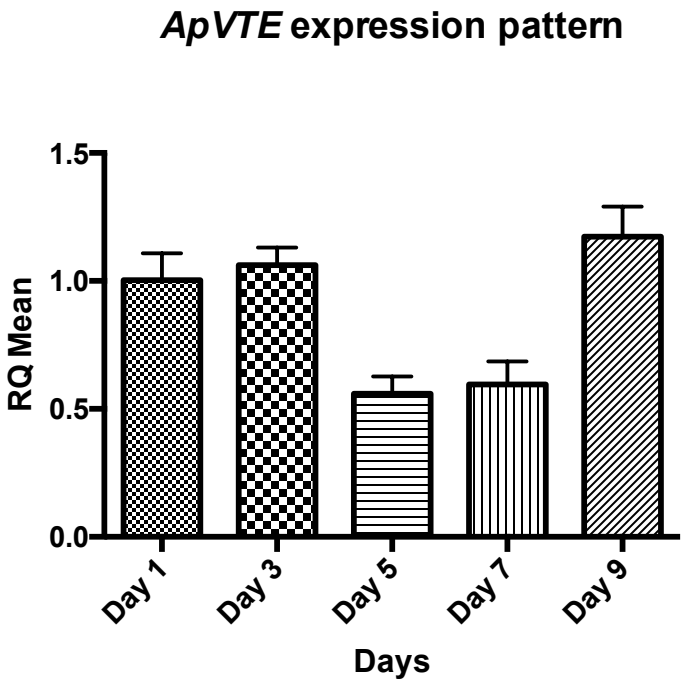

Figure 3-31 ***ApVTE* gene expression at different life stages of *A. pisum.*** Columns show the levels of transcript relative to *GADPH* transcript (internal standard) as estimated by qPCR, normalised to *ApVTE* level in stage 1 = 1.0. Error bars indicate standard errors of the mean for 3 technical replicates. Number of insects for each treatment n=5.

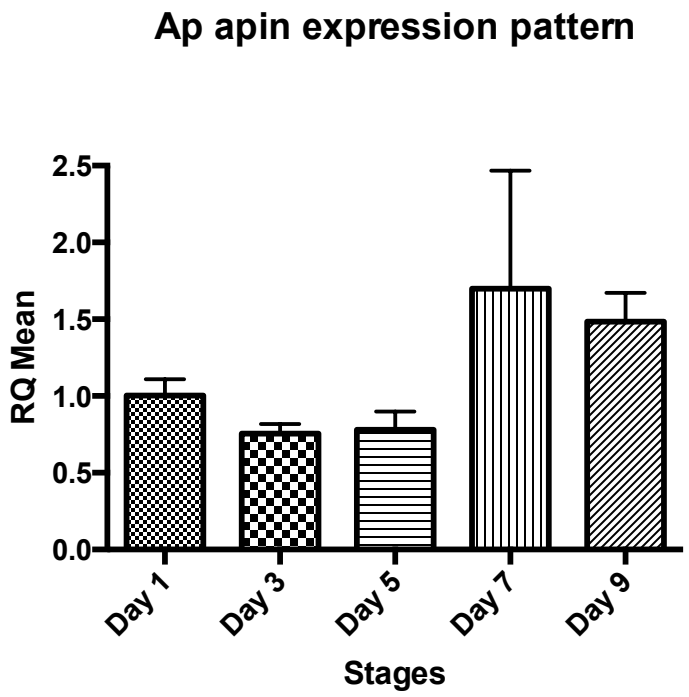

Figure 3-32 ***ApAPIN* gene expression at different life stages of *A. pisum.*** Columns show the levels of transcript relative to *GADPH* transcript (internal standard) as estimated by qPCR, normalised to *ApAPIN* level in stage 1 = 1.0. Error bars indicate standard errors of the mean for 3 technical replicates. Number of insects for each treatment n=5.

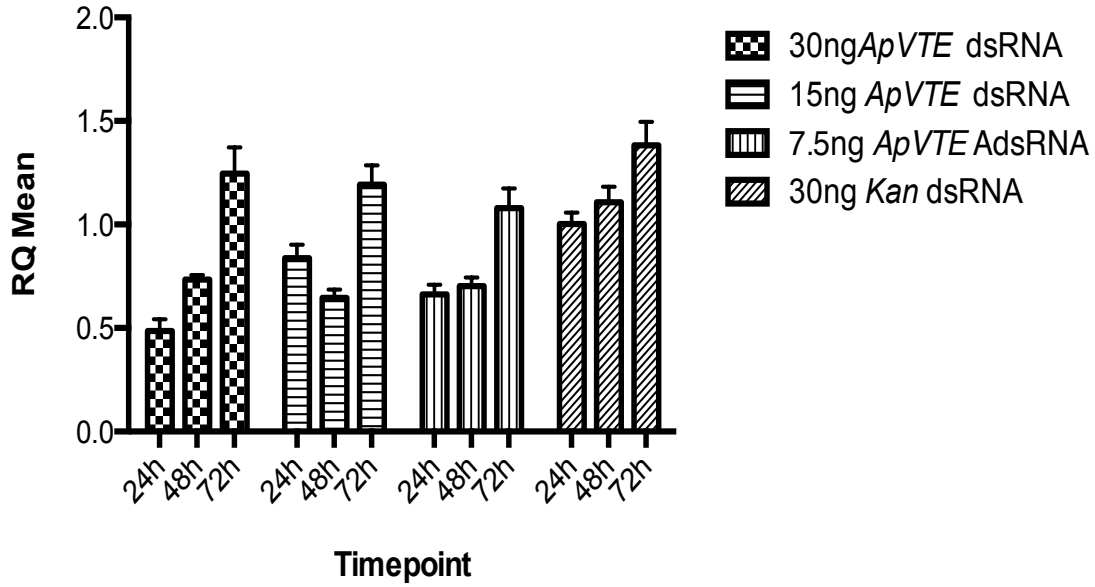

Figure 3-33 ***ApVTE* gene expression after injection of *ApVTE* dsRNA.**
Columns show the levels of transcript relative to *GADPH* transcript (internal standard) as estimated by qPCR, normalised to *ApVTE* level in 24h control = 1.0. Error bars indicate standard errors of the mean for 3 technical replicates. Number of insects for each treatment n=5. Control Kan 30ng and *ApVTE* 30ng treatment show significant difference by ANOVA with P<0.0001, ****.

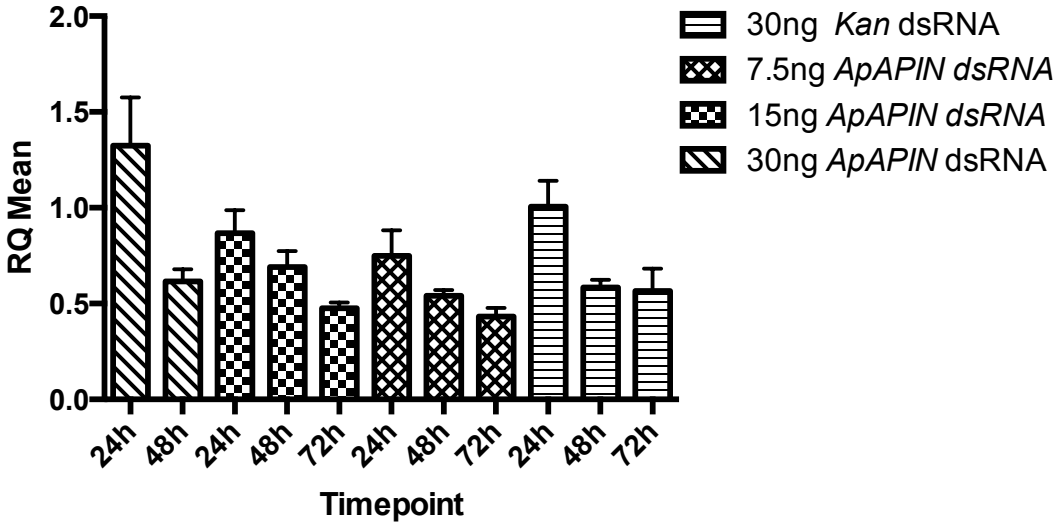

Figure 3-34 ***ApAPIN* gene expression after injection of *ApAPIN* dsRNA.**
Columns show the levels of transcript relative to *GADPH* transcript (internal standard) as estimated by qPCR, normalised to *ApAPIN* level in 24h control = 1.0. Error bars indicate standard errors of the mean for 3 technical replicates. Number of insects for each treatment n=5. Difference between treatments is not significant (ANOVA).

(A)

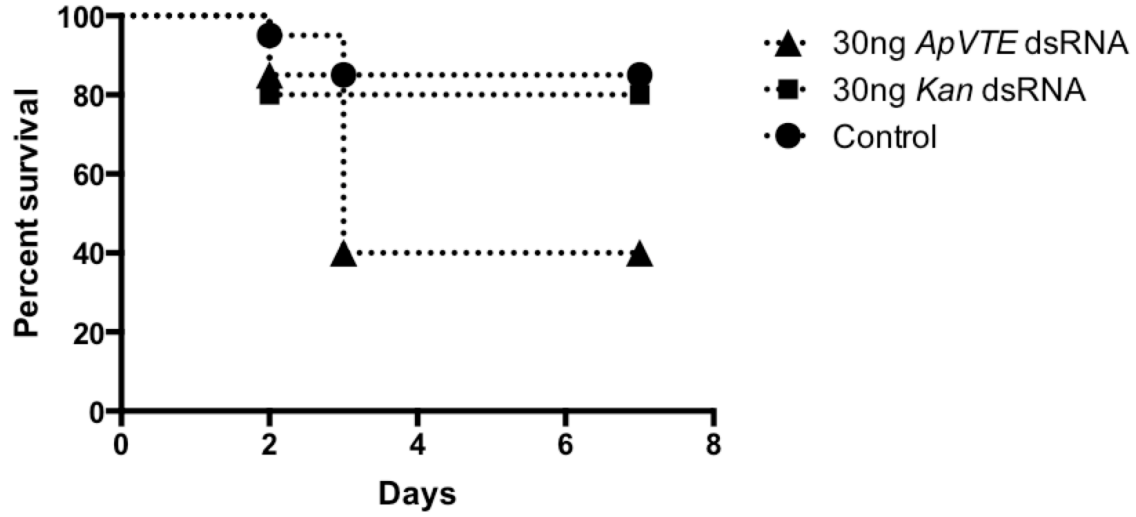

(B)

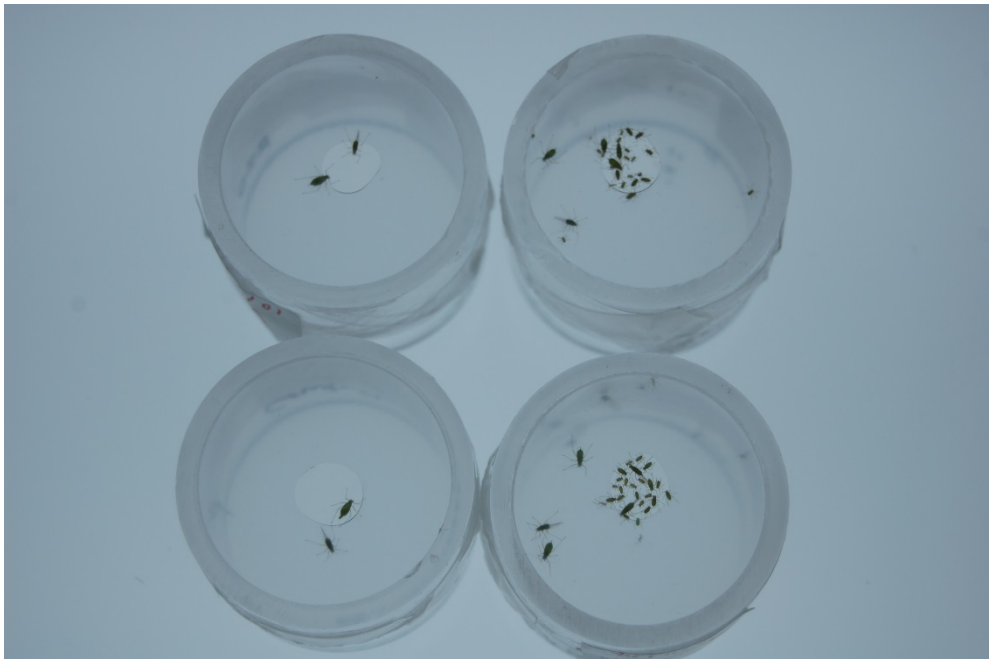

Figure 3-35 **Phenotypes of *A. pisum* injected with 30ng *ApVTE* dsRNA.**

Panel A: Survival after injection of dsRNA as shown. Number of insects used for each treatment n=20. Difference between *Kan* 30ng and *ApVTE* 30ng treatment is significant by Log-rank (Mentel-Cox) test with P=0.0299, *.

Panel B: Surviving aphids after 10 days; *ApVTE* dsRNA-fed (left dishes) and controls (right dishes). Surviving control aphids have produced nymphs.

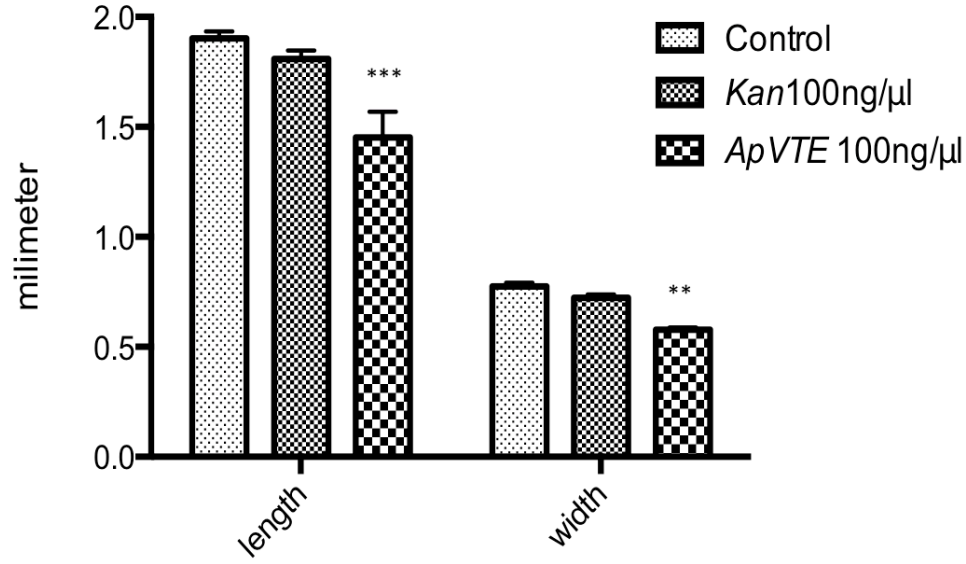

A: *A. pisum* fed with 100ng/µl *ApVTE* dsRNA

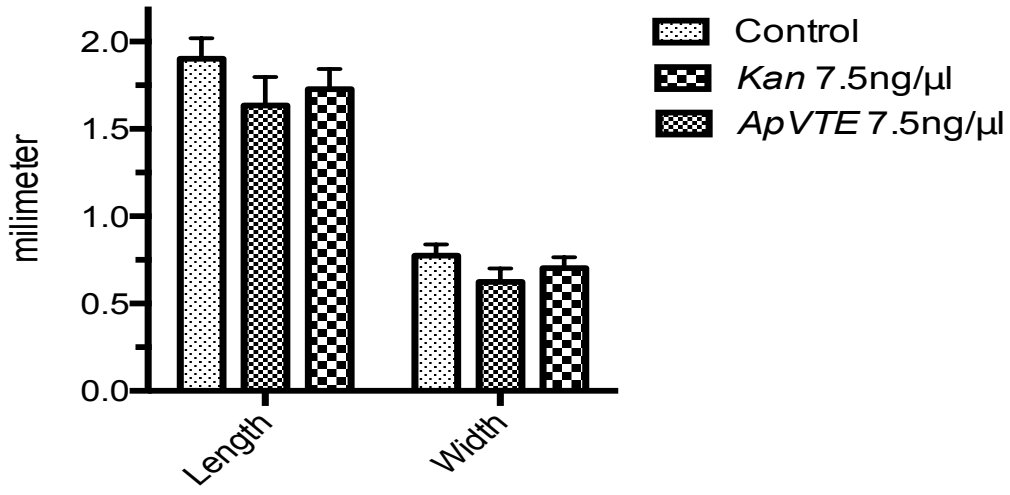

B: *A. pisum* fed with 7.5ng/µl *ApVTE* dsRNA

Figure 3-36 **Growth parameters (length and width at day 10) in aphids fed *ApVTE* dsRNA**. Error bars indicate ±SE of mean. Number of insects used for each treatment n=20. Mean length in 100ng/µl *ApVTE* dsRNA fed aphids is significant different from control treatement (ANOVA, P<0.001, ***). Mean width in 100ng/µl *ApVTE* dsRNA fed aphids is significant different from control aphid (ANOVA, P<0.01, **).

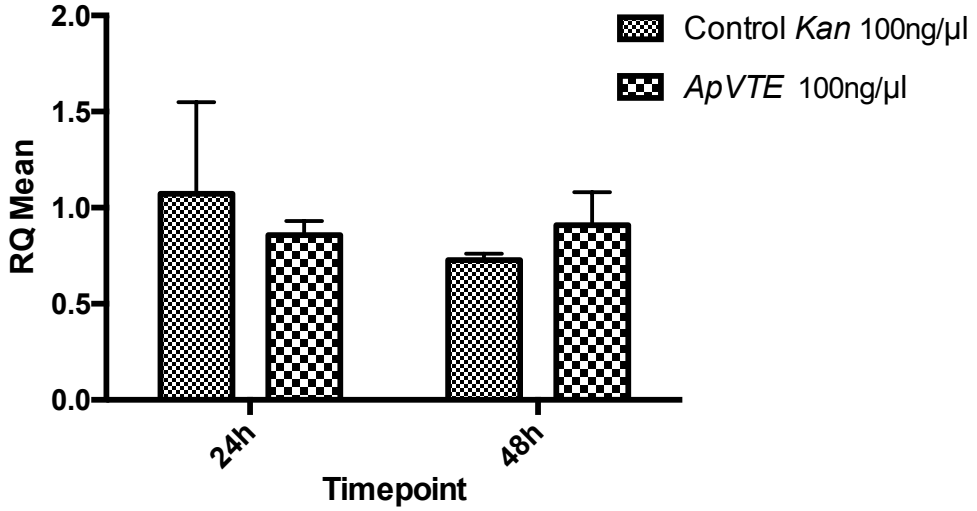

Figure 3-37 ***ApVTE* gene expression after feeding *ApVTE* dsRNA.** Columns show the levels of transcript relative to *GADPH* transcript (internal standard) as estimated by qPCR, normalised to *ApVTE* level in 24h control = 1.0. Error bars indicate standard errors of the mean for 3 technical replicates. Number of insects for each treatment n=5. Difference between treatments is not significant (ANOVA).

3.3 Discussion

RNAi experiments in *T. castaneum*, *M. domestica*, and *D. radicum* and *A. pisum* were conducted by both microinjection and feeding of dsRNA in order to demonstrate that they are differently susceptible to RNAi. V-ATPase is a membrane-bound protein that acts as a proton pump to establish the pH gradient within the gut lumen of many insects, and a previous study performed by Baum *et al.* (2007) demonstrated that silencing this gene prevents growth of Western corn rootworm larvae feeding on transgenic corn plants. Inhibitor of apoptosis (*APIN* or *thread*) gene is another target gene candidate tested. Downregulation of *thread* gene by RNAi has been demonstrated in Drosophila (Igaki *et al.* 2002) and mosquito *Aedes aegypti* (Rodriguez *et al.* 2002); down regulation in Drosophila cell cultures causes cell death by apoptosis.

A successful RNAi response in insects relies on several parameters such as dsRNA length, concentration, sequence, gene target, tissue and different uptake mechanisms (Bellés 2010).

In this work, dsRNAs against insect specific *VTE* and *thread* genes were designed to conform to a target length 277bp, which considered to be of sufficient length for dsRNA cell uptake, and to cover matching stretches of sequence in the homologous genes. Previous studies revealed that dsRNA between 50-100bp lengths is required for efficient systemic RNAi in *C. elegans* (Parrish *et al.* (2000); Winston *et al.* (2002)). In *T. castaneum*, injection of dsRNA against EGFP of 69bp was efficient in knocking down EGFP in transgenic *T. castaneum* larvae, but a 31bp fragment was not able to induce RNAi response (Miller *et al.* 2012), The author concluded that the failure of activation of RNAi by the short fragment was due to failure of the dsRNA being taken up by the cells. This was shown by injecting 30bp dsRNA into *T. castaneum* embryos at the syncytial blastoderm stage, when embryogenesis cell membranes have not yet formed around the multiple nuclei and therefore the dsRNA can be injected directly into each cell. Under these conditions, the dsRNA around 30bp were capable of knocking down EGFP expression, as 89% of the hatched larvae showed no EGFP expression. A similar result in western corn rootworm was also reported by Bolognesi *et al.* (2012) who showed that at least 60bp dsRNA was required for an RNAi response in artificial diet bioassays. In this chapter, 50ng *TcAPIN* and *TcVTE* dsRNA (277bp) efficiently induced gene downregulation as well as causing significant mortality as a phenotype in larvae by injection and feeding (Figure 3-3, Figure 3-4, Figure 3-5 and Figure 3-6). Moreover, the *TcVTE* gene was proved to be downregulated by closely related *Tribolium species T. confusum VTE* dsRNA. Several stretches of ≥20 bases with sequence identity are present between *T. castaneum* and *T. confusum* VTE transcripts which suggest *T. confusum* siRNA with sufficient length complementary to *T.*

castaneum VTE gene was produced and induced a cross species RNAi effect (Figure 3-7and Figure 3-8). Injection of dsRNA at a lower dose was investigated, *Tribolium* larvae injected with 10ng *TcAPIN* dsRNA resulted in approx. 50% *TcAPIN* gene downregulation as early as 5h post injection. After 10 days, more efficient *TcAPIN* gene downregulation was detected which suggests a spreading systemic RNAi response in *Tribolium* (Figure 3-10). According to the studies investigated by Miller *et al.* (2012), injection of 7ng dsRNA (480bp length) led to 90% reduction in transcript levels whereas injection of 0.7ng caused 50% gene downregulation. Previous studies performed by Tomoyasu and Denell (2004) also showed that the injection of GFP transgenic *T. castaneum* larvae with GFPdsRNA was able to inhibit GFP expression and inhibition continued through pupal and adult stages, and injected dsRNA was detected in entire bodies rather than being localized near the site of injection. Moreover, parental RNAi was also observed by Bucher *et al.* (2002), injection of dsRNA into mother's haemolymph led to target gene knock down in offspring embryos. These results suggest that there could be an amplification step occurring like *C. elegans* through another mechanism due to the absence of RdRP or a efficient mechanism of take up and/ or store dsRNA.

In terms of feeding, less than 1 week old *T. castaneum* exposed to diets containing dsRNA induced gene downregulation as well as mortality (Figure 3-11, Figure 3-12 and Figure 3-13). According to the result reported by Whyard *et al.* (2009), neonates exposed to diet containing 2.5ng *TcVTE* dsRNA/mg flour continuously for 7 days resulted in 50% mortality. Compared to the result reported by Whyard *et al.* (2009), much higher dsRNA concentrations (250ng/mg and 500ng/mg) were applied to *T. castaneum* larvae in this work to achieve mortality. Instead of feeding dsRNA continuously to *T. castaneum* larvae for 7 days, diets containing higher concentrations of dsRNAs were prepared at the beginning of the assay without any changes during the assay. However, the result regarding the stability of dsRNA in *T. castaneum* diet reveals that only slightly degraded dsRNA were observed after 72h, and more obvious degradation was found after 120h (chapter 5). A colleague from Newcastle University demonstrated that feeding *T. castaneum* with diet containing 50ng *TcVTE* dsRNA/mg diet induced detectable *TcVTE* gene downregulation but not mortality (Tempel Nakasu 2014). According to the mortality assay (Figure 3-12), *TcVTE* dsRNA is more efficient in causing larval mortality in *T. castaneum* than *TcAPIN* dsRNA. This could due to the more abundant *VTE* transcript encoding a protein which is required for a fundamental biological process throughout the whole larvae at different developmental stages (Figure 3-1) whereas *APIN* transcripts are expressed at a high level when larvae approach pupation (Figure 3-2), being needed to prevent uncontrolled apoptosis associated with tissue remodelling.

In *M. domestica* and *D. radicum*, the *APIN* gene expresses at low levels throughout insect development as compared to the pre-pupal stage. APIN gene expression reached to the highest level during pre-pupa stage where significant gene downregulation was observed following injection of dsRNA. This data agrees well with the result from *Drosophila* (Chintapalli *et al.* 2007). Successful RNAi effects were achieved by microinjection of specific *APIN* dsRNA into *M. domestica* and *D. radicum* larvae (Figure 3-19 and Figure 3-20), which led to increased apoptotic activity. Injection bioassays revealed a dose-dependent pattern mortality for both *M. domestica* and *D. radicum* larvae (Figure 3-21, (2) and Figure 3-22, (2)) which indicated that the *APIN* gene is good candidate of using RNAi against dipteran insect pests.

Cross injection of *DrAPIN* dsRNA into *M. domestica* larvae also resulted in significant *MdAPIN* gene downregulation which indicated that RNAi can be effective across closely related Dipteran species. However, when the two APIN gene sequences are aligned, no stretch of sequence identity of more than 20bp is found, although a stretch of >20bp has only a single base mismatch. Therefore, the RNAi effect in Dipterans appears to tolerate to small number of imperfect matches between siRNA and target gene sequence. However, the RNAi effect seems to be stage-dependent. In present work, *M. domestica* adult mortality and *APIN* gene expression was unaffected whether *MdAPIN* dsRNA was delivered via injection or feeding.

In order to use RNAi as a potential method for crop protection, feeding dsRNA in artificial diet to larvae of *M. domestica* was investigated. Neither feeding purified dsRNA nor bacteria expressing dsRNA induced any RNAi response in *M. domestica* larvae (Figure 3-28 and Figure 3-29). Whyard *et al.* (2009) reported that soaking young stage larvae in Lipofectamine 2000 (Invitrogen) liposome-encapsulated long dsRNA for 1h resulted in 50% reduction of *β-glucuronidase* (GUS) activity in larval gut of transgenic strain of *D. melanogaster* carrying a ubiquitously-expressed *gus* gene. They claimed that soaking newly hatched Drosophila larvae in *gus*-dsRNA for 1 hour without the aid of transfection reagents led to a ‘weak’ RNAi response, in which only 20% gene downregulation was detected. This may indicate that the transfection reagents could somehow protect ingested dsRNA from degradation in the very active Drosophila digestive system before its uptake into cells. Therefore, an efficient dsRNA delivery method will need to be optimised to apply RNAi as a strategy of crop protection.

Compared to beetles and flies, the *A. pisum* exhibited a limited RNAi response. Weak endogenous gene downregulation (50%) can be only achieved by injection of *ApVTE*

dsRNA at high amount (30ng/nymph which equivalent to 42ng/mg insect) shown in Figure 3-33. In terms of the weight of injected insects, 10ng dsRNAs induces significant gene downregulation by injection into pre-pupa stage *T. castaneum* larvae weighing 3.1mg (3 ng/mg insect), injection of 125ng dsRNA also induced downregulation *M. domestica* and *D. radicum* larvae which weigh 18mg and 16.7mg, respectively (6.9 and 7.5 ng/mg insect). However, injection of 30ng dsRNA in 5 days old *A. pisum* that weighed 0.7mg can only induce weak gene downregulation. Moreover, *ApVTE* gene downregulation was transient, only lasting for 48h. *ApVTE* recovered to the level comparable to control treatment at 72h post injection. Injection of *ApAPIN* dsRNA failed to provoke any response in *A. pisum* which could indicate that the RNAi response in *A. pisum* may be gene-dependent. Actually, previous results regarding RNAi in aphids are various. Whyard *et al.* (2009) reported that 50% aphid mortality was achieved by feeding *ApVTE* dsRNA. However, when the same experiment was repeated by Christiaens *et al.* (2014) the later paper reported a negative result, namely that feeding *ApVTE* dsRNA to aphids failed to cause mortality. In this work, aphid fitness parameters (width and length) were affected by feeding 100ng/µl *ApVTE* dsRNA (Figure 3-36). Therefore, future work could perform feeding *ApVTE* dsRNA continuously to *A. pisum* to observe effects on fitness and reproduction.

Studies investigating RNAi in aphid by delivery of dsRNA via transgenic plants, but not via artificial diet or microinjection, achieved more promising results. In 2012, Mao and Zeng developed dsRNA against *A. pisum* hunchback (*Aphb*) gene where its loss-of-function resulted in segmentation defects in the next generation. *Aphb* gene was reported to be significantly downregulated, leading to aphid lethality by continuous feeding of Aphp dsRNA (Mao and Zeng 2012). Another study regarding green peach aphid (*Myzus persicae*) by Pitino *et al.* (2011) demonstrated that up to 60% *MpC002 (*expressed in salivary glands*)* and *Rack-1* (expressed in gut) gene expression can be downregulated by feeding on transgenic plants which continuously express dsRNAs. As a result, silenced peach aphids showed reduced fecundity.

Chapter 4 Production of recombinant protein containing dsRNA-binding domain in *E. coli* and *P. pastoris*

4.1 Introduction

RNA interference (RNAi) is the mechanism of downregulation of expression of specific genes through introducing double-stranded RNA, which has been widely used for investigating gene function in insects, particularly in the model insect *Drosophila melanogaster* (Kennerdell and Carthew (1998); Kennerdell and Carthew (2000);Misquitta and Paterson (1999)). In *C. elegans*, a systemic RNAi effect can be introduced by feeding bacteria expressing dsRNA (Timmons and Fire (1998); Timmons *et al.* (2001)) or by soaking nematodes in dsRNA solution (Tabara *et al.* 1998). However, due to the lack of genes encoding RNA-dependent RNA polymerase (RdRP), the enzyme involved in RNA amplification which produces systemic RNAi effects, most RNAi effects in insects have relied on microinjection of nanogram amounts of synthesised dsRNA into insect haemolymph. The absence of RdRP in insects means that the RNAi effect may be limited to the cells that are exposed to dsRNA; input of dsRNA into haemolymph is required to allow it to access cells throughout the insect. Previous research has identified that different insect species show variable sensitivity to RNAi and some species are totally insensitive (Bellés (2010); Terenius *et al.* (2011)). For achieving a successful RNAi effect by microinjection in insects, dsRNA must remain in a non-degraded state for a sufficient period to allow dsRNA to be taken up by insect cells. Rapid degradation of dsRNA by ribonucleases in the haemolymph could result in failure of uptake and intracellular processing of dsRNA, and lead to absence of an RNAi effect as a consequence. In terms of crop protection, producing an RNAi effect by microinjection of dsRNA is not possible in the field. In order to achieve RNAi effects in insects by feeding, the insect gut is the first barrier for dsRNA to survive; degradation of dsRNA in the gut will prevent intact dsRNA reaching any insect cells.

To address potential problems of dsRNA stability in insect haemolymph and gut lumen, the experiments in this chapter describe the development of a dsRNA-fusion protein delivery system. A double-stranded RNA binding protein, the third dsRNA-binding domain (DRBD3) from *Drosophila staufen,* was selected to conjugate dsRNA forming a protein-RNA complex that could improve the stability of dsRNA and protect it from degradation from insect haemolymph and gut lumen. To achieve sufficient RNAi effect through feeding, dsRNA must be transported from gut lumen into cells as an intact molecule. The snowdrop lectin, GNA, is known to act as a molecular carrier which is transported across the insect gut, from the lumen to the haemolymph, and has

been shown to co-transport other proteins, such as spider toxins (Fithes et al., 2004), when produced as a recombinant fusion protein. GNA fused with DRBD3, was developed as a recombinant protein to improve dsRNA delivery in insects, and to produce 'systemic' RNAi effect by transporting of the complex to the insect haemolymph.

The dsRNA binding protein (DRBP) staufen was first identified in *Drosophila.* It is a 1026 amino acid protein which is important for maturation and localization of maternal mRNAs (St Johnston *et al.* 1991). It was the first protein to be identified as a determinant of cell polarity. It is reported to anchor *bicoid* mRNA at the anterior of the *Drosophila* oocyte and *oskar* mRNA to the posterior of the oocyte (Johnston *et al.* 1989) at different development stages. After fertilization, a concentration gradient of bicoid protein is produced by the translation of *bicoid* mRNA at different locations within the oocyte; the gradient defines the anterior pattern of the embryo. The *staufen* gene product is found to be involved in the last stage of *bicoid* RNA localization when the RNA moves from the anterior cortex into the cytoplasm in oocytes (Johnston *et al.* 1989). After the eggs have been laid, *bicoid* mRNA is anchored by the *staufen* product to the anterior pole of the egg to determine the anterior position (Johnston *et al.* (1989); Ferrandon *et al.* (1994)). *Bicoid* mRNA encodes a homeodomain protein which forms a morphogen gradient that specifies the head and thorax (Driever *et al.* 1990). Posterior polarity is defined by accumulation of the product of the *oskar* gene which define the place of formation of the pole plasm that contains a germline and posterior determinant encoded by *nanos* mRNA, important for abdomen development (Ephrussi *et al.* (1991); Kim-Ha *et al.* (1991)). Also, staufen plays an important role during the asymmetric divisions of *Drosophila* embryonic neuroblasts and their daughter cells, ganglion mother cells (GMCs). In these cells, it associates with *prospero* mRNA but not prospero protein. Failure of localization of *staufen* or of *pros* RNA results in changes of GMC development in embryos (Broadus *et al.* 1998). Regions of the 3'UTRs of *bicoid, oskar* and *prospero* form long stem-loop structures with extensive dsRNA regions, that are necessary for interact with *staufen* (Kim-Ha *et al.* 1993). However, how staufen recognizes these transcripts is still unclear.

Staufen protein has four or five conserved dsRNA binding domains (DRBDs) of 65-70 amino acids depending on the species, and folds into an αββββα structure (Bycroft *et al.* 1995). For *Drosophila* staufen, DRBD1, 3 and 4 have been shown to bind to dsRNA *in vitro* (St Johnston *et al.* (1992); Micklem *et al.* (2000)). Due to the presence of a conserved proline-rich insertion that separates DRBD2 into half, DRBD2 does not show dsRNA binding activity. DRBD2 dsRNA binding activity is shown to be

recovered by removing this insertion (Micklem *et al.* 2000). DRDB5 is less conserved and no dsRNA binding activity is reported. Although DRBD2 and DRBD5 are not involved with dsRNA binding, DRBD2 and DRBD5 are required for localization and interaction with *oskar*, *bicoid* and *prospero* mRNAs (Micklem *et al.* 2000). Previous researches have shown that DRBDs bind to dsRNA, but not to single-stranded RNA or DNA, dsDNA (St Johnston *et al.* (1992); Bass *et al.* (1994); Clarke and Mathews (1995); Bevilacqua and Cech (1996)). It is interesting that DRBDs do not recognize nucleotide sequences and do not contact bases directly, but instead contact through 2'-OH groups in the ribose sugars and the phosphate backbone of RNA. The optimal binding is found with dsRNA stem loops of 12 uninterrupted base pairs or longer (Ramos *et al.* 2000). Introduction of unpaired bases in the helical structure of dsRNA reduces the binding with DRBD3(Ramos *et al.* 2000). DRBDs specifically bind the A-form double helix of dsRNA in which the minor groove is less deep and wider than the minor groove in the B-form double stranded nucleic acid structure adopted by DNA. Ramos et al. identified three regions of the DRBD3 from *Drosophila* staufen that are important for dsRNA binding, which are helix α1, loop 2 and loop 4. Mutations of amino acids in each of these regions either abolish or reduce RNA binding activity, whereas dsRNA binding activity was not affected by the mutation of surface residues in other regions. The amino acid sequences in these regions which were identified as necessary for dsRNA binding are strongly conserved from *Drosophila* staufen to staufen in humans (Ramos *et al.* 2000). DRBD3 plays a further role in RNA binding, in that helix α1 of DRBD3 is found to interact with the single-stranded loop in a stem-loop RNA structure.

In this chapter, recombinant fusion proteins containing DRBD3, Trx/RBD3 and Trx/RBD3/GNA were constructed and expressed in *E. coli* using a pET32 expression vector. RBD3 and RBD3/GNA were also expressed in *P. pastoris*. Transport of Trx/RBD3 and RBD3/GNA across the insect gut was demonstrated by western blotting.

4.2 Results

4.2.1 Expression of recombinant RNA binding proteins using *E. coli* as expression host

4.2.1.1 Preparation of expression constructs

Sequences encoding the RNA binding domains RBD1 and RBD3 from the *Drosophila melanogaster staufen* gene (Figure 4-1), containing codon optimisation for expression in yeast, were synthesised by a commercial supplier Shinegene (sequences shown in Figure 4-2). The sequences were transferred into the expression vector pET32, so that the resulting construct directed expression of a fusion protein containing thioredoxin (Trx), fused N-terminally to the RNA binding domain, with a $(His)_6$ tag fused C-terminally to the RBD, The amino acid sequences are shown in Figure 4-3. These proteins were designated Trx/RBD1 and Trx/RBD3.

Further constructs were also prepared which contained the coding sequence for snowdrop lectin, GNA, fused C-terminally to the RBD1 or RBD3 RNA-binding domain. These constructs also contained a C-terminal $(His)_6$ tag. The predicted sizes of the Trx/RBD and Trx/RBD/GNA fusion proteins are 24 and 35kDa, respectively. A typical construct is illustrated (Figure 4-4), and the predicted sequences of the coding regions of the constructs are shown in Figure 4-5. These proteins were designated Trx/RBD1/GNA and Trx/RBD3/GNA.

Recombinant DNA cloning was carried out in an *E. coli* cloning host. All constructs were verified by DNA sequencing.

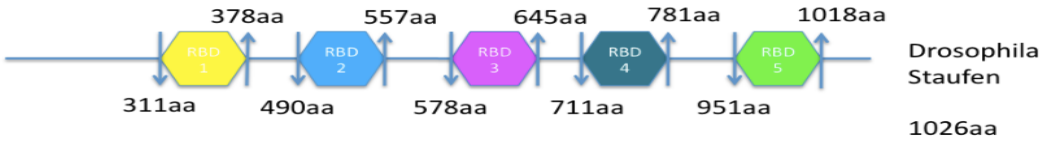

Dmstau

MQHNVHAARPAPHIRAAHHHSHSHAHMHLHPGMEQHLGPSLQQQQQPPPPQQPPHRDLHARLNHHHLHAQQQQQQQTSSNQAGAVAA
AGAAYHHGNINSNSGSNISSNSNQMQKIRQQHQHLSSSNGLLGNQPPGPPPQAFNPLAGNPAALAYNQLPPHPPHHMAAHLGSYAAPP
PHYYMSQAKPAKYNHYGSNANSNSGSNNSNSNYAPKAILQNTYRNQKVVVPPVVQEVTPVPEPPVTTNNATTNSTSNSTVIASEPVTQ
EDTSQKPETRQEPASADDHVSTGNIDATGALSNEDTSSSGRGGKDKTPMCLVNELARYNKITHQYRLTEERGPAHCKTFTVTLMLGDE
EYSADGFKIKKAQHLAASKAIEETMYKHPPPKIRRSEEGGPMRTHITPTVELNALAMKLGQRTFYLLDPTQIPPTDSIVPPEFAGGHL
LTAPGPGMPQPPPPPAYALRQRLGNGFVPIPSQPMHPHFFHGPGQRPFPPKFPSRFALPPPLGAHVHHGPNGPFPSVPTPPSKITLFV
GKQKFVGIGRTLQQAKHDAAARALQVLKTQAISASEEALEDSMDEGDKKSPISQVHEIGIKRNMTVHFKVLREEGPAHMKNFITACIV
GSIVTEGEGNGKKVSKKRAAEKMLVELQKLPPLTPTKQTPLKRIKVKTPGKSGAAAREGSVVSGTDGPTQTGKPERRKRLNPPKDKLI
DMDDADNPITKLIQLQQTRKEKEPIFELIAKNGNETARRREFVMEVSASGSTARGTGNSKKLAKRNAAQALFELLEAVQVTPTNETQS
SEECSTSATMSAVTAPAVEATAEGKVPMVATPVGPMPGILILRQNKKPAKKRDQIVIVKSNVESKEEEANKEVAVAAEENSNNSANSG
DSSNSSSGDSQATEAASESALNTSTGSNTSGVSSNSSNVGANTDGNNHAESKNNTESSSNSTSNTQSAGVHMKEQLLYLSKLLDFEVN
FSDYPKGNHNEFLTIVTLSTHPPQICHGVGKSSEESQNDAASNALKILSKLGLNNAMK

Figure 4-1 **Schematic diagram and amino acid sequence of the product of the *Drosophila melanogaster staufen* gene showing the 5 RNA-binding domains (coloured regions).** The *staufen* gene from *Drosophila melanogaster* encodes a protein which is involved in polarity determination during embryo development. It contains five similar copies of a domain which potentially binds dsRNA. RNA binding is specific for dsRNA, but is not sequence-specific.

RBD1 (73 residues, 219bp)

```
K   D   K   T   P   M   C   L   V   N   E   L   A   R
AAG GAT AAG ACT CCA ATG TGT TTG GTT AAC GAA TTG GCT AGA
 Y   N   K   I   T   H   Q   Y   R   L   T   E   E   R
TAC AAC AAG ATT ACT CAT CAA TAC AGA TTG ACT GAA GAA AGA
 G   P   A   H   C   K   T   F   T   V   T   L   M   L
GGT CCA GCT CAT TGT AAG ACT TTT ACT GTT ACT TTG ATG TTG
 G   D   E   E   Y   S   A   D   G   F   K   I   K   K
GGT GAT GAA GAA TAC TCT GCT GAT GGT TTT AAG ATT AAG AAG
 A   Q   H   L   A   A   S   K   A   I   E   E   T   M
GCT CAA CAT TTG GCT GCT TCT AAG GCT ATT GAA GAA ACT ATG
 Y   K   H
TAC AAG CAT
```

RBD3 (73 residues, 219bp)

```
D   K   K   S   P   I   S   Q   V   H   E   I   G   I
GAT AAG AAG TCT CCA ATT TCT CAA GTT CAT GAA ATT GGT ATT
 K   R   Q   M   T   V   H   F   K   V   L   R   E   E
AAG AGA CAA ATG ACT GTT CAT TTT AAG GTT TTG AGA GAA GAA
 G   P   A   H   M   K   N   F   I   T   A   C   I   V
GGT CCA GCT CAT ATG AAG AAG TTT ATT ACT GCT TGT ATT GTT
 G   S   I   V   T   E   G   E   G   N   G   K   K   V
GGT TCT ATT GTT ACT GAA GGT GAA GGT AAG GGT AAG AAG GTT
 S   K   K   R   A   A   E   K   M   L   V   E   L   Q
TCT AAG AAG AGA GCT GCT GAA AAG ATG TTG GTT GAA TTG CAA
 K   L   P
AAG TTG CCA
```

Figure 4-2 **Nucleotide and derived amino acid sequences of synthetic RBD1 and RBD3.** Highlighting indicates modification of original AAC (N) to CAA(Q) (highlighted in blue) to remove a potential N-linked glycosylation site for RBD3.

MSDKIIHLTDDSFDTDVLKADGAILVDFWAEWCGPCKMIAPILDEIADEYQGKLTVAK
LNIDQNPGTAPKYGIRGIPTLLLFKNGEVAATKVGALSKGQLKEFLDANLAGSGSGH
MHHHHHHSSGLVPRGSGMKETAAAKFERQHMDSPDLGTDDDDKAMADIGSKDKT
PMCLVNELARYNKITHQYRLTEERGPAHCKTFTVTLMLGDEEYSADGFKIKKAQHLA
ASKAIEETMYKHKLAAALEHHHHHH

Thioredoxin Enterokinase site RNA Binding Domain 1 His(6) tag

(A) Amino acid sequence for expression construct for Trx/RBD1 in *E.coli* BL21(DE3)

MSDKIIHLTDDSFDTDVLKADGAILVDFWAEWCGPCKMIAPILDEIADEYQGKLTVAK
LNIDQNPGTAPKYGIRGIPTLLLFKNGEVAATKVGALSKGQLKEFLDANLAGSGSGH
MHHHHHHSSGLVPRGSGMKETAAAKFERQHMDSPDLGTDDDDKAMADIGSDKKS
PISQVHEIGIKRQMTVHFKVLREEGPAHMKNFITACIVGSIVTEGEGNGKKVSKKRAA
EKMLVELQKLPKLAAALEHHHHHH

Thioredoxin Enterokinase site RNA Binding Domain 3 His(6) tag

(B) Amino acid sequence for expression construct for Trx/RBD3 in *E. coli* BL21(DE3)

Figure 4-3 Amino acid sequences for predicted products of Trx/RBD expression constructs

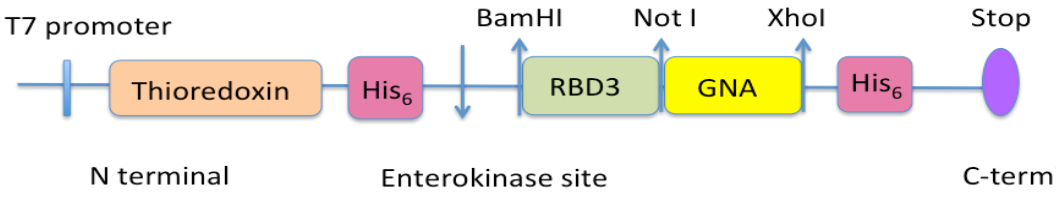

Figure 4-4 **Schematic diagram of an expression construct for a typical fusion protein, Trx/RBD3/GNA in pET32.**

The RBD1 coding sequence was cloned C-terminal to the thioredoxin sequence, $(His)_6$ tag and enterokinase cleavage site, between BamHI and NotI restriction sites. The GNA coding sequence was inserted between Not I and Xho I sites, C-terminal to the RBD1 coding sequence. A further $(His)_6$ tag is present C-terminal to the GNA sequence.

MSDKIIHLTDDSFDTDVLKADGAILVDFWAEWCGPCKMIAPILDEIADEYQGKLTVAK
LNIDQNPGTAPKYGIRGIPTLLLFKNGEVAATKVGALSKGQLKEFLDANLAGSGSGH
MHHHHHHSSGLVPRGSGMKETAAAKFERQHMDSPDLGTDDDDKAMADIGSKDKT
PMCLVNELARYNKITHQYRLTEERGPAHCKTFTVTLMLGDEEYSADGFKIKKAQHLA
ASKAIEETMYKHKLAAADNILYSGETLSTGEFLNYGSFVFIMQEDCNLVLYDVDKPIW
ATNTGGLSRSCFLSMQTDGNLVVYNPSNKPIWASNTGGQNGNYVCILQKDRNVVIY
GTDRWATGLEHHHHHH

Thioredoxin Enterokinase site RNA Binding Domain 1 GNA His(6) tag

(A) Amino acid sequence for expression construct for Trx/RBD1/GNA in *E.coli* BL21(DE3)

MSDKIIHLTDDSFDTDVLKADGAILVDFWAEWCGPCKMIAPILDEIADEYQGKLTVAK
LNIDQNPGTAPKYGIRGIPTLLLFKNGEVAATKVGALSKGQLKEFLDANLAGSGSGH
MHHHHHHSSGLVPRGSGMKETAAAKFERQHMDSPDLGTDDDDKAMADIGSDKKS
PISQVHEIGIKRQMTVHFKVLREEGPAHMKNFITACIVGSIVTEGEGKGKKVSKKRAA
EKMLVELQKLPKLAAADNILYSGETLSTGEFLNYGSFVFIMQEDCNLVLYDVDKPIW
ATNTGGLSRSCFLSMQTDGNLVVYNPSNKPIWASNTGGQNGNYVCILQKDRNVVIY
GTDRWATGLEHHHHHH

(B) Amino acid sequence for expression construct for Trx/RBD3/GNA in *E.coli* BL21(DE3)

Thioredoxin Enterokinase site RNA Binding Domain 3 GNA His(6) tag

Figure 4-5 **Amino acid sequence for expression construct for Trx/RBD/GNA in *E. coli* BL21 (DE3).**

Coding sequences for RNA binding domain 1 and 3 containing 73 amino acid residues are inserted into the MCS of the expression vector pET32a, between BamHI and NotI restriction enzyme sites. GNA is introduced by restriction enzyme NotI and XhoI C-terminal to the RBD coding sequences. Trx, the fusion protein tag containing 109 amino acid residues precedes RBD with six His residues in between the fusion for detection of fusion protein and purification using metal affinity chromatography.

4.2.1.2 Expression of RNA binding proteins in PET32 vector in *E. coli*

Selected clones of expression constructs for RNA binding proteins were transferred to *E. coli* BL21 DE3 as expression host. Bacterial clones were grown to late logarithmic phase and expression was induced by adding IPTG. Soluble and insoluble protein fractions from uninduced and induced cultures were analysed by SDS-PAGE, the uninduced samples being used as controls (Figure 4-6. A). Bands of the predicted size for Trx/RBD1 and Trx/RBD/GNA fusion proteins (27kDa and 35kDa, respectively) were produced as the major components of the insoluble protein fractions from induced bacteria, but were not present in uninduced bacteria. Although the soluble protein fractions from induced bacteria contained more protein than those from uninduced bacteria, there were no apparent difference in the band patterns, suggesting that little, if any, of the recombinant protein produced as a result of induction was soluble. These initial experiments suggested that most, or all of the recombinant proteins produced in this expression system were insoluble, although proteins were being produced in large amounts, estimated as 100-150 mg/l of *E. coli* culture. Analysis of protein fractions by western blotting using anti-$(His)_6$ tag antibodies confirmed the identity of the bands identified as representing Trx/RBD and Trx/RBD/GNA fusion proteins; representative results are shown in Figure 4-6 (B) for Trx/RBD1. The band detected by the antibodies is of the correct predicted size. This blot shows that small amounts of insoluble protein are produced in uninduced cultures (presumably as a result of "leaky" expression from the *tac* promoter in pET32a) and that after induction some soluble fusion protein is actually present, even though it is not visible on a stained gel. However, it confirms that most of the recombinant protein is produced as an insoluble fraction after induction.

In order to determine whether soluble recombinant protein could be produced in the *E. coli* expression system, conditions for induction of expression were manipulated to attempt to enhance protein folding. Initial experiments showed no benefit from expression at lower temperature, 25°C compared to 30°C, for either Trx/RBD or Trx/RBD/GNA proteins (Figure 4-7 and Figure 4-8). Most, if not all the recombinant proteins were still present in the insoluble protein fractions after induction. Using different concentrations of IPTG in the inducing medium also had little effect on the solubility of the resulting proteins (Figure 4-9), with no increase in recombinant protein in the soluble fraction being observed.

Decreasing the temperature for inducing expression of the recombinant proteins to 15°C proved successful in enabling expression of soluble or partially soluble fusion proteins. Results for Trx/RBD3 fusion protein are shown in Figure 4-10. When induced at 15°C, this recombinant protein is wholly present in the soluble protein fraction. The

expression levels of soluble fusion proteins from Trx/RBD1, Trx/RBD1/GNA and Trx/RBD3/GNA cultures induced at 15°C were approximately 25mg/L.

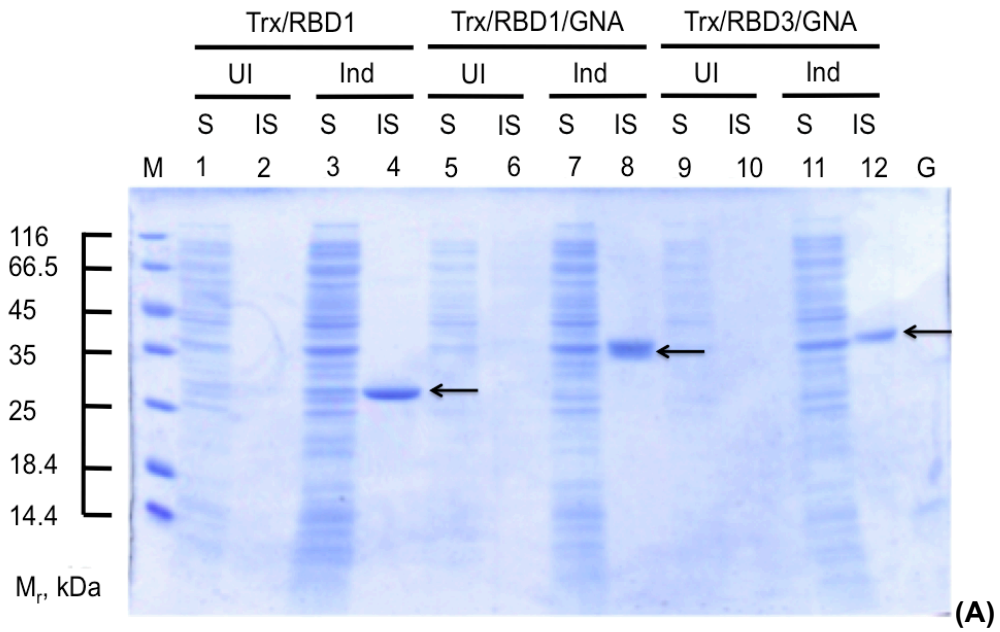

Figure 4-6 **(A) Expression of recombinant thioredoxin-RNA binding domain fusion proteins in *E. coli* BL21 (DE3) at 15°C. SDS-PAGE gel stained with Coomassie Blue.**

Lanes 1 and 2 show Trx/RBD1 uninduced soluble (S) and insoluble fractions (IS). Lanes 3 and 4 show Trx/RBD1 induced soluble (IS) and insoluble fractions (II). Trx/RBD1 shows a fusion protein of approx. 27kDa. Lanes 5 and 6 show Trx/RBD1/GNA uninduced soluble and insoluble fractions. Lanes 7 and 8 show Trx/RBD1/GNA induced soluble and insoluble fractions. Trx/RBD1/GNA shows a fusion protein of approx. 35kDa. Lanes 9 and 10 show Trx/RBD3/GNA uninduced soluble and insoluble fractions. Lanes 11 and 12 show Trx/RBD3/GNA induced soluble and insoluble fractions. Trx/RBD3/GNA shows a fusion protein of approx. 35kDa. Lane 13 shows a 12kDa band of GNA (1μg; as a standard). Lane M represents a molecular weight marker (SDS7) = 116, 66.2, 45, 35, 25, 18.4, 14.4 kDa. 1μl from each fraction was loaded on SDS-PAGE.

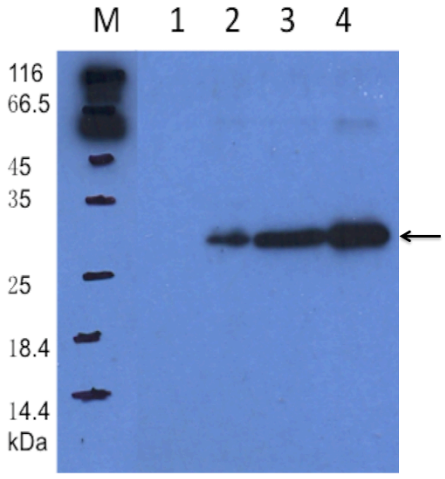

(B)

Figure 4-6 **(B) Confirmation of Trx/RBD1 recombinant protein expression by western blotting.**

Western blotting result shows Uninduced soluble fraction (US) of Trx/RBD1 in lane 1, Lane 2 shows Uninduced insoluble fraction (UI), lane 3 shows Induced soluble fraction (IS) and Lane 4 shows Induced insoluble fraction (II). Lane M represents a molecular weight marker (SDS7) = 116, 66.2, 45, 35, 25, 18.4, 14.4 kDa.

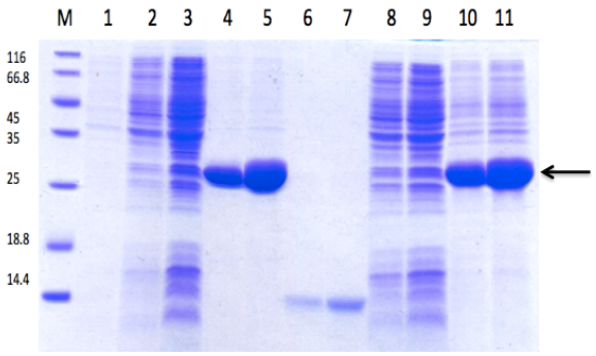

Figure 4-7 **Expression of induced recombinant Trx-RBD1 fusion protein at 25°C and 30°C. SDS-PAGE gel stained with Coomassie Blue**

Lane 1 shows 3μl Trx/RBD1 from uninduced soluble fractions. Lane 2 and 3 shows 2μl and 4μl Trx/RBD1 induced soluble fractions at 25°C. 2μl and 4μl Trx/RBD1 (27kDa) induced insoluble fractions at 25°C are shown in lanes 4 and 5. Lanes 6 and 7 shows 2μg and 4μg 12kDa band of GNA as standards. Lanes 8 and 9 shows 2μl and 4μl Trx/RBD1 induced soluble fractions at 30°C whereas 2μl and 4μl Trx/RBD1 from induced insoluble fractions at 30°C are shown in lanes 10 and 11. Lane M represents a molecular weight marker (SDS7) = 116, 66.2, 45, 35, 25, 18.4, 14.4 kDa.

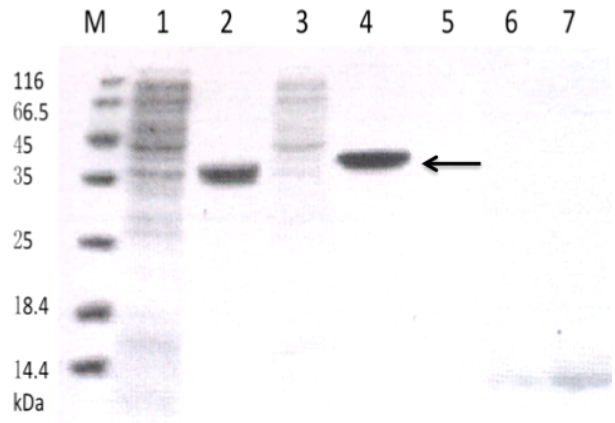

Figure 4-8 **Expression of induced recombinant Trx/RBD/GNA fusion protein at 25°C. SDS-PAGE gel stained with Coomassie Blue.**

Induced soluble and insoluble fractions of Trx/RBD1/GNA are shown in lane 1 and 2. Trx/RBD3/GNA induced soluble and insoluble fractions are shown in lane 3 and 4. Twelve-kilodalton band of GNA (1μg, 2μg, 4μg as a standard) are shown in lane 5, 6 and 7. One microliter from each fractions were loaded on SDS-PAGE. Lane M represents a molecular weight marker (SDS7) = 116, 66.2, 45, 35, 25, 18.4, 14.4 kDa.

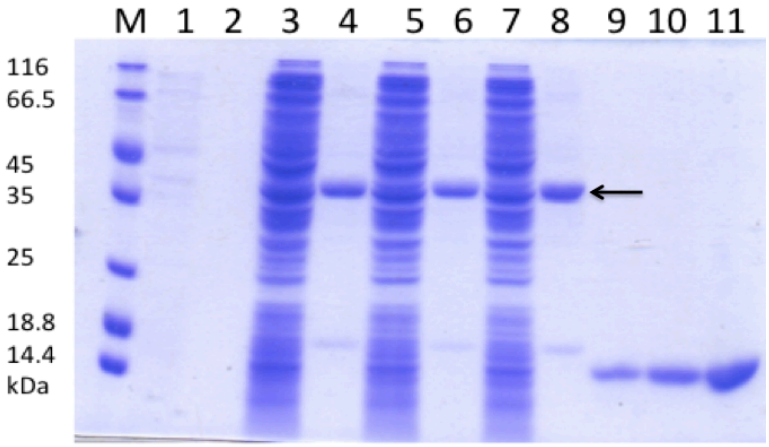

Figure 4-9 **Analysis of expression of recombinant Trx/RBD3/GNA protein in *E. coli* induced by 1mM, 2mM and 2.5mM IPTG by SDS-PAGE.**

Soluble and insoluble fractions from uninduced Trx/RBD3/GNA cell culture are shown in lane 1 and 2. Soluble and insoluble fractions from Trx/RBD3/GNA cell cultures induced at final concentrations of IPTG at 1mM, 2mM and 2.5mM are shown in lanes Lanes 3,4; 5,6; 7,8: Twelve-kilodalton band of GNA (1μg, 2μg, 4μg as a standard) are shown in lane 9-11. One microliter from each fraction was loaded on SDS-PAGE. Lane M represents a molecular weight marker (SDS7) = 116, 66.2, 45, 35, 25, 18.4, 14.4 kDa.

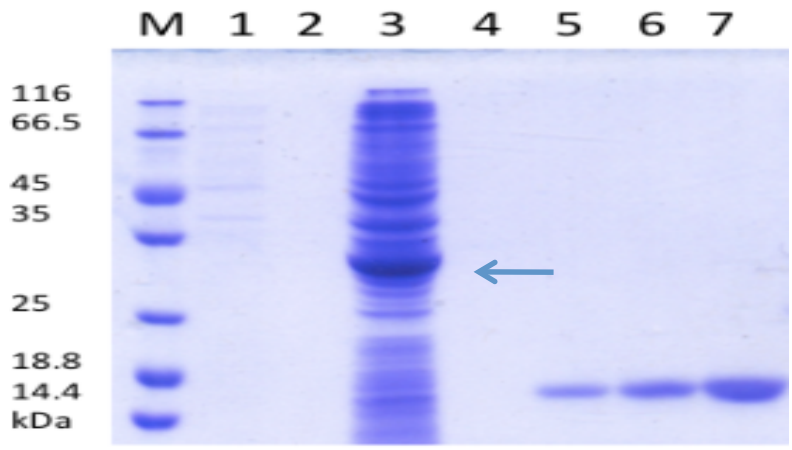

Figure 4-10 **Analysis of expression of Trx/RBD3 protein in *E. coli* at 15°C by SDS-PAGE**

Soluble and insoluble fractions from uninduced Trx/RBD3 cell cultures are shown in lanes 1 and 2. Soluble and insoluble fractions from induced Trx/RBD3 cell cultures are shown in lane 3 and 4. Twelve-kilodalton band of GNA (1μg, 2μg, 4μg as a standard) are shown in lane 5-7. The band identified as Trx/RBD3 protein (approx. 27kDa) is indicated by an arrow. One microliter from each fraction was loaded on SDS-PAGE. Lane M represents a molecular weight marker (SDS7) = 116, 66.2, 45, 35, 25, 18.4, 14.4 kDa.

4.2.2 Purification of Trx/RBD and Trx/RBD/GNA fusion proteins expressed in *E. coli*

The purification of recombinant proteins exploited the $(His)_6$ tag incorporated into the pET32 vector-encoded sequence, and the C-terminal $(His)_6$ tag added to the fusion proteins containing GNA. Conditions for elution of the proteins were checked using "empty" vector which expressed the tagged Trx protein only. Cells were pelleted after induction of the protein, and a soluble protein fraction was prepared and subjected to metal affinity chromatography. Results are shown in Figure 4-11. The Trx recombinant protein bound tightly to a nickel affinity column, and could be eluted by including with 200mM imidazole in the column buffer, with only small additional amounts eluting at 400mM imidazole. Very little recombinant protein eluted at 25mM imidazole, which therefore made a good wash solution to remove non-specifically bound *E. coli* proteins. Approximately 7mg thioredoxin was purified from a 50ml induced cell culture, and the eluted protein can be estimated as at least 90% pure, based on staining of the 20kDa thioredoxin band compared to other bands in the fraction eluted at 200mM imidazole. These conditions were used as a basis for purifying recombinant fusion proteins.

Purification of Trx/RBD3 from the soluble protein fraction of an *E. coli* culture containing the appropriate expression construct is shown in Figure 4-12. The culture was induced at 15°C overnight. Soluble proteins extracted from the cell pellet were loaded onto a nickel affinity column, which was washed successively with binding buffer, and buffer containing 25mM, 200mM and 400mM imidazole. Trx/RBD3 bound more tightly to the column than Trx alone, and was not eluted in 200mM imidazole (tracks 3 and 4); washing with 400mM imidazole was necessary to elute the fusion protein. The eluted Trx/RBD3 gave a major band of 30kDa on SDS-PAGE (tracks 5 and 6) with minimal amounts of contaminating proteins indicated by minor bands on the gel. Approximately 3.5mg Trx/RBD3 fusion protein was purified from 50ml cell culture pellet.

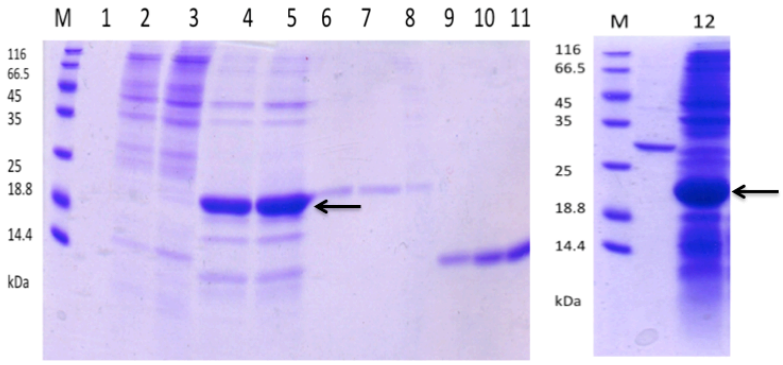

Figure 4-11 **Expression and purification of thioredoxin from transformed empty pET32 vector.**

Binding buffer wash fraction (10μl) is shown in lane 1. Thioredoxin washed fraction and peak drop in volume of 10μl with 25mM imidazole in 1XBB are shown in lane 2 and 4, whereas 10μl eluted fraction and peak drop with 200mM imidazole in 1XBB are shown in lane 6 and 7. Lane 8 shows 1μl induced insoluble thioredoxin fraction. Twelve-kilodalton band of GNA (1μg, 2μg, 4μg as a standard) are shown from lane 9-11. Induced soluble thioredoxin (5μl) shows protein at 20kDa as indicated by arrow in lane 12. Lane M represents a molecular weight marker (SDS7) = 116, 66.2, 45, 35, 25, 18.4, 14.4 kDa.

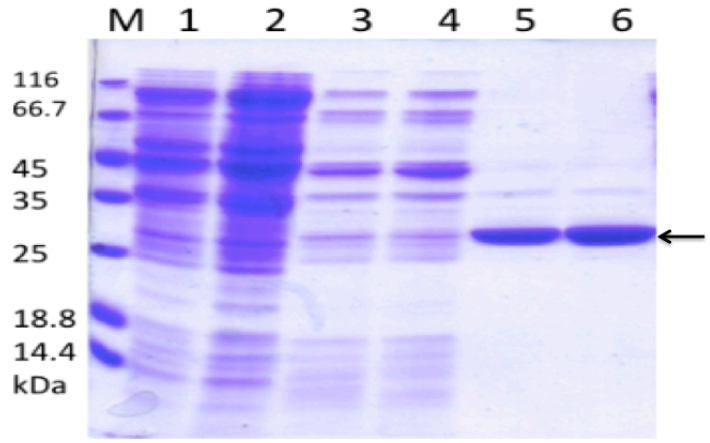

Figure 4-12 **Purification of Trx/RBD3 from soluble protein fraction of *E. coli* cell cultures.**

Wash fraction and peak drop eluted with 25mM imidazole are shown in lane 1 and 2. Elution fraction and peak drop from elution with 200mM imidazole are shown in lane 3 and 4, elution with 400mM imidazole are shown in lane 5 and 6. Eluted Trx/RBD3 shows protein at 27kDa as indicated by arrow in lane 5 and 6. Ten microliter from all fractions was loaded on SDS-PAGE. Lane M represents a molecular weight marker (SDS7) = 116, 66.2, 45, 35, 25, 18.4, 14.4 kDa.

Purification of the Trx/RBD/GNA fusion proteins from soluble protein fractions from *E. coli* cells containing appropriate expression constructs induced at 15°C overnight did not yield similarly successful results. Although some fusion protein was recovered, the eluted proteins were obtained in poor yield and with much lower levels of purity. Results are summarised in Figure 4-13 (A), which shows an analysis of fractions from the purifications of Trx/RBD/GNA proteins by SDS-PAGE.

The Trx/RBD/GNA fusion proteins appeared to bind relatively poorly to the nickel affinity column, as shown by the presence of a band of approx. 35kDa in the 10mM imidazole wash fractions (lanes 2, 3, 7, 8). When bound proteins were subsequently eluted in buffer containing 400mM imidazole, a band corresponding to Trx/RBD1/GNA was only present in low amount as a minor component in the eluted fraction and peak drop (lanes 4, 5). A band corresponding to Trx/RBD3/GNA was the major component in the eluted fraction and peak drop (lanes 9, 10) but was still only obtained in low yield. Analysis of the fractions by western blotting (Figure 4-13 B) showed that the fusion protein was eluted in 400mM imidazole, and that no immunoreactivity was observed in fractions from the 10mM imidazole wash, suggesting that the 35kDa band observed at lower imidazole concentrations represents a contaminating *E. coli* protein.

Attempts to purify fusion proteins by exploiting denaturing conditions are discussed in a later section (4.2.10).

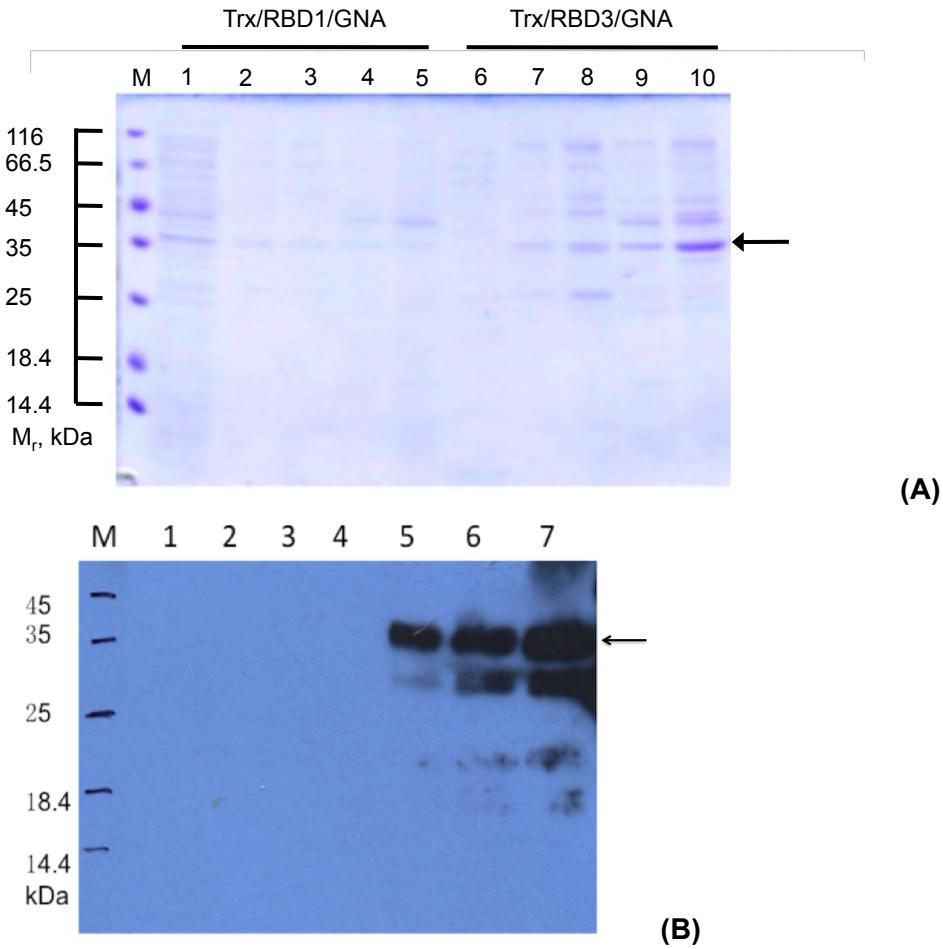

Figure 4-13 **Purification of induced soluble recombinant Trx/RBD1/GNA and Trx/RBD3/GNA fusion protein in *E. coli* BL21 (DE3). SDS-PAGE gel stained with Coomassie Blue**.

(A): Induced soluble fractions of Trx/RBD1/GNA and Trx/RBD3/GNA culture supernatant are shown in lanes 1 and 6, respectively. Trx/RBD1/GNA and Trx/RBD3/GNA fractions washed with 10mM Imidazole are shown in lanes 2 and 7, and peak drops are shown in lanes 3 and 8. Lanes 4 and 9 shows Trx/RBD1/GNA and Trx/RBD3/GNA eluted fractions with 400mM Imidazole, and peak drops are in lanes 5 and 10. The Trx/RBD/GNA fusion protein band at approx. 35kDa is indicated by an arrow. Ten microliter of all fractions were loaded. Lane M represents a molecular weight marker (SDS7).

(B): Identification of recombinant fusion proteins by Western blotting

Fractions from the purification of Trx/RBD3/GNA were probed with anti-(His)6 antibodies. Ten microlitre samples were loaded. Lane 1 shows flow-through fraction from metal affinity column. Lane 2 shows fraction washed with 1XBB. Lanes 3 and 4 shows wash fraction containing 10mM imidazole. Lanes 5 and 6 show eluted fraction and peak drop containing 400mM imidazole. Soluble protein fraction from *E. coli* expressing Trx/RBD3/GNA after induction is shown in lane 7.

4.2.3 Downstream processing of purified recombinant proteins

The purified recombinant proteins were eluted from the metal affinity column in buffer containing 200mM-400mM imidazole, which must be removed as it is toxic to insects and would interfere with use of the fusion proteins in making protein-RNA complexes.

In an initial experiment, the peak of Trx/RBD3/GNA protein eluted in 400mM imidazole was dialysed againt sodium phosphate buffer containing 10% glycerol and 0.15M NaCl. A precipitate was formed on dialysis, and after several changes of buffer, the supernatant and pellet were seperated by centrifugation and analysed by SDS-PAGE. Results are shown in Figure 4-14. No Trx/RBD3/GNA fusion protein remained in the supernatant (lane 4), indicating that all the fusion protein had precipitated out on removal of imidazole. The insoluble protein cannot show biological activity and is useless for further applications.

To investigate conditions for downstream processing which could retain biological activity in the fusion proteins, thioredoxin expressed from "empty" pET32a vector was again used as a model system. This protein was processed by passage through a PD-10 desalting column that had been pre-equilibrated in deionised water; results are shown in Figure 4-15. The eluted peak of protein remained soluble (lanes 1-5). It was collected, flash-frozen and lyophilised; the resulting protein powder was fully soluble in a non-denaturing buffer (phosphate-buffered saline), with no evidence for any remaining insoluble material being observed.

A similar process was used to treat the Trx/RBD3 and Trx/RBD3/GNA fusion proteins eluted from the metal affinity chromatography column. The proteins remained soluble after desalting into deionised water using a PD-10 column (Figure 4-16). Protein-containing fractions were flash-frozen and lyophilised. The freeze dried proteins (with thioredoxin as a comparison) were resuspended in 1XPBS and soluble and insoluble fractions were separated by centrifugation, and analysed by SDS-PAGE. Results are shown in Figure 4-17. This experiment confirmed that recombinant thioredoxin showed 100% solubility in1XPBS after lyophilisation. The Trx/RBD3 fusion protein showed approx. 70% solubility, although some Trx/RBD3 could be detected in the insoluble fraction (lanes 2 and 7). In contrast, little of the Trx/RBD3/GNA fusion protein was soluble after lyophilisation, and only the insoluble fraction contained a prominent 35kDa fusion protein band (lanes 3 and 8).

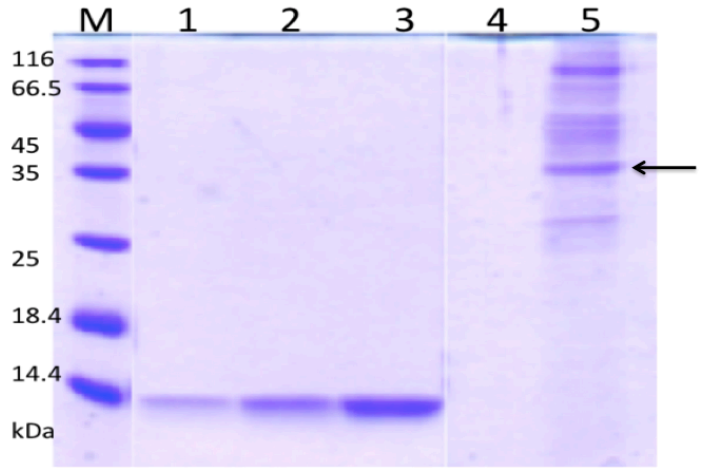

Figure 4-14 **Downstream processing of Trx/RBD3/GNA after purification.**
Purified Trx/RBD3/GNA was dialysed against sodium phosphate buffer containing 10% glycerol and 0.15M NaCl. Twelve-kilodalton band of GNA (1μg, 2μg, 4μg as a standard) are shown from lanes 1-3. Lane 4 shows soluble fraction after dialysis and lane 5 shows insoluble fraction after dialysis. Trx/RBD3/GNA fusion protein is represented by the 35kDa band in the insoluble fraction as indicated by arrow. Lane M represents a molecular weight marker (SDS7).

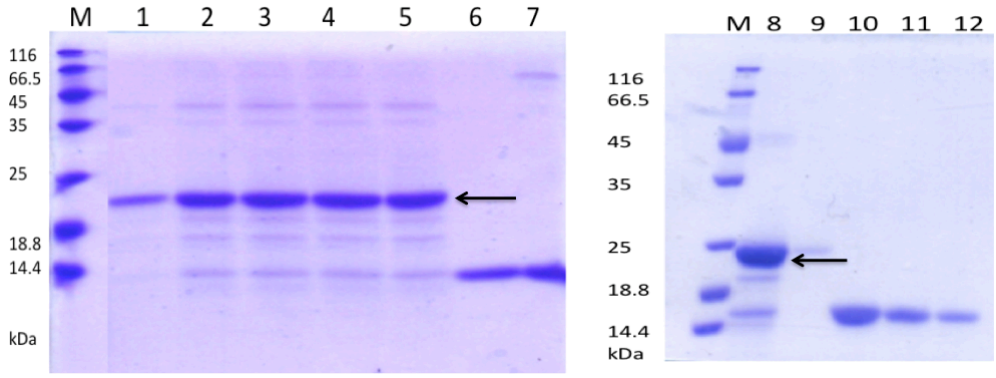

Figure 4-15 **Downstream processing of recombinant thioredoxin.**
Purified thioredoxin was desalted into deionised water on a PD-10 column. Ten microlitre of eluted protein fractions are shown from lanes 1-5. After desalting, Thioredoxin was freeze dried and re-suspended in 1XPBS. Lane 8 shows desalted thioredoxin after lyophilisation and dissolving in phosphate-buffered saline. Lane 9 shows 5μl of eluted thioredoxin fractions from desalting PD-10 column. Twelve-kilodalton band of GNA (2μg, 4μg as a standard) are shown in lane 6 and 7. Lanes 10-12 shows 4μg, 2μg and 1μg GNA standard. Lane M represents a molecular weight marker (SDS7).

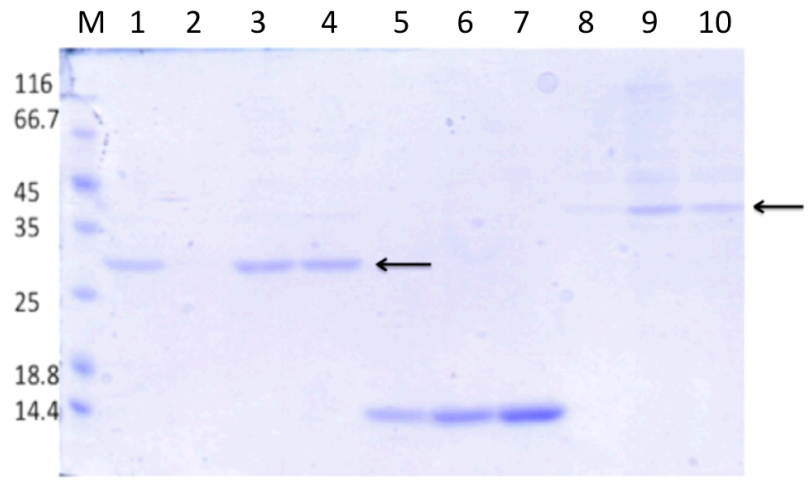

Figure 4-16 **Desalting Trx/RBD3 and Trx/RBD3GNA fusion proteins on a PD-10 column**

Lanes 1-4 shows 5μl of eluted Trx/RBD3 fractions from PD-10 column. The band at 27kDa represents Trx/RBD3 as indicated by arrow. Twelve-kilodalton band of GNA (1μg, 2μg, 4μg as a standard) are shown in lanes 5-7. Lanes 8-10 shows 5μl of eluted Trx/RBD3/GNA fractions from PD-10 column. The band at 35kDa represents Trx/RBD3/GNA. Lane M represents a molecular weight marker (SDS7).

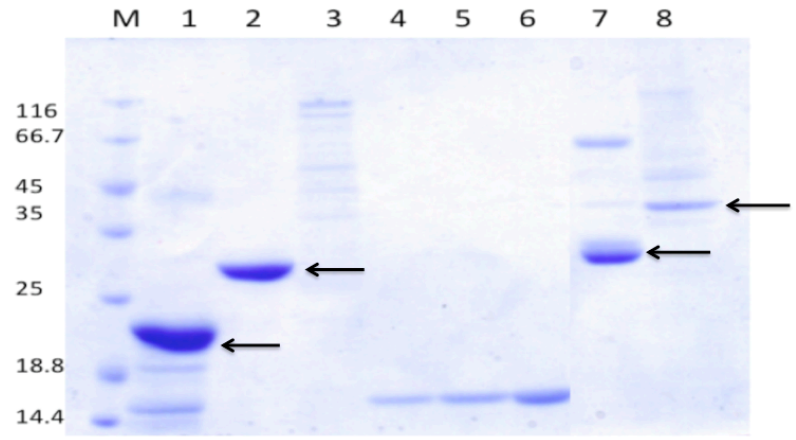

Figure 4-17 **Solubility of Trx, and Trx/RBD3 and Trx/RBD3/GNA fusion proteins in PBS after lyophilisation**

Lane 1-3 represents 10μg soluble fraction of thioredoxin, 5μg soluble fraction of Trx/RBD3 (27kDa) and soluble fraction of Trx/RBD3/GNA (35kDa), respectively. Twelve-kilodalton band of GNA (1μg, 2μg, 4μg as a standard) are shown in lanes 4-6. Lanes 7 and 8 show insoluble fraction of Trx/RBD3 and Trx/RBD3/GNA, respectively. Lane M represents a molecular weight marker (SDS7).

4.2.4 Expression of RBD3/GNA in the periplasm of *E. coli*

Secretion of recombinant protein into the periplasmic space was attempted in order to produce soluble RBD3/GNA protein in *E. coli* system. The vector pET22, containing the *E. coli* periplasmic secretion signal sequence from *pelB* was used to produce an expression construct for recombinant protein production. The schematic diagram and sequences of PelB/RBD3/GNA is shown in Figure 4-18; the *pelB* leader sequence was introduced N-terminal to the RBD3 coding sequence, and a $(His)_6$ tag was arranged C-terminal to the GNA coding sequence (Figure 4-19). The predicted size of the PelB/RBD3/GNA fusion protein is 24.5 kDa. After introduction into the BL21(DE3) expression strain, fusion protein production was induced by addition of IPTG. After induction, fractions corresponding to periplasmic proteins, soluble cytoplasmic proteins and insoluble proteins were purified from *E. coli* cells, and analysed by SDS-PAGE and western blotting. Results are summarised in Figure 4-20. The stained SDS-PAGE gel shows evidence of PelB/RBD3/GNA production, but only in the insoluble protein fraction (panel A, lane 6); the prominnent band at approx. 25kDa could be pelB/RBD3/GNA whereas the lower band around 24kDa could be RBD3/GNA without pelB leader sequence. The Western blot has overloaded in the corresponding track, but confirms that immunoreactivity is strongly present in the insoluble fraction. Very little potential pelB/RBD3/GNA can be detected in periplasmic fraction (Figure 4-20 A and B, lane 2; a possible trace of soluble fusion protein is indicated by an arrow in panel B). This method was not successful in producing soluble recombinant protein.

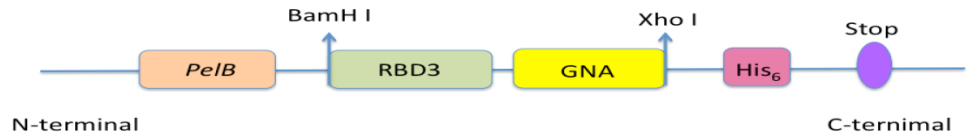

Figure 4-18 **Schematic diagram of an expression construct for the fusion protein, PelB/RBD3/GNA in pET22b+.**

ATGAAATACCTGCTGCCGACCGCTGCTGCTGGTCTGCTGCTCCTCGCTGCCCAG
CCGGCGATGGCCATGGATATCGGAATTAATTCGGATCC*C**GATAAGAAGTCTCC*A
ATTTCTCAAGTTCATGAAATTGGTATTAAGAGACAAATGACTGTTCATTTTAAGG
TTTTGAGAGAAGAAGGTCCAGCTCATATGAAGAACTTTATTACTGCTTGTATTGT
TGGTTCTATTGTTACTGAAGGTGAAGGTAAGGGTAAGAAGGTTTCTAAGAAGAG
AGCTGCTGAAAAGATGTTGGTTGAATTGCAAAAGTTGCCAAAGCTTGCGGCCGC
CGACAATATTTTGTACTCCGGTGAGACTCTCTCTACAGGGGAATTTCTCAACTAC
GGAAGTTTCGTTTTTATCATGCAAGAGGACTGCAATCTGGTCTTGTACGACGTGG
ACAAGCCAATCTGGGCAACAAACACAGGTGGTCTCTCCCGTAGCTGCTTCCTCA
GCATGCAGACTGATGGGAACCTCGTGGTGTACAACCCATCGAACAAACCGATTT
GGGCAAGCAACACTGGAGGCCAAAATGGGAATTACGTGTGCATCCTACAGAAG
GATAGGAATGTTGTGATCTACGGAACTGATCGTTGGGCCACTGGA*CTCGAG*CAC
CACCACCACCACCACTGA

MKYLLPTAAAGLLLLAAQPAMAMDIGINSDPDKKSPISQVHEIGIKRQMTVHFKVLRE
EGPAHMKNFITACIVGSIVTEGEGKGKKVSKKRAAEKMLVELQKLPKLAAADNILYS
GETLSTGEFLNYGSFVFIMQEDCNLVLYDVDKPIWATNTGGLSRSCFLSMQTDGNLV
VYNPSNKPIWASNTGGQNGNYVCILQKDRNVVIYGTDRWATGLEHHHHHH.

Figure 4-19 **Nucleotide and derived amino acid sequences of synthetic RBD3/GNA in PET22b+ vector**

pelB leader sequence, RBD3 coding sequence, GNA coding sequence, His_6 tag

Extra **c** highlighted in blue is added into sequence to get right frame.

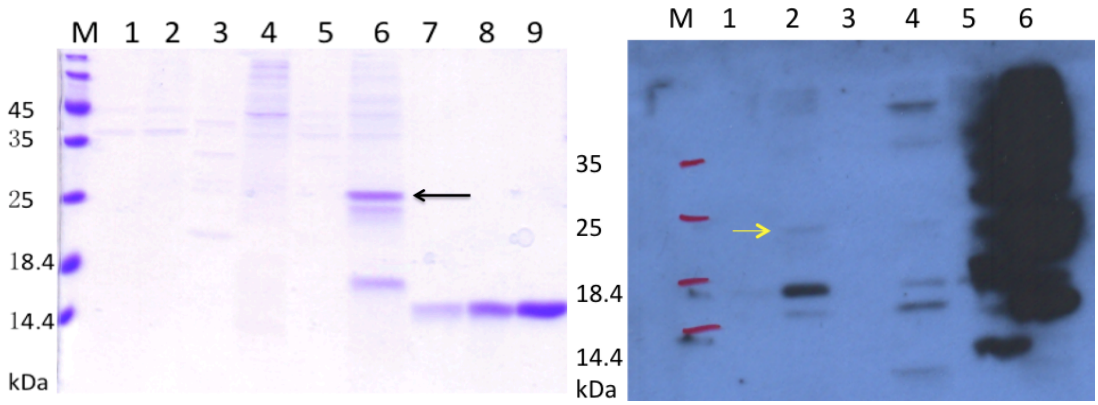

(A) (B)

Figure 4-20 **SDS-PAGE analysis and western blotting confirmation of recombinant RBD3/GNA expression in cytoplasm and periplasm.**

Lanes 1 and 2 show periplasmic fractions from uninduced and induced cell culture checked on SDS-PAGE (A) and blot (B). Lanes 3 and 4 show cytoplasmic fractions from uninduced and induced cell culture on SDS-PAGE (A) and blot (B). Lanes 5 and 6 show Insoluble fractions from uninduced and induced cell culture on SDS-PAGE (A) and blot (B). Twelve-kilodalton band of GNA (1μg, 2μg, 4μg as a standard) are shown in lanes 7-9. pelB/RBD3/GNA was predicted as 24kDa as indicated by arrow.

4.2.5 Expression of recombinant proteins containing RBD domains in the yeast *Pichia pastoris*

The difficulties experienced in trying to produce soluble recombinant Trx/RBD/GNA fusion proteins in *E. coli* as an expression host reflect previous work, in which GNA itself has been expressed in bacterial hosts. The recombinant GNA was found to be insoluble after expression in *E. coli*, and although purification by denaturation-renaturation can be made to work, recovery of soluble protein was poor and non-reproducible (Longstaff *et al.* 1998). In contrast, GNA can be produced in the eukaryotic microorganism *Pichia pastoris* as a functional, soluble protein secreted into culture medium in high yield (Baumgartner *et al.* 2003). Expression of RBD/GNA fusion proteins was thus attempted in this host with the aim of generating soluble, functional products.

Constructs encoding RBD3 fused C-terminally to the yeast α-mating factor prepropeptide, and N-terminally to myc and $(His)_6$ tags, and RBD3 fused C-terminally to the yeast mating factor prepropeptide, and N-terminally to a GNA coding sequence with C-terminal myc and $(His)_6$ tags were assembled in the vector pGAPZα. This shuttle vector is propagated and manipulated in *E. coli*, and can be linearised and transfromed into *P. pastoris*, where it integrates into the genome by homologous recombination. Yeast transformants thus contain an integrated genomic copy of the expression construct, whose promoter directs constitutive expression of the recombinant protein. The yeast α-mating factor sequence directs the recombinant protein into the yeast secretory pathway, and consequently it can be purified from the culture supernatant. The constructs are described by block diagrams and predicted sequences of their products in Figure 4-21. The predicted molecular weights of the recombinant proteins after removal of the α-mating factor prepropeptide are 9.21 kDa for RBD3, and 21.18 kDa for RBD3/GNA.

Construct assembly was carried out by restriction-ligation after PCR of appropriate fragments, and resulting plasmids were checked by sequencing prior to transformation of *Pichia pastoris* strain (SMD1168). Recombinant yeast were selected on plates containing zeocin, the selectable marker included on the vector pGAPZα.

Screening recombinant RBD3 yeast clones by analysis of culture supernatants by Western blotting detected clones showing low levels of expression of a polypeptide of approx. 10kDa, assumed to correspond to RBD3. The best expressing clone was selected. A similar screening analysis of recombinant RBD3/GNA yeast clones allowed selection of several clones which were expressing a polypeptide of approx. 20kDa, close to the size predicted for RBD3/GNA. The best expressing clone was again selected.

(A)

N-terminal C-terminal

ATGAGATTTCCTTCAATTTTTACTGCTGTTTTATTCGCAGCATCCTCCGCATTAGC
TGCTCCAGTCAACACTACAACAGAAGATGAAACGGCACAAATTCCGGCTGAAG
CTGTCATCGGTTACTCAGATTTAGAAGGGGATTTCGATGTTGCTGTTTTGCCATT
TTCCAACAGCACAAATAACGGGTTATTGTTTATAAATACTACTATTGCCAGCATT
GCTGCTAAAGAAGAAGGGGTATCTCTCGAGAAAAGAGAGGCTGA**AGCTGCAGC**
AGATAAGAAGTCTCCAATTTCTCAAGTTCATGAAATTGGTATTAAGAGACAAATG
ACTGTTCATTTTAAGGTTTTGAGAGAAGAAGGTCCAGCTCATATGAAGAACTTTA
TTACTGCTTGTATTGTTGGTTCTATTGTTACTGAAGGTGAAGGTAAGGGTAAGAA
GGTTTCTAAGAAGAGAGCTGCTGAAAAGATGTTGGTTGAATTGCAAAAGTTGCC
AGTCGACCATCATCATCATCATCATTGA

MRFPSIFTAVLFAASSALAAPVNTTTEDETAQIPAEAVIGYSDLEGDFDVAVLPFSNS
TNNGLLFINTTIASIAAKEEGVSLEKREAE**AAA**DKKSPISQVHEIGIKRQMTVHFKVLR
EEGPAHMKNFITACIVGSIVTEGEGKGKKVSKKRAAEKMLVEQKLP**VD**HHHHHH.

α-factor signal sequence, **RBD3 coding sequence**, **His_6 tag**

(A) Schematic diagram and amino acid sequence of an expression construct for RBD3 in pGAPZαB

(B)

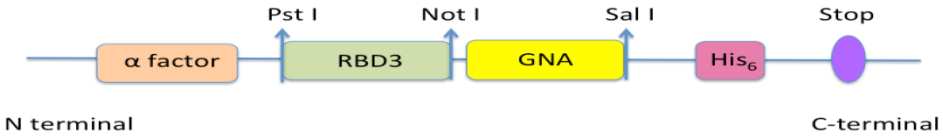

ATGAGATTTCCTTCAATTTTTACTGCTGTTTTATTCGCAGCATCCTCCGCATTAGC
TGCTCCAGTCAACACTACAACAGAAGATGAAACGGCACAAATTCCGGCTGAAG
CTGTCATCGGTTACTCAGATTTAGAAGGGGATTTCGATGTTGCTGTTTTGCCATT
TTCCAACAGCACAAATAACGGGTTATTGTTTATAAATACTACTATTGCCAGCATT
GCTGCTAAAGAAGAAGGGGTATCTCTCGAGAAAAGAGAGGCTGAAGCTGCAGC
AGATAAGAAGTCTCCAATTTCTCAAGTTCATGAAATTGGTATTAAGAGACAAATG
ACTGTTCATTTTAAGGTTTTGAGAGAAGAAGGTCCAGCTCATATGAAGAACTTTA
TTACTGCTTGTATTGTTGGTTCTATTGTTACTGAAGGTGAAGGTAAGGGTAAGAA
GGTTTCTAAGAAGAGAGCTGCTGAAAAGATGTTGGTTGAATTGCAAAAGTTGCC
AGCGGCCGCCGATAACATTTTGTACTCTGGTGAAACTTTGTCTACTGGTGAATTT
TTGAACTACGGTTCTTTTGTTTTTATTATGCAAGAAGATTGTAACTTGGTTTTGTA
CGATGTTGATAAGCCAATTTGGGCTACTAACACTGGTGGTTTGTCCAGATCTTGT
TTTTTGTCTATGCAAACTGATGGTAACTTGGTTGTTTACAACCCATCTAACAAGC
CAATTTGGGCTTCTAACACTGGTGGTCAAAACGGTAACTACGTTTGTATTTTGCA
AAAGGATAGAAACGTTGTTATTTACGGTACTGATAGATGGGCTACTGGTGTCGA
CCATCATCATCATCATCATTGA

MRFPSIFTAVLFAASSALAAPVNTTTEDETAQIPAEAVIGYSDLEGDFDVAVLPFSNS
TNNGLLFINTTIASIAAKEEGVSLEKREAEAAADKKSPISQVHEIGIKRQMTVHFKVLR
EEGPAHMKNFITACIVGSIVTEGEGKGKKVSKKRAAEKMLVELQKLPAAADNILYSG
ETLSTGEFLNYGSFVFIMQEDCNLVLYDVDKPIWATNTGGLSRSCFLSMQTDGNLVV
YNPSNKPIWASNTGGQNGNYVCILQKDRNVVIYGTDRWATGVDHHHHHH.

α-factor signal sequence, RBD3 coding sequence, GNA coding sequence, His6 tag

(B) Schematic diagram and amino acid sequence of an expression construct for RBD3/GNA in pGAPZαB

Figure 4-21 Schematic diagrams and amino acid sequences of expression constructs for RBD3 and RBD3/GNA in pGAPZαB

4.2.6 Purification of recombinant proteins containing RBD3 from *P. pastoris* culture supernatant

4.2.6.1 Purification of RBD3

RBD3 was purified from yeast culture supernatant by metal affinity chromatography as described for purification of Trx/RBD3 from *E. coli*. Yeast culture supernantant after fermentation was diluted x4 with binding buffer, and was loaded directly onto a nickel-NTA-agarose column. After washing, the column was eluted with binding buffer containing 400mM imidazole. results are shown in Figure 4-22. The protein fraction eluted from the affinity column at 400mM imidazole contained a polypeptide of approx. 10 kDa mol. wt. which was assumed to be RBD3; however, this material was contaminted by a yeast protein of approx. 55 kDa (Figure 4-22, panel A, lanes 3-5).

The eluted protein was concentrated by centrifugal concentrator and dialysed into RNA binding buffer. A small amount of protein precipitated out under these conditions (Figure 4-22, panel B, lanes 16 and 17), but most remained soluble (lanes 14-15).

The results showed that purification of recombinant RBD3 from yeast culture supernatant was feasible, but yileds were very low, and the final product was inferior in purity to the soluble recombinant protein produced in *E. coli*. This method for producing recombinant RBD3 was not taken further.

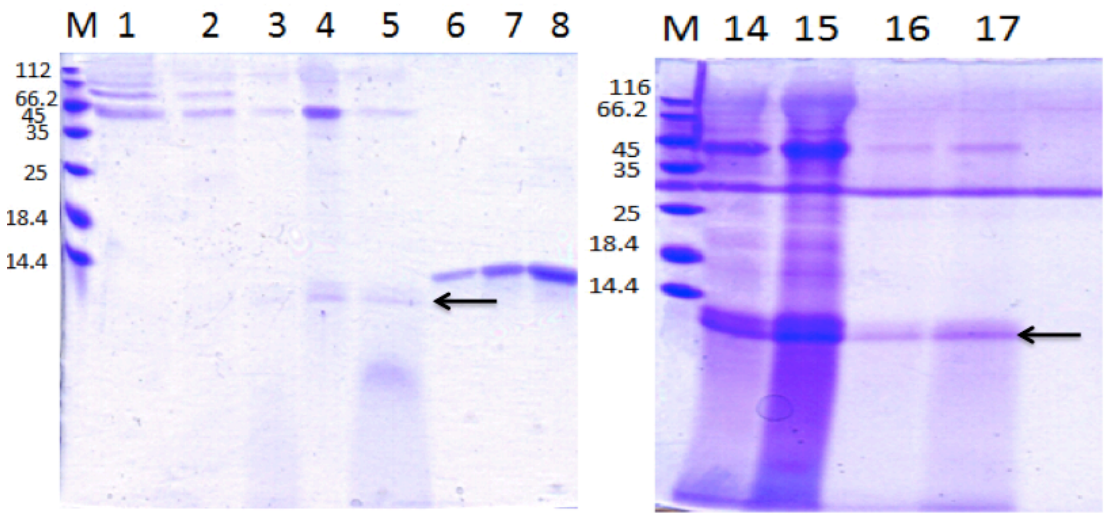

(A) (B)

Figure 4-22 **SDS-PAGE analysis of fractions from purification of RBD3 from *P. pastoris* culture supernatant.**

Panel A: Lanes 1 and 2 show 20μl of RBD3 culture supernatant and 20μl of peak drop from 10mM imidazole wash, respectively. Lanes 3 and 5 show 10μl of fraction eluted by 400mM imidazole. Lane 4 shows 20μl of peak drop from 400mM imidazole elution. Twelve-kilodalton band of GNA (1μg, 2μg, 4μg as a standard) are shown in lanes 6-8. Panel B: Lanes 14 and15 shows 2μg and 5μg RBD3 soluble protein after concentration. Insoluble RBD3 protein after concentration are show in lane. 16 and 17. Lane M represents a molecular weight marker (SDS7).

4.2.7 Purification of RBD3/GNA by metal affinity chromatography under different pH conditions

The selected *P. pastoris* clone expressing RBD3/GNA was grown on a larger scale in a 5 L laboratory fermentation system. After 4 days fermentation at 30°C, 2.5 L of culture supernatant were harvested and filtered by 2.7μM and 0.7μM filter before purification. RBD3/GNA was purified from culture supernatant by metal affinity chromatography on a column of immobilised nickel. To achieve better protein recovery efficiency, several purification methods were applied.

First, purification of RBD3/GNA under native conditions was performed by diluting yeast supernatant with 4XBB pH 7.4. The pH of diluted yeast supernatant was around 4 before loading. As the stained SDS-PAGE result shown in Figure 4-23, Purification of RBD3/GNA from the yeast culture supernatant gave a product of the expected size visible as a band on SDS-PAGE (see Figure 4-23, panel B, lanes 5 and 6; arrowed band), although this was present in small amount, and other polypeptides were also present in the eluted fraction. However, analysis of the culture supernatant by SDS-PAGE followed by Western blotting probed with anti-GNA antibodies showed bands at the expected size for the RBD3/GNA fusion protein and a GNA cleavage product (Figure 4-23, panel C, lanes 1,2). These bands were also present in the fraction eluted from the column in 200mM imidazole, and thus are likely to represent the RBD3/GNA fusion protein, which has been produced in soluble form in *P. pastoris.* The RBD3/GNA band is indicated by an arrow in the Figure 4-23 panel C. RBD3/GNA is also in the fraction eluted by 0.4M imidazole (Figure 4-23 panel c lane 5) suggest that some of the RBD3/GNA bounds to column tightly and most of cleaved GNA can be eluted in 0.4M imidazole fraction. The solubility of RBD3/GNA is maintained after dialysis against both distilled water and 0.02M sodium phosphate buffer (Figure 4-23 panel C lane 7 and lane 9). RBD3/GNA shows more solubility in 0.02M sodium phosphate buffer than distilled water. The yield of fermented RBD3/GNA was approx.10mg/L and about 0.8 mg RBD3/GNA was recovered from 300ml supernatant that contained approx. 3mg fusion protein.

Secondly, the purification of RBD3/GNA was also carried out at pH 5.5 by adding 4XBB pH 9.0. The nickel-NTA column was washed with 0.01M imidazole to remove unbound protein and RBD3/GNA was eluted in 0.2M imidazole. Western blotting of fractions from the purification using anti-GNA antibody is shown in Figure 4-24. RBD3/GNA was detected in the fraction eluted with 0.2M imidazole. After dialysis against 0.02M sodium phosphate buffer followed by centrifugation, RBD3/GNA was found in soluble supernatant (Figure 4-24.B lane 2) with no protein detected in insoluble fraction (Figure

4-24.B lane 1). However, there is no obvious improvement of RBD3/GNA protein recovery efficiency compared to purification at pH 4.

Finally, the purification of RBD3/GNA was performed from freeze dried culture supernatant powder that was re-suspended in 1XBB at pH 7.4. Washing and elution were carried out with 0.01M imidazole and 0.2M imidazole as mentioned above; results are shown in fig.4.25. Whereas higher mol. wt. polypeptides did not bind to the column, major protein components of culture supernatant with polypeptides approx. 25 and 50kDa were washed off in binding buffer containing 10mM imidazole. RBD3/GNA were eluted in 0.2M imidazole fraction. Pooled 0.2M imidazole fractions were dialysed against distilled water overnight at 4°C followed by freeze drying. Pooled 0.01M washed fractions were dialysed against 0.02M sodium phosphate buffer followed by concentration by a centrifugal filtration system. Analysis of fractions by SDS-PAGE showed that detectable RBD3/GNA was washed out from column by 0.01M imidazole (Figure 4-25 panel B, lane 4), but that RBD3/GNA protein was purified in reasonable yield by elution with 0.2M imidazole (Figure 4-25 panel A, lanes 3, 4 and 7, 8). Approx. 1.3mg RBD3/GNA was recovered from 300ml yeast supernatant.

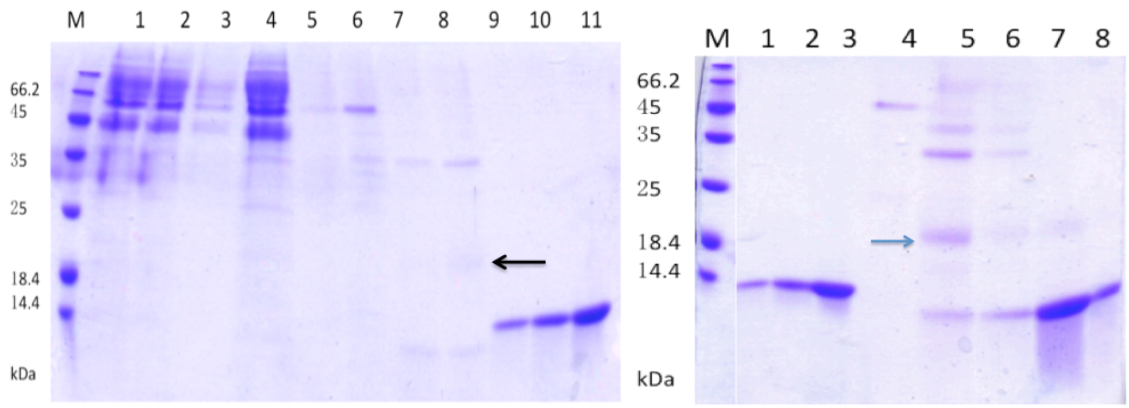

(A) (B)

Figure 4-23 **Purification of RBD3/GNA from culture supernatant of *P. pastoris* by nickel affinity chromatography at pH 4**

(A, B) Analysis of fractions by SDS-PAGE; results from 2 separate column purifications RBD3/GNA supernatant is shown in lanes 1 and 2 (A) and RBD3/GNA supernatant diluted in in 1Xbinding buffer (pH 4) is shown in lane 3 (A). Lane 4 (A) shows flow-through protein fraction. Lanes 5 and 6 (A) and B4 showsfraction and peak drop from 10mM imidazole wash. Lanes 7 and 8 (A) and 5 and 6 (B) show fraction and peak drop from elution with 200mM imidazole. Lanes 7 and 8 (B) shows fraction and peak drop from elution with 400mM imidazole. Twelve-kilodalton band of GNA (1μg, 2μg, 4μg as a standard) are shown in lanes 9-11 (A) and 1-3 (B).

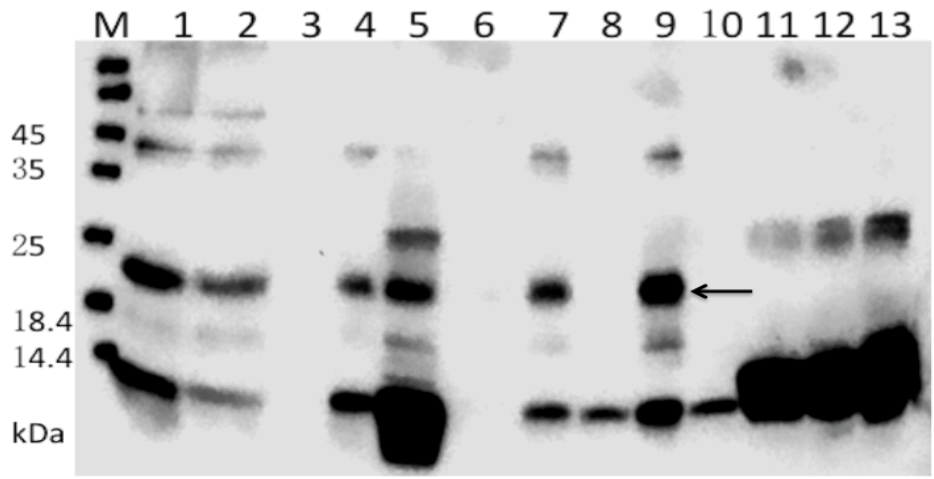

(C)

(C) **Analysis of fractions from purification of RBD3/GNA produced by *P. pastoris* by Western blotting, probed with anti-GNA antibodies**

Lanes 1 and 2 show culture supernatant of *P. pastoris* clone expressing RBD3/GNA. Lane 3, 4 and 5 show 10mM imidazole wash fraction, 200mM imidazole elution fraction, and 400mM imidazole elution fraction from nickel affinity chromatography, respectively. Lane 7 and 8 show soluble and insoluble fractions after dialysis of purified RBD3/GNA against water, respectively. Lane 9 and 10 show soluble and insoluble fraction after dialysis of purified RBD3/GNA against 20mM sodium phosphate buffer, respectively. Twelve-kilodalton band of GNA (1μg, 2μg, 4μg as a standard) are shown in lanes 11-13. Band of expected size for RBD3/GNA fusion protein is indicated by arrow.

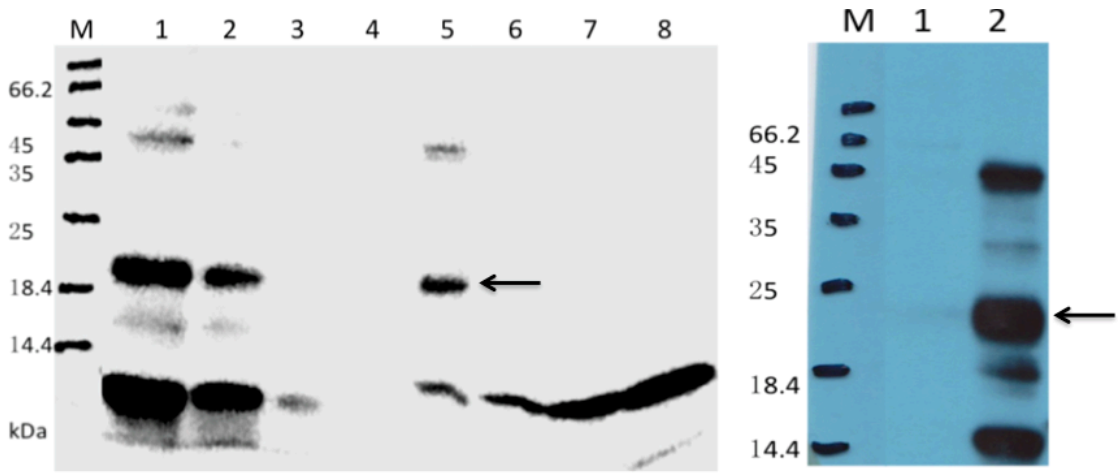

(A) (B)

Figure 4-24 **Purification of RBD3/GNA from culture supernatant of *P. pastoris* by nickel affinity chromatography at pH 5.5**

Panel A: Lane 1 and 2 show RBD3/GNA neat supernatant and the supernatant diluted in 1Xbinding buffer (pH 5.5). Lane 3 shows flow-through fraction from nickel column. Lanes 4 and 5 show fraction from 10mM imidazole wash and elution with 200mM imidazole. Twelve-kilodalton band of GNA (30ng, 50ng, 100ng as a standard) are shown in lanes 6-8. After dialysis against 0.02M sodium phosphate buffer, RBD3/GNA can be detected in soluble fraction (lane 2, B) whereas no fusion protein was found in insoluble fraction (lane 1, B).

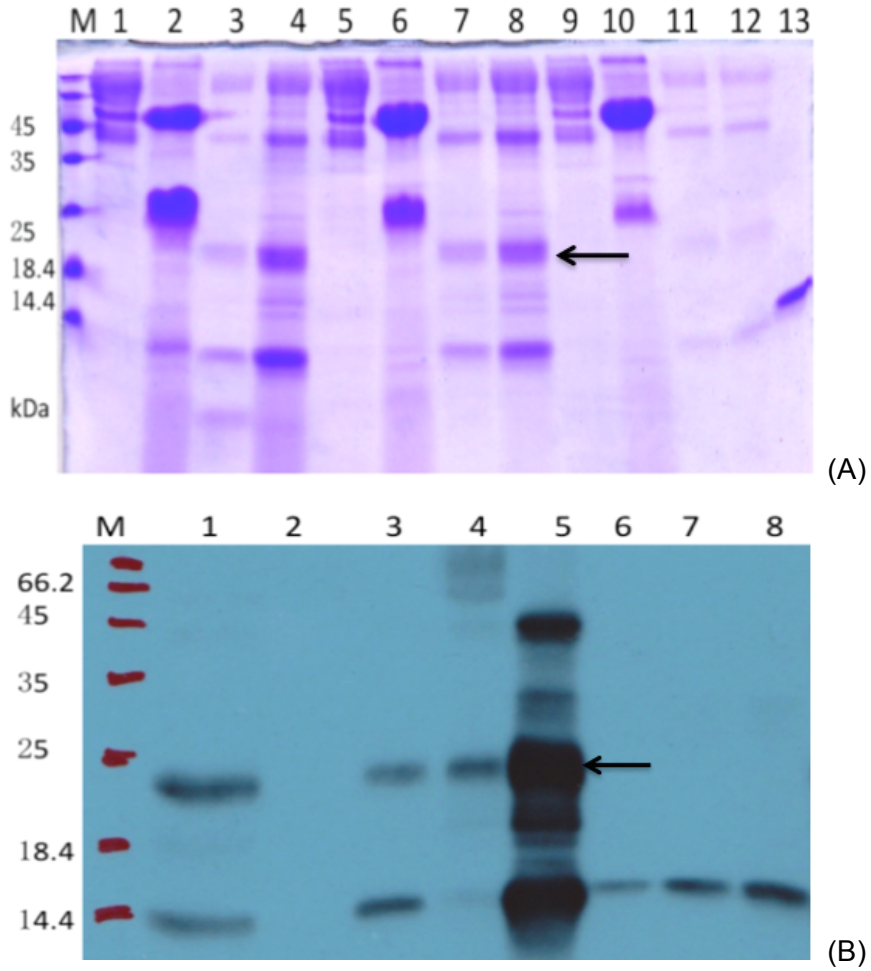

Figure 4-25 **Purification of RBD3/GNA from dialysed freeze dry supernatant powder pH 7.4**

A: Analysis of fractions by SDS-PAGE; results from 3 separate purifications. Flow-throughs are shown in lanes 1, 5 and 9 and eluted peak drop from 10mM imidazole washes are shown in lanes 2, 6 and 10. Elution fractions and peak drops with 200mM imidazole are shown in lanes 3, 7, 11 and lanes 4, 8 and 12, respectively. Twelve-kilodalton band of 2μg GNA as a standard is shown in lane 13.

B**:** Western blotting of purification of RBD3/GNA from freeze dried supernatant powder pH 7.4 by GNA antibody**.** Lane 1 shows RBD3/GNA supernatant. Lane 2 shows fraction from 0.01M imidazole wash. After concentration, fraction was check in lane 4. Lane 3 and 5 shows fraction eluted in 0.2M imidazole (RBD3/GNA indicated by arrow) and RBD3/GNA after lypophilisation, respectively. Twelve-kilodalton band of GNA (30, 50, and 100ng as a standard) are shown in lanes 6-8.

4.2.8 Purification of RBD3/GNA by gel filtration chromatography

Freeze dried RBD3/GNA supernatant powder was re-suspended in 0.02M sodium phosphate buffer and loaded onto a Sephacryl S-200 gel filtration column which was equilibrated in 0.02M sodium phosphate buffer. As the result shown in Figure 4-26, gel filtration failed to separate yeast proteins in the culture supernatant from RBD3/GNA. Large amounts of proteins above 35kDa were still presented in all fractions analysed.

4.2.9 Purification of RBD3/GNA under denaturing conditions at pH 6

As the His tag will be exposed to nickel column and thus increase the chance of binding when protein was unfolded, purification of RBD3/GNA was performed under denaturing conditions by metal affinity chromatography in the presence of 6M urea. Results are shown in Figure 4-27.

Analysis by western blotting using anti-GNA antibodies (Figure 4-27) confirmed that RBD3/GNA was successfully purified by elution with 0.2M imidazole, and that no residual fusion protein was observed in wash fraction. However, purified RBD3/GNA failed to refolded after dialysis against 0.02M sodium phosphate buffer with a gradient dilution of urea (see Figure 4-27 lane 5), and only insoluble protein was present.

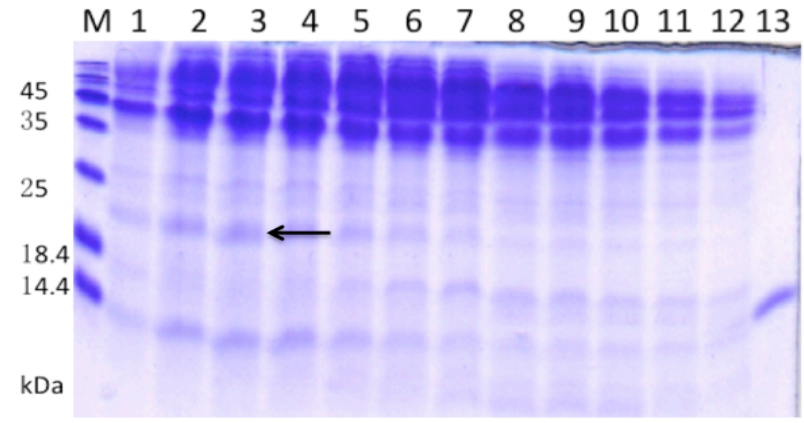

Figure 4-26 **Purification of RBD3/GNA by gel filtration chromatography**
Fractions eluted from the column containing protein (lanes 1-12; fractions 21-44) were analysed by SDS-PAGE. Twelve-kilodalton band of 2μg GNA as a standard is shown in lane 13.

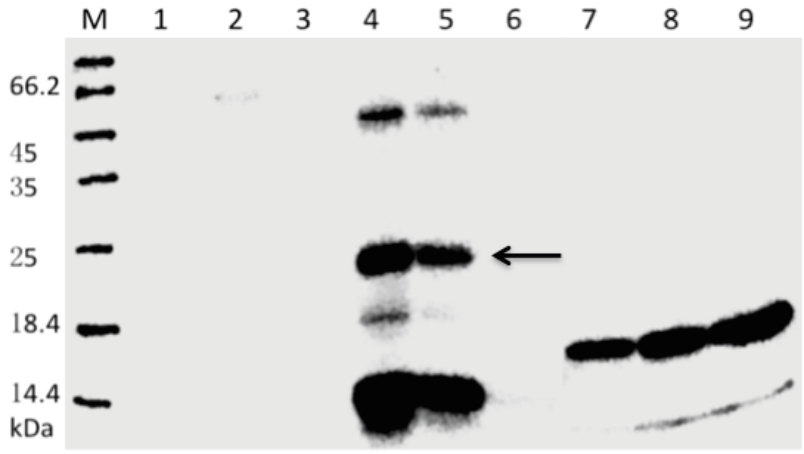

Figure 4-27 **Western Blot of purification of RBD3/GNA under denaturing conditions probed with anti-GNA antibody**
Lanes 1 and 3 show fraction washed with 1XBB containing 6M urea and 10mM imidazole containing 6M urea. Lane 2 shows Flow-through. Eluted RBD3/GNA in 0.2M imidazole is shown in lane 4. Dialysised insoluble and soluble fractions of RBD3/GNA are shown in lanes 5 and 6, respectively. Twelve-kilodalton band of GNA (30, 50 and 100ng as a standard) are shown in lanes 7-9. Five-microlire from each samples were used for western blotting.

4.2.10 Processing of recombinant proteins by denaturation-renaturation

The insoluble protein fractions from *E. coli* strains expressing Trx/RBD1 and Trx/RBD/GNA fusion proteins showed clean single bands on SDS-PAGE, in high yield, and thus offer a source to recover recombinant proteins without further purification. These insoluble fractions were dissolved in 6M urea to provide material for experiments to determine whether renaturation could produce functional proteins.

Insoluble Trx/RBD1 and Trx/RBD/GNA fractions solubilised in 6M urea were dialysed against a gradient dilution of urea to 0.5M, and were stored at 0.5M urea and 0.5mM DTT. This process was successful in maintaining protein solubility, in that no precipitation was observed. However, when the refolded Trx/RBD1 was tested in a RESMA assay no dsRNA binding activity was observed, as no dsRNA mobility shift was detected. Refolded Trx/RBD3/GNA was also checked for biological activity of the GNA by aggutination assay (shown in Figure 4-29, row 6). The result indicated that GNA had lost any activity. Therefore, the refolding of Trx/RBD1 AND Trx/RBD3/GNA against urea and DTT was unsuccessful in allowing biological activity to be restored.

When the insoluble Trx/RBD and Trx/RBD/GNA fractions after refolding in 0.5M urea were dialysed against 20mM sodium phosphate solutions without urea, but containing decreasing concentrations of DTT to zero, extensive precipitation of proteins was observed, with little material remaining in the soluble fraction after separation by centrifugation, result shown in Figure 4-28. These samples were tested for REMSA (results shown in Figure 4-34 lane 7 and 8). No dsRNA mobility shift deteced suggesting that the Trx/RBD/GNA fusion protein had failed to renature.

4.2.11 Confirmation of protein activity by agglutination assays

The biological activity of the GNA part of recombinant fusion proteins was tested by an agglutination assay using rabbit erythrocytes. Results are shown in Figure 4-28. A positive agglutination reaction results in erthrocytes forming a layer over the bottom of the well (e.g. GNA positive control, row1 wells A-E; lowest agglutination concentration = 6 μg ml^{-1}). In a negative reaction, shown in row 2, no agglutination allows the erythrocytes to settle into the bottom of the well to form a "pellet" (e.g. row 2, wells A-J). Soluble RBD3/GNA from *P. pastoris* which had been purified under native conditions at pH 7.4 showed agglutination activity (lowest agglutination concentration = 31 μg ml^{-1}) showing that the GNA part of the fusion was functional. However, none of the GNA-containing fusion proteins which had been purified via processes involving denaturation and refolding showed any agglutination activity.

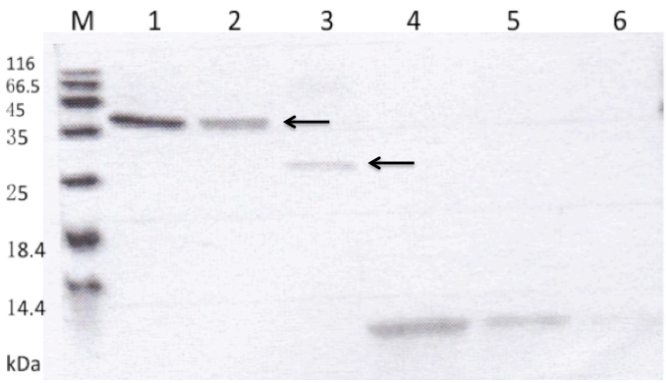

Figure 4-28 **Attempted refolding of Trx/RBD and Trx/RBD/GNA fusion proteins**. Recombinant proteins were dissolved in 6M urea and dialysed against sodium phosphate buffer containing DTT to a final concentration of 0.5M urea. Soluble and insoluble fractions were separated by centrifugation. Lanes 1, 2 and 3 show soluble Trx/RBD3/GNA, Trx/RBD1/GNA and Trx/RBD1, respectively. Twelve-kilodalton band of GNA (1μg, 2μg, 4μg as a standard) are shown in lanes 4, 5 and 6.

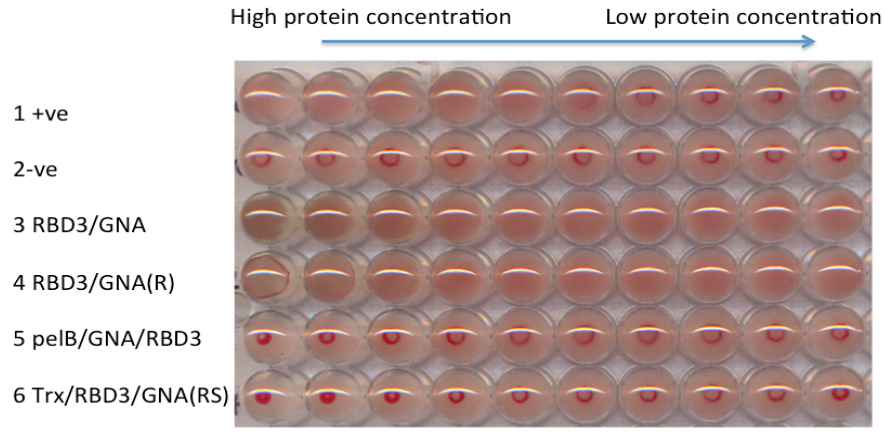

Figure 4-29 **GNA agglutination assay by agglutination**

Each row of wells contains a serial dilution (left to right) of the protein from 1μg μl^{-1}, and the same amount of rabbit erythrocyte suspension. GNA (starting concentration 100ng/μl) as positive control is shown in row 1 and negative control was performed by using 1XPBS (row 2). RBD3/GNA soluble and refolded RBD3/GNA proteins produced in *P. pastoris* are shown in rows 3 and 4, respectively. Refolded pelB/GNA/RBD3 and Trx/RBD3/GNA produced in *E. coli* are shown in rows 5 and 6.

4.2.12 Production of Labelled RNAs and Assays of RNA-Binding Activity of Recombinant Proteins

4.2.12.1 Production of synthetic ss and dsRNAs

Synthetic single stranded (ss) RNAs were produced by *in vitro* transcription of linearized plasmid templates, using T7 RNA polymerase. RNAs were purified by treatment with DNase followed by precipitation, and RNA was quantified by UV absorbance at 260nm. The yield of ssRNA from 1μg of DNA template was routinely around 100μg. dsRNAs were prepared by annealing similar amounts of synthetic sense and antisense strands. All synthetic RNA products were analysed by agarose gel electrophoresis to check for integrity, and to provide a semiquantitative estimate of RNA amount. Typical results are shown in Figure 4-30.

4.2.12.2 Detection of Biotin-labelled RNAs on dot blot and after gel electrophoresis

Single-stranded (ss) RNAs were 3'-end labelled with biotin using biotinylated cytidine bisphosphate and T4 RNA ligase, and purified by chloroform:isomyl alcohol extraction, and precipitation. Biotin-labelled dsRNAs were prepared by annealing separately labelled strands together. To test the senstivity of the detection method, 2μl "dots" of different concentrations of biotin-labelled RNAs were pipetted onto a positively charged nylon membrane and detected using stabilized streptavidin-horseradish peroxidase as shown in Figure 4-31. Dot blots showed that amounts $<3x10^{-17}$ moles of a labelled control ssRNA (biotinylated iron responsive elements (IRE) RNA) supplied with the labelling kit could be readily detected. RNAs labelled using the kit gave less strong signals at similar amounts, but amounts of the order of $4x10^{-16}$ moles (7×10^{-11} g) of both single and double stranded labelled RNAs were readily detectable, with no apparent difference in sensitivity between ssRNA and dsRNA. Sensitivity of detection of labelled dsRNAs after separation by 6% polyacrylamide gel electrophoresis was tested. In this case the separated bands were blotted onto nylon membrane and detected as for dot-blots. As shown in Figure 4-32.B, a minimum of 10 ng labelled dsRNA could be visualised as a single band after gel electrophoresis. The markedly lower sensitivity of the gel method may reflect inefficient transfer from the gel.

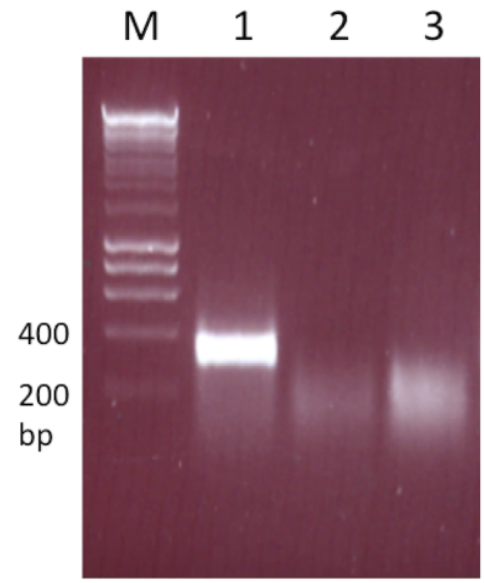

Figure 4-30 ***In vitro*** **transcription of RNAs**

Lanes 2, 3 show single stranded RNAs (*TcVTE* sense and antisense strand respectively; 277 bases) and double stranded RNA produced by annealing ssRNAs shown in lane 1. M: DNA ladder.

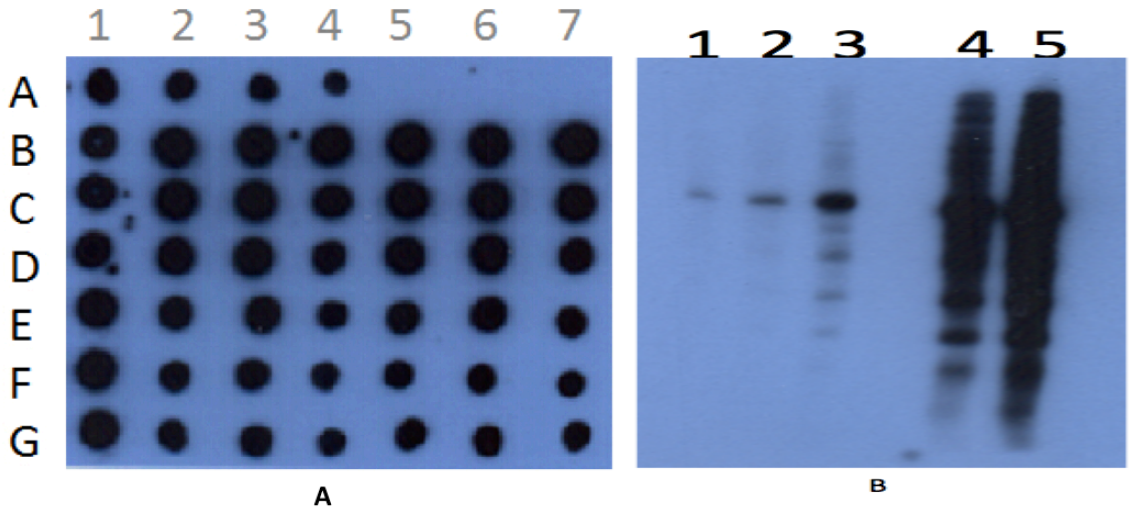

Figure 4-31 **Biotin-lablled ssRNA and dsRNA**

(A) Dot blot of biotinylated ssRNAs and dsRNAs**.** A1-A5 show 1, 0,75, 0.5, 0.25 and 0nM Labeled IRE control RNA provided from Kit. B1-G1 show 1, 0.5, 0.25, 0.125, 0.0625 and 0.0312nM Labeled IRE control RNA. B2-G2, B3-G3, B4-G4, B5-G5, B6-G6 and B7-G7 show 66.8, 33.4, 16.7, 8.35, 4.17, 2.08nM *MdVTE* (Sense) ssRNA, *MdVTE* (Antisense)ssRNA, *MbVTE* (Sense) ssRNA, *MbVTE* (Antisense) ssRNA, *MdVTE* dsRNA and *MbVTE* dsRNA, respectively. **(B)** Detection of labelled *MbVTE* dsRNA on 6%TBE polyacrylamide gel. The amoutn of 10ng, 20ng, 50ng, 200ng, 500ng labelled *MbVTE* dsRNA are shown in lanes 1-5.

4.2.13 RNA Binding Assays using Blotted Proteins

Following a procedure used to show the RNA-binding activity of *staufen* RBD domains (Micklem *et al.* 2000), protein samples were separated on normal SDS-PAGE and blotted onto nitrocellulose membrane. The membrane was then probed with biotin-labelled dsRNA (a 277 bp fragment from the *D. radicum V-type ATPase* gene was used), and RNA binding was detected using a streptavidin-HRP conjugate. The assays were carried out under conditions where proteins on the membrane were probed directly after blotting, or were subjected to denaturation in 6M urea followed by renaturation in a series of washes of lower urea concentrations, with similar results.

This method for detecting RNA-binding activity proved non-viable when biotin-labelled dsRNA was used as a probe on cell extracts or culture supernatants, due to the presence of small amounts of biotin-containing contaminating proteins in all the samples analysed. These contaminants were detected by the streptavidin-HRP conjugate as bands present in negative controls. Representative results are shown in Figure 4-32. *E. coli* cell extracts (Lanes 2, 3 and 5) gave bands in the region 14-25 kDa, which were present in the negative "empty vector" control (lane 2) even when no labelled RNA probe was used (panel D). Proteins purified from *E. coli* could contain small amounts of a contaminating biotin-containing band at approx. 22 kDa (lane 2). In highly purified samples, this band was absent (lanes 4, 6), but in these samples, no RNA binding was observed (panels B and C). Culture supernatants from *P. pastoris*, whether expressing RBD-domain containing proteins or not, contained a high molecular weight contaminants which contained biotin, as shown by reaction with streptavidin-HRP conjugate (panel D, lanes 7-11), and variable amounts of a band at approx. 25 kDa which also reacted with streptavidin. No evidence for specific RNA-binding proteins was observed in any of these blot assays.

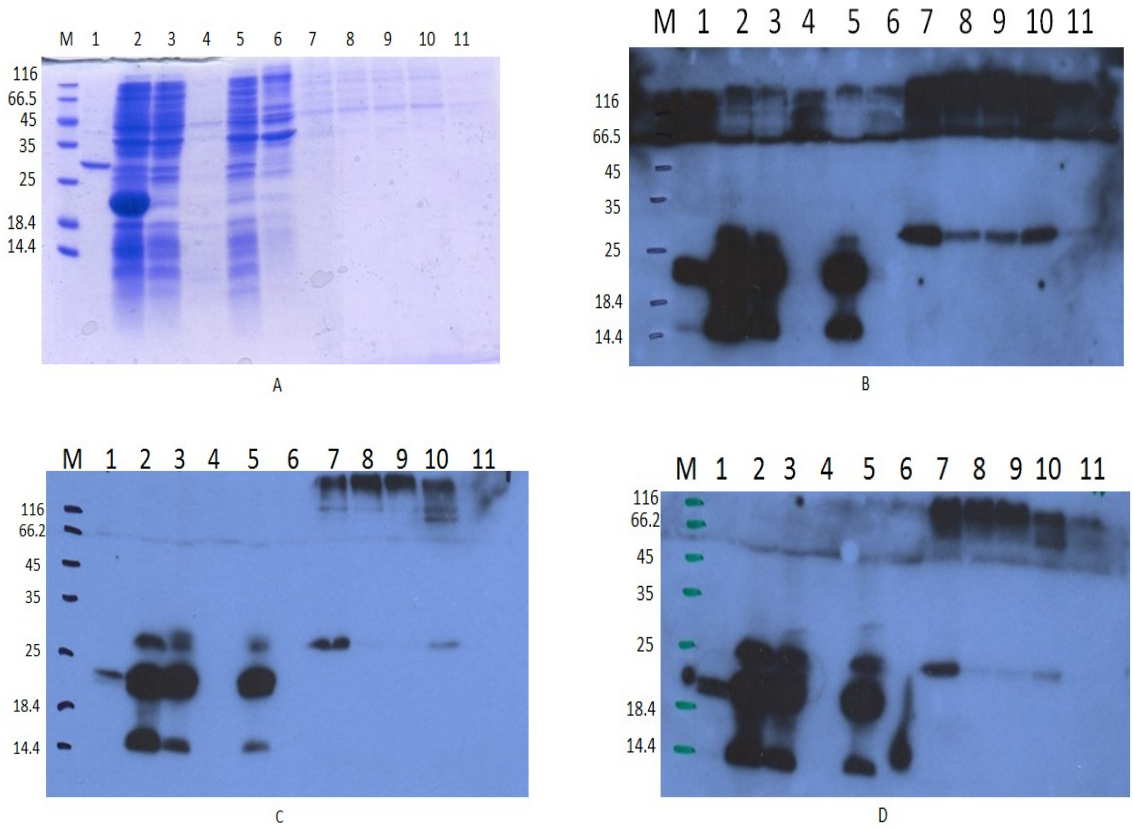

Figure 4-32 **Probing protein blots with biotin-labelled RNA cannot be used to demonstrate RNA binding.**

Stained SDS-PAGE gel of protein samples is shown in panel A and blot probed with labelled dsRNA and single-stranded RNA are shown in panel B and C, respectively. Blot treated with streptavidin-HRP conbjugate without probing with labelled RNA (negative control) is shown in panel D. Each panel contains the following lanes: lane 1 shows purified RBD1/Trx fusion protein. Lanes 2, 3 and 5 show soluble protein fraction from *E. coli* expressing Trx protein (negtive control), RBD1/GNA and Trx/RBD3/GNA, respectively. Purified fraction of Trx/RBD1/GNA and Trx/RBD3/GNA fusion protein is shown in lanes 4 and 6. Culture supernatant from SMD yeast (negive control), RBD1, RBD1/GNA, RBD3 and RBD3/GNA in *P. pastoris* are shown in lanes 7-11.

4.2.14 RNA Electrophoretic Mobility Shift Assays (REMSA) using biotin labelled dsRNA

The failure to detect RNA-binding activity in recombinant fusion proteins containing RBD domains after SDS-PAGE suggested that an assay which could be carried out using non-denatured protein would be necessary to show biological activity. An RNA electrophoretic mobility shift assay (REMSA) to demonstrate the formation of protein-RNA complexes was selected as a suitable method. The technique was evaluated using the positive control reaction provided in the Pierce biotin labelling kit, which involves interaction of an IRE-element binding protein in a liver extract with its target RNA. Results are shown in Figure 4-33. The interaction results in the formation of a complex with reduced mobility on gel electrophoresis, which is clearly visualised after blotting and detection of biotin-labelled RNA. Further experiments (data not presented) showed that no interaction was observed when labelled insect RNAs were tested.

When similar assays were carried out to show interactions of purified recombinant proteins containing RBD domains with dsRNAs, results were less clear-cut. Typical results are shown in Figure 4-34. Proteins produced in *Pichia* could not be assayed using this method due to the presence of contaminants which gave high levels of background reactivity in the biotin detection reaction; this resulted in tracks containing smears (see lane 3, Figure 4-34), which could not be interpreted as unambiguous evidence for the formation of protein-RNA complexes. In addition, all recombinant proteins produced in *E. coli* which had been subjected to denaturation-renaturation procedures during purification failed to show evidence for complex formation with labelled dsRNA, which was shown by the labelled RNA control running to the same position on the gel as the labelled RNA mixed with recombinant protein, or by dsRNA degradation. Since Trx/RBD1 and Trx/RBD1/GNA could not be produced as soluble proteins in *E. coli*, the binding activity of the RBD1 domain could not be demonstrated in recombinant proteins.

The data shown in Figure 4-34 suggests evidence for complex formation between the recombinant protein and dsRNA for Trx/RBD3/GNA produced in *E. coli*, which had been produced and purified as a soluble protein. Further work was carried out to demonstrate that the RBD3 domain produced as a soluble protein in *E. coli* was biologically active.

Figure 4-33 **Electrophoretic Mobility Shift Assays (REMSA); Control for Binding**

Control biotin IRE-RNA (16.25nM) is shown in lane 1 and control biotin IRE-RNA with added liver extract protein the formation of a protein-RNA complex is indicated by the arrow which is shown in lane 2.

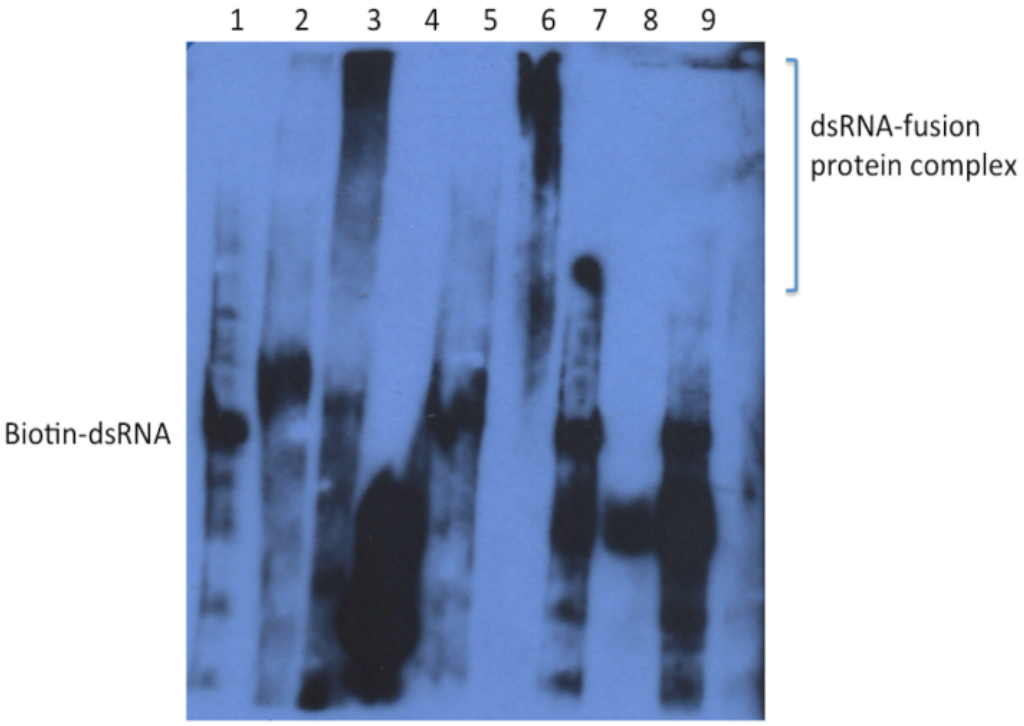

Figure 4-34 **RNA Electrophoretic mobility shift assay (REMSA) of recombinant proteins containing RBD domains**.

Negtive controls used for this assay were 10ng biotin-MbVTE dsRNA (lane 1) and the reaction of 10ng biotin-MbVTE dsRNA incubated with 2μg GNA (lane 2). Smearing and background is detected after inucating 10ng biotin-dsRNA incubated with RBD3/GNA produced in *P. pastoris* (lane 3). Additional negative control is soluble fraction of induced 'empty' pET32 vector expressing Trx (lane 4). Lanes 5 and 6 show 10ng biotin-dsRNA incubated with 2μg purified Trx/RBD1/GNA and Trx/RBD3/GNA (peak drops from nickel affinity column) whereas lanes 7, 8 show 10ng biotin-dsRNA incubated with 2μg Trx/RBD1/GNA and Trx/RBD3/GNA purified under denaturing conditions. Lane 9 shows 10ng biotin-dsRNA incubated with 2μg Trx/RBD1 purified under denaturing conditions.

4.2.15 RNA-binding activity of RBD3-containing recombinant proteins

Trx/RBD3 fusion protein purified from soluble *E.coli* cell fractions showed dsRNA binding activity, assayed by REMSA (Figure 4-35). Incubation of 2.5μg of recombinant protein with 10ng biotin-labelled dsRNA caused a clear mobility shift, whereas incubation of lower amounts of recombinant protein (0.5μg and 1μg) gave no clear mobility shift. Thioredoxin and GNA protein were incubated with labelled dsRNA as negative controls; no shift was observed with 2.5μg of either protein, showing that the mobility shift observed in lane 9 of Figure 4-35 must be due to the RBD3 domain. Although this result demonstrates binding activity, the recombinant protein is present in large excess over the dsRNA target when binding is observed (approx. 2000-fold, on a molar basis) which suggests that the protein is either only partially biologically active, or that the binding constant for the interaction is relatively high.

Similar results were obtained with the Trx/RBD3/GNA fusion protein produced as a soluble protein in *E. coli*. This protein became insoluble after lyophilisation following purification by metal affinity chromatography, and thus in order to carry out a REMSA assay, the eluted peak fraction of Trx/RBD3/GNA from the nickel column was used directly for the binding assay. Ten nanograms biotin dsRNA was incubated with varying amounts of Trx/RBD3/GNA fusion protein, from 50ng to 2μg; results are shown in Figure 4-36.A mobility shift in the dsRNA band was observed consistently when ≥750ng of recombinant fusion protein was added to the labelled RNA (panel A, lanes 4-8; panel B, lane 5). Again, although these results suggest that recombinant RNA binding domain RBD3 has dsRNA binding activity, whereas GNA and thioredoxin controls do not, the amount of protein required to show a mobility shift is in large excess over the dsRNA.

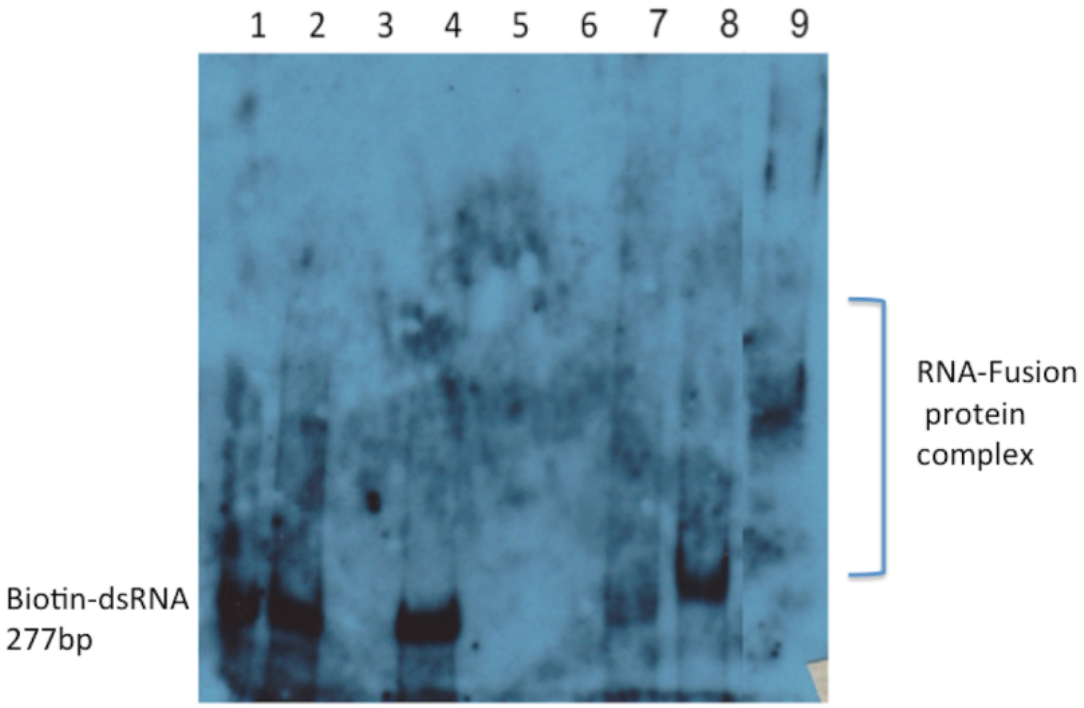

Figure 4-35 **RNA-binding activity of Trx/RBD3 shown by REMSA**

Negtive control is shown in lane 1 represent 10ng biotinylated dsRNA. Negtive controls were used as 2.5μg protein (i.e. without incubating with dsRNA) that are Thioredoxin (lane 3), GNA (lane 5) and Trx/RBD3 (lane 6). Lanes 2, 4 show 10ng biotinylated dsRNA incubated with 2.5μgThioredoxin and GNA, respectively. Lanes 7-9 show 0.5μg, 1μg and 2.4μg Trx/RBD3 incubated with 10ng biotinylated dsRNA.

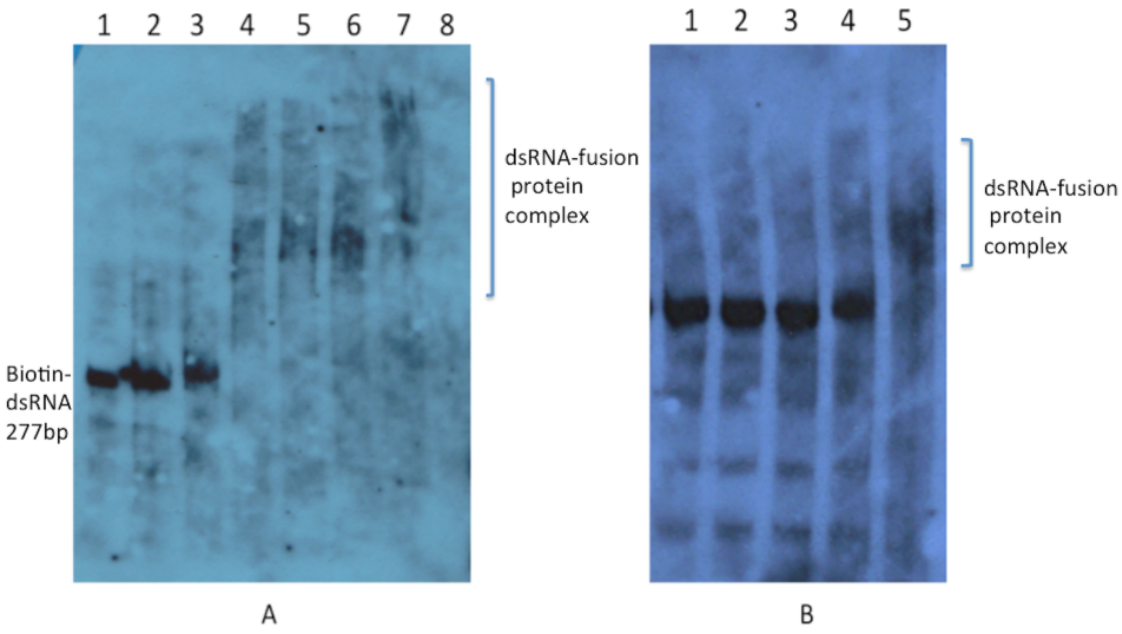

Figure 4-36 **RNA-binding activity of Trx/RBD3/GNA shown by REMSA**

Panel A and B show independent replicates.

A: Lane 1 shows 10ng biotinylated dsRNA (i.e. without incubating with protein) as negative control. Additional negive control is 2μg Trx/RBD3/GNA (lane 8). Lanes 2-7 show 300ng, 500ng, 750ng, 1ug, 1.5μg and 2μg Trx/RBD3/GNA incubated with 10ng biotinylated dsRNA.

B: Lanes 1-5 show 50ng, 100ng, 250ng, 500ng and 1μg Trx/RBD3/GNA fusion protein incubated with 10ng biotinylated dsRNA.

4.2.16 REMSA assays with FITC-labelled dsRNA

To investigate the possibility that biotin-labelling dsRNA was interfering with RBD3 binding, an alternative labelling system was used.

When carrying out *in vitro* transcription to produce RNA, T7 RNA polymerase can incorporate modified 5'-initiating nucleosides based on guanosine. These modified nucleotides can incorporate chemical functionality which introduces reactive groups for bioconjugation. One of the 5'-deoxyguanosine derivatives, 5'-deoxy-5'-hydrazinylguanosine (see Figure 4-37; 1) is used to enable the RNA transcripts to be labelled with a fluorophore such as FITC, giving the conjugate shown in Figure 4-37 (2). 5'-deoxy-5'-hydrazinylguanosine 1 was introduced during *in vitro* transcription of a 200bp RNA fragment derived from the *T. castaneum* V-type ATPase encoding sequence; FITC was added after the initial initiation and transcription completed. The labelling reaction was initiated and quenched by pH adjustment. Unincorporated 5'-deoxy-5'-hydrazinylguanosine 1 and FITC were removed by gel filtration using spin columns.

Analyses of the FITC labelled dsRNA by gel electrophoresis on 6% native TBE polyacrylamide gels are shown in Figure 4-38. Imaging 2ng, 5ng and 10ng FITC-dsRNA showed that the lowest amount could be detected as a band of the expected indicated size (panel A). FITC-dsRNA also shows single band on a similar gel stained by ethidium bromide at final concentration of 0.5mg/ml in 200ml 0.5X TBE buffer. (panel B).

The results of FITC-dsRNA mobility shift assays using purified Trx/GNA produced as a soluble recombinant protein in *E. coli* are shown in Figure 4-39. The labelled FITC-dsRNAs are detected in by inherent fluorescence using a phosphorimager (panel A) or by staining with ethidium bromide (panel B). Labelled dsRNA is detected as a band towards the bottom of the gel (lane 1), and no evidence of complex formation with thioredoxin or GNA is observed (lanes 7 and 8). In this assay, the formation of a dsRNA-Trx/RBD3 complex shifts the dsRNA band to the top of the gel over the entire range of amounts of fusion protein used (1-8ng; lanes 2-5). The results show that Trx/RBD3 has binding activity towards FITC-labelled dsRNA. The assays shown in Figure 4-39, when compared to those of Figure 4-35 and Figure 4-36, suggest much stronger binding of Trx/RBD3, shown by the almost complete absence of mobility of the complex on gel electrophoresis. Even when a higher amount of dsRNA is used in the assay (Figure 4-39, panel B) no evidence for the presence of uncomplexed dsRNA is seen.

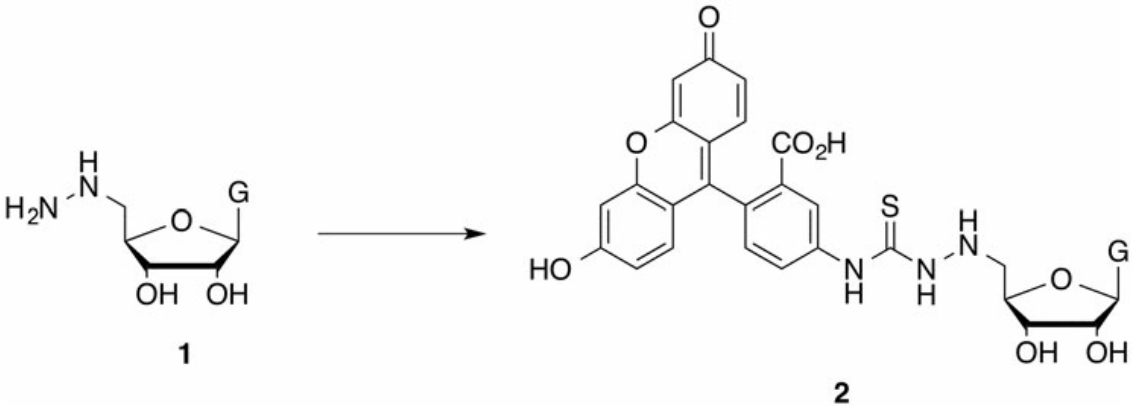

Figure 4-37 **Modification of the 5'-hydrazinyl functional group of 5'-deoxy-5'-hydrazinylguanosine with FITC**. (M. Skipsey et al. 2013)

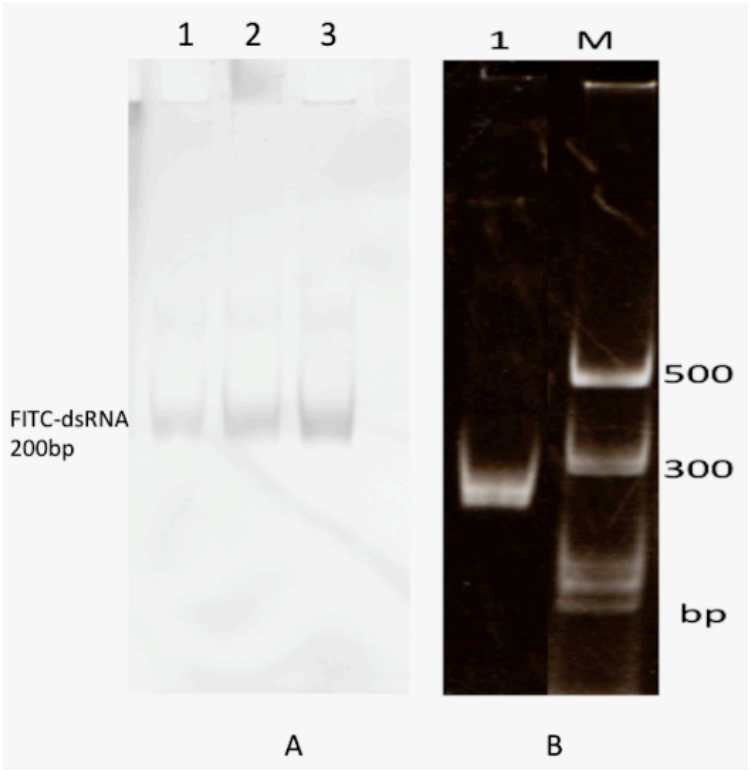

Figure 4-38 **Visualisation of FITC-labelled dsRNA by inherent fluorescence and by staining.**

A: Lanes 1-3 show 2ng, 5ng and 10ng FITC-*TcVTE* dsRNA on 6% TBE polyacrylamide gel visualised by endogenous fluorescence using a Typhoon phosphorimager.

B: Lane 1 shows 100ng FITC-*TcVTE* dsRNA on 6% TBE polyacrylamide gel stained with ethidium bromide. M: dsRNA marker

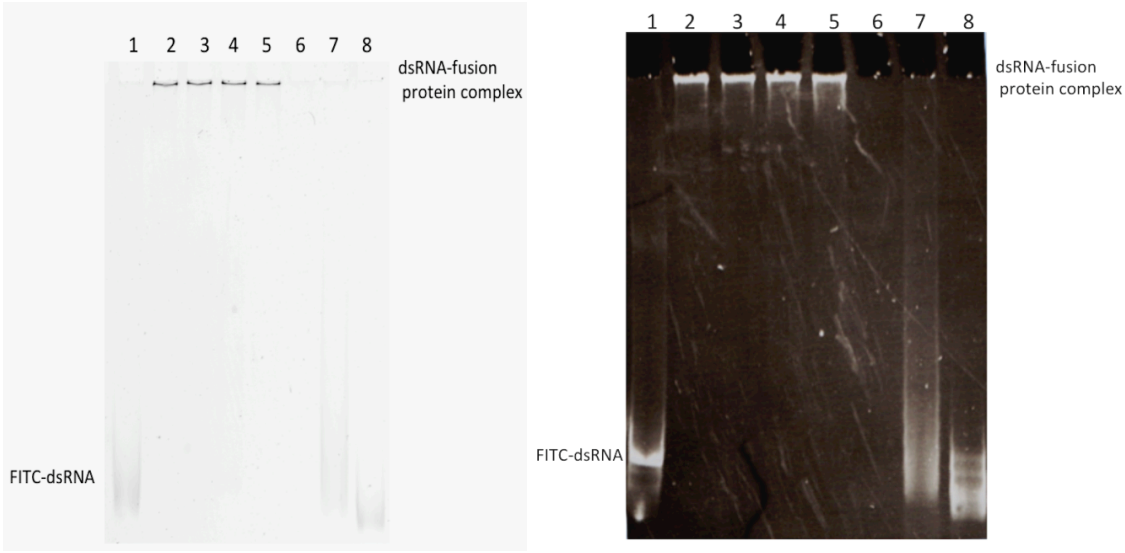

(A) (B)

Figure 4-39 **Trx/RBD3 fusion protein binds to FITC-dsRNA demonstrated by RNA Electrophoresis Mobility shift assays.**

(A) 6%TBE polyacrylamide gel of FITC-dsRNA mobility shift assay visualised by Typhoon phosphorimager.

Negtive controls are 5ng FITC-dsRNA (lane 1) and 8μg Trx/RBD3 fusion protein (lane 6). Lanes 2-5 show 5ng FITC-dsRNA incubated with 1μg, 2μg, 4μg and 8μg Trx/RBD3 fusion protein. Lanes 7 and 8 show 5ng FITC-dsRNA incubated with 8μg thioredoxin and GNA proteins respectively.

(B) 6% TBE polyacrylamide gel of FITC-dsRNA mobility shift assay stained with ethidium bromide

Negtive controls are 20ng FITC-dsRNA (lane 1) and 8μg Trx/RBD3 fusion protein (lane 6). Lanes 2-5 show 20ng FITC-dsRNA incubated with 1μg, 2μg, 4μg and 8μg Trx/RBD3 fusion protein Lanes 7 and 8 show 20ng FITC-dsRNA incubated with 8μg thioredoxin and GNA proteins respectively.

4.2.17 REMSA assays with unlabelled dsRNA

The results in Figure 4-39 show that when assays are carried out *in vitro*, with amounts of RNA that can be visualised by ethidium bromide staining, it is not necessary to label dsRNA to show mobility shifts due to protein binding. This is advantageous in that any interference with the protein-RNA interaction caused by labelling the RNA can be avoided. Further assays were thus carried out with unlabelled dsRNA.

A REMSA assay using a constant amount of dsRNA incubated with varying amounts of Trx/RBD3 from 2ng to 2μg was carried out, and visualised using polyacrylamide gel electrophoresis and ethidium bromide staining. Results are shown in Figure 4-40. 50ng *T. castaneum APIN* dsRNA (300 bp) was used in each binding reaction; the molar equivalent of Trx/RBD3 GNA is approx. 7ng. In the assay, no mobility shift of dsRNA is apparent when incubating Trx/RBD3 fusion protein with 2, 5 or 10ng of protein (Figure 4-40, lanes 2-4). When 40ng Trx/RBD3 protein is used, the band of uncomplexed RNA is decreased significantly, and evidence for protein-RNA complexes is seen in the form of a smear up the gel. Because RBD3 is a non-specific dsRNA binding protein, and binds at multiple sites on the RNA molecule, distinct complexes are not visualised (Figure 4-40, lane 5). Uncomplexed dsRNA is still present when 80ng of Trx/RBD3 is added, but not when 300ng or greater is added Figure 4-40, lanes 5-6). When dsRNA is incubated with 300ng-1μg Trx/RBD3 fusion protein, all the dsRNA is complexed, and the complexes become of higher mol. wt., as shown by a shift of the smear up the gel; finally, when 2 μg protein is added to 50ng dsRNA, all the RNA is present in the form of a high mol. wt. complex that hardly enters the gel (Figure 4-40 lanes 7-9). The binding constant, K_d, of Trx/RBD3 with dsRNA can be estimated from the amount necessary to convert approx. 50% of uncomplexed RNA to complexed RNA; the value is approx. $8x10^{-8}$M. Recombinant thioredoxin was used as a control to show that addition of protein alone has no effect an dsRNA mobility (Figure 4-40 lane 11).

A similar REMSA assay was carried out using the same dsRNA with varying amounts of purified recombinant RBD3/GNA fusion protein produced in *P. pastoris*. The result is shown in Figure 4-41. GNA, used as a negative control, shows that protein alone has no effect on RNA mobility (Figure 4-41 lane 11). However, all amounts of RBD3/GNA used affect dsRNA mobility; amounts of dsRNA from 1-50ng RBD3/GNA increase the mobility of the dsRNA (Figure 4-41, lanes 2-6), whereas amounts >50ng result in the formation of high mol. wt. complexes (Figure 4-41, lanes 7-9). Addition of 800ng RBD3/GNA results in a high. mol. wt. complex.

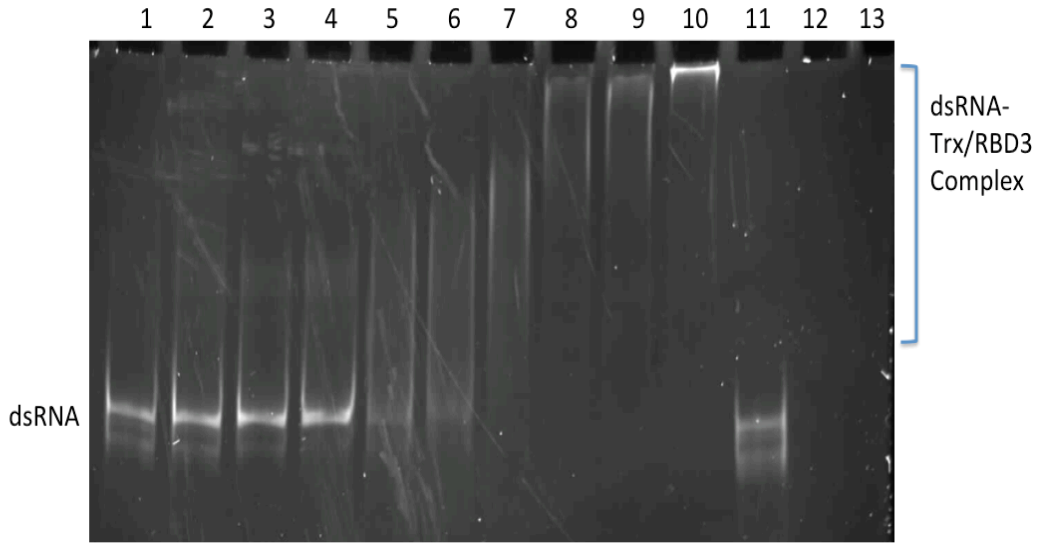

Figure 4-40 **RESMA assay by using increasing amount of Trx/RBD3 fusion protein incubated with 50ng dsRNA. (TBE gel stained with ethidium bromide)**

Negative controls are 50ng *TcAPIN* dsRNA (i.e. without incubating with protein) shown in lane 1, and 2μg thioredoxin and Trx/RBD3 (i.e. without incubating with dsRNA) shown in lanes 12 and 13 respectively. Additional negtive control is applied by using 50ng dsRNA incubated with 2μg Thioredoxin (lane 11). Lanes 2-10 show 50ng dsRNA incubated with 2ng, 5ng, 10ng, 40ng, 80ng, 300ng, 700ng, 1μg and 2μg Trx/RBD3 fusion protein.

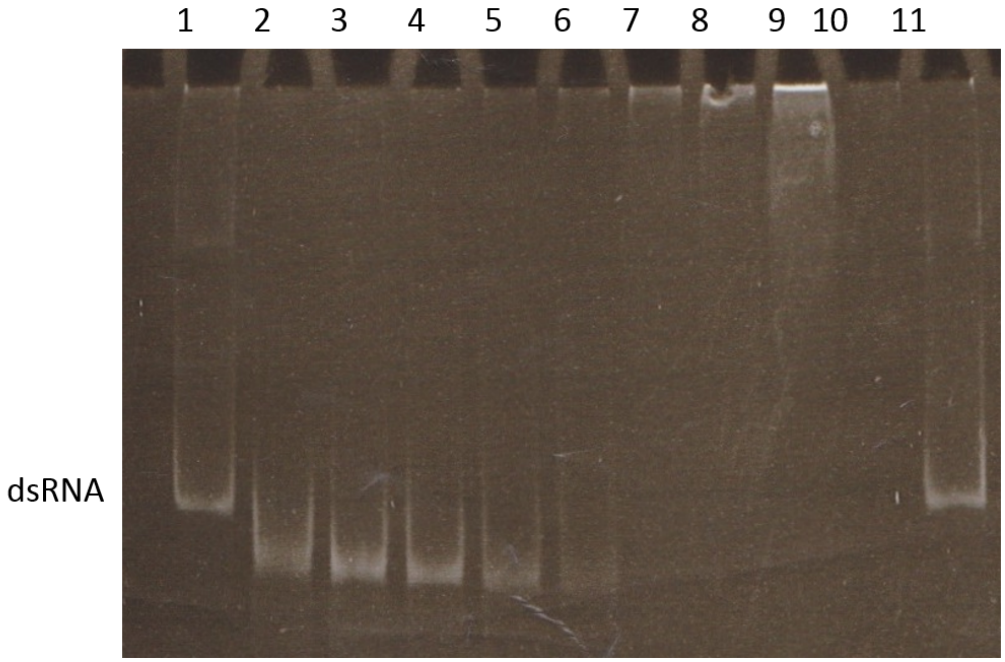

Figure 4-41 **RESMA assay by using increasing amount of RBD3/GNA fusion protein incubated with 50ng dsRNA. (TBE gel stained with ethidium bromide)**

Negtive controls are 50ng *TcAPIN* dsRNA (lane 1, i.e. without protein) and 800ng RBD3/GNA fusion protein (lane 10, i.e. without dsRNA). Additional negative control is using 50ng dsRNA incubated with 800ng GNA (lane 11). Lanes 2-9 show 50ng *TcAPIN* dsRNA incubated with 1ng, 5ng, 10ng, 50ng, 80ng, 150ng, 400ng, 800ng RBD3/GNA fusion protein.

4.2.18 Detection of Trx/RBD3 and RBD3/GNA in *A. pisum* by western blotting

Fusion proteins were fed to aphids as components of the liquid diet. Trx/RBD3 was detected in diet and *A. pisum* gut sample by using an anti-$(His)_6$ antibody (recognises tag on recombinant protein), but not in haemolymph or honeydew, demonstrating that Trx/RBD3 is not able to transport from *A. pisum* gut to haemolymph as expected (Figure 4-42 A). In terms of detection of RBD3/GNA, GNA as positive control can be detected in all different tissues (gut, haemolymph and honeydew) which suggests that GNA was able to transport cross the aphid gut epithelium to the circulatory space (Figure 4-42 B). However, RBD3/GNA was not visualized in any other samples apart from diet. The band reacting with antibodies observed around 10kDa in gut and haemolymph lanes is most likely to represent GNA resulting from cleavage of RBD3/GNA fusion protein in aphid gut.

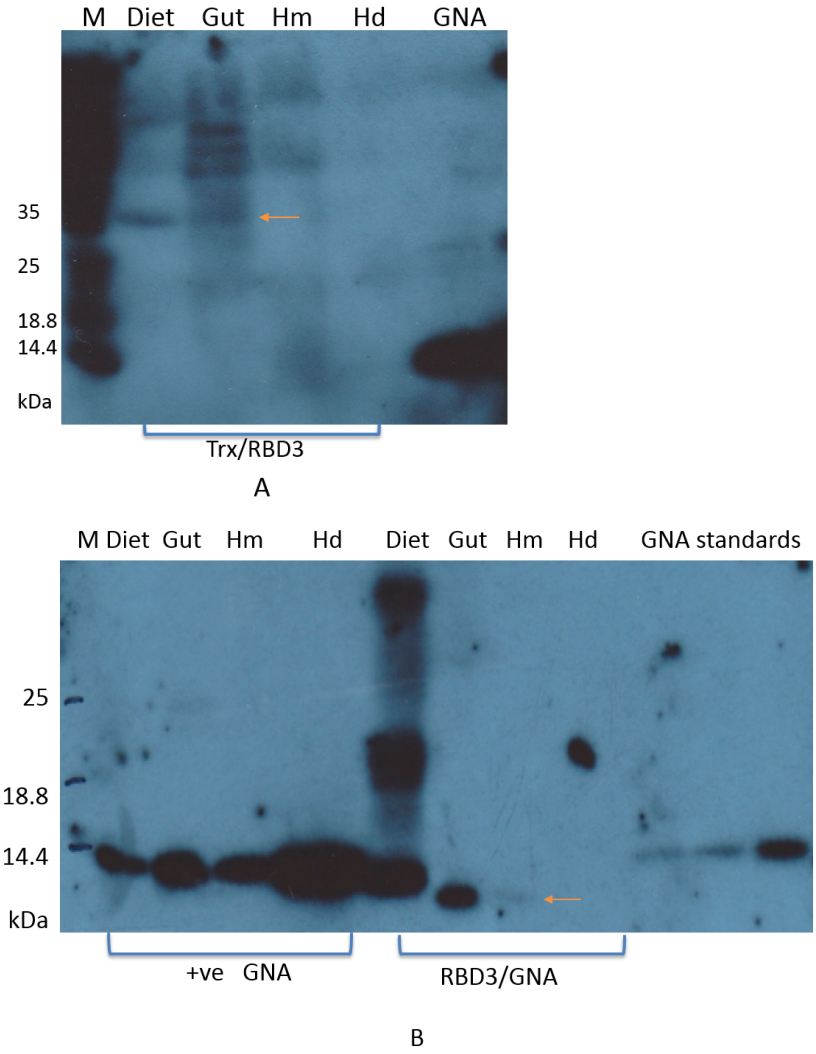

Figure 4-42 **Western blot using anti-His (A) and anti-GNA (B) demonstrating the transportation of Trx/RBD3 (A) and RBD3/GNA (B) in *A. pisum* circulatory system after feeding.**

A Trx/RBD3 is detected in aphid diet and gut extract (Gut, arrowed) after feeding for 48h but not presented in haemolymph or honeydew (Hd). Fifty-nanograms GNA is used as positive control for the blot (GNA standard).

B GNA used as positive control shows that it transports from aphid gut to the haemolymph (Hm) It is detectable in honeydew (Hd) as well. However, RBD3/GNA can be detected only in diet (Diet), cleaved GNA is found in aphid gut extract (Gut) and haemolymph (Hm, arrowed). Ten, 20 and 30ng GNA used as standard and positive control for the blot.

4.3 Discussion and Conclusion

In this chapter, constructs for expressing the dsRNA-binding domain RBD3 from *Drosophila* staufen were designed. Expression of the domain as a fusion protein with thioredoxin (Trx) in *E. coli,* using a pET32 expression vector was successful in giving a functional product. The expression level of Trx/RBD3 was approx. 180mg per litre of induced bacterial culture. After purification and desalting from induced soluble fraction, approximately 60% soluble Trx/RBD3 could be recovered. Most of the protein was lost during extended concentration of protein solutions by filter centrifugation. The most concentrated Trx/RBD3 sample achieved was 3mg/ml in 20mM sodium phosphate buffer.

RBD3/GNA was successfully produced as a soluble protein, in yields of approx. 10mg/L, by *P. pastoris*. However, purification from culture supernatant proved a problem, and the recovery level was low. The best recovery level was achieved by purifying from freeze dried supernatant re-suspended in 1XBB at pH 7.4. Overall, small amounts of soluble protein were produced by dialysis of eluted fractions after metal affinity chromatography, with dialysis into 20mM sodium phosphate buffer, pH 7.2, giving the most successful result, as shown in fig. 4.25 panel B, lane 5. This material was used in subsequent assays of RNA binding.

Further research into optimising expression conditions, and improving downstream processing, would be necessary before *P. pastoris* could be considered as a viable host for expressing RBD-containing fusion proteins.

Assaying the binding activity of the recombinant protein by RESMA shows that Trx/RBD3 binds to dsRNA to cause a mobility shift on a stained TBE polyacrylamide gel. The binding constant K_d is estimated at approx. $8x10^{-8}$M in this work. In a previous study reported by (Ramos *et al.* 1999), the binding constant of dsRNA binding domains was estimated as 10^{-6}M or higher by NMR. This could be due to using short dsRNA which is 12bp, whereas the assays reported here used a 277bp double helix designed for causing RNAi effect in insects. The RBD3-dsRNA recognition is mediated by loop2 and loop4 of RBD3 interacting with adjacent minor and major grooves of dsRNA. However, the 12bp dsRNA designed by Ramos et al. was capped by an exceptionally stable C (UUGG) G tetraloop. Their results revealed that helix α 1 of RBD3 interacts with the tetraloop by contacting both the RNA bases and sugars (Ramos *et al.* 1999). The interactions between helix α 1 and capped dsRNA releases extra binding energy, but could also provide preference of certain RNA sequences. The failure to include a "loop" structure in the dsRNA used in the assays reported here might lead to a weaker interaction, but the estimated K_d is lower than that reported by Ramos *et al.* (1999),

which suggests the protein binds better to a longer dsRNA. Another factor in the binding activity of RBD3 is the length and exact sequence of the "domain" used for assays. Previous studies performed by St Johnston *et al.* (1992) and Ramos *et al.* (2000) used a staufen RBD3 sequence with an additional 10 residues beyond the end of the domain (Figure 4-43). A protein containing just the dsRNA binding domain (65 amino acids) showed weak binding activity (St Johnston *et al.* 1992). The recombinant RBD3-containing proteins constructed in this work (70 aa) is 6 amino acid less on both N-terminal and C-terminal sides compared to the sequences previously used. This could affect the binding constant estimated from REMSA, but again, the estimated binding constant is actually lower than previous estimates, suggesting stronger binding. Therefore, the additional residues omitted from the present constructs compared to those used previously do not seem to be important for strong dsRNA binding activity. However, it has been proved that deletion of two or three amino acids from N terminal of the RNA-binding domain itself result in inactivity in RNA binding.

In terms of the binding conditions, dsRNA and Trx/RBD3 was incubated in 1Xbinding buffer containing 50mM Tris-HCL (pH 8), 5mM EDTA, 1mM DTT, 100ug/ml BSA and 5% glycerol. The mixture was incubated on ice for 20 minutes which gave the conditions used to estimate the binding constant. Ramos *et al.* (1999) performed the binding reaction in 10mM PO_4^{-}, 3mM DTT at pH 6.5 and incubated at 27 °C. They claimed that neither pH range between 5.5 and 6.8 nor the temperature from 6, 27 and 34 °C will affect the binding. However, significant decrease in binding was observed when 5mM Mg^{2+} was added in the reaction; this could be due to the aggregation or interaction with RNA (Ramos *et al.* 1999).

A similar buffer condition used for REMSA was performed by Bass *et al.* (1994). They identified *Xenopus* proteins containing two dsRNA binding domains and an auxiliary domain rich in arginine and glycine (RG domain). The estimated Kd is $2.7x10^{-9}$M for a synthetic 36bp dsRNA without extra loop. Binding is significantly reduced with the amino-terminal domain alone. Compared to staufen RBD3 used in this work. It suggests that a fusion protein containing multiple binding RNA-binding domains could provide stronger binding activity. Although previous research suggested that the RG domain lends cooperativity to the overall nucleic acid binding when associated with the RNA recognized motif (RRM) (Cobianchi *et al.* (1988); Nadler *et al.* (1991)), there was no significant differences in binding efficiency with proteins lacking the RG domain (Bass *et al.* 1994).

The experiments described here show that dsRNA was successfully bound with Trx/RBD3. Despite this success, several improvements could be made to the system to achieve stronger binding and better protection. First, use of a stem-loop dsRNA with a tetraloop with a well-studied C (UUGG) G sequence could enhance the binding, as this

single stranded loop structure will increase additional binding sites with the helix α 1 of Trx/RBD3. Secondly, the amino acid sequence region for binding dsRNA used in the construct could include the additional 10 residues on either side of 65 amino acid RBD3 domain to achieve stronger dsRNA binding activity. RBD3 is expressed successfully as soluble protein in pET32 system, therefore mutation N to Q for optimizing the condition of yeast expression in not necessary, although this mutation will not affect dsRNA binding. Lastly, a fusion protein with multiple copies of the RBD3 domain could result in stronger binding, reducing the number of fusion protein molecules necessary to bind to cover the dsRNA. This would reduce the molar ratio of fusion protein: target RNA necessary to give protection.

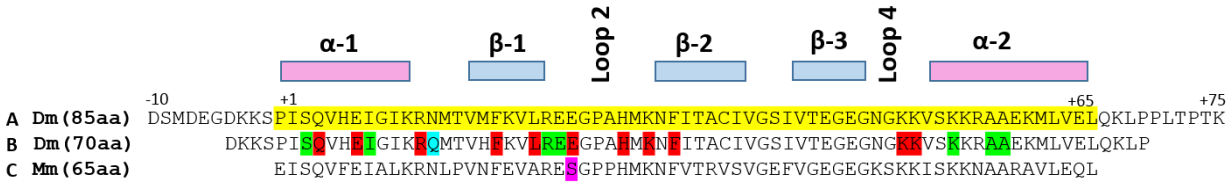

Figure 4-43 **Alignment of RBD3 sequence from staufen homologues of *Drosophila melanogaster* (Dm) and *Mus musculus* (Mm).**

A: 85 amino acids region containing staufen RBD3 selected by previous studies shows strong dsRNA binding activity. Staufen RBD3 of 65 amino acids is highlighted in yellow.

B: 70 amino acids region containing staufen RBD3 constructed as fusion protein in this work. Mutants in RBD3 either reduce or abolish dsRNA binding activity. Q replaces N for the convenience of yeast expression. Fortunately, this mutant does not reduce or abolish dsRNA binding activity.

C: RBD3 of 65 amino acids *from M. Musculus* selected by Kawaguchi *et al*., (2009). S replaces E in *M. musculus*. Mutation of E in *D. melanogaster* cause inactive of dsRNA binding activity. This sequence different could cause different efficiency of dsRNA binding activity. Adapted from Ramos *et al.* (1999).

Chapter 5 The persistence and stability of dsRNA against insect tissues and its improvement by conjugating with recombinant protein containing dsRNA-binding domain

5.1 Introduction

The results in Chapter 3 demonstrate that there are differences in the RNAi efficiencies among insect species from different orders. Robust and long-lasting RNAi effect is proved in *T. castaneum*, RNAi-induced gene downregulation was also detected in two Dipteran species: *M. domestica* and *D. radicum*, but only a weak and transient RNAi response was observed in *A. pisum*. Since dsRNA must be taken up into cells to generate siRNA which leads to subsequent degradation of target mRNA, stability of dsRNA to degradation in the extracellular environment could be a major factor in determining the efficiency of RNAi effects. Degradation of of dsRNA would lead to poor uptake, and a less sensitive RNAi response. Data concerning the stability of dsRNA in the haemolymph and gut extract of *T. castaneum*, *D. radicum* and *A. pisum* are presented in this chapter, and examined to determine whether correlations between dsRNA persistence and sensitivity to RNAi effects can be drawn.

To address potential problems of dsRNA stability in insect haemolymph and gut lumen, protection by forming complexes with the RNA-binding fusion proteins Trx/RBD3 and RBD3/GNA was considered. Enhancement of stability of dsRNA conjugated with RBD3-containing fusion proteins against the ribonucleases in insect haemolymph and gut extract is investigated.

5.2 Result

5.2.1 The stability of dsRNA in insect diet

5.2.1.1 The stability of dsRNA in *T. castaneum* diet

Stability of dsRNA in the presence of *T. castaneum* larvae in flour disks were assessed. Samples of disks were taken at different time points after exposure to larvae, and dsRNA was extracted and analysed by electrophoresis on 1% agarose gel. Results are shown in Figure 5-1. Intact dsRNA can be detected in the diet up to 72h after feeding, as shown by the prominent band at approx. 380 bp (same as input dsRNA). However, the gel also shows multiple bands of lower mobility as a result of mixing dsRNA with wheat flour, possibly as a result of the formation of complexes between the dsRNA and wheat proteins. At 120h post feeding, the lower mobility bands disappear, and a broader smeared dsRNA band is present on the gel, which is indicative of dsRNA degradation. Despite the longer-term indications of degradation, the experiment establishes that feeding dsRNA as a component of diet in *Tribolium* spp. is a viable procedure.

5.2.1.2 The stability of dsRNA in *A. pisum* diet

The stability of dsRNA in aphid diet was investigated by using FITC-labelled dsRNA. The aphid liquid diet is a sterile mixture of defined chemicals, and dsRNA is stable over at least 5 days when dissolved (results not shown); diet containing dsRNA which was not exposed to aphids was used as control treatment. To evaluate dsRNA degradation caused by the secreted products of the aphid salivary gland, aphids were allowed to feed on diet containing dsRNA; diet samples were examined at two different time points, 5h and 72h. Samples from different treatments were then extracted and loaded on 6% TBE gel followed by visualization. Results are shown in Figure 5-2. After 5h feeding, the dsRNA band was almost the same as the control treatment was detected, suggesting no degradation. Intact dsRNA can still be detected in the diet after 72h exposure to aphid feeding, although partial dsRNA degradation was observed compared to control treatment.

5.2.2 The stability of dsRNA in *A. pisum* honeydew *in vitro*

Aphid honeydew was collected from insects confined in a 1.5ml plastic tube. Total protein from collected honeydew was measured by BCA assay and 20μg, 50μg and 100μg total protein was incubated with dsRNA in a 20μl reaction at 25°C for 30 min. The result in Figure 5-3 shows that slightly degraded dsRNA signal was found in reaction containing 100μg total protein, but degradation by the lower amounts of

honeydew protein is very limited. The result shows that dsRNA degradation by *A. pisum* gut contents is limited in extent.

5.2.3 Protein estimation of insect haemolymph and gut samples

Gut samples were dissected from 50 late stage *A. pisum*, 30 *T. castaneum* larvae at the pre-pupal stage, and 20 *D. radicum* at pre-pupal larvae stage; soluble protein extracts were prepared from each sample, in total volumes of 50μl 1XPBS, in 60μl 1XPBS and 100μl 1XPBS respectively. Protein concentrations in the extracts were 6μg/μl in *A. pisum* gut sample, 7μg/μl in *T. castaneum* larvae gut sample and 16μg/μl in *D. radicum* larvae gut sample. Each *A. pisum* gut contained about 6μg protein whereas flour beetle larvae gut and *D. radicum* larval guts contained approx. 15μg and 80μg respectively. Haemolymph samples were collected from 50 late stage *A. pisum* s and 50 *T. castaneum* pre-pupal stage larvae in a final volume of 80μl 1XPBS containing PTU, and from 40 *D. radicum* pre-pupa stage larvae in 80μl 1XPBS containing PTU. Protein concentrations in *A. pisum* and *T. castaneum* larvae haemolymph samples were approximately 10μg/μl, and in the *D. radicum* larvae haemolymph sample the total protein concentration was approx. 50μg/μl according to the BCA assay.

5.2.4 dsRNA is rapidly degraded in *A. pisum* and *D. radicum* gut extract but not in *T. castaneum* (*In vitro*)

An *In vitro* experiment was performed to investigate the persistence of dsRNA in insects' gut. Initial experiments contained 200ng dsRNA incubated with an increasing amount of protein presented in insects gut extracts. 200ng dsRNA were incubated with *D. radicum* and *T. castaneum* larval gut extracts containing 3μg, 7μg, 14μg, 21μg and 28μg total proteins. *A. pisum* gut extract contain 1μg, 2μg, 4μg, 8μg and 10μg protein was used for incubating dsRNA. The reactions were incubated at 25°C for 30 minutes and the integrity of dsRNA was examined on agarose gel (Figure 5-4. Incubation of dsRNA in gut extract isolated from late stage *A. pisum* and *D. radicum* larvae, resulted in fading and smearing of dsRNA on the gel (Figure 5-4 A and B). Weakening and smearing of dsRNA began to occur after incubation in *A. pisum* and *D. radicum* gut extract containing 3μg protein. More significant decrease of dsRNA signal was observed with higher amount of protein presented in gut extracts. dsRNA was completely undetectable after incubation with extract contain 4μg protein in *A. pisum* gut and 12μg protein in *D. radicum* gut *in vitro*. The control treatments indicated that dsRNA is relatively stable molecule and is not liable to degradation, whereas dsRNA was degraded rapidly in insects gut extract from *A. pisum* and *D. radicum* larvae extracts.

However, the situation in *T. castaneum* showed different pattern (Figure 5-4.C). When incubating dsRNA with 3μg, 7μg and 14μg *T. castaneum* larval gut extract, dsRNA showed decreased size gradually rather than smearing and weakening on the gel. The smaller dsRNA began to show weak signal after incubating with gut extract containing 21μg protein and became undetectable when incubating with gut extract containing 28μg protein. The results could be interpreted as a result of different types of ribonucleases present in insects gut that are able to degrade dsRNA. It is predicted as endoribonucleases in aphid gut and *D. radicum* larvae gut that degrades dsRNA internally whereas exoribonucleases in *T. castaneum* gut sample degrades dsRNA on 5' and 3' prime ends of it.

5.2.5 The rates of persistence of dsRNA against insect gut extract are different

Another assay was carried out for comparing the degradation efficiency of dsRNA of ribonucleases presented in different insects. Firstly, gut extract from different insects were normalised to same amount (3μg) followed by incubating dsRNA in gut extracts for different time points. 200ng dsRNA were incubated in gut extracts containing 3μg total protein for 1min, 5min, 15min and 30min. The result is shown in Figure 5-5. After 1 min incubation, dsRNA incubated with *A. pisum* gut extract showed weakening signal which can be interpreted as degradation whereas dsRNA incubated with other two gut extracts containing same amount of protein were not affected. dsRNA was completedly degraded in *A. pisum* gut extract after 5min and partly degraded dsRNA in *D. radicum* gut extract was observed. Smaller size of dsRNA was found in reaction containing *T. castaneum* gut extract after 15min incubation whereas dsRNA in other two gut samples were completely degraded. A significantly smaller size of dsRNA was presented in *T. castaneum* gut extract after 30 min incubation.

A similar assay was performed to investigate the persistence of dsRNA when exposed to an amount of gut extract containing total protein equivalent to a single gut of each insect species (Figure 5-6). Each *A. pisum* gut contains about 6μg protein, whereas flour beetle larvae gut and *D. radicum* larvae contain 15μg and 80μg respectively. The reactions were incubated for 1min, 15min and 30min. dsRNA was degraded completely after incubation with *D. radicum* larval gut extract for 1min whereas dsRNA incubated with *A. pisum* extract shows weaken signal after 1min. The strongest signal was detected in reaction that dsRNA incubated with *T. castaneum* larval gut extract after 1 min. After 15min incubation, dsRNA incubated with *A. pisum* gut extract was fully degraded whereas partly degraded dsRNA was observed in reaction that incubated with *T. castaneum* larval gut extract. Smaller size of dsRNA was more obvious in

reaction contain *T. castaneum* larval gut extract after 30 min incubation.

5.2.6 The rates of persistence of dsRNA against insects haemolymph are variable

The persistence of dsRNA in insect haemolymph were also investigated. DsRNAs were incubated with same amount of protein (25μg) present in insect haemolymph samples. The result in Figure 5-7 shows that dsRNA is degraded rapidly in *A. pisum* haemolymph, as a weaker signal was observed after 1min incubation. The band had completed disappeared in *A. pisum* haemolymph after 5 min incubation. Weakened dsRNA bands with decreased sizes were detected in both *D. radicum* and *T. castaneum* larval haemolymph after 5 min incubation. However, the signal was much stronger in *T. castaneum* larval haemolymph than *D. radicum* sample. After incubation for 30min, dsRNA with decreased size in intact form still can be detected in *T. castaneum* treatment whereas smearing of dsRNA was shown in *D. radicum* treatment. The results regarding stability of dsRNA in insect haemolymph and gut samples suggest that dsRNA was relatively stable and did not degrade under the experimental conditions utilized unless insect gut extract or haemolymph was present. Intact dsRNAs as positive controls were observed in each experiment eliminating the possibility that PBS responsible for dsRNA degradation, rather than insect haemolymph and gut extract.

5.2.7 Improvement of stability of dsRNA by conjugation with Trx/RBD3 against degradation by insect haemolymph *in vitro*

Experiments were carried out to determine whether the Trx/RBD3 fusion protein was able to improve the stability of dsRNA against degradation by enzymes present in insect haemolymph, through the formation of a complex which protected the RNA from the activity of RNases. DsRNA (200ng; approx. 1 pmole) or dsRNA conjugated with Trx/RBD3 (200ng plus 10μg protein; approx. 300-fold molar excess of protein) were mixed with different insect haemolymph samples.

Without the protection of Trx/RBD3, 200ng *Ap VTE* dsRNA started to be degraded by *A. pisum* haemolymph containing 5μg protein after 1 minute, as non-degraded and partly degraded dsRNA are both presented in reaction according to the result shown in Figure 5-8. Degradation is seen as a reduction in the band intensity of intact dsRNA, and appearance of a "smear" of RNA of lower molecular weight. After incubation with haemolymph for 15min, no intact dsRNA remains, although an RNA band at a smaller size than the positive control is present, indicating that dsRNA is degraded by exoribonucleases presented in *A. pisum* haemolymph. When conjugated with 10μg Trx/RBD3, dsRNA is able to maintain its intact form against ribonucleases for at least 15 minutes. Even after 30 minutes, dsRNA conjugated with Trx/RBD3 can still protect

part of dsRNA from cleavage by ribonucleases whereas dsRNA alone without any protection by Trx/RBD3 shows extensive degradation, with reduction to smaller size and weak signal. Trx was used as a negative control which shows no inhibition activity at all. The result shows that the RBD3 domain in the fusion protein Trx/RBD3 improves the stability of dsRNA against degradation by enzymes present in *A. pisum* haemolymph.

Similar experiments were performed using haemolymph collected from *T. castaneum* larvae. Results are shown in Figure 5-9. Haemolymph of *T. castaneum* was found to contain comparatively little RNase activity, and an amount equivalent to 25μg protein had to be used to observe significant degradation in controls. Under these conditions, dsRNA started to be degraded by ribonucleases after 15min incubation, and dsRNA size difference is observed, similar to that seen for *A. pisum*. With conjugated with Trx/RBD3, dsRNA is fully protected as intact form against *T. castaneum* haemolymph until 30 minutes, the latest time point investigated.

In contrast to *T. castaneum* haemolymph, haemolymph from *D. radicum* contained high levels of RNase activity, as shown in the results in Figure 5-10, where effects of an amount of haemolymph containing 25μg protein was used. DsRNA was completely degraded in haemolymph containing 25μg protein without being conjugated with Trx/RBD3 at 1 minute, the earliest time point tested. Trx/RBD3 was able to inhibit the degradation against *D. radicum* haemolymph for up to 15 minutes, as shown by intact dsRNA still being detectable.

The differing activities of RNases in the different insect haemolymph samples was a feature of these assays. Five times more protein in *T. castaneum* haemolymph sample than *A. pisum* was used to achieve a similar level of degradation. DsRNA was partly degraded in *A. pisum* haemolymph containing 5ug protein after 1min (Figure 5-8) but not in *T. castaneum* haemolymph containing 25μg protein at this time point. However, after 15 min and 30 min the quantitative level of degradation is similar, although there are qualitative differences in that dsRNA shows two different sized bands with *T. castaneum* haemolymph (Figure 5-9), but not with aphid haemolymph. Compared to the ribonucleases presented *T. castaneum* haemolymph, *D. radicum* shows more efficient degradation when same amount of protein was tested. DsRNA was entirely degraded in *D. radicum* haemolymph after 1min (Figure 5-10) whereas dsRNA partly degraded in *T. castaneum* sample after 30 minutes (Figure 5-9). To conclude, the ribonucleases in *A. pisum* haemolymph shows the highest efficiency between the other two species, and the ribonucleases in *D. radicum* haemolymph are more efficient as degrading dsRNA than *T. castaneum*.

All the haemolymph assays agree in showing that the RBD3 domain of fusion protein Trx/RBD3 is able to improve the stability of dsRNA and reduce the rate of degradation

of dsRNA by insect haemolymph, whereas an equivalent amount of Trx alone does not do so.

5.2.8 Improvement of stability of dsRNA by conjugated with Trx/RBD3 against degradation by insect gut extract *in vitro*.

Protection of dsRNA against degradation by RNases present in insect gut extracts was investigated by assays similar to those described for haemolymph extracts. DsRNA (200ng; approx. 1 pmole) or dsRNA conjugated with Trx/RBD3 (200ng plus 10μg protein; approx. 300-fold molar excess of protein) were mixed with different insect gut extract samples.

A. pisum gut extract containing 2μg protein was incubated with dsRNA or dsRNA-Trx/RBD3 conjugate for 1min, 15min and 30min. After incubation, all reactions were subjected to phenol / chloroform/ isoamyl alcohol (25:24:1) to recover the residual dsRNA. The result in Figure 5-11 shows that dsRNA is degraded gradually by *A. pisum* gut extract containing 2μg protein after 1 min, with little intact dsRNA left at 15 min. Two hundard nanograms dsRNA is completed degraded after 30 min. However, *ApVTE* dsRNA after conjugation with 10ug Trx/RBD3 is effectively protected against RNases in *A. pisum* gut extract for 30 minutes, with minimal degradation being observed.

T. castaneum gut extract containing 25μg protein was used for testing the activity of Trx/RBD3 (Figure 5-12, A). Reactions were prepared as same as *A. pisum*. *TcAPIN* dsRNA was completely degraded in 25μg gut extract after 1min. After conjugated with Trx/RBD3, dsRNA was effectively protected. There is a rapid degradation to produce RNAs of two different sizes (1min time point), but after this initial reaction, no further degradation of the smaller band is observed over 30 mins, showing that the greater part of the dsRNA is protected. An additional experiment was performed to confirm that stabilization of dsRNA was "dose dependent" and could be increased by conjugating with increasing amount of Trx/RBD3. 200ng *Tc APIN* dsRNA was conjugated with increasing amount of Trx/RBD3 (0μg, 2μg, 4μg, 8μg, 10μg, 14μg) against 25μg gut extract. The experiment was carried out at 25 °C for 30 minutes. Result shown in Figure 5-12B. The conjugates with higher amounts of RBD3 gave a distinct RNA band, as observed previously, but with amounts of Trx/RBD3 <10μg, there was evidence of degradation of this band, which were "dose dependent" in that the less protein was present, the more degradation was seen. These results establish the dsRNA protection conferred by RBD3, and show that the stability of dsRNA can be improved when more Trx/RBD3 is present in the reaction, probably as more binding reaction occurs.

The *D. radicum* gut extract contained a high level of RNase activity as shown in the results of Figure 5-13). *DrAPIN* dsRNA is completely degraded in gut extract containing

15μg protein after 1min. Part of dsRNA is protected by Trx/RBD3 against gut extract for 1min. However, no intact dsRNA is detected after 15min even when conjugated with Trx/RBD3.

5.2.9 Stability of dsRNA conjugated with RBD3/GNA from *P. pastoris* against degradation by *A. pisum* gut extract *in vitro*.

Two-hundard nanograms *ApVTE* dsRNA was incubated with 10μg Trx/RBD3/GNA or RBD3/GNA against 2μg protein from *A. pisum* gut extract. However, neither of the conjugates were able to reduce the degradation of dsRNA by *A. pisum* extract (**Figure 5-14** A and B). In terms of dsRNA incubated with Trx/RBD3/GNA, smearing and weakening of the dsRNA band began to present after incubation in gut extract for just 1min in both treatment without Trx/RBD3/GNA (**Figure 5-14**A, lane 2) and with Tx/RBD3/GNA (Figure 5-14A, lane 5), after 15min the dsRNA band in all tested samples had completely disappeared (**Figure 5-14**A, lanes 4 and 7). The result indicates that dsRNA was not conjugated or protected by Trx/RBD3/GNA which confirm that Trx/RBD3/GNA does not bind dsRNA.

In Figure 5-14, B, dsRNA alone shows smearing on the gel and partial degradation after incubation with gut extract for 1 min (Lane 2), and no intact dsRNA is present after 15 min (Lane 4). Pre-treatment by conjugation with RBD3/GNA resulted in complete degradation (Lanes: 5-7) of the nucleic acid at all time points. It is possible that the purified RBD3/GNA actually contained RNase activity, since inclusion of the fusion protein enhanced degradation rather than retarding it.

5.2.10 Comparison of gene downregulation by dsRNA and dsRNA-Trx/RBD3 conjugates.

In order to show that conjugation with RBD3 did not prevent dsRNA from producing an RNAi effect, experiments were carried out in which the effects of injecting similar amounts of conjugated and non-conjugated dsRNA into insects were compared.

Previous results in *A. pisum* suggested that approx. 50% downregulation of the *ApVTE* gene can be achieved by injection of 7.5ng *ApVTE* dsRNA. Therefore *ApVTE* dsRNA was selected to compare the gene downregulation by conjugating with Trx/RBD3. After injection, total RNA was isolated from aphids and analysed by real-time PCR. Results are shown in Figure 5-15. Insects injected with 5ng *ApVTE* dsRNA showed 40% downregulation of gene expression after 48h, consistent with previous results. Insects injected with the same amount of dsRNA in the form of *ApVTE*-Trx/RBD3 conjugates showed no decrease in *ApVTE* gene expression, similar to the control treatments (Aphids injected with buffer or Trx/RBD3). At 72h post injection, the gene expression

level was similar in all treatments; neither the dsRNA-injected, nor conjugate-injected insects, differed from control treatments (ANOVA). These results suggested that conjugation could interfere with the RNAi effect in aphids, although there is only a weak RNAi effect under any circumstances.

Experiments carried out in *T. castaneum*, using the *TcAPIN* gene as target for downregulation, gave a different outcome. Ten nanograms dsRNA with or without conjugation to RBD3, was injected into pre-pupal stage larvae and samples were collected at four different time points, including 2h and 5h post injection, to determine whether conjugation affected short-term RNAi effects. The results shown in
Figure 5-16 demonstrate that 10ng *APIN* dsRNA causes gene downregulation as early as 5h after dsRNA injection, but not after 2h. When conjugated with Trx/RBD3, *TcAPIN* dsRNA causes approx. 40% *APIN* gene downregulation after 2h, while *TcAPIN* dsRNA only shows no downregulation when compared to control treatments (ANOVA, $p<0.0001$). At the 5h and subsequent timepoints, the RNAi effect caused by dsRNA is similar whether or not it is conjugated to RBD3. At 10days after injection, approx.75% *APIN* gene downregulation is observed in insects injected with either dsRNA or dsRNA-conjugates compare same treatmens at 5h and 24h timepoints (ANOVA, $p<0.0001$). *APIN* gene downregulation is more effective at 10days than 5h after injection which illustrates the systemic, long-lasting RNAi effect produced by dsRNA in *Tribolium* spp., as described by other workers.

Results obtained from injected conjugated and non-conjugated dsRNA into *D. radicum* larvae also suggested that conjugation does not prevent observation of an RNAi effect, as shown in Figure 5-17. This experiment only used a single time point after injection, but approx. 40% down-regulation of the *DrAPIN* gene was observed for both *APIN* dsRNA compared to control Trx/RBD3 treatment, difference is significant (ANOVA with $P<0.05$), but difference is not significant between control Trx/RBD3 treatment and *APIN* dsRNA-Trx/RBD3 conjugate treatment (ANOVA test).

To conclude, the balance of evidence suggests that the RBD3/dsRNA conjugate is still capable of producing an RNAi effect; the failure to observe this in aphids may be due to choice of time points for sampling, or the poor RNAi response in these insects.

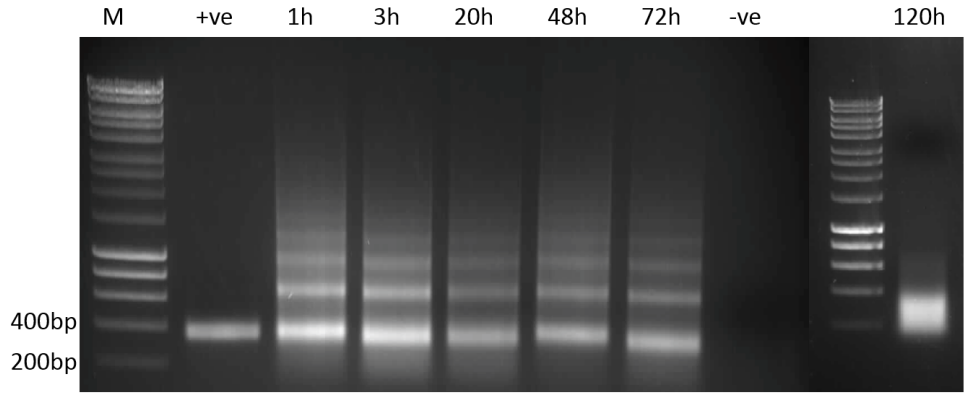

Figure 5-1 **Stability of dsRNA wheat flour disks exposed to *T. castaneum* larvae.** Lane +ve denotes 200ng dsRNA control in nuclease free water (i.e. no flour mixed or *T. castaneum* larvae fed on), Lane -ve control shows flour diet with *T. castaneum* larvae, but without dsRNA. Total RNA was extracted from disks exposed for the times indicated, 2μl from samples of each timepoints were loaded and analysed by agarose gel electrophoresis. Decreased signal was detected after 20h compared to 1h and 3h time points, which suggest dsRNA was partially degraded. The results for the 120h time point are from a separate gel, with a different molecular weight marker scale (two lanes on right of figure). After 120h, no intact band on gel was shown, indicating dsRNA degradation.

Figure 5-2 **dsRNA was degraded in diet after feeding *A. pisum* for 72h.**
dsRNA was mixed with *A. pisum* diet for 5h and 72h time point, diet with *A. pisum* fed on was collected after 5h and 72h time points as indicated. +ve control denotes diet mixed with dsRNA collected after 72h without *A. pisum* fed on. Afterwards, *A. pisum* diet containing dsRNA was extracted by chloroform extraction and analysised on 6% TBE polyacrylamide gel.

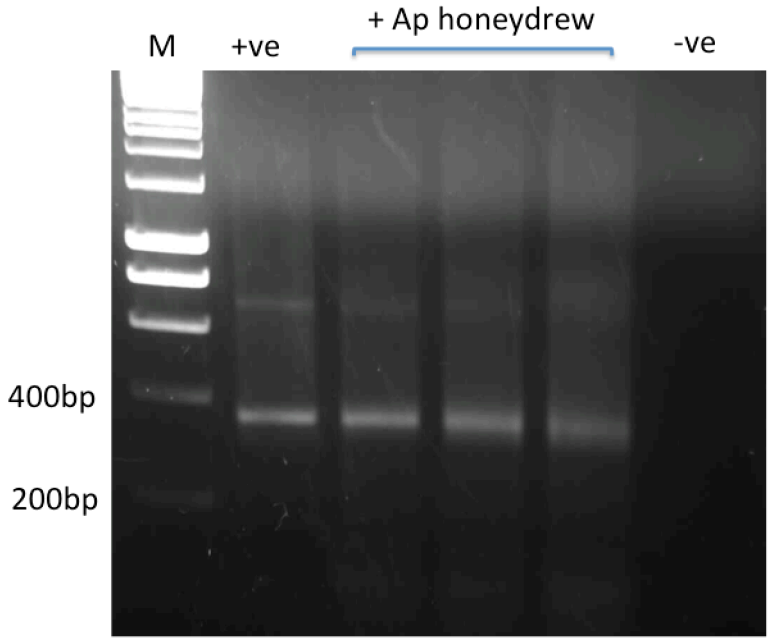

Figure 5-3 ***In vitro*** **experiment suggest dsRNA was degraded by the RNase presented in aphid honeydew**

An amount of 200ng dsRNA were incubated with 20μg, 50μg and 100μg total protein from honeydew in 20μl reaction at 25°C for 30min. Lane +ve control denotes 200ng dsRNA in 1XPBS (i.e. no honeydew added), Lane -ve control shows honeydew containing 100μg total protein with no added dsRNA.

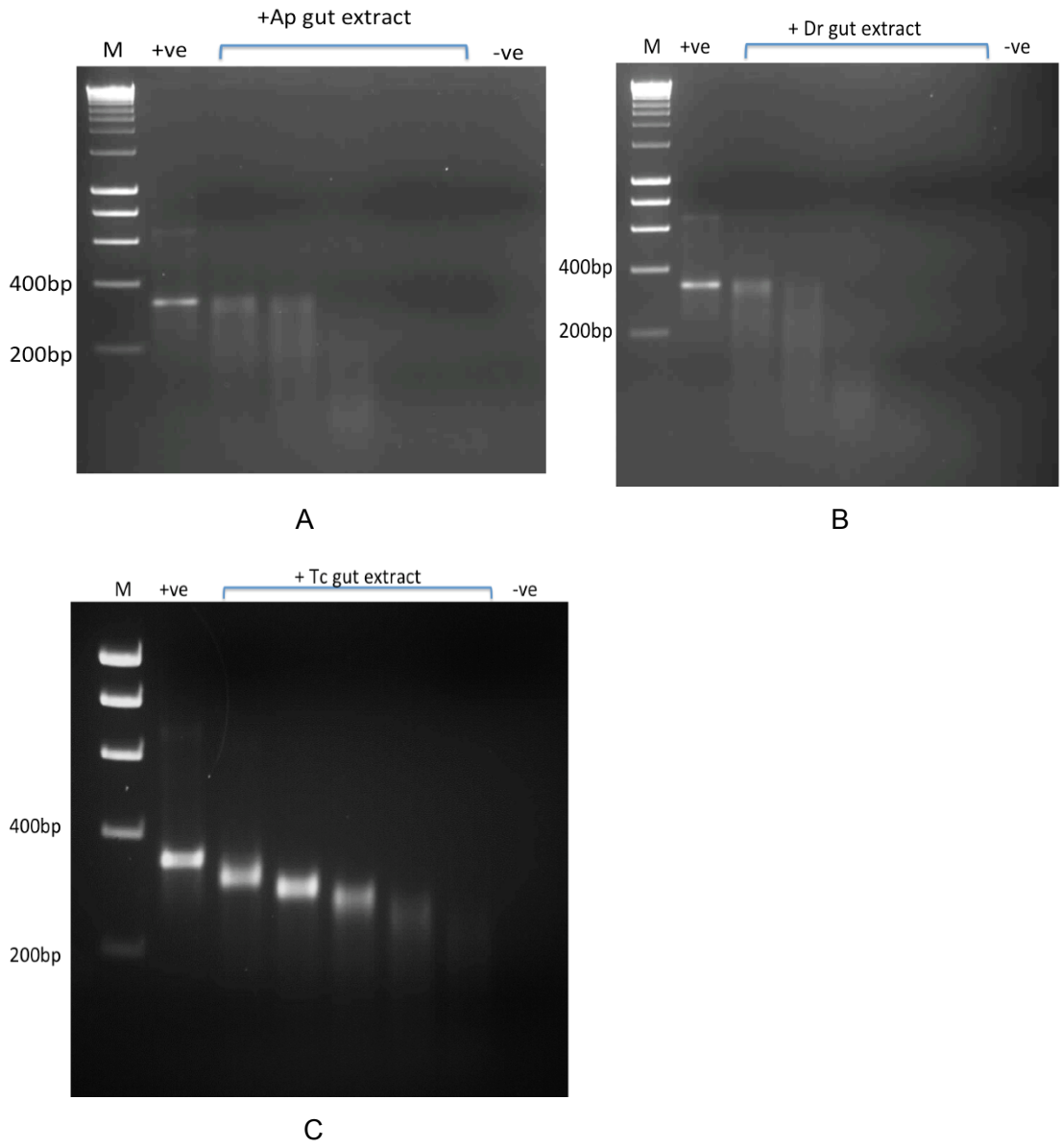

Figure 5-4 ***In vitro* experiment indicated that dsRNA is rapidly degraded in *A. pisum* and *D. radicum* larval gut but not in *T. castaneum* larval gut extract.**

Aliquots (200 ng) of dsRNA were incubated with gut extracts prepared from *A. pisum* (Ap), *T. castaneum* (Tc) and *D. radicum* (Dr) larval guts for 30 minutes. +ve denotes dsRNA control (i.e. no added protein), -ve control shows gut extracts with no added dsRNA. A: An amount of 200ng dsRNA incubated with *A. pisum* gut extract containing 1μg, 2μg, 4μg, 8μg and 10μg protein. B: 200ng dsRNA were incubated with *D. radicum* larval gut extract. C: *T. castaneum* larval gut extract containing 3μg, 7μg, 14μg, 21μg and 28μg total proteins. Rapid and complete dsRNA degradation were detected in *A. pisum* (A) and *D. radicum* extract (B). dsRNA was degraded at slow rate with size-decreasing pattern in *T. castaneum* gut extract (C).

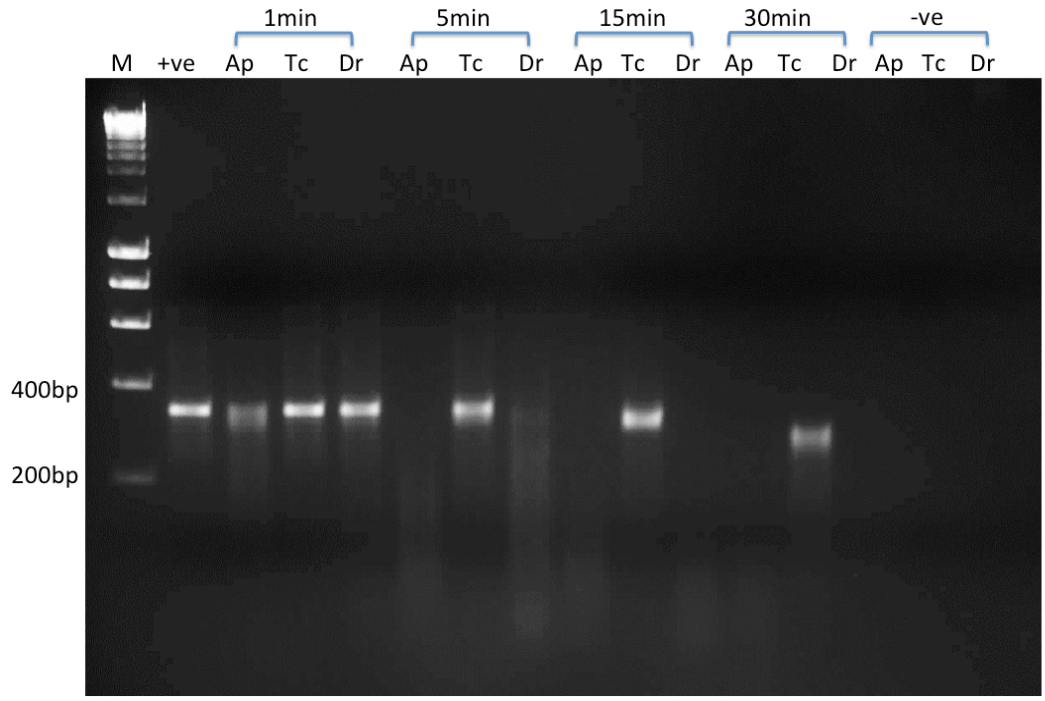

Figure 5-5 ***In vitro*** **experiment showing variability in the persistence and stability of dsRNA in gut extracts from different insect species.** Aliquots (200 ng) of dsRNA were incubated with gut extracts (3 ug total protein in each case) prepared from *A. pisum* (Ap), *T. castaneum* (Tc) and *D. radicum* larval guts for specified time points. +ve denotes dsRNA control (i.e. no added protein), -ve control shows gut extracts with no added dsRNA. The RNase presented in *A. pisum* gut extract showed the most rapid RNA degradation ability as dsRNA was partly degraded after 1min incubation. After 5min incubation, dsRNA incubated with *D. radicum* larval gut extract showed smearing signal. dsRNA were detectable in reaction contain *T. castaneum* larval gut extract after 15min. Instead of showing smearing and weaken signal in *A. pisum* and *D. radicum* gut extract, gradually decreased size of dsRNA was observed in *T. castaneum* until 30 min after incubation.

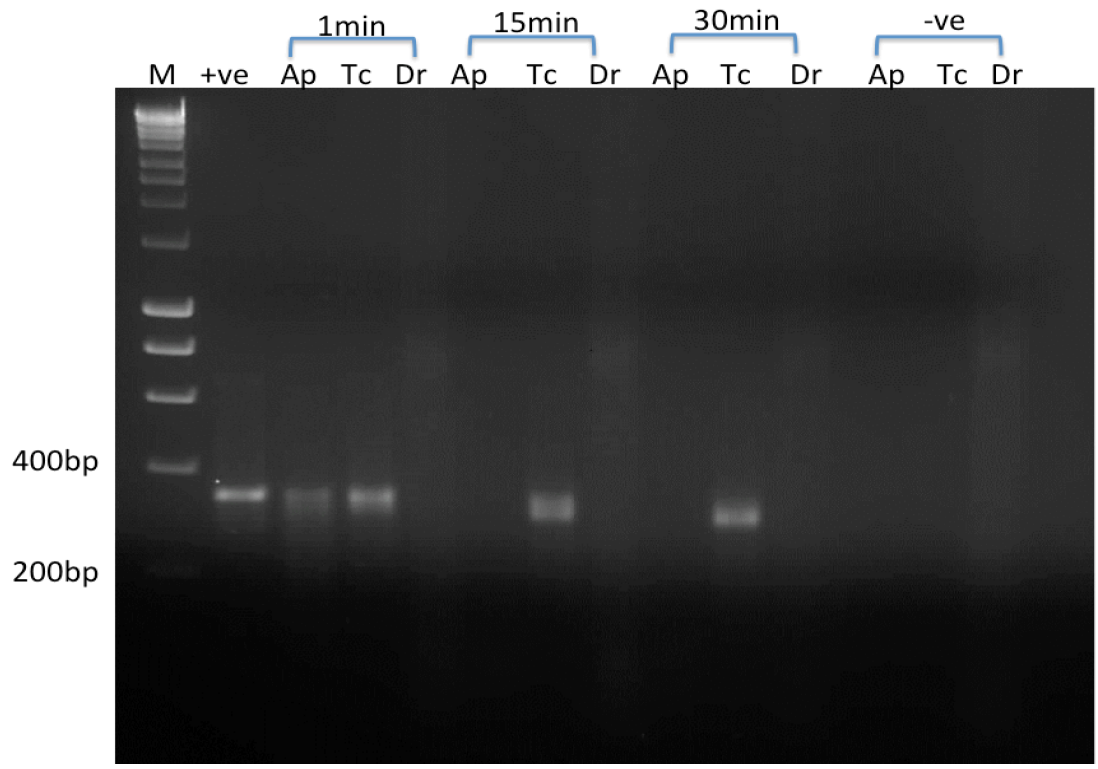

Figure 5-6 ***In vitro*** **experiment showing variability in the persistence and stability of dsRNA in gut extracts from different insect species.**

Aliquots (200 ng) of dsRNA were incubated with gut extracts (the amount of total protein equal to sigle gut in each insects in each case) prepared from *A. pisum* (Ap), *T. castaneum* (Tc) and *D. radicum* (Dr) larval guts for specified time points. +ve denotes dsRNA control (i.e. no added protein), -ve control shows gut extracts with no added dsRNA. dsRNA was not detectable in *D. radicum* reaction after 1min incubation, and weaken signal was shown in *A. pisum* reaction after 1min. After 15 min incubation, dsRNA was completely degraded in *A. pisum* reaction. dsRNA in *T. castaneum* reaction showed signal with decreased size after 30min.

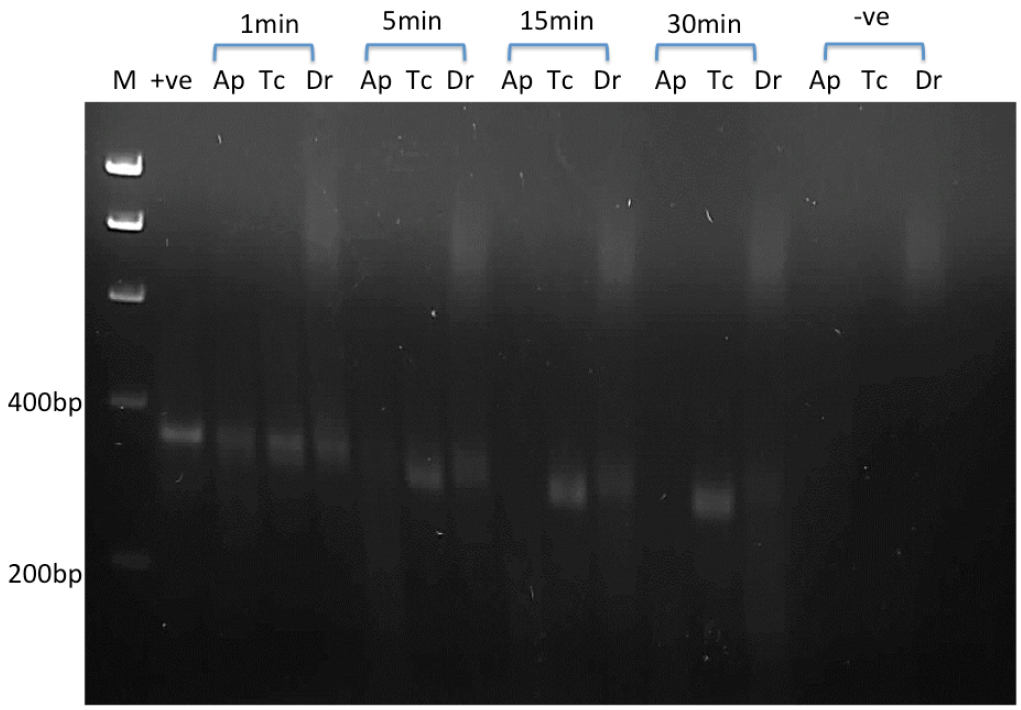

Figure 5-7 ***In vitro*** **experiment showing variability in the persistence and stability of dsRNA in cell-free haemolymph efrom different insect species.**

Aliquots (200 ng) of dsRNA were incubated with cell-free insect haemolymph (25ug total protein in each case) prepared from *A. pisum* (Ap), *T. castaneum* (Tc) and *D. radicum* (Dr) larval haemolymph for specified time points. +ve denotes dsRNA control (i.e. no added protein), -ve control shows gut extracts with no added dsRNA.

When dsRNA incubated with insect haemolymph extract, *A. pisum* extract degrades dsRNA at the highest rate than other two species. Smearing and weakening signal from *A. pisum* treatment was detected after 1 min incubation; the signal was completely disappeared after 5mins. dsRNA incubated with *D. radicum* larval haemolymph extract showed relatively slow rate of degradation. Weakening signal is still detectable after 15 min. In terms of *T. castaneum* larval extract, a slow rate of degradation was observed. As the figure shows dsRNA with partly intact form was still detectable after 30min incubation, the latest time point assayed.

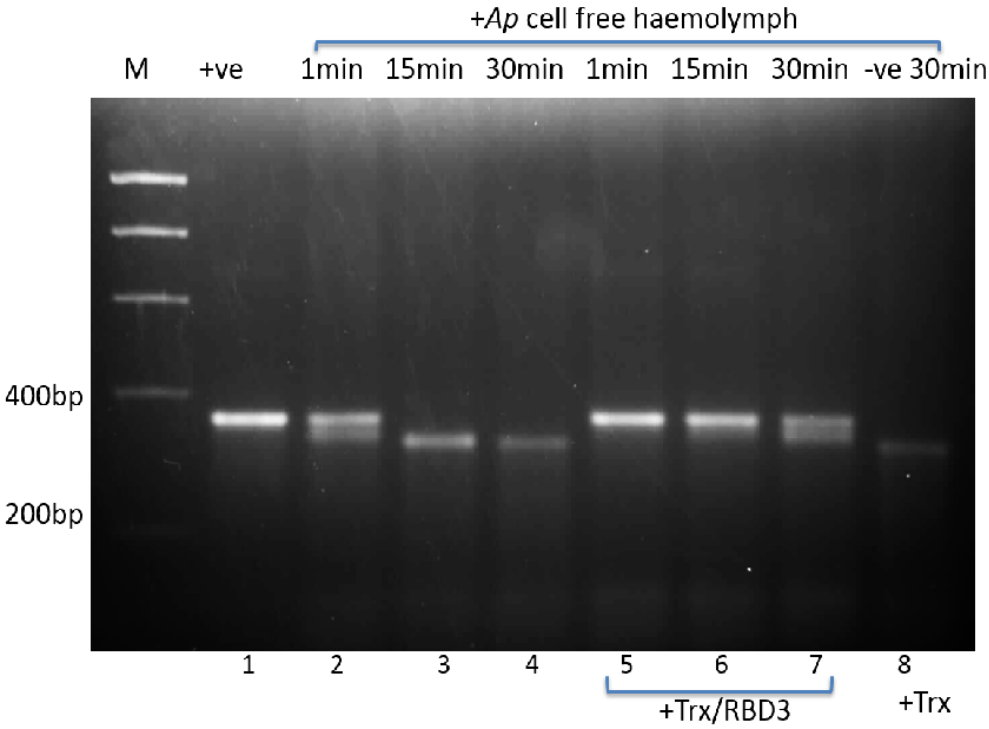

Figure 5-8 **Improvement of stability of dsRNA by Trx/RBD3 against *A. pisum* haemolymph.**

Aliquots (200 ng) of *ApVTE* dsRNA were incubated with cell-free *A. pisum* (Ap) haemolymph at 25°C for specified time points. +ve denotes dsRNA control incubated in 1XPBS containing PTU (i.e. no added haemolymph or Trx/RBD3) for 30 min (Lane 1). -ve control shows dsRNA incubated with 10μg Trx against haemolymph containing 5μg for 1min (Lane 8). Lanes 2-4 show 200ng *ApVTE* dsRNA incubated with *A. pisum* haemolymph containing 5μg protein for 1, 15 and 30 min. Lanes 5-7 show 200ng *ApVTE* dsRNA conjugated with 10μg Trx/RBD3 and incubated with *A. pisum* haemolymph containing 5μg protein for 1, 15 and 30 min.

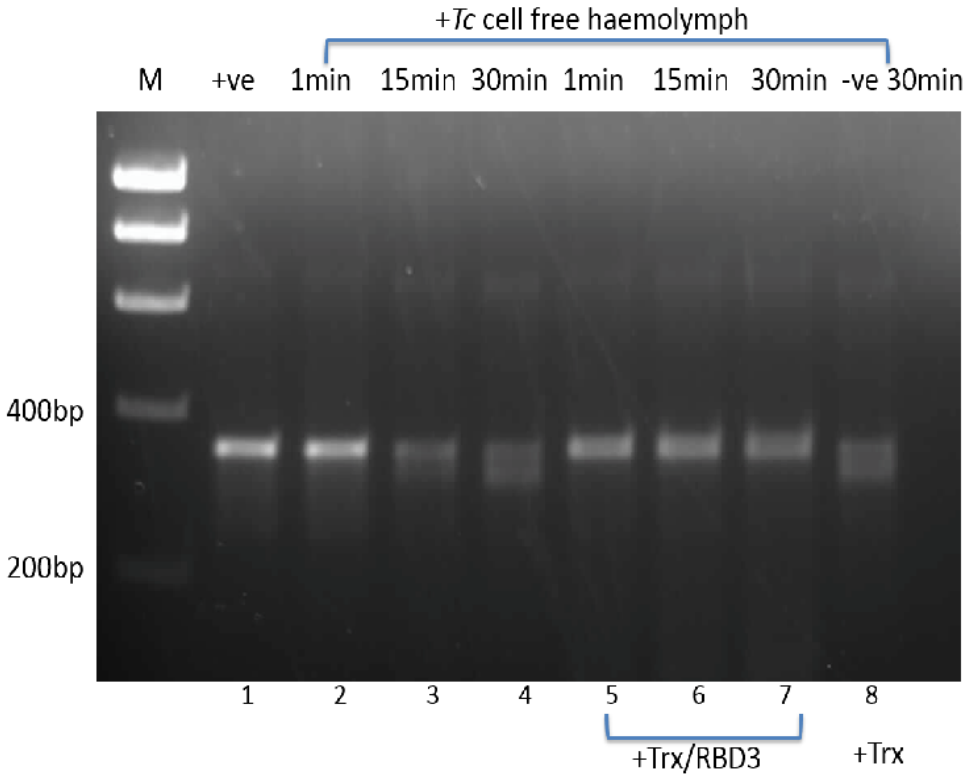

Figure 5-9 **Improvement of stability of dsRNA by Trx/RBD3 against *T. castaneum* haemolymph.**

Aliquots (200 ng) of *TcAPIN* dsRNA were incubated with cell-free *T. castaneum* (Tc) larval haemolymph at 25°C for specified time points. +ve denotes dsRNA control incubated in 1XPBS containing PTU (i.e. no added haemolymph or Trx/RBD3) for 30 min (Lane 1). -ve control shows dsRNA incubated with 10μg Trx against haemolymph containing 25μg for 1min (Lane 8). Lanes 2-4 show 200ng *Tc APIN* dsRNA incubated with *T. castaneum* haemolymph containing 25μg protein for 1, 15 and 30 min. Lanes 5-7 show 200ng *TcAPIN* dsRNA conjugated with 10μg Trx/RBD3 and incubated with *T. castaneum* haemolymph containing 25μg protein for 1, 15 and 30 min.

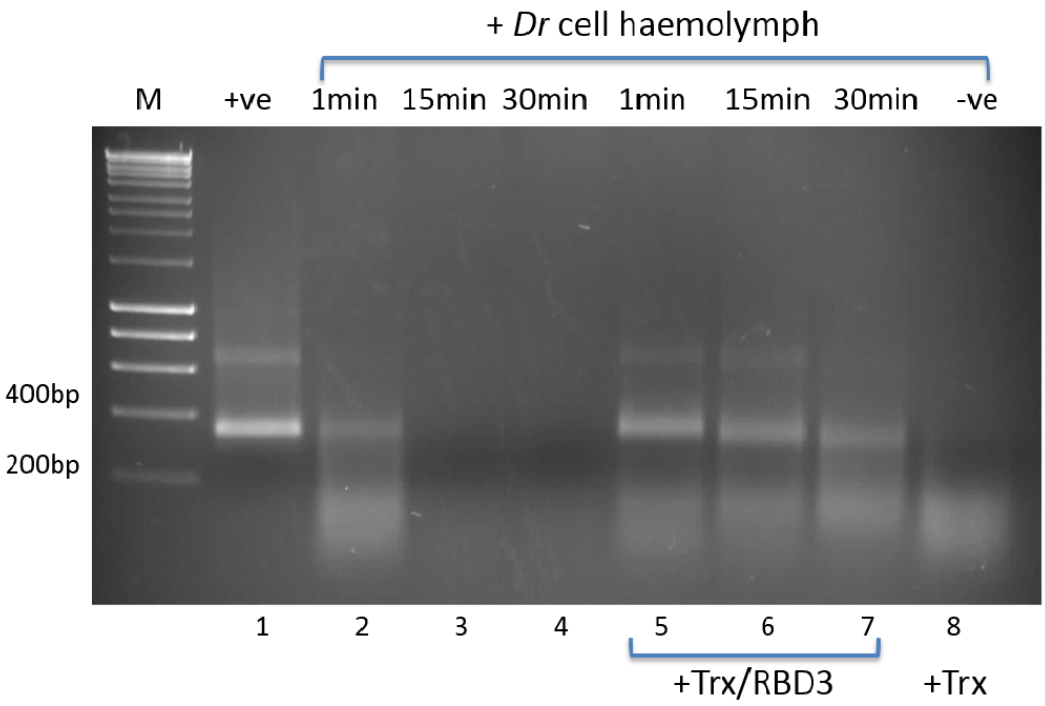

Figure 5-10 **Improvement of stability of dsRNA by Trx/RBD3 against *D. radicum* haemolymph**

Aliquots (200 ng) of *DrAPIN* dsRNA were incubated with cell-free *D. radicum* larval haemolymph at 25°C for specified time points. +ve denotes dsRNA control incubated in 1XPBS containing PTU (i.e. no added haemolymph or Trx/RBD3) for 30 min (Lane 1). -ve control shows dsRNA incubated with 10μg Trx against haemolymph for 1min (Lane 8). Lanes 2-4 show 200ng *DrAPIN* dsRNA incubated with *D. radicum* haemolymph containing 25μg protein for 1, 15 and 30 min. Lanes 5-7 show 200ng *DrAPIN* dsRNA conjugated with 10μg Trx/RBD3 and incubated with *D. radicum* haemolymph containing 5μg protein for 1, 15 and 30 min.

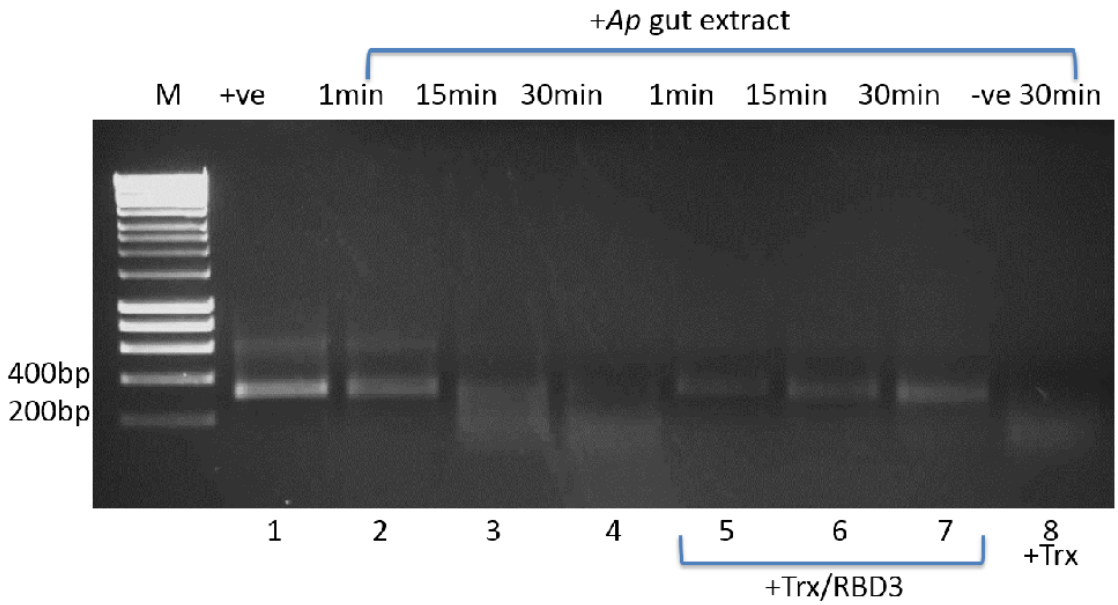

Figure 5-11 **Improvement of stability of dsRNA by Trx/RBD3 against *A. pisum* gut extract.**

Aliquots (200 ng) of *ApVTE* dsRNA were incubated with *A. pisum* (Ap) gut extract at 25°C for specified time points. +ve denotes dsRNA control incubated in 1XPBS (i.e. no added gut extract or Trx/RBD3) for 30 min (Lane 1). -ve control shows dsRNA incubated with 10μg Trx against gut extracts for 1min (Lane 8). Lanes 2-4 show 200ng *ApVTE* dsRNA in 1XPBS incubated with 2μg *A. pisum* gut extract at 25 °C for 1min, 15min and 30min. Lanes 5-7 show 200ng *ApVTE* dsRNA conjugated with 10μg Trx/RBD3 and incubated with 2μg *A. pisum* gut extract at 25 °C for 1min, 15min and 30min.

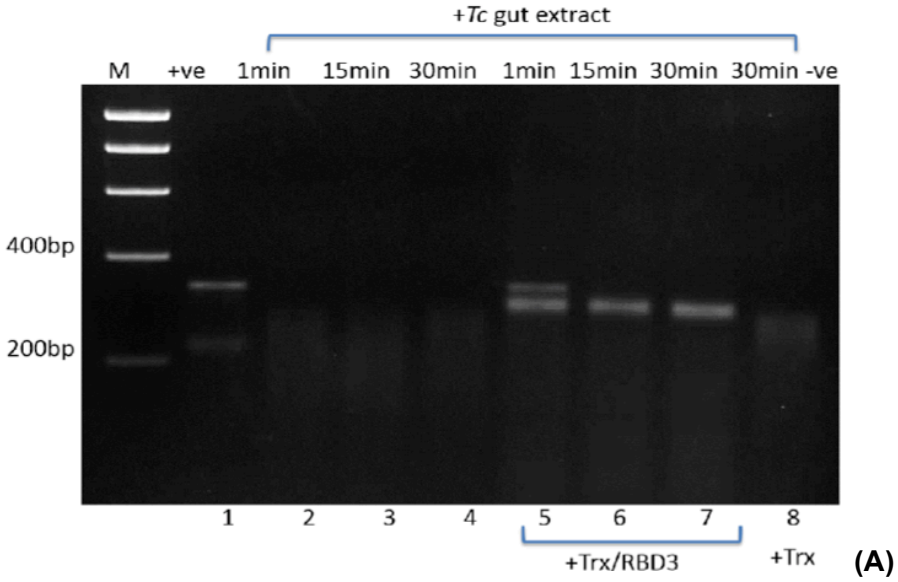

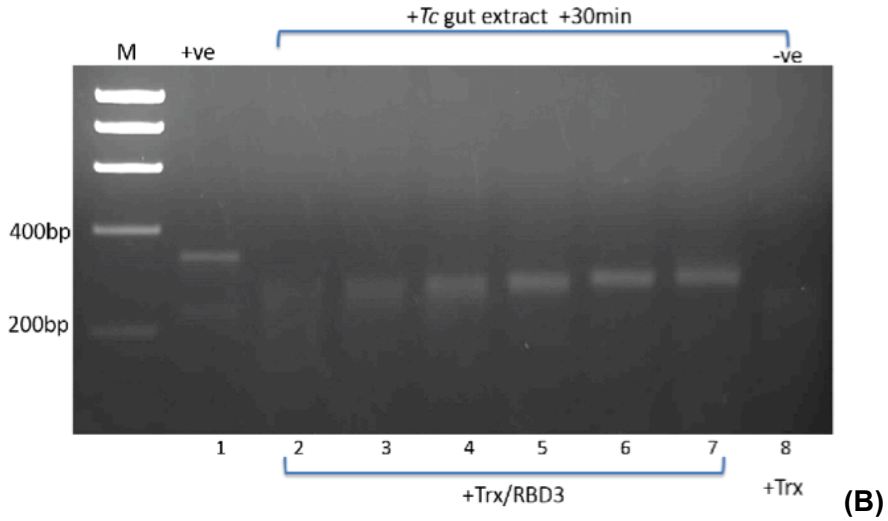

Figure 5-12 **Improvement of stability of dsRNA by Trx/RBD3 against *T. castaneum* gut extract**

Aliquots (200 ng) of *TcAPIN* dsRNA were incubated with *T. castaneum* larval gut extract at 25°C for specified time points. +ve denotes dsRNA control incubated in 1XPBS (i.e. no added gut extract or Trx/RBD3) for 30 min (A&B: Lane 1). -ve control shows dsRNA incubated with 10μg Trx (A: Lane 8) or 14μg Trx (B: Lane 8) against gut extracts for 1min (A) or 30min (B). (A): Lanes 2-4 show 200ng *TcAPIN* dsRNA in 1XPBS incubated with 25μg *T. castaneum* gut extract at 25 °C for 3 different timpoints. Lanes 5-7 show 200ng *TcAPIN* dsRNA conjugated with 10μg Trx/RBD3 and incubated with 25μg *T. castaneum* gut extract at 25 °C for 3 different timepoints.

(B): Lanes 2-7 show 200ng *TcAPIN* dsRNA conjugated with 0μg, 2μg, 4μg, 8μg, 10μg, 14μg against 25μg gut extract at 25 °C for 30 minutes.

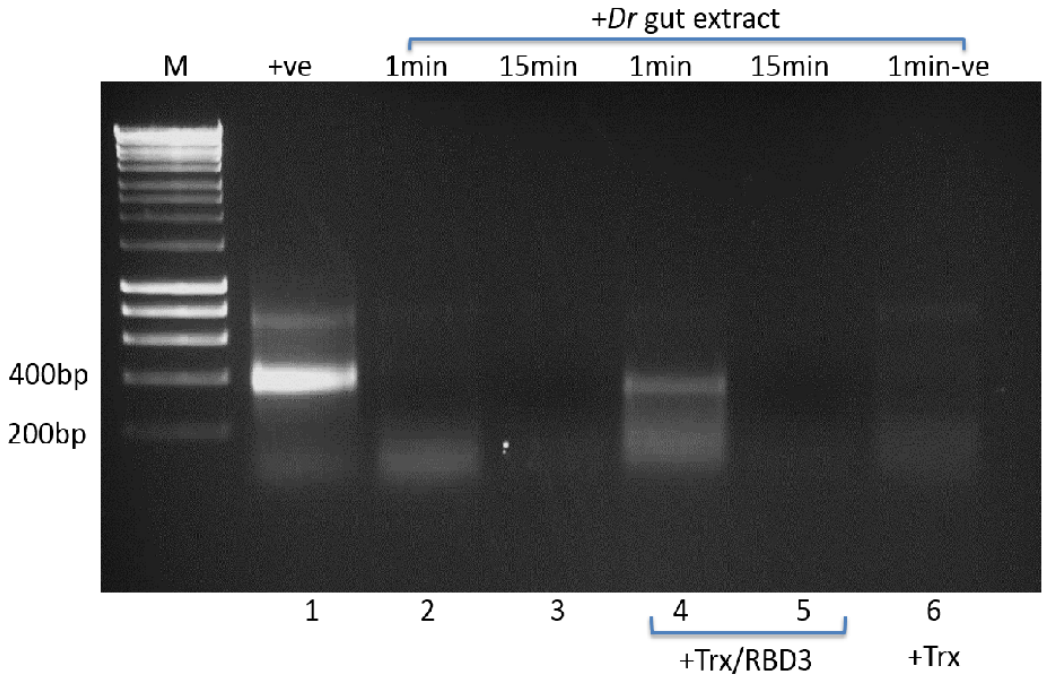

Figure 5-13 **Improvement of stability of dsRNA by Trx/RBD3 against *D. radicum* gut extract**

Aliquots (200 ng) of dsRNA were incubated with *D. radicum* larval gut extract at 25°C for specified time points. +ve denotes dsRNA control incubated in 1XPBS (i.e. no added gut extract or Trx/RBD3) for 30 min (Lane 1). -ve control shows dsRNA incubated with 10μg Trx against gut extracts for 1min (Lane 8). Lanes 2-3 show 200ng *DrAPIN* dsRNA in 1XPBS incubated with 15μg *D. radicum* gut extract at 25 °C for 1min, 15min. Lanes 4-5 show 200ng *DrAPIN* dsRNA conjugated with 10μg Trx/RBD3 and incubated with 15μg *D. radicum* gut extract at 25 °C for 1min, 15min.

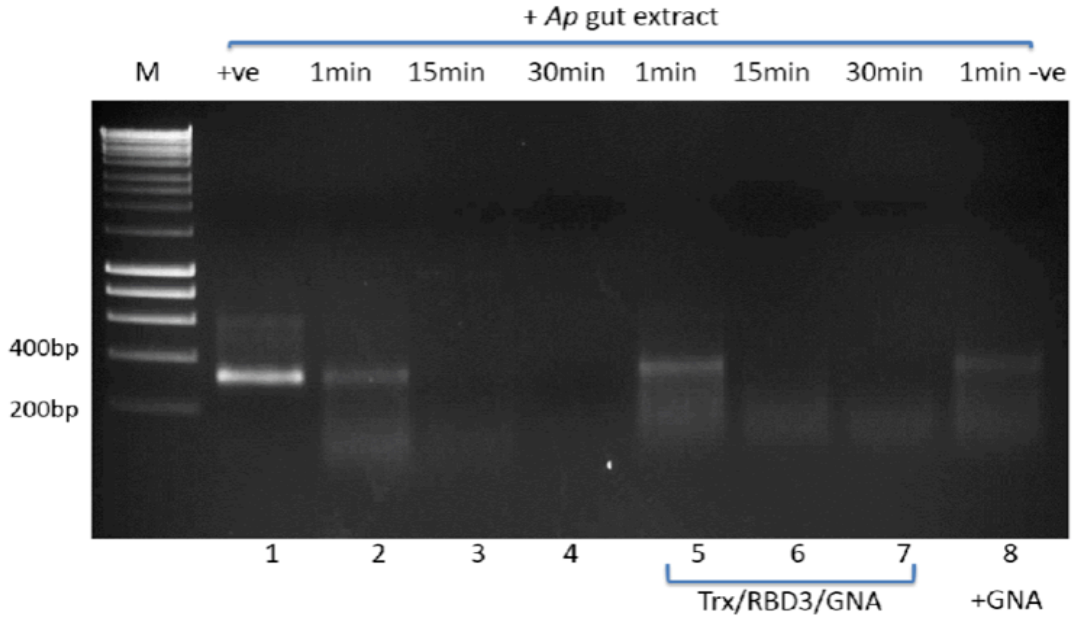

(A)

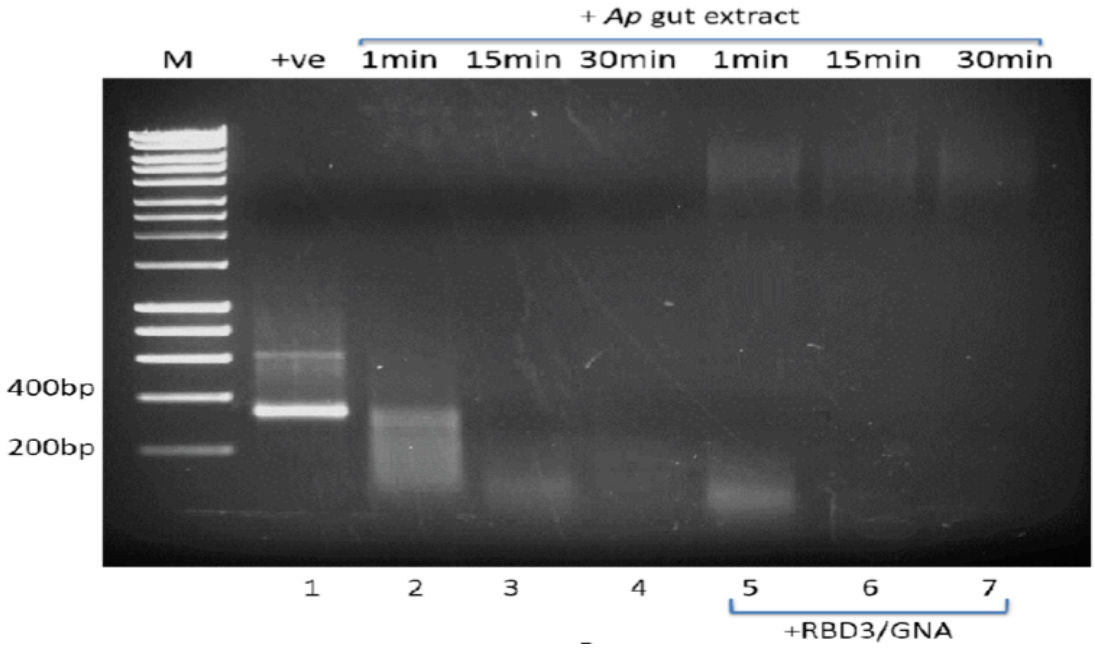

(B)

Figure 5-14 **Stability of dsRNA conjugated with Trx/RBD3/GNA and RBD3/GNA against *A. pisum* gut extract**

Aliquots (200 ng) of *ApVTE* dsRNA were incubated with *A. pisum* gut extract at 25°C for specified time points. +ve denotes dsRNA control incubated in 1XPBS (i.e. no added gut extract, Trx/RBD3GNA or RBD/GNA) for 30 min (A&B: Lane 1). -ve control shows dsRNA incubated with 10μg GNA against gut extracts for 1min (Lane 8). A&B: Lanes 2-4 show 200ng *ApVTE* dsRNA in 1XPBS incubated with 2μg *A. pisum* gut extract at 25 °C for 1min, 15min and 30min. Lanes 5-7 show 200ng *ApVTE* dsRNA in 1XPBS conjugated with Trx/RBD3/GNA (A) or RBD3/GNA (B) against *A. pisum* gut extract at 25 °C for 1min, 15min and 30min.

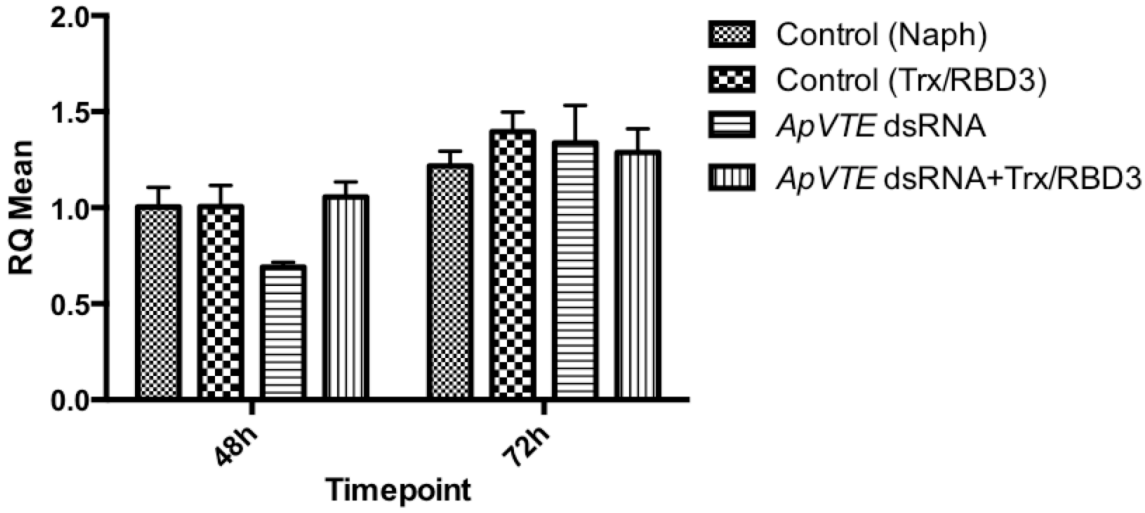

Figure 5-15 **Comparison of gene downregulation by injection of *ApVTE*dsRNA and *ApVTE* dsRNA-Trx/RBD3 conjugate by qRT-PCR.**

Five days old aphid nymphs injected with 20mM Sodium phosphate buffer (Naph) as negative control. Injections were carried out with protein Trx/RBD3 as an additional negative control. Nymphs injected with 5ng *ApVTE* dsRNA was treated as positive control. Trx/RBD3 was incubated with *ApVTE* dsRNA for binding prior injection. Columns show the levels of transcript relative to *GADPH* transcript (internal standard), normalised to Control (Naph) 48h=1.0. Error bars indicate standard errors of the mean for 3 technical replicates. Number of insects used for each treatment n=5. Difference between treatments is not significant (ANOVA).

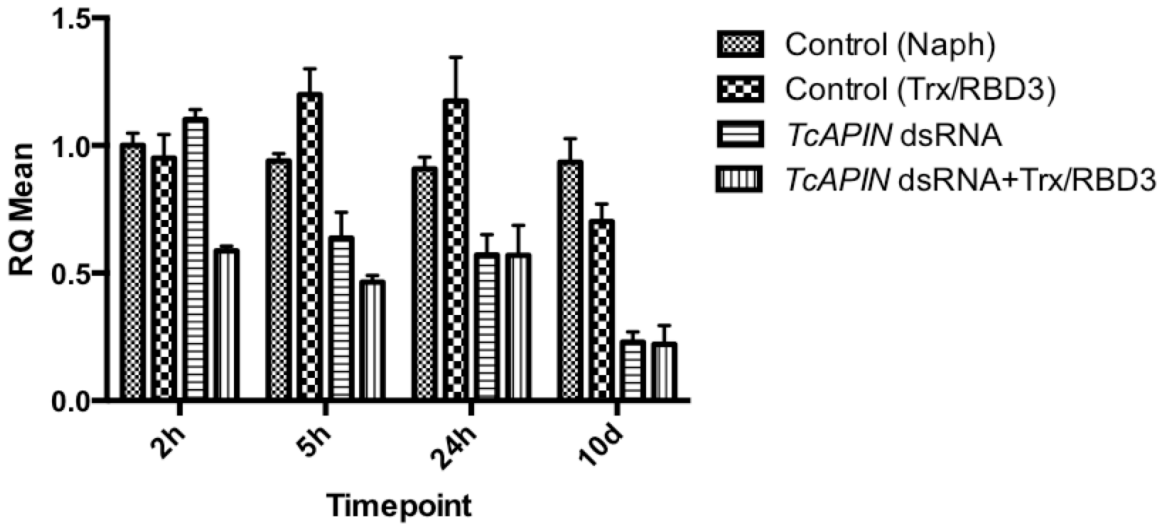

Figure 5-16 **Comparison of gene downregulation by injection of *TcAPIN* dsRNA and *TcAPIN* dsRNA-Trx/RBD3 conjugate by qRT-PCR.**

Pre-pupa stage *T. castaneum* larvae injected with 20mM Sodium phosphate buffer (Naph) and Trx/RBD3 were treated as negative control. Larvae injected with 10ng *TcAPIN* dsRNA was treated as positive control. Trx/RBD3 was incubated with *TcAPIN* dsRNA for binding prior injection. Columns show the levels of transcript relative to *GADPH* transcript (internal standard), normalised to Control (Naph) 48h= 1.0. Error bars indicate standard errors of the mean for 3 technical replicates. Number of insects used for each treatment n=5 (ANOVA with $p<0.0001$, ****).

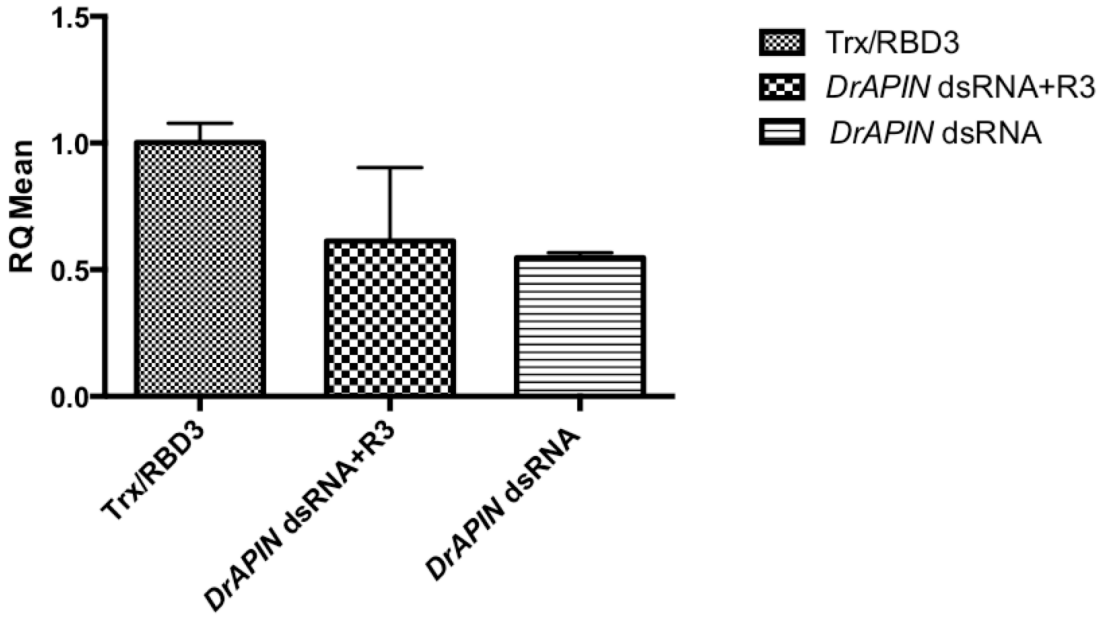

Figure 5-17 **Comparison of gene downregulation by injection of *DrAPIN* dsRNA and *DrAPIN* dsRNA-Trx/RBD3 conjugate by qRT-PCR**

Third instar *D. radicum* larvae injected with Trx/RBD3 were treated as negative control. Larvae injected with 100ng *DrAPIN* dsRNA was treated as positive control. Trx/RBD3 was incubated with *DrAPIN* dsRNA for binding prior injection. Columns show the levels of transcript relative to *GADPH* transcript (internal standard), normalised to Control (Trx/RBR3) =1.0. Error bars are mean value from 3 technical replicates. Number of insects used for each treatment n=5. Difference between Trx/RBD3 treatment and DrAPIN dsRNA treatment is significant by ANOVA test with $p<0.05$, *. No significant difference between Trx/RBD3 and conjugate treatment (ANOVA).

5.3 Discussion

As various sensitivities of RNAi in insects were observed, efforts were made to investigate the potential parameters could be responsible for this difference. For efficient RNAi response, the persistence of intact dsRNA need to be long enough in extracellular environment for its uptake by cells after delivering by injection and feeding. The stability of dsRNA in insect diets were firstly investigated and results suggest that the amount of dsRNA exposed to *A. pisum* via feeding was less than expected. Intact dsRNA was found in aphid diet with aphids feeding, although some of the dsRNA was degraded. In *T. castaneum* diet, however, intact dsRNA was found to survive for much longer term. *In vitro* and *in vivo* experiments of persistence and stability of dsRNA in aphid salivary secretions and haemolymph were also examined by Christiaens *et al.* (2014). Degraded dsRNA in aphid diet was detected after 84h whereas rapid degradation was found in aphid haemolymph after 12h. Similar result was also reported by Allen and Walker III (2012) in another hemipteran, the tarnished plant bug *Lygus lineolaris*, that the secretions from salivary glands were able to degrades dsRNA in the diet. In this work, intact dsRNA was found in aphid diet with aphids feeding after 72h, although some of the dsRNA was degraded. Moreover, the stability of dsRNA was also tested *in vitro* against *A. pisum* honeydew, slightly degraded dsRNA was found which indicated that the RNase presented in gut cell degraded dsRNA rather than the RNase from ingested content in *A. pisum*.

In vitro experiments using cell-free haemolymph and gut extract, which eliminating the possibility that any disappearance of dsRNA could be explained by uptake into cells. The result shows that synthetic dsRNA molecules are rapidly and completely degraded in *A. pisum* haemolymph extract, moderately degraded in *D. radicum* larval haemolymph extract, but degraded with a slow rate in *T. castaneum* haemolymph extract (Fig. 5.5). DsRNA in *T. castaneum* haemolymph extract presented a size-decreasing pattern at different time points whereas completely smearing and weakening signals were observed in other two species. The result in *T. castaneum* haemolymph extract suggest that the nature of RNases could be exoribonuclease activity rather than endonuclease activity. It has already documented in previous literature that the action of endogenously expressed nucleases could be detrimental for RNAi response. Although robust systemic RNAi response has been proved in *C. elegans*, worm tissues such as gonad and neurons are unusually refractory to RNAi whereas all other tissues are susceptible to RNAi (Kennedy *et al.* 2004). In *C. elegans*, a nuclease encoded by the *eri-1* (enhanced RNAi-1) gene was identified and it expresses at high level in worm gonad and neurons. Enhanced RNAi response and greater accumulation of siRNAs than wild type animals were found in *eri-1* mutant

worms (Kennedy *et al.* 2004). Moreover, *eri-1* homologues, *meri-1* (mouse enhance RNAi-1) was found in mice and RNAi against meri-1 result in enhanced sensitivity of RNAi in mice (Hong *et al.* 2005). An enzyme with dsRNAse activity was also been identified in lepidopteran insect, the silkworm *B. mori* (Arimatsu *et al.* 2007). Furthermore, rapid degradation of dsRNA occurs in haemolymph of RNAi-insensitive *A. pisum*, and relatively fast degradation in *D. radicum*, but not in the haemolymph of the RNAi-sensitive *T. castaneum* larval extract indicates the persistence of dsRNA against nucleases in insect extracellular environment could be the key factor in determining the success of RNAi experiments. However, limited information of dsRNA-specific nucleases in insects that could interfere with RNAi is amendable. More efforts should be made to identify the endoribonucleases and exoribonucleases.

Gene downregulation as well as mortality were observed in dsRNA fed *T. castaneum*, but not in other two species. Thus the persistence of dsRNA against *A. pisum*and *D. radicum* gut extracts were compared with *T. castaneum* gut extract as the insect gut is the first barrier for dsRNA after being ingested orally. When analysing dsRNA with same concentration of total protein from three insect gut extracts, the result revealed a rapid and completely dsRNA degradation in *A. pisum* gut extract, moderately fast degradation in *D. radicum* larval gut extract. However, in *T. castaneum*, larval gut extract degraded dsRNA at very slow rate. The result indicates that RNAi induced gene downregulation is restricted to cells in *A. pisum* and *D. radicum* guts. Similar to the result of dsRNA degradation in *T. castaneum* haemolymph extract, dsRNA was degraded with decreasing size and can survive for a much longer time than in other two insect gut extracts. The result could lead to hypothesis that dsRNA degraded by exoribonucleases rather than endoribonucleases at slow rate and remain partly intact and this allow form allow survival for a longer time and uptake of dsRNA by cells in *T. castaneum* larvae. The stability of dsRNA was also tested against total protein equivalent to single gut of each insect, and dsRNA was found to be degraded at highest rate in *D. radicum* larval gut extract due to the highest amount of protein (80μg). However, the total protein extracted and tested in this work may not truly reflect the real situation *in vivo*.

Experiments *in vitro* showed that conjugation to Trx/RBD3 was able to reduce the rate of degradation of dsRNA when exposed to insect haemolymph. These results were consistent across different species, and gave direct evidence for the utility of conjugate formation in protecting dsRNA. The effects of conjugation of dsRNA to Trx/RBD3 *in vivo* after injection into haemolymph could thus be predicted to be extension or improvement of the RNAi effect induced by injected dsRNA. However, it is also possible that the dsRNA could be prevented from showing any RNAi effect as a

result of conjugation, due to lack of uptake into cells, or availability for the RNAi machinery being blocked. The results in *A. pisum* suggest that conjugation with Trx/RBD3 does somehow interfere with RNAi effect. However, the injected *T. castaneum* shows different result pattern. DsRNA-Trx/RBD3 conjugate injection shows a faster RNAi response than dsRNA injection only (from results at 2h post injection). The improved RNAi response could due to more intact dsRNAs being maintained in *T. castaneum* haemolymph before they are transported into different cells.

In terms of using RBD3 to protect dsRNA from biodegradation, dsRNA-Trx/RBD3 complexes were assayed against different insect haemolymph and gut extracts. The results demonstrated that Trx/RBD3 is able to improve the stability of dsRNA and reduce the rate of degradation by the ribonucleases present in insect haemolymph and gut extract. A recent study investigated improvement of the stability of dsRNA by conjugating RBD3 from the *Mus musculus* Staufen (Kawaguchi *et al.* 2009). Unexpectedly, the recombinant RBD3 was not able to improve the stability of siRNA against fetal bovine serum (FBS), but showed some protection of shRNA that has a stem loop structure. The amino acid sequence alignment between *D. melanogaster* and *M. musculus* is shown in figure 4.43 (in chapter 4). As figure 4.43, indicates that RBD3 from *Mus musculus* chosen by Kawaguchi *et al.* (2009), contained only the 65 amino acid domain. This could be one of the reasons for inefficient binding in their results. Another issue could be RBD3 from different species shows different efficiency of dsRNA binding activity. For example, both of the domains are required for optimal dsRNA binding by human dsRNA-dependent protein kinase (PKR), and mutations in one domain are more damaging than in the other (Green and Mathews 1992). However, a synthetic 24 amino acid peptide containing only part of the RNA-binding domain from intact 345 amino acid human immunodeficiency virus type 1 transactivation response RNA binding protein (TRBP) shows efficient dsRNA binding activity (Gatignol *et al.* 1993).

Positive results were obtained with insect gut extracts *in vitro*, showing that dsRNA in Trx/RBD3 conjugates showed enhanced resistance to nuclease activity in all the insect species examined. However, neither Trx/RBD3/GNA nor RBD3/GNA were able to improve dsRNA stability against *A. pisum* gut extract. This could due to the bad protein sample preparation, as little soluble Trx/RBD3/GNA from induced *E. coli* cells can be purified and large amount of protein precipitation was observed during dialysis and concentrating steps. Although RBD3/GNA can be produced as a soluble protein from *P. pastoris,* REMSA assays do not show consistent evidence for dsRNA binding activity, and the assays with aphid gut extract showed no evidence for improving dsRNA stability. Indeed, results from REMSA (chapter 4) and other assays suggest that

RBD3/GNA from *P. pastoris* may itself be contaminated with nuclease activity, making any protective effect difficult to observe.

Chapter 6 General discussion

Gene silencing through RNAi is a useful reverse genetic technique that has revolutionized the study of gene function in insect species, particularly in non-model insects. The generation of a loss-of-function phenotype by depletion of a chosen transcript has been recognised as a potential method for linking genes to processes in many different fields of insect biology (Bellés 2010), as well as for developing medical treatments (Tiemann and Rossi 2009). Unfortunately, recent studies regarding RNAi in insects have revealed that there is clear variability in the susceptibility of insect species to RNAi. Terenius *et al.* (2011) reviewed RNAi experiments in Lepidopteran species, and concluded that there is variation in RNAi efficiency of the technique related to insect species, tissues and target gene selected. Moreover, cases of contrasting results from similar experiments have also been reported. Low reproducibility of RNAi experiments in Hemipteran insects, such as aphids, were also noticed.

This thesis describes work that has attempted to explore the mechanistic reason underlying the differing susceptibility to RNAi in different insects, in the context of testing the potential for using RNAi for crop protection. RNAi responses in insects from three different orders (*T. castaneum*, Coleopteran*; M. domestica* and *D. radicum*, Dipteran and *A. pisum* from Hemiptera) were selected and compared. To standardise the RNAi experimental parameters in insects, a conserved region from the sequence of *V-type ATPase E* subunit of insects was chosen for designing dsRNA with same length (277bp). Similarly, comparable dsRNAs were also selected from the *APIN* (*Inhibitor of Apoptosis*) gene, although in this case the sequences were more variable in length due to differences in the target genes. The dose of dsRNA used was considered in relation to the relative sizes of the insects on a weight basis. Assessment of the efficacy of gene knockdowns was determined by using real time qPCR.

In this work, a robust systemic RNAi response was observed in *T. castaneum* larvae by both injection and feeding of dsRNAs against *TcVTE* and *TcAPIN* genes. A phenotype resulting from the RNAi effect was observed, and down-regulation of target genes was confirmed by qPCR. These results (Chapter 3) agree well with previous studies (Tomoyasu and Denell (2004); Arakane *et al.* (2005); Whyard *et al.* (2009); (Miller *et al.* 2012)). Successful target *APIN* downregulation and phenotype were also achieved in two Dipteran species which are *M. domestica* and *D. radicum* larvae, however the RNAi effect rely on microinjection of dsRNA and was found to be stage dependent (RNAi response was not detected in *M. domestica* adult). Feeding dsRNA to Dipteran larvae failed to provoke any RNAi response (Chapter 3). In terms of *A. pisum*, limited silencing was observed (Chapter 3). 'Weak' gene downregulation and phenotype were achieved only by injection of *ApVTE* dsRNA. Feeding *ApVTE* dsRNA did not result in

any phenotype effects on either survival or fitness parameters. Attempts to silence *ApAPIN* gene was completely unsuccessful either by injection or feeding. The results with aphids contrast with those for flour beetle, and cannot be explained by stability of dsRNA in the diet; even though dsRNA survived for a longer time during feeding in *T. confusum* diet than in *A. pisum* liquid diet, it was present in both for long enough to produce an RNAi effect if the timescale of the effect produced by injection is indicative.

For a better understanding the various sensitivities to RNAi in these three insects, attempts were made to investigate the persistence of dsRNA in both insect haemolymph and gut extract. Rapid and complete degradation of dsRNA was found to occur in RNAi insensitive *A. pisum* haemolymph. Previous studies performed by Christiaens *et al.* (2014) also demonstrated a fast dsRNA degradation in *A. pisum* haemolymph. Compared to *A. pisum* haemolymph, dsRNA is degraded slower rate in *D. radicum* larval haemolymph. In the haemolymph of the RNAi-sensitive *T. castaneum* larvae, partial degradation of dsRNA was observed at a slow rate than other two tested insects. These findings could explain the weak RNAi effects in *A. pisum*, as exogenous dsRNA delivered by injection was broken down rapidly in aphid haemolymph before its uptake by cells where the RNAi process takes place. Fast degradation was also observed in larval haemolymph of *D. radicum*. However, significant RNAi response was achieved after injection of dsRNA into *D. radicum* larvae. This indicated that dsRNA survived for sufficiently long for its uptake by cells in *D. radicum* larvae. In terms of *T. castaneum*, dsRNA with a long survival period could be the first parameter for RNAi, as a result of sufficient dsRNA uptake by cells.

Rapid degradation of dsRNA in haemolymph could be an adaption for evolutionary response to a heavy viral loads that led to the constitutive expression of active RNases against viral RNAs. Aphids are sap-sucking insects that can damage crops by transmitting viral diseases. Historical exposure of *A. pisum* to viral infection may have resulted in an active RNA degradation ability against virus. The result of dsRNA feeding experiment also indicated that the products of *A. pisum* salivary glands were able to degrade some of dsRNA in the diet. In Dipteran species, the model insect *D. melanogaster* is relatively insensitive to exogenous dsRNA. The effectiveness of dsRNA in this species appears to differ over different developmental stages; in larvae dsRNA was found to be only incorporated in hemocyte cells in the hemolymph (Miller *et al.* 2008), but in adults and embryos it is able to penetrate into different tissues (Tomoyasu *et al.* 2008).

Apart from the differences in dsRNA degradation mechanism in insects' extracellular environment, another most important factor for a robust RNAi response is the amplification and export of the dsRNA signal in the cells initially targetted, so that the RNAi effect spreads through cells and tissues in the organism. As mentioned in chapter

1, the transitive RNAi in *C. elegans* relies on the production of secondary dsRNA by an RNA-dependent RNA polymerase (RdRP) whereas the systemic property is dependent on the gene *sid-1*, which encodes a multitransmembrane domain protein and is recognized as a channel for transporting dsRNA. A comparison of RNAi related genes between *C. elegans* and insects revealed that the core RNAi machinery enzymes like Dicer and Argonaute are conserved in *C. elegans* and insects (Tomoyasu *et al.* 2008), which indicated that the poor sensitivity in some insect species is restricted to transmission of interfering signal though cells and tissues rather than core machinery (Bellés 2010). The evidence from Miller *et al.* (2008) demonstrated that over-expression of dsRNA within the cells could trigger RNAi responses in *D. melanogaster* tissues that are known for resistance to systemic RNAi. In terms of SID genes, a single orthologue of *sid-1* is identified in each of the bee (Winston *et al.* 2002), louse and aphid genomes, whereas three orthologues are observed in moth *Bombyx* and the beetle *Tribolium* (Tomoyasu *et al.* 2008). The variation in the number of *sid-1* genes could lead to different susceptibility to RNAi in different insect species.

It is necessary to identify and compare the identity of the enzymes responsible for dsRNA degradation in insect haemolymph and gut of *A. pisum* and *T. castaneum*. Ion exchange chromatography and affinity chromatography could be applied to separated protein fractions. The ability of dsRNA degradation of the isolated protein fraction could be assessed by incubating protein sample with dsRNA using agarose gel-based system validated in chapter 5. Fractionation of protein may require several repeated experiments using sensitive affinity chromatography to achieve a sample only containing one protein. Identification of the protein sequence and domain could be examined by loading onto SDS-PAGE followed by MALDI-TOF mass spectrometry.

A strategy based on RNA-binding proteins was explored in this thesis to stabilise dsRNA by protecting it from degradation Trx/RBD3 was expressed as soluble active fusion protein from *E. coli* system and the dsRNA binding property was confirmed by REMSA system. The estimated binding constant K_d is approx. $8x10^{-8}$M in this work (Chapter 4). Compared to previous study using short dsRNA (12bp) with extra tetraloop, longer dsRNA with sufficient length 277bp to induce RNAi response resulted in stronger binding. The stability of dsRNA was successfully improved by Trx/RBD3 conjugation against RNases from tested insects haemolymph and gut extract (Chapter 4). However, since the RNAi response is a cellular process, dsRNA needs to be recognized and processed by Dicer and Argonaute protein in the pathway after being imported into cells. Conjugation with Trx/RBD3 could lead to a potential risk of blocking the process of dsRNA uptake into cells, since there is a possibility that Trx/RBD3-

dsRNA would fail to be taken up by the cell as a conjugated form. Luckily, the conjugate showed more rapid RNAi response than dsRNA injection however only in *T. castaneum* (Chapter 4), but not in *A. pisum*. The result in *A. pisum* suggest that the conjugate does somehow interfere with RNAi effect (Chapter 4), although the RNAi induced gene downregulation in *A. pisum* is limited (Chapter 3).

Alternative strategies to stabilise dsRNA by using chemical modification were investigated by previous researchers. Morrissey *et al.* (2005a), (Morrissey *et al.* 2005b) chemically substituted all 2'-OH residues on siRNA targeted to hepatitis B virus with 2'F, 2'O-Me or 2'H residues. The stabilized siRNA was then incorporated in a specialized liposome to form a stable nucleic-acid-lipid particle (SNALP). The authors reported that a longer half-life of siRNA-SNALP in mice plasma and liver (*in vivo*) after administration which led to an RNAi effect after applying lower doses with less frequency. Another study performed by Layzer *et al.* (2004) modified siRNA with 2'-flouro (2'-F) pyrimidine result in increased stability and a prolonged half-life in human plasma compared to 2'-OH containing siRNAs. But improved stability did not lead to enhanced gene inhibition in mice after injection. Liu *et al.* (2012) developed a solid phase method for peptide-siRNA covalent conjuagets based on click chemistry. The conjugation of peptides and siRNAs through a 1,2,3,-triazole linker. Alkynyl nucleoside analogue 'clikced' onto a peptide-derivatized Controlled Pore Glass (CPG) followed by oligonucleotides synthesis. The results show that the 3'-snese strand conjugate maintained gene silencing activity. However, the silencing activity of 3'-antisense strand conjuagate is decreased (Liu *et al*., 2012).

In order to address limitations of RNAi effects after feeding dsRNA in insects due to the poor transport of RNA to the circulatory system, recombinant proteins Trx/RBD3/GNA and RBD3/GNA were expressed in *E. coli* and *P. pastoris*, respectively. However, due to the insolubility of Trx/RBD3/GNA, the dsRNA binding assay of Trx/RBD3/GNA did not show convincing binding ability (Chapter 4). Although RBD3/GNA can be produced from yeast as soluble protein, REMSA indicates that RBD3/GNA degrades dsRNA rather than protecting dsRNA from degradation. Moreover, neither the assays with aphid gut extract showed evidence for improving dsRNA stability (Chapter 4).

Previous studies indicated that production of GNA in *E. coli* system could be problematic, but soluble and active GNA was successfully purified and refolded from inclusion bodies of induced *E. coli* cells by Longstaff *et al.* (1998). Briefly, induced cells pellet was lysed and inclusion bodies were prepared in 10mM $MgCl_2$ and 1mM $MnCl_2$ to increase enzyme activity. The inclusion bodies were then precipitated by adding 2 vol. 0.2M NaCl, 1% deoxycholate, 1% Nonidet P-40, 20 mM Tris/HCl pH 7.5, 2 mM EDTA followed by centrifugation. The inclusion bodies were then solubilised in buffer

containing 6M urea and purified from metal-affinity column. Unbound protein was washed off by buffer containing 6M urea and column was was rinsed with 60Mm imidazole in buffer containing decreasing amounts of urea (6, 4, 2, 1, 0.5, 0.25 and 0.125M). Refolded GNA was eluted with buffer containing 300mM imidazole and dialysed against 50mm Tris/HCl pH 7.9. GNA purified from this method showed activity of specific mannose binding property and toxicity towards rice brown planthopper (*N. lugens*) (Longstaff *et al.* 1998). The inclusion bodies from induced Trx/RBD3/GNA in this work shows a single and clean product (Chapter 4). Refolding Trx/RBD3/GNA from induced inclusion bodies according to method developed by Longstaff *et al.* (1998) may lead to active fusion protein product.

Different approaches could be also applied for transporting dsRNA according to previous literature. Fusion proteins with two cell-penetrating peptides (CPP): human transcriptional factor Hph-1-Hph-1, and a double-stranded RNA binding domain from human Dicer was constructed for siRNA delivery to a heart transplant model (Li *et al.* 2014). CPP transfers siRNA through covalent and noncovalent associations and should able to transport the dsRBD/siRNA complex into cells. A much higher percentage of target GAPDH mRNA in Hela cells was downregulated by Hph-1-Hph-1-dsRBD-siRNA than either siRNA only or treatment using Lipofectamine^{TM} RNAiMAX for siRNA delivery (Li *et al.* 2014). *In vivo* evidence by using FAM-siRNA bound with Hph-1-Hph-1-dsRBD-siRNA demonstrated that the complex entered the heart and was distributed throughout (Li *et al.* 2014). Another successful delivery method was use chitosan/dsRNA nanoparticle to silence chitin synthase genes though feeding in the African malaria mosquito, *Anopheles gambiae* (Zhang *et al.* 2010). Chitosan/dsRNA nanoparticles were formed by self-assembly of polycations with dsRNA though electrostatic interaction between amino groups of chitosan and phosphate groups of dsRNA (Zhang *et al.* 2010). After feeding chitosan/dsRNA against chitin synthesis particles to third instar mosquito larvae, chitin content is decreased by 33.8%, and resulted in increased susceptibility of the larvae to diflubenzuron, and calcofluor white or dithiothreitol (Zhang *et al.* 2010).

References:

Allen, M. L. and Walker III, W. B. (2012) 'Saliva of Lygus lineolaris digests double stranded ribonucleic acids', *Journal of Insect Physiology*, 58(3), 391-396.

Ambrosini, G., Adida, C. and Altieri, D. C. (1997) 'A novel anti-apoptosis gene, survivin, expressed in cancer and lymphoma', *Nature Medicine*, 3(8), 917-921.

Arakane, Y., Muthukrishnan, S., Beeman, R. W., Kanost, M. R. and Kramer, K. J. (2005) 'Laccase 2 is the phenoloxidase gene required for beetle cuticle tanning', *Proceedings of the National Academy of Sciences of the United States of America*, 102(32), 11337-11342.

Arakawa, T. (1995) 'Phenylthiourea, an Effective Inhibitor of the Insect Haemolymph Melanization Reaction, Interferes with the Detection of Lipoprotein Hydroperoxide', *Applied Entomology and Zoology*, 30(3), 443-449.

Araujo, R., Santos, A., Pinto, F., Gontijo, N., Lehane, M. and Pereira, M. (2006) 'RNA interference of the salivary gland nitrophorin 2 in the triatomine bug Rhodnius prolixus (Hemiptera: Reduviidae) by dsRNA ingestion or injection', *Insect Biochemistry and Molecular Biology*, 36(9), 683-693.

Aravin, A. A., Hannon, G. J. and Brennecke, J. (2007) 'The Piwi-piRNA pathway provides an adaptive defense in the transposon arms race', *Science*, 318(5851), 761-764.

Arimatsu, Y., Kotani, E., Sugimura, Y. and Furusawa, T. (2007) 'Molecular characterization of a cDNA encoding extracellular dsRNase and its expression in the silkworm, Bombyx mori', *Insect Biochemistry and Molecular Biology*, 37(2), 176-183.

Bachan, S. and Dinesh-Kumar, S. P. (2012) 'Tobacco rattle virus (TRV)-based virus-induced gene silencing' in *Antiviral Resistance in Plants* Springer, 83-92.

Bass, B. L., Hurst, S. R. and Singer, J. D. (1994) 'Binding properties of newly identified Xenopus proteins containing dsRNA-binding motifs', *Current Biology*, 4(4), 301-314.

Baum, J. A., Bogaert, T., Clinton, W., Heck, G. R., Feldmann, P., Ilagan, O., Johnson, S., Plaetinck, G., Munyikwa, T. and Pleau, M. (2007) 'Control of coleopteran insect pests through RNA interference', *Nature Biotechnology*, 25(11), 1322-1326.

Baumgartner, P., Harper, K., Raemaekers, R. J., Durieux, A., Gatehouse, A. M., Davies, H. V. and Taylor, M. A. (2003) 'Large-scale production and purification of recombinant Galanthus nivalis agglutinin (GNA) expressed in the methylotrophic yeast Pichia pastoris', *Biotechnology Letters*, 25(15), 1281-1285.

Bellés, X. (2010) 'Beyond Drosophila: RNAi in vivo and functional genomics in insects', *Annual Review of Entomology*, 55, 111-128.

Bernstein, E., Caudy, A. A., Hammond, S. M. and Hannon, G. J. (2001) 'Role for a bidentate ribonuclease in the initiation step of RNA interference', *Nature*, 409(6818), 363-366.

Berthelet, J. and Dubrez, L. (2013) 'Regulation of apoptosis by inhibitors of apoptosis (IAPs)', *Cells*, 2(1), 163-187.

Beug, S. T., Cheung, H. H., LaCasse, E. C. and Korneluk, R. G. (2012) 'Modulation of immune signalling by inhibitors of apoptosis', *Trends in Immunology*, 33(11), 535-545.

Bevilacqua, P. C. and Cech, T. R. (1996) 'Minor-groove recognition of double-stranded RNA by the double-stranded RNA-binding domain from the RNA-activated protein kinase PKR', *Biochemistry*, 35(31), 9983-9994.

Beyenbach, K. W. and Wieczorek, H. (2006) 'The V-type H+ ATPase: molecular structure and function, physiological roles and regulation', *Journal of Experimental Biology*, 209(4), 577-589.

Birnbaum, M., Clem, R. and Miller, L. (1994) 'An apoptosis-inhibiting gene from a nuclear polyhedrosis virus encoding a polypeptide with Cys/His sequence motifs', *Journal of Virology*, 68(4), 2521-2528.

Boisson, B., Jacques, J. C., Choumet, V., Martin, E., Xu, J., Vernick, K. and Bourgouin, C. (2006) 'Gene silencing in mosquito salivary glands by RNAi', *FEBS Letters*, 580(8), 1988-1992.

Bolognesi, R., Ramaseshadri, P., Anderson, J., Bachman, P., Clinton, W., Flannagan, R., Ilagan, O., Lawrence, C., Levine, S. and Moar, W. (2012) 'Characterizing the mechanism of action of double-stranded RNA activity against western corn rootworm (Diabrotica virgifera virgifera LeConte)'. *PloS ONE,* 7(10),e47534.

Broadus, J., Fuerstenberg, S. and Doe, C. Q. (1998) 'Staufen-dependent localization of prospero mRNA contributes to neuroblast daughter-cell fate', *Nature*, 391(6669), 792-795.

Broemer, M., Tenev, T., Rigbolt, K. T., Hempel, S., Blagoev, B., Silke, J., Ditzel, M. and Meier, P. (2010) 'Systematic in vivo RNAi analysis identifies IAPs as NEDD8-E3 ligases', *Molecular Cell*, 40(5), 810-822.

Bucher, G., Scholten, J. and Klingler, M. (2002) 'Parental RNAi in Tribolium (Coleoptera)', *Current Biology*, 12(3), R85-R86.

Bycroft, M., Grünert, S., Murzin, A., Proctor, M. and St Johnston, D. (1995) 'NMR solution structure of a dsRNA binding domain from Drosophila staufen protein reveals homology to the N-terminal domain of ribosomal protein S5', *The EMBO Journal*, 14(14), 3563.

Casida, J. E. and Durkin, K. A. (2013) 'Neuroactive insecticides: targets, selectivity, resistance, and secondary effects', *Annual Review of Entomology*, 58, 99-117.

Cerritelli, S. M. and Crouch, R. J. (2009) 'Ribonuclease H: the enzymes in eukaryotes', *FEBS Journal*, 276(6), 1494-1505.

Chandraratna, D., Lawrence, N., Welchman, D. P. and Sanson, B. (2007) 'An in vivo model of apoptosis: linking cell behaviours and caspase substrates in embryos lacking DIAP1', *Journal of Cell Science*, 120(15), 2594-2608.

Chapman, E. J. and Carrington, J. C. (2007) 'Specialization and evolution of endogenous small RNA pathways', *Nature Reviews Genetics*, 8(11), 884-896.

Chintapalli, V. R., Wang, J. and Dow, J. A. (2007) 'Using FlyAtlas to identify better Drosophila melanogaster models of human disease', *Nature Genetics*, 39(6), 715-720.

Christiaens, O., Swevers, L. and Smagghe, G. (2014) 'DsRNA degradation in the *A. pisum* (Acyrthosiphon pisum) associated with lack of response in RNAi feeding and injection assay', *Peptides*, 53, 307-314.

Chung, W.-J., Okamura, K., Martin, R. and Lai, E. C. (2008) 'Endogenous RNA interference provides a somatic defense against Drosophila transposons', *Current Biology*, 18(11), 795-802.

Cino, J. (1999) 'High-yield protein production from Pichia pastoris yeast: a protocol for benchtop fermentation', *American Biotechnology Laboratory*, 17, 10-13.

Ciudad, L., Bellés, X. and Piulachs, M.-D. (2007) 'Structural and RNAi characterization of the German cockroach lipophorin receptor, and the evolutionary relationships of lipoprotein receptors', *BMC Molecular Biology*, 8(1), 1-10.

Clarke, P. A. and Mathews, M. (1995) 'Interactions between the double-stranded RNA binding motif and RNA: definition of the binding site for the interferon-induced protein kinase DAI (PKR) on adenovirus VA RNA', *RNA*, 1(1), 7-20.

Clarke, T. E. and Clem, R. J. (2003) 'Insect defenses against virus infection: the role of apoptosis', *International Reviews of Immunology*, 22(5-6), 401-424.

Cobianchi, F., Karpel, R., Williams, K., Notario, V. and Wilson, S. (1988) 'Mammalian heterogeneous nuclear ribonucleoprotein complex protein A1. Large-scale overproduction in Escherichia coli and cooperative binding to single-stranded nucleic acids', *Journal of Biological Chemistry*, 263(2), 1063-1071.

Crickmore, N., Zeigler, D., Feitelson, J., Schnepf, E., Van Rie, J., Lereclus, D., Baum, J. and Dean, D. (1998) 'Revision of the nomenclature for the Bacillus thuringiensis pesticidal crystal proteins', *Microbiology and Molecular Biology Reviews*, 62(3), 807-813.

Crook, N. E., Clem, R. and Miller, L. (1993) 'An apoptosis-inhibiting baculovirus gene with a zinc finger-like motif', *Journal of Virology*, 67(4), 2168-2174.

Czech, B., Malone, C. D., Zhou, R., Stark, A., Schlingeheyde, C., Dus, M., Perrimon, N., Kellis, M., Wohlschlegel, J. A. and Sachidanandam, R. (2008) 'An endogenous small interfering RNA pathway in Drosophila', *Nature*, 453(7196), 798-802.

Davies, S. A., Goodwin, S. F., Kelly, D. C., Wang, Z., Sözen, M. A., Kaiser, K. and Dow, J. A. (1996) 'Analysis and inactivation of vha55, the gene encoding the vacuolar ATPase B-subunit in Drosophila melanogaster reveals a larval lethal phenotype', *Journal of Biological Chemistry*, 271(48), 30677-30684.

Dogan, T., Harms, G. S., Hekman, M., Karreman, C., Oberoi, T. K., Alnemri, E. S., Rapp, U. R. and Rajalingam, K. (2008) 'X-linked and cellular IAPs modulate the stability of C-RAF kinase and cell motility', *Nature Cell Biology*, 10(12), 1447-1455.

Dou, H., Finberg, K., Cardell, E. L., Lifton, R. and Choo, D. (2003) 'Mice lacking the B1 subunit of H+-ATPase have normal hearing', *Hearing Research*, 180(1), 76-84.

Douglas, A. and Prosser, W. (1992) 'Synthesis of the essential amino acid tryptophan in the A. pisum (Acyrthosiphon pisum) symbiosis', *Journal of Insect Physiology*, 38(8), 565-568.

Down, R. E., Fitches, E. C., Wiles, D. P., Corti, P., Bell, H. A., Gatehouse, J. A. and Edwards, J. P. (2006) 'Insecticidal spider venom toxin fused to snowdrop lectin is toxic to the peach-potato aphid, Myzus persicae (Hemiptera: Aphididae) and the rice brown planthopper, Nilaparvata lugens (Hemiptera: Delphacidae)', *Pest Management Science*, 62(1), 77-85.

Down, R. E., Gatehouse, A. M., Hamilton, W. D. and Gatehouse, J. A. (1996) 'Snowdrop lectin inhibits development and decreases fecundity of the glasshouse potato aphid (Aulacorthum solani) when administered in vitro and via transgenic plants both in laboratory and glasshouse trials', *Journal of Insect Physiology*, 42(11), 1035-1045.

Driever, W., Siegel, V. and Nusslein-Volhard, C. (1990) 'Autonomous determination of anterior structures in the early Drosophila embryo by the bicoid morphogen', *Development*, 109(4), 811-820.

Du, T. and Zamore, P. D. (2005) 'microPrimer: the biogenesis and function of microRNA', *Development*, 132(21), 4645-4652.

Dupoux, A., Cartier, J., Cathelin, S., Filomenko, R., Solary, E. and Dubrez-Daloz, L. (2009) 'cIAP1-dependent TRAF2 degradation regulates the differentiation of monocytes into macrophages and their response to CD40 ligand', *Blood*, 113(1), 175-185.

Eckelman, B., Drag, M., Snipas, S. and Salvesen, G. (2008) 'The mechanism of peptide-binding specificity of IAP BIR domains', *Cell Death & Differentiation*, 15(5), 920-928.

Elbashir, S. M., Harborth, J., Lendeckel, W., Yalcin, A., Weber, K. and Tuschl, T. (2001a) 'Duplexes of 21-nucleotide RNAs mediate RNA interference in cultured mammalian cells', *Nature*, 411(6836), 494-498.

Elbashir, S. M., Lendeckel, W. and Tuschl, T. (2001b) 'RNA interference is mediated by 21-and 22-nucleotide RNAs', *Genes & Development*, 15(2), 188-200.

Eleftherianos, I., Foster, S., Williamson, M. and Denholm, I. (2008) 'Characterization of the M918T sodium channel gene mutation associated with strong resistance to pyrethroid insecticides in the peach-potato aphid, Myzus persicae (Sulzer)', *Bulletin of Entomological Research*, 98(02), 183-191.

Ephrussi, A., Dickinson, L. K. and Lehmann, R. (1991) 'Oskar organizes the germ plasm and directs localization of the posterior determinant nanos', *Cell*, 66(1), 37-50.

FAO. (2009) How to feed the world 2050. Available at http://www.fao.org/fileadmin/templates/wsfs/docs/Issues_papers/HLEF2050_Global_Agriculture.pdf

FAO. (2011) The state of the world's land and water resources for food and agriculture. Available at http://www.fao.org/docrep/017/i1688e/i1688e.pdf

Febvay, G., Delobel, B. and Rahbé, Y. (1988) 'Influence of the amino acid balance on the improvement of an artificial diet for a biotype of Acyrthosiphon pisum (Homoptera: Aphididae)', *Canadian Journal of Zoology*, 66(11), 2449-2453.

Ferrandon, D., Elphick, L., Nüsslein-Volhard, C. and St Johnston, D. (1994) 'Staufen protein associates with the 3′ UTR of bicoid mRNA to form particles that move in a microtubule-dependent manner', *Cell*, 79(7), 1221-1232.

Ffrench-Constant, R. H. (2013) 'The molecular genetics of insecticide resistance', *Genetics*, 194(4), 807-15.

Filipowicz, W. (2005) 'RNAi: the nuts and bolts of the RISC machine', *Cell*, 122(1), 17-20.

Finch, S. and Coaker, T. (1969) 'A method for the continuous rearing of theD. radicumErioischia brassicae (Bch.) and some observations on its biology', *Bulletin of Entomological Research*, 58(03), 619-627.

Fire, A., Xu, S., Montgomery, M. K., Kostas, S. A., Driver, S. E. and Mello, C. C. (1998) 'Potent and specific genetic interference by double-stranded RNA in Caenorhabditis elegans', *Nature*, 391(6669), 806-811.

Fitches, E., Edwards, M. G., Mee, C., Grishin, E., Gatehouse, A. M., Edwards, J. P. and Gatehouse, J. A. (2004) 'Fusion proteins containing insect-specific toxins

as pest control agents: snowdrop lectin delivers fused insecticidal spider venom toxin to insect haemolymph following oral ingestion', *Journal of Insect Physiology*, 50(1), 61-71.

Fitches, E., Woodhouse, S. D., Edwards, J. P. and Gatehouse, J. A. (2001) 'In vitro and in vivo binding of snowdrop (Galanthus nivalis agglutinin; GNA) and jackbean (Canavalia ensiformis; Con A) lectins within tomato moth (Lacanobia oleracea) larvae; mechanisms of insecticidal action', *Journal of Insect Physiology*, 47(7), 777-787.

Fitches, E. C., Bell, H. A., Powell, M. E., Back, E., Sargiotti, C., Weaver, R. J. and Gatehouse, J. A. (2010) 'Insecticidal activity of scorpion toxin (ButaIT) and snowdrop lectin (GNA) containing fusion proteins towards pest species of different orders', *Pest Management Science*, 66(1), 74-83.

Fitches, E. C., Pyati, P., King, G. F. and Gatehouse, J. A. (2012) 'Fusion to snowdrop lectin magnifies the oral activity of insecticidal ω-hexatoxin-Hv1a peptide by enabling its delivery to the central nervous system', *PLoS ONE*, 7(6), e39389.

Fu, K.-Y., Guo, W.-C., Lü, F.-g., Liu, X.-p. and Li, G.-Q. (2014) 'Response of the vacuolar ATPase subunit E to RNA interference and four chemical pesticides in Leptinotarsa decemlineata (Say)', *Pesticide Biochemistry and Physiology*, 114, 16-23.

Fukuto, T. R. (1990) 'Mechanism of action of organophosphorus and carbamate insecticides', *Environmental Health Perspect*, 87, 245-54.

Garbutt, J. S., Bellés, X., Richards, E. H. and Reynolds, S. E. (2013) 'Persistence of double-stranded RNA in insect hemolymph as a potential determiner of RNA interference success: evidence from Manduca sexta and Blattella germanica', *Journal of Insect Physiology*, 59(2), 171-178.

Garthwaite, D., Thomas, M., Parrish, G., Smith, L. and Barker, I. (2008) 'Pesticide usage survey report 224: Arable Crops in Britain', *FERA, York*.

Gatehouse, J. A. and Price, D. R. (2011) 'Protection of crops against insect pests using RNA interference', *Insect Biotechnology* Springer, 145-168.

Gatignol, A., Buckler, C. and Jeang, K. (1993) 'Relatedness of an RNA-binding motif in human immunodeficiency virus type 1 TAR RNA-binding protein TRBP to human P1/dsI kinase and Drosophila staufen', *Molecular and Cellular Biology*, 13(4), 2193-2202.

Geley, S. and Müller, C. (2004) 'RNAi: ancient mechanism with a promising future', *Experimental Gerontology*, 39(7), 985-998.

Green, S. R. and Mathews, M. B. (1992) 'Two RNA-binding motifs in the double-stranded RNA-activated protein kinase, DAI', *Genes & Development*, 6(12b), 2478-2490.

Grube, A., Donaldson, D., Kiely, T. and Wu, L. (2011) 'Pesticides industry sales and usage', *US EPA, Washington, DC*.

Gu, L. and Knipple, D. C. (2013) 'Recent advances in RNA interference research in insects: Implications for future insect pest management strategies', *Crop Protection*, 45, 36-40.

Guo, S. and Kemphues, K. J. (1995) 'par-1, a gene required for establishing polarity in C. elegans embryos, encodes a putative Ser/Thr kinase that is asymmetrically distributed', *Cell*, 81(4), 611-620.

Gyrd-Hansen, M. and Meier, P. (2010) 'IAPs: from caspase inhibitors to modulators of NF-κB, inflammation and cancer', *Nature Reviews Cancer*, 10(8), 561-574.

Hamilton, A. J. and Baulcombe, D. C. (1999) 'A species of small antisense RNA in posttranscriptional gene silencing in plants', *Science*, 286(5441), 950-952.

Hammond, S. M., Bernstein, E., Beach, D. and Hannon, G. J. (2000) 'An RNA-directed nuclease mediates post-transcriptional gene silencing in Drosophila cells', *Nature*, 404(6775), 293-296.

Hartig, J. V., Tomari, Y. and Förstemann, K. (2007) 'piRNAs—the ancient hunters of genome invaders', *Genes & Development*, 21(14), 1707-1713.

Heckel, D. G. (2012) 'Insecticide Resistance After Silent Spring', *Science*, 337(6102), 1613-1614.

Hester, G., Kaku, H., Goldstein, I. J. and Wright, C. S. (1995) 'Structure of mannose-specific snowdrop (Galanthus nivalis) lectin is representative of a new plant lectin family', *Nature Structural & Molecular Biology*, 2(6), 472-479.

Higgins, D. R. and Cregg, J. M. (1998) 'Introduction to Pichia pastoris', *Pichia Protocols*, 1-15.

Hinds, M. G., Norton, R. S., Vaux, D. L. and Day, C. L. (1999) 'Solution structure of a baculoviral inhibitor of apoptosis (IAP) repeat', *Nature Structural & Molecular Biology*, 6(7), 648-651.

Hogervorst, P. A., Ferry, N., Gatehouse, A. M., Wäckers, F. L. and Romeis, J. (2006) 'Direct effects of snowdrop lectin (GNA) on larvae of three aphid predators and fate of GNA after ingestion', *Journal of Insect Physiology*, 52(6), 614-624.

Hong, J., Qian, Z., Shen, S., Min, T., Tan, C., Xu, J., Zhao, Y. and Huang, W. (2005) 'High doses of siRNAs induce eri-1 and adar-1 gene expression and reduce the efficiency of RNA interference in the mouse', *Biochem. J*, 390, 675-679.

Igaki, T., Yamamoto-Goto, Y., Tokushige, N., Kanda, H. and Miura, M. (2002) 'Down-regulation of DIAP1 Triggers a NovelDrosophila Cell Death Pathway Mediated by Dark and DRONC', *Journal of Biological Chemistry*, 277(26), 23103-23106.

Inoue, H., Noumi, T., Nagata, M., Murakami, H. and Kanazawa, H. (1999) 'Targeted disruption of the gene encoding the proteolipid subunit of mouse vacuolar H+-ATPase leads to early embryonic lethality', *Biochimica et Biophysica Acta (BBA)-Bioenergetics*, 1413(3), 130-138.

Irles, P., Bellés, X. and Piulachs, M. D. (2009) 'Identifying genes related to choriogenesis in insect panoistic ovaries by Suppression Subtractive Hybridization', *BMC Genomics*, 10(1), 206.

James, C., Teng, P., Arujanan, M., Aldemita, R. R., Flavell, R. B., Brookes, G. and Qaim, M. (2015) 'Invitational Essays to Celebrate the 20th Anniversary of the Commercialization of Biotech Crops (1996 to 2015): Progress and Promise'. *ISAAA Brief,* No. 51. ISAAA: Ithaca, NY, USA.

Johnston, D. S., Driever, W., Berleth, T., Richstein, S. and Nüsslein-Volhard, C. (1989) 'Multiple steps in the localization of bicoid RNA to the anterior pole of the Drosophila oocyte', *Development*, 107(Supplement), 13-19.

Junge, W., Lill, H. and Engelbrecht, S. (1997) 'ATP synthase: an electrochemical ransducer with rotatory mechanics', *Trends in Biochemical Sciences*, 22(11), 420-423.

Junge, W. and Nelson, N. (2005) 'Nature's rotary electromotors', *Science*, 308(5722), 642-644.

Kane, P. M. (1995) 'Disassembly and reassembly of the yeast vacuolar H+-ATPase in vivo', *Journal of Biological Chemistry*, 270(28), 17025-17032.

Kane, P. M. (2000) 'Regulation of V-ATPases by reversible disassembly', *FEBS letters*, 469(2), 137-141.

Kane, P. M. (2012) 'Targeting reversible disassembly as a mechanism of controlling V-ATPase activity', *Current Protein & Peptide Science*, 13(2), 117.

Kawaguchi, Y., Danjo, K., Okuda, T. and Okamoto, H. (2009) 'Improving the stability of short hairpin RNA against fetal bovine serum using the third double-stranded RNA-binding domain from Staufen protein', *Biological and Pharmaceutical Bulletin*, 32(2), 283-288.

Kennedy, R. and Collier, R. (2000) 'Pests and diseases of field vegetables', *Pest and Disease Management Handbook*, 185-257.

Kennedy, S., Wang, D. and Ruvkun, G. (2004) 'A conserved siRNA-degrading RNase negatively regulates RNA interference in C. elegans', *Nature*, 427(6975), 645-649.

Kennerdell, J. R. and Carthew, R. W. (1998) 'Use of dsRNA-mediated genetic interference to demonstrate that frizzled and frizzled 2 act in the wingless pathway', *Cell*, 95(7), 1017-1026.

Kennerdell, J. R. and Carthew, R. W. (2000) 'Heritable gene silencing in Drosophila using double-stranded RNA', *Nature Biotechnology*, 18(8), 896-898.

Kim-Ha, J., Smith, J. L. and Macdonald, P. M. (1991) 'oskar mRNA is localized to the posterior pole of the Drosophila oocyte', *Cell*, 66(1), 23-35.

Kim-Ha, J., Webster, P. J., Smith, J. L. and Macdonald, P. M. (1993) 'Multiple RNA regulatory elements mediate distinct steps in localization of oskar mRNA', *Development*, 119(1), 169-178.

Kirst, H. A., Michel, K. H., Mynderase, J. S., Chio, E. H., Yao, R. C., Nakasukasa, W. M., Boeck, L., Occlowitz, J. L., Paschal, J. W. and Deeter, J. B. (1992) 'Discovery, isolation, and structure elucidation of a family of structuraly unique, fermentation-derived tetracyclic macrolides', *ACS Symposium Series*, 504, 214-225.

Klattenhoff, C. and Theurkauf, W. (2008) 'Biogenesis and germline functions of piRNAs', *Development*, 135(1), 3-9.

Koehler, H.-R. and Triebskorn, R. (2013) 'Wildlife Ecotoxicology of Pesticides: Can We Track Effects to the Population Level and Beyond?', *Science*, 341(6147), 759-765.

Kumar, P., Pandit, S. S. and Baldwin, I. T. (2012) 'Tobacco rattle virus vector: a rapid and transient means of silencing Manduca sexta genes by plant mediated RNA interference', *PloS One*, 7(2), e31347.

Laemmli, U. K. (1970) 'Cleavage of structural proteins during the assembly of the head of bacteriophage T4', *Nature*, 227, 680-685.

Layzer, J. M., McCaffrey, A. P., Tanner, A. K., Huang, Z., Kay, M. A. and Sullenger, B. A. (2004) 'In vivo activity of nuclease-resistant siRNAs', *RNA*, 10(5), 766-771.

Lee, Y. S., Nakahara, K., Pham, J. W., Kim, K., He, Z., Sontheimer, E. J. and Carthew, R. W. (2004) 'Distinct roles for Drosophila Dicer-1 and Dicer-2 in the siRNA/miRNA silencing pathways', *Cell*, 117(1), 69-81.

Li, H., Zheng, X., Koren, V., Vashist, Y. K. and Tsui, T. Y. (2014) 'Highly efficient delivery of siRNA to a heart transplant model by a novel cell penetrating peptide-dsRNA binding domain', *International Journal of Pharmaceutics*, 469(1), 206-213.

Li, X., Zhang, M. and Zhang, H. (2011) 'RNA interference of four genes in adult Bactrocera dorsalis by feeding their dsRNAs', *PloS ONE*, 6(3), e17788.

Lipkin, A., Kozlov, S., Nosyreva, E., Blake, A., Windass, J. and Grishin, E. (2002) 'Novel insecticidal toxins from the venom of the spider Segestria florentina', *Toxicon*, 40(2), 125-130.

Lisi, S., Mazzon, I. and White, K. (2000) 'Diverse domains of THREAD/DIAP1 are required to inhibit apoptosis induced by REAPER and HID in Drosophila', *Genetics*, 154(2), 669-678.

Liu, J., Carmell, M. A., Rivas, F. V., Marsden, C. G., Thomson, J. M., Song, J.-J., Hammond, S. M., Joshua-Tor, L. and Hannon, G. J. (2004) 'Argonaute2 is the catalytic engine of mammalian RNAi', *Science*, 305(5689), 1437-1441.

Liu, J., Swevers, L., Iatrou, K., Huvenne, H. and Smagghe, G. (2012) 'Bombyx mori DNA/RNA non-specific nuclease: expression of isoforms in insect culture cells, subcellular localization and functional assays', *Journal of Insect Physiology*, 58(8), 1166-1176.

Liu, Y., Wang, X.-F., Chen, Y., Zhang, L.-H. and Yang, Z.-J. (2012) 'A solid-phase method for peptide–siRNA covalent conjugates based on click chemistry', *Medicinal Chemistry Communications*, 3(4), 506-511.

Liu, Y., Ye, X., Jiang, F., Liang, C., Chen, D., Peng, J., Kinch, L. N., Grishin, N. V. and Liu, Q. (2009) 'C3PO, an endoribonuclease that promotes RNAi by facilitating RISC activation', *Science*, 325(5941), 750-753.

Longstaff, M., Powell, K. S., Gatehouse, J. A., Raemaekers, R., Newell, C. A. and Hamilton, W. (1998) 'Production and purification of active snowdrop lectin in Escherichia coli', *European Journal of Biochemistry*, 252(1), 59-65.

Lu, M., Lin, S.-C., Huang, Y., Kang, Y. J., Rich, R., Lo, Y.-C., Myszka, D., Han, J. and Wu, H. (2007) 'XIAP induces NF-κB activation via the BIR1/TAB1 interaction and BIR1 dimerization', *Molecular Cell*, 26(5), 689-702.

Luo, Y., Wang, X., Yu, D. and Kang, L. (2012) 'The SID-1 double-stranded RNA transporter is not required for systemic RNAi in the migratory locust', *RNA Biology*, 9(5), 663-671.

Lynch, J. A. and Desplan, C. (2006) 'A method for parental RNA interference in the wasp Nasonia vitripennis', *NATURE PROTOCOLS-ELECTRONIC EDITION-*, 1(1), 486.

Mao, J. and Zeng, F. (2012) 'Feeding-based RNA intereference of a gap gene is lethal to the A. pisum, Acyrthosiphon pisum'. PloS ONE 7 (11), e48718.

Mao, Y.-B., Cai, W.-J., Wang, J.-W., Hong, G.-J., Tao, X.-Y., Wang, L.-J., Huang, Y.-P. and Chen, X.-Y. (2007) 'Silencing a cotton bollworm P450 monooxygenase gene by plant-mediated RNAi impairs larval tolerance of gossypol', *Nature Biotechnology*, 25(11), 1307-1313.

Marivin, A., Berthelet, J., Plenchette, S. and Dubrez, L. (2012) 'The inhibitor of apoptosis (IAPs) in adaptive response to cellular stress', *Cells*, 1(4), 711-737.

Marshansky, V. and Futai, M. (2008) 'The V-type H+-ATPase in vesicular trafficking: targeting, regulation and function', *Current Opinion in Cell Biology*, 20(4), 415-426.

Marshansky, V., Rubinstein, J. L. and Grüber, G. (2014) 'Eukaryotic V-ATPase: novel structural findings and functional insights', *Biochimica et Biophysica Acta (BBA)-Bioenergetics*, 1837(6), 857-879.

Martinez, J., Patkaniowska, A., Urlaub, H., Lührmann, R. and Tuschl, T. (2002) 'Single-stranded antisense siRNAs guide target RNA cleavage in RNAi', *Cell*, 110(5), 563-574.

Martinez, J. and Tuschl, T. (2004) 'RISC is a 5′ phosphomonoester-producing RNA endonuclease', *Genes & Development*, 18(9), 975-980.

Matranga, C. and Zamore, P. D. (2007) 'Small silencing RNAs', *Current Biology*, 17(18), R789-R793.

Matthews, G. A. (1999) Application of pesticides to crops (p. 325), *World Scientific*. London, United Kingdom: Imperial College Press.

Meier, P., Silke, J., Leevers, S. J. and Evan, G. I. (2000) 'The Drosophila caspase DRONC is regulated by DIAP1', *The EMBO Journal*, 19(4), 598-611.

Meier, T., Polzer, P., Diederichs, K., Welte, W. and Dimroth, P. (2005) 'Structure of the rotor ring of F-Type Na+-ATPase from Ilyobacter tartaricus', *Science*, 308(5722), 659-662.

Micklem, D. R., Adams, J., Grünert, S. and St Johnston, D. (2000) 'Distinct roles of two conserved Staufen domains in oskar mRNA localization and translation', *The EMBO Journal*, 19(6), 1366-1377.

Miller, S. C., Brown, S. J. and Tomoyasu, Y. (2008) 'Larval RNAi in Drosophila?', *Development Genes and Evolution*, 218(9), 505-510.

Miller, S. C., Miyata, K., Brown, S. J. and Tomoyasu, Y. (2012) 'Dissecting systemic RNA interference in the *T. castaneum* Tribolium castaneum: parameters affecting the efficiency of RNAi', PloS ONE 7(10), e47431.

Misquitta, L. and Paterson, B. M. (1999) 'Targeted disruption of gene function in Drosophila by RNA interference (RNA-i): a role for nautilus in embryonic somatic muscle formation', *Proceedings of the National Academy of Sciences*, 96(4), 1451-1456.

Mito, T., Nakamura, T., Bando, T., Ohuchi, H. and Noji, S. (2011) 'The advent of RNA interference in entomology', *Entomological Science*, 14(1), 1-8.

Morrissey, D. V., Blanchard, K., Shaw, L., Jensen, K., Lockridge, J. A., Dickinson, B., McSwiggen, J. A., Vargeese, C., Bowman, K. and Shaffer, C. S. (2005a) 'Activity of stabilized short interfering RNA in a mouse model of hepatitis B virus replication', *Hepatology*, 41(6), 1349-1356.

Morrissey, D. V., Lockridge, J. A., Shaw, L., Blanchard, K., Jensen, K., Breen, W., Hartsough, K., Machemer, L., Radka, S. and Jadhav, V. (2005b) 'Potent and persistent in vivo anti-HBV activity of chemically modified siRNAs', *Nature Biotechnology*, 23(8), 1002-1007.

Murata, Y., Sun-Wada, G.-H., Yoshimizu, T., Yamamoto, A., Wada, Y. and Futai, M. (2002) 'Differential localization of the vacuolar H+ pump with G subunit isoforms (G1 and G2) in mouse neurons', *Journal of Biological Chemistry*, 277(39), 36296-36303.

Nadler, S. G., Merrill, B. M., Roberts, W. J., Keating, K. M., Lisbin, M. J., Barnett, S. F., Wilson, S. H. and Williams, K. R. (1991) 'Interactions of the A1 heterogeneous nuclear ribonucleoprotein and its proteolytic derivative, UP1, with RNA and DNA: evidence for multiple RNA binding domains and salt-dependent binding mode transitions', *Biochemistry*, 30(11), 2968-2976.

Napoli, C., Lemieux, C. and Jorgensen, R. (1990) 'Introduction of a chimeric chalcone synthase gene into petunia results in reversible co-suppression of homologous genes in trans', *The Plant Cell*, 2(4), 279-289.

Nelson, H. and Nelson, N. (1990) 'Disruption of genes encoding subunits of yeast vacuolar H (+)-ATPase causes conditional lethality', *Proceedings of the National Academy of Sciences*, 87(9), 3503-3507.

Nishi, T. and Forgac, M. (2002) 'The vacuolar (H+)-ATPases—nature's most versatile proton pumps', *Nature Reviews Molecular Cell Biology*, 3(2), 94-103.

Nossal, N. G. and Heppel, L. A. (1966) 'The release of enzymes by osmotic shock from Escherichia coli in exponential phase', *Journal of Biological Chemistry*, 241(13), 3055-3062.

Obbard, D. J., Gordon, K. H., Buck, A. H. and Jiggins, F. M. (2009) 'The evolution of RNAi as a defence against viruses and transposable elements', *Philosophical Transactions of the Royal Society B: Biological Sciences*, 364(1513), 99-115.

Orme, M. and Meier, P. (2009) 'Inhibitor of apoptosis proteins in Drosophila: gatekeepers of death', *Apoptosis*, 14(8), 950-960.

Orr, N., Shaffner, A. J., Richey, K. and Crouse, G. D. (2009) 'Novel mode of action of spinosad: Receptor binding studies demonstrating lack of interaction with known insecticidal target sites', *Pesticide Biochemistry and Physiology*, 95(1), 1-5.

Palauqui, J. C., Elmayan, T., Pollien, J. M. and Vaucheret, H. (1997) 'Systemic acquired silencing: transgene-specific post-transcriptional silencing is transmitted by grafting from silenced stocks to non-silenced scions', *The EMBO Journal*, 16(15), 4738-4745.

Parrish, S., Fleenor, J., Xu, S., Mello, C. and Fire, A. (2000) 'Functional anatomy of a dsRNA trigger: differential requirement for the two trigger strands in RNA interference', *Molecular Cell*, 6(5), 1077-1087.

Peumans, W. J. and Van Damme, E. (1995) 'Lectins as plant defense proteins', *Plant Physiology*, 109(2), 347.

Pillai, R. S., Bhattacharyya, S. N. and Filipowicz, W. (2007) 'Repression of protein synthesis by miRNAs: how many mechanisms?', *Trends in Cell Biology*, 17(3), 118-126.

Pitino, M., Coleman, A. D., Maffei, M. E., Ridout, C. J. and Hogenhout, S. A. (2011) 'Silencing of aphid genes by dsRNA feeding from plants', *PloS ONE*, 6(10), e25709.

Porcar, M., Grenier, A.-M., Federici, B. and Rahbé, Y. (2009) 'Effects of Bacillus thuringiensis δ-endotoxins on the A. pisum (Acyrthosiphon pisum)', *Applied and Environmental Microbiology*, 75(14), 4897-4900.

Powell, K. S., Spence, J., Bharathi, M., Gatehouse, J. A. and Gatehouse, A. M. (1998) 'Immunohistochemical and developmental studies to elucidate the mechanism of action of the snowdrop lectin on the rice brown planthopper, Nilaparvata lugens (Stal)', *Journal of Insect Physiology*, 44(7), 529-539.

Price, D. R. and Gatehouse, J. A. (2008) 'RNAi-mediated crop protection against insects', *Trends in Biotechnology*, 26(7), 393-400.

Pridgeon, J. W., Zhao, L., Becnel, J. J., Strickman, D. A., Clark, G. G. and Linthicum, K. J. (2008) 'Topically applied AaeIAP1 double-stranded RNA kills female adults of Aedes aegypti', *Journal of Medical Entomology*, 45(3), 414-420.

Ramos, A., Bayer, P. and Varani, G. (1999) 'Determination of the structure of the RNA complex of a double-stranded RNA-binding domain from Drosophila Staufen protein', *Biopolymers*, 52(4), 181-196.

Ramos, A., Grünert, S., Adams, J., Micklem, D. R., Proctor, M. R., Freund, S., Bycroft, M., St Johnston, D. and Varani, G. (2000) 'RNA recognition by a Staufen double-stranded RNA-binding domain', *The EMBO Journal*, 19(5), 997-1009.

Raymond-Delpech, V., Matsuda, K., Sattelle, B. M., Rauh, J. J. and Sattelle, D. B. (2005) 'Ion channels: molecular targets of neuroactive insecticides', *Invertebrate Neuroscience*, 5(3-4), 119-133.

Ren, D., Cai, Z., Song, J., Wu, Z. and Zhou, S. (2014) 'dsRNA uptake and persistence account for tissue-dependent susceptibility to RNA interference in the migratory locust, Locusta migratoria', *Insect Molecular Biology*, 23(2), 175-184.

Rodriguez, A., Chen, P., Oliver, H. and Abrams, J. M. (2002) 'Unrestrained caspase-dependent cell death caused by loss of Diap1 function requires the Drosophila Apaf-1 homolog, Dark', *The EMBO Journal*, 21(9), 2189-2197.

Romano, N. and Macino, G. (1992) 'Quelling: transient inactivation of gene expression in Neurospora crassa by transformation with homologous sequences', *Molecular Microbiology*, 6(22), 3343-3353.

Ronco, M., Uda, T., Mito, T., Minelli, A., Noji, S. and Klingler, M. (2008) 'Antenna and all gnathal appendages are similarly transformed by homothorax knock-down in the cricket Gryllus bimaculatus', *Developmental Biology*, 313(1), 80-92.

Saleh, M.-C., van Rij, R. P., Hekele, A., Gillis, A., Foley, E., O'Farrell, P. H. and Andino, R. (2006) 'The endocytic pathway mediates cell entry of dsRNA to induce RNAi silencing', *Nature Cell Biology*, 8(8), 793-802.

Sen, G. L. and Blau, H. M. (2006) 'A brief history of RNAi: the silence of the genes', *The FASEB Journal*, 20(9), 1293-1299.

Seto, A. G., Kingston, R. E. and Lau, N. C. (2007) 'The coming of age for Piwi proteins', *Molecular Cell*, 26(5), 603-609.

Silke, J. and Brink, R. (2010) 'Regulation of TNFRSF and innate immune signalling complexes by TRAFs and cIAPs', *Cell Death & Differentiation*, 17(1), 35-45.

Silke, J., Kratina, T., Chu, D., Ekert, P. G., Day, C. L., Pakusch, M., Huang, D. C. and Vaux, D. L. (2005) 'Determination of cell survival by RING-mediated regulation of inhibitor of apoptosis (IAP) protein abundance', *Proceedings of the National Academy of Sciences of the United States of America*, 102(45), 16182-16187.

Siomi, M. C., Sato, K., Pezic, D. and Aravin, A. A. (2011) 'PIWI-interacting small RNAs: the vanguard of genome defence', *Nature Reviews Molecular Cell Biology*, 12(4), 246-258.

Song, J.-J., Smith, S. K., Hannon, G. J. and Joshua-Tor, L. (2004) 'Crystal structure of Argonaute and its implications for RISC slicer activity', *Science*, 305(5689), 1434-1437.

St Johnston, D., Beuchle, D. and Nüsslein-Volhard, C. (1991) 'Staufen, a gene required to localize maternal RNAs in the Drosophila egg', *Cell*, 66(1), 51-63.

St Johnston, D., Brown, N. H., Gall, J. G. and Jantsch, M. (1992) 'A conserved double-stranded RNA-binding domain', *Proceedings of the National Academy of Sciences*, 89(22), 10979-10983.

Sumner, J.-P., Dow, J. A., Earley, F. G., Klein, U., Jäger, D. and Wieczorek, H. (1995) 'Regulation of plasma membrane V-ATPase activity by dissociation of peripheral subunits', *Journal of Biological Chemistry*, 270(10), 5649-5653.

Tabara, H., Grishok, A. and Mello, C. C. (1998) 'RNAi in C. elegans: soaking in the genome sequence', *Science*, 282(5388), 430-431.

Tempel Nakasu, E. Y. (2014) 'Effects of w-ACTX-Hv1a/GNA, a novel protein biopesticide targeting voltage-gated calcium ion channels, on target and non-target arthropod species'.Unpublised PhD Thesis. Newcastle University.

Terenius, O., Papanicolaou, A., Garbutt, J. S., Eleftherianos, I., Huvenne, H., Kanginakudru, S., Albrechtsen, M., An, C., Aymeric, J.-L. and Barthel, A. (2011) 'RNA interference in Lepidoptera: an overview of successful and unsuccessful studies and implications for experimental design', *Journal of Insect Physiology*, 57(2), 231-245.

Thornberry, N. A. and Lazebnik, Y. (1998) 'Caspases: enemies within', *Science*, 281(5381), 1312-1316.

Tian, H., Peng, H., Yao, Q., Chen, H., Xie, Q., Tang, B. and Zhang, W. (2009) 'Developmental control of a lepidopteran pest Spodoptera exigua by ingestion of bacteria expressing dsRNA of a non-midgut gene', *PLoS ONE*, 4(7), e6225.

Tiemann, K. and Rossi, J. J. (2009) 'RNAi-based therapeutics–current status, challenges and prospects', *EMBO Molecular Medicine*, 1(3), 142-151.

Timmons, L., Court, D. L. and Fire, A. (2001) 'Ingestion of bacterially expressed dsRNAs can produce specific and potent genetic interference in Caenorhabditis elegans', *Gene*, 263(1), 103-112.

Timmons, L. and Fire, A. (1998) 'Specific interference by ingested dsRNA', *Nature*, 395(6705), 854-854.

Toenniessen, G. H., O'Toole, J. C. and DeVries, J. (2003) 'Advances in plant biotechnology and its adoption in developing countries', *Current Opinion in Plant Biology*, 6(2), 191-198.

Tolia, N. H. and Joshua-Tor, L. (2007) 'Slicer and the argonautes', *Nature Chemical Biology*, 3(1), 36-43.

Tomoyasu, Y. and Denell, R. E. (2004) 'Larval RNAi in Tribolium (Coleoptera) for analyzing adult development', *Development Genes and Evolution*, 214(11), 575-578.

Tomoyasu, Y., Miller, S. C., Tomita, S., Schoppmeier, M., Grossmann, D. and Bucher, G. (2008) 'Exploring systemic RNA interference in insects: a genome-wide survey for RNAi genes in Tribolium', *Genome Biology*, 9(1), R10.

Trung, N. P., Fitches, E. and Gatehouse, J. A. (2006) 'A fusion protein containing a lepidopteran-specific toxin from the South Indian red scorpion (Mesobuthus tamulus) and snowdrop lectin shows oral toxicity to target insects', *BMC Biotechnology*, 6(1), 18.

Turner, C., Davy, M., MacDiarmid, R., Plummer, K., Birch, N. and Newcomb, R. (2006) 'RNA interference in the light brown apple moth, Epiphyas postvittana (Walker) induced by double-stranded RNA feeding', *Insect Molecular Biology*, 15(3), 383-391.

Ulvila, J., Parikka, M., Kleino, A., Sormunen, R., Ezekowitz, R. A., Kocks, C. and Rämet, M. (2006) 'Double-stranded RNA is internalized by scavenger receptor-mediated endocytosis in Drosophila S2 cells', *Journal of Biological Chemistry*, 281(20), 14370-14375.

Van Damme, E. J., Allen, A. K. and Peumans, W. J. (1987) 'Isolation and characterization of a lectin with exclusive specificity towards mannose from snowdrop (Galanthus nivalis) bulbs', *FEBS Letters*, 215(1), 140-144.

Vaux, D. L., Haecker, G. and Strasser, A. (1994) 'An evolutionary perspective on apoptosis', *Cell*, 76(5), 777-779.

Vitavska, O., Merzendorfer, H. and Wieczorek, H. (2005) 'The V-ATPase subunit C binds to polymeric F-actin as well as to monomeric G-actin and induces cross-linking of actin filaments', *Journal of Biological Chemistry*, 280(2), 1070-1076.

Vitte-Mony, I., Korneluk, R. and Diaz-Mitoma, F. (1997) 'Role of XIAP protein, a human member of the inhibitor of apoptosis (IAP) protein family, in phytohemagglutinin-induced apoptosis of human T cell lines', *Apoptosis*, 2(6), 501-509.

Walter, D., Wissing, S., Madeo, F. and Fahrenkrog, B. (2006) 'The inhibitor-of-apoptosis protein Bir1p protects against apoptosis in S. cerevisiae and is a substrate for the yeast homologue of Omi/HtrA2', *Journal of Cell Science*, 119(9), 1843-1851.

Wang, S. L., Hawkins, C. J., Yoo, S. J., Müller, H.-A. J. and Hay, B. A. (1999) 'The Drosophila caspase inhibitor DIAP1 is essential for cell survival and is negatively regulated by HID', *Cell*, 98(4), 453-463.

Wang, Y., Zhang, H., Li, H. and Miao, X. (2011) 'Second-generation sequencing supply an effective way to screen RNAi targets in large scale for potential application in pest insect control', *PLoS ONE*, 6(4), e18644.

Wertz, I. and Dixit, V. (2010) 'Regulation of death receptor signaling by the ubiquitin system', *Cell Death & Differentiation*, 17(1), 14-24.

Whyard, S., Singh, A. D. and Wong, S. (2009) 'Ingested double-stranded RNAs can act as species-specific insecticides', *Insect Biochemistry and Molecular Biology*, 39(11), 824-832.

Winston, W. M., Molodowitch, C. and Hunter, C. P. (2002) 'Systemic RNAi in C. elegans requires the putative transmembrane protein SID-1', *Science*, 295(5564), 2456-2459.

Xie, Y., Bodnaryk, R. and Fields, P. (1996) 'A rapid and simple flour-disk bioassay for testing substances active against stored-product insects', *The Canadian Entomologist*, 128(05), 865-875.

Xu, W. and Han, Z. (2008) 'Cloning and phylogenetic analysis of sid-1-like genes from aphids', *Journal of Insect Science*, 8(1), 30.

Yang, S., Pyati, P., Fitches, E. and Gatehouse, J. A. (2014) 'A recombinant fusion protein containing a spider toxin specific for the insect voltage-gated sodium ion channel shows oral toxicity towards insects of different orders', *Insect Biochemistry and Molecular Biology*, 47, 1-11.

Yuan, S., Yu, X., Topf, M., Dorstyn, L., Kumar, S., Ludtke, S. J. and Akey, C. W. (2011) 'Structure of the Drosophila apoptosome at 6.9 Å resolution', *Structure*, 19(1), 128-140.

Zamore, P. D. and Haley, B. (2005) 'Ribo-gnome: the big world of small RNAs', *Science*, 309(5740), 1519-1524.

Zha, W., Peng, X., Chen, R., Du, B., Zhu, L. and He, G. (2011) 'Knockdown of midgut genes by dsRNA-transgenic plant-mediated RNA interference in the hemipteran insect Nilaparvata lugens', *PLoS ONE* 6(5), e20504.

Zhang, X., Zhang, J. and Zhu, K. (2010) 'Chitosan/double-stranded RNA nanoparticle-mediated RNA interference to silence chitin synthase genes through larval feeding in the African malaria mosquito (Anopheles gambiae)', *Insect Molecular Biology*, 19(5), 683-693.

Zhu, F., Xu, J., Palli, R., Ferguson, J. and Palli, S. R. (2011) 'Ingested RNA interference for managing the populations of the Colorado potato beetle, Leptinotarsa decemlineata', *Pest Management Science*, 67(2), 175-182.

Zhuang, M., Guan, S., Wang, H., Burlingame, A. L. and Wells, J. A. (2013) 'Substrates of IAP ubiquitin ligases identified with a designed orthogonal E3 ligase, the NEDDylator', *Molecular Cell*, 49(2), 273-282.

Appendix A.

GAPDH gene sequence cloned from *D. radicum*

ATCCATCGGCGCTGGTTTTGCGGTGCCGCCGTCGATAAAGGTGCTGCCGTTGGTAGCTGTTAAC
GATCCCTTCATCGATGTTAACTACATGGTATACTTGTTCAAATTCGATTCGACCCACGGTCGTT
TCAAGGGCACCGTCGCTGCTGAAGATGGCAAATTGGTAGTCAACGGTCAAAAGATCACCGTTTT
CAGTGAACGCGACCCTGCCAACATTAACTGGGCTAGCGCTGGCGCTGAATATGTTGTAGAATCG
ACTGGTGTCTTCACCACCATCGAAAAAGCTTCTCTCCATTTCAAGGGTGGTGCCAAGAAGGTAG
TCATCTCTGCCCCCTCTGCTGATGCCCCCATGTTTGTGTGCGGTGTTAACTTGGATGCCTACAC
ACCCGACATGAAGGTAGTCTCCAATGCTTCCTGCACAACCAACTGTTTGGCTCCCTTGGCCAAG
GTTATCAACGATAACTGGGAAATCGTAGAGGGTTTCATGATCCACTGTCCATGCCACTACTGCC
ACCCAAAAGACCGTTGACGGTCCATCTGGCAAATTGTGGCGCGATGGACGTGGCATCTTGCTGA
AAAACTCGAGCC

qPCR primers are highlighted in yellow (Forward) and green (Reverse)

Appendix B.

Drosophilia *thread* (*APIN*) and *V-type ATPase E subunit* expression atlas

http://flyatlas.org/atlas.cgi

thread (CG12284) = 500-1500 in different larval tissues
V-type ATPase E (CG1088) = 1500-5000 in different larval tissues = 2-4x higher

From Flybase - thread

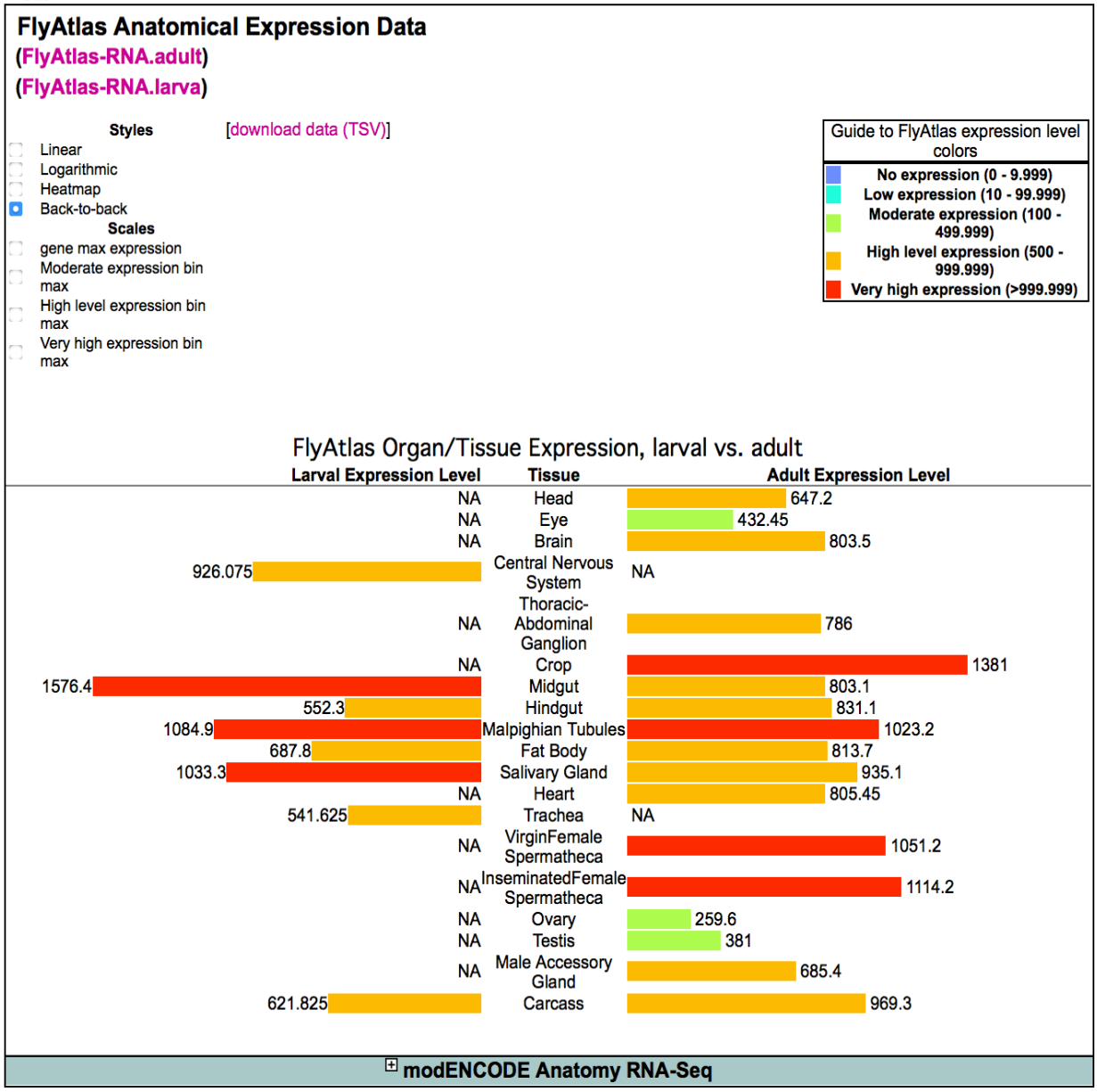

V-type ATPase E

FlyAtlas Anatomical Expression Data

(FlyAtlas-RNA.adult)

(FlyAtlas-RNA.larva)

Styles [download data (TSV)]

- Linear
- Logarithmic
- Heatmap
- Back-to-back

Scales

- gene max expression
- Moderate expression bin max
- High level expression bin max
- Very high expression bin max

Guide to FlyAtlas expression level colors

- **No expression (0 - 9.999)**
- **Low expression (10 - 99.999)**
- **Moderate expression (100 - 499.999)**
- **High level expression (500 - 999.999)**
- **Very high expression (>999.999)**

FlyAtlas Organ/Tissue Expression, larval vs. adult

Larval Expression Level	Tissue	Adult Expression Level
NA	Head	2099.5
NA	Eye	1648.475
NA	Brain	2409.8
1587.925	Central Nervous System	NA
NA	Thoracic-Abdominal Ganglion	2972.3
NA	Crop	2093.2
4646.5	Midgut	4330.8
5110.6	Hindgut	5075
3979.8	Malpighian Tubules	6448.4
1624.6	Fat Body	1276.9
3937.6	Salivary Gland	1131
NA	Heart	1734.975
2608.475	Trachea	NA
NA	VirginFemale Spermatheca	1569.4
NA	InseminatedFemale Spermatheca	1706.6
NA	Ovary	1498.5
NA	Testis	777.3
NA	Male Accessory Gland	1730.4
2754.05	Carcass	1771.3